POSTHARVEST DISEASES OF FRUIT AND VEGETABLE: METHODS AND MECHANISMS OF ACTION

EDITED BY: Khamis Youssef, Antonio Ippolito and Sergio Ruffo Roberto
PUBLISHED IN: Frontiers in Microbiology

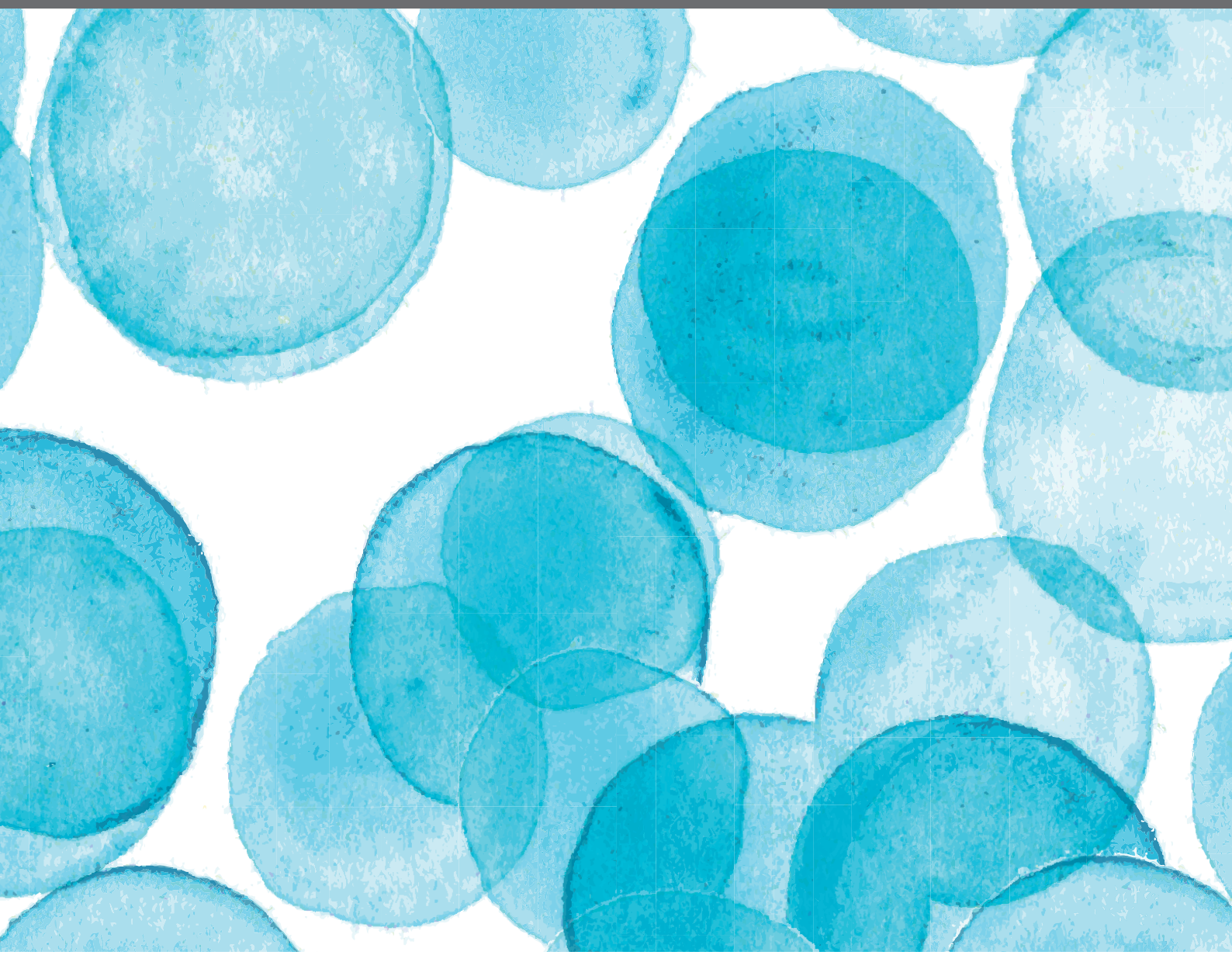

frontiers Research Topics

frontiers

ISSN 1664-8714
ISBN 978-2-88976-093-0
DOI 10.3389/978-2-88976-093-0

About Frontiers

Frontiers is more than just an open-access publisher of scholarly articles: it is a pioneering approach to the world of academia, radically improving the way scholarly research is managed. The grand vision of Frontiers is a world where all people have an equal opportunity to seek, share and generate knowledge. Frontiers provides immediate and permanent online open access to all its publications, but this alone is not enough to realize our grand goals.

Frontiers Journal Series

The Frontiers Journal Series is a multi-tier and interdisciplinary set of open-access, online journals, promising a paradigm shift from the current review, selection and dissemination processes in academic publishing. All Frontiers journals are driven by researchers for researchers; therefore, they constitute a service to the scholarly community. At the same time, the Frontiers Journal Series operates on a revolutionary invention, the tiered publishing system, initially addressing specific communities of scholars, and gradually climbing up to broader public understanding, thus serving the interests of the lay society, too.

Dedication to Quality

Each Frontiers article is a landmark of the highest quality, thanks to genuinely collaborative interactions between authors and review editors, who include some of the world's best academicians. Research must be certified by peers before entering a stream of knowledge that may eventually reach the public - and shape society; therefore, Frontiers only applies the most rigorous and unbiased reviews.
Frontiers revolutionizes research publishing by freely delivering the most outstanding research, evaluated with no bias from both the academic and social point of view. By applying the most advanced information technologies, Frontiers is catapulting scholarly publishing into a new generation.

What are Frontiers Research Topics?

Frontiers Research Topics are very popular trademarks of the Frontiers Journals Series: they are collections of at least ten articles, all centered on a particular subject. With their unique mix of varied contributions from Original Research to Review Articles, Frontiers Research Topics unify the most influential researchers, the latest key findings and historical advances in a hot research area! Find out more on how to host your own Frontiers Research Topic or contribute to one as an author by contacting the Frontiers Editorial Office: frontiersin.org/about/contact

POSTHARVEST DISEASES OF FRUIT AND VEGETABLE: METHODS AND MECHANISMS OF ACTION

Topic Editors:
Khamis Youssef, Agricultural Research Center (Egypt), Egypt
Antonio Ippolito, University of Bari Aldo Moro, Italy
Sergio Ruffo Roberto, State University of Londrina, Brazil

Citation: Youssef, K., Ippolito, A., Roberto, S. R., eds. (2022). Postharvest Diseases of Fruit and Vegetable: Methods and Mechanisms of Action. Lausanne: Frontiers Media SA. doi: 10.3389/978-2-88976-093-0

Table of Contents

frontiers | Frontiers in Microbiology

EDITORIAL
published: 13 April 2022
doi: 10.3389/fmicb.2022.900060

Editorial: Post-harvest Diseases of Fruit and Vegetable: Methods and Mechanisms of Action

Khamis Youssef[1,2]*, *Antonio Ippolito*[3]* and *Sergio Ruffo Roberto*[4]*

[1] Agricultural Research Center, Plant Pathology Research Institute, Giza, Egypt, [2] Agricultural and Food Research Council, Academy of Scientific Research and Technology (ASRT), Cairo, Egypt, [3] Department of Soil, Plant and Food Science, University of Bari Aldo Moro, Bari, Italy, [4] Agricultural Research Center, State University of Londrina, Londrina, Brazil

Keywords: shelf-life, fruit, post-harvest pathology, vegetables, fungi

Editorial on the Research Topic

Post-harvest Diseases of Fruit and Vegetable: Methods and Mechanisms of Action

INTRODUCTION

Post-harvest losses of fruit and vegetables are very high and sometimes reach 50% and more in some developing countries due to pathological and physiological deterioration (Smilanick et al., 2006). This loss is due to inappropriate handling and lack of right methods and means to prevent diseases. Fruits and vegetables are susceptible to severe losses caused by several plant pathogenic fungi including *Botrytis cinerea, Alternaria alternata, Penicillium italicum, P. digitatum, P. expansum, Monilia fructicola, M. laxa, Colletotrichum gloeosporioides, Rhizopus stolonifer, Botryiodiplodia theobromae etc.,* after harvest. Chemical fungicides are the primary means to control such diseases. However, several constrains have limited their use including fungicide resistance, market pressure regarding residues and concerns of environmental and human health (Hashim et al., 2019). In this context, safe alternative means to control post-harvest diseases of fruits and vegetables are needed to be developed (Lachhab et al., 2015; Salem et al., 2016). Several investigations have documented the strong antimicrobial activity of various alternatives including biological control using antagonistic microorganisms, physical means such as low temperatures, modified and controlled atmospheres, heat, irradiation, and generally regarded as safe (GRAS) substances such as salts, sanitizers, plant extracts, and essential oils. Also, many efforts have been done to understand their mode of action to improve their use, especially at large scale in the field.

The aim of this Research Topic was to present the latest results of controlling post-harvest diseases of fruit and vegetables using new alternative control means and understanding their mechanism of action. Eleven articles were accepted for this Research Topic dealing with table grapes, strawberries, avocados, mangoes, papayas, apples, and pears. In this context, Godana et al. investigated the mechanism by which *Pichia anomala* induced with chitosan (1% w/v) controls blue mold disease in table grapes caused by *Penicillium expansum*. The results of the study showed that chitosan (1% w/v) significantly increased the yeast β-1,3-glucanase, catalase (CAT), and malondialdehyde (MDA) activities. Furthermore, *P. anomala* alone or induced with chitosan significantly increased the table grapes enzymatic activities of Polyphenol oxidase (PPO), phenylalanine ammonia-lyase (PAL), peroxidase (POD), and catalase compared to the control. The RT-qPCR results also confirmed that the genes of these major disease defense enzymes were up-regulated when the table grapes were treated with *P. anomala*.

OPEN ACCESS

Edited and reviewed by:
Aldo Corsetti,
University of Teramo, Italy

***Correspondence:**
Khamis Youssef
youssefeladawy@arc.sci.eg
Antonio Ippolito
antonio.ippolito@uniba.it
Sergio Ruffo Roberto
sroberto@uel.br

Specialty section:
This article was submitted to Food Microbiology, a section of the journal Frontiers in Microbiology

Received: *19 March 2022*
Accepted: *24 March 2022*
Published: *13 April 2022*

Citation:
Youssef K, Ippolito A and Roberto SR (2022) Editorial: Post-harvest Diseases of Fruit and Vegetable: Methods and Mechanisms of Action. Front. Microbiol. 13:900060. doi: 10.3389/fmicb.2022.900060

In China, as Novel Loop-Mediated Isothermal Amplification Detection Methods, Fu et al. isolated two bacterial strains (*Pseudomonas aeruginosa* and *Serratia marcescens*) from rotten post-harvest Fuzi. Two loop-mediated isothermal amplification (LAMP) methods targeting the gyrase B subunit (gyrB) gene of *P. aeruginosa* and the phosphatidylinositol glycan C (pigC) gene of *S. marcescens* were successfully developed, and it was found that the target genes were highly specific to the two pathogens.

Morales-Cedeño et al. evaluated the role of strain SER3 from the recently discovered *Rouxiella badensis* as a biocontrol agent. SER3 was isolated from the phyllosphere of decaying strawberry fruit (*Fragaria* × *ananassa* Duch.) and showed different grades of antagonism against 20 fungal pathogens of berries, based on confrontation assays, due to the action of its diffusible and volatile compounds. A comparison of the genomic properties of *R. badensis* SER3 and other close bacterial relatives showed several genes with potential functions in biocontrol activities, such as those encoding siderophores, non-ribosomal peptide synthetases, and polyketide synthases.

In a scientific collaboration between South Africa, Turkey and Italy Sivakumar et al. developed a comprehensive review on the impact of edible coatings, essential oils, and their nano formulations on post-harvest decay anthracnose of avocados, mangoes, and papayas. The authors summarized and analyzed the recent advances and trends in the use of these alternative post-harvest treatments on anthracnose decay in the mentioned fruit crops.

In apples, Deng et al. verified the use of sodium hydrosulfide against *Penicillium expansum* and it promoted the synthesis of endogenous hydrogen sulfide (H_2S), hydrogen peroxide (H_2O_2), and nitrogen oxide (NO). Sodium hydrosulfide treatment enhanced the activities of phenylalanine ammonia-lyase, cinnamate 4-hydroxylase, p-coumarate:coenzyme A ligase isoenzymes, caffeoyl-CoA-O-methyltransferase, caffeic acid-O-methyltransferase, ferulic acid-5-hydroxylase, cinnamyl-CoA reductase, and cinnamyl-alcohol dehydrogenase. In Belgium, in the same fruit crop, Naets et al. verified that the early activation of the mevalonate pathway in fruits challenged by *Botrytis cinerea* correlated with reduced susceptibility during post-harvest storage. The authors demonstrated a clear transcriptional activation of secondary metabolism and a correlation between the early transcriptional activation of the mevalonate pathway and reduced susceptibility, expressed as a reduction in resulting lesion diameters. Also in apples, Sun, Liu, et al. used *Serratia plymuthica* to suppress apple ring rot on post-harvest apple fruit caused by *Botryosphaeria dothidea*. The treatment significantly reduced the titratable acidity content, enhanced the soluble sugar content, vitamin C, and their ratio, and maintained the firmness of the fruits. In another study on apples, Yuan et al. investigated the role of *Bacillus velezensis* Strain P2-1 as a biocontrol agent against apple post-harvest decay caused by *Botryosphaeria dothidea*. The authors summarized that PCR and qRT-PCR assays revealed that strain P2-1 harbored the gene clusters required for biosynthesis of antifungal lipopeptides and polyketides. Sun, Duan, et al. used dimethyl trisulfide to manage ring rot disease. The authors concluded that soluble sugar, vitamin C, and soluble sugar/titratable acidity ratio of the dimethyl trisulfide-treated fruit were significantly higher as compared to the control. Finally, in apple cv. Fuji, Ackah et al. summarized that chitosan accelerated apple wound healing by activating the phenylpropanoid pathway and stimulating enzymatic browning of wounds.

Some interesting results on "Doyenne du Comice" pear were obtained by Zhang et al. 1-methylcyclopropene was highly effective in reducing disease incidence and induced multiple changes of the fungal and bacterial microbiota. This study was the first comprehensive analysis of the microbiome response to 1-methylcyclopropene in post-harvest pear fruit, and reveals the relationship between fruit decay and microbial composition in pear fruit.

AUTHOR CONTRIBUTIONS

KY, SR, and AI: writing—review and editing. All authors contributed to the article and approved the submitted version.

REFERENCES

Hashim, A. F., Youssef, K., and Abd-Elsalam, K. A. (2019). Ecofriendly nanomaterials for controlling gray mold of table grapes and maintaining postharvest quality. *Euro. J. Plant Pathol.* 154, 377–388. doi: 10.1007/s10658-018-01662-2

Lachhab, N., Sanzani, S. M., Fallanaj, F., Youssef, K., Nigro, F., Boselli, M., et al. (2015). Protein hydrolysates as resistance inducers for controlling green mould of citrus fruit. *Acta Horticult.* 1065, 1593–1598. doi: 10.17660/ActaHortic.2015.1065.203

Salem, E. A., Youssef, K., and Sanzani, S. M. (2016). Evaluation of alternative means to control postharvest Rhizopus rot of peaches. *Sci. Horticult.* 198, 86–90. doi: 10.1016/j.scienta.2015.11.013

Smilanick, J. L., Brown, G. E., and Eckert, J. W. (2006)"The biology and control of postharvest diseases," in *Fresh Citrus Fruits, 2nd edn*, eds W. F. Wardowski, W. M. Miller, D. J. Hall, and W. Grierson (Longboat Key, FL; Florida Science Source Inc.). p. 339–96.

Conflict of Interest: The authors declare that the research was conducted in the absence of any commercial or financial relationships that could be construed as a potential conflict of interest.

frontiers in Microbiology

ORIGINAL RESEARCH
published: 22 July 2021
doi: 10.3389/fmicb.2021.704519

Pichia anomala Induced With Chitosan Triggers Defense Response of Table Grapes Against Post-harvest Blue Mold Disease

*Esa Abiso Godana[1], Qiya Yang[1], Lina Zhao[1], Xiaoyun Zhang[1], Jizhan Liu[2] and Hongyin Zhang[1]**

[1] School of Food and Biological Engineering, Jiangsu University, Zhenjiang, China, [2] School of Agricultural Engineering, Jiangsu University, Zhenjiang, China

To study the mechanism by which *Pichia anomala* induced with chitosan (1% w/v) controls blue mold disease in table grapes caused by *Penicillium expansum*, this study evaluated alterations in three yeast enzymatic activities. The changes in the five primary disease defense-related enzymes and two non-enzyme activities of table grapes were assayed. The results of the study showed that chitosan (1% w/v) significantly increased the yeast β-1,3-glucanase, catalase (CAT), and malondialdehyde (MDA) activities. Furthermore, *P. anomala* alone or induced with chitosan (1% w/v) significantly increased the table grapes enzymatic activities of Polyphenol oxidase (PPO), phenylalanine (PAL), peroxidase (POD), and catalase (CAT) compared to the control. The RT-qPCR results also confirmed that the genes of these major disease defense enzymes were up-regulated when the table grapes were treated with *P. anomala*. The highest results were recorded when the fruit was treated by yeast induced with chitosan (1% w/v). The phenolic compounds, in addition to their nutritional value, can also increase the antimicrobial properties of table grapes. The current experiment determined that the total phenol and flavonoid contents of table grapes showed the highest results for fruits treated by *P. anomala* induced with chitosan compared with the control. Generally, the increment of these fruit enzymatic and non-enzymatic activities shows improved table grape defense against the pathogenic fungus. The induction of the yeast with chitosan also increases its bio-control efficacy against the pathogen. This study will enable future detailed investigation in the yeast pathogen control mechanisms and the use of yeasts as bio-pesticides.

Keywords: grape, post-harvest disease, *Pichia anomala*, *Penicillium expansum*, enzyme activity, total phenol and flavonoid

OPEN ACCESS

Edited by:
Khamis Youssef, Agricultural Research Center, Egypt

Reviewed by:
Kamal A. M. Abo-Elyousr, Assiut University, Egypt
Rachid Lahlali, Ecole Nationale d'Agriculture de Meknès, Morocco

***Correspondence:**
Hongyin Zhang
zhanghongyin126@126.com

Specialty section:
This article was submitted to Food Microbiology, a section of the journal Frontiers in Microbiology

Received: *03 May 2021*
Accepted: *31 May 2021*
Published: *22 July 2021*

Citation:
Godana EA, Yang Q, Zhao L, Zhang X, Liu J and Zhang H (2021) Pichia anomala Induced With Chitosan Triggers Defense Response of Table Grapes Against Post-harvest Blue Mold Disease. Front. Microbiol. 12:704519. doi: 10.3389/fmicb.2021.704519

Abbreviations: CAT, catalase; MDA, malondialdehyde; PPO, Polyphenol oxidase; PAL, phenylalanine; POD, peroxidase.

INTRODUCTION

The United Nations has indicated that for the first time in recent history world hunger is on the rise. It is clear that we are not going to be able to meet the global food shortage crisis by simply producing more food as we did during the "Green Revolution." Even with our most advanced food production technologies, we are going to fall far short of producing enough food to feed the world's increasing population, which is expected to reach 9.6 billion by 2050. To feed this growing population, we must save substantially more food than we currently produce. Until recent years, a disproportionate amount of our resources have been invested in the production of food (95%) while only (5%) has been dedicated to the post-harvest preservation of food. This has left us with tremendous post-harvest "Skill Gaps" and "Technology Gaps" in developing countries.

Of the total food produced for human consumption in the world, one-third is lost or wasted every year. This amounts to an approximate cost of $680 billion in developed countries and around $310 billion in developing countries (Sawicka, 2019). When we compare industrialized and developing countries, a similar amount of food is wasted (670 and 630 million tons, respectively). Of this massive world food loss, fruits and vegetables take the largest share. Generally, post-harvest loss of these perishables is estimated from 40 to 50%. Although there are different causes for post-harvest losses for these perishables, post-harvest diseases are major contributing factors. Therefore, the control of post-harvest diseases could significantly help to reduce this massive food loss after production, providing a sustainable solution to increase food availability, reduce pressure on natural resources, eliminate hunger, and improve farmers' living conditions (Sawicka, 2019).

Due to their physiological nature, table grapes are highly susceptible to post-harvest diseases. *Penicillium expansum* is the primary causal agent of blue mold disease in table grapes (Zoffoli and Latorre, 2011; Sanzani et al., 2013). This destructive pathogen colonizes the fruit surface and causes massive economic loss during storage and shipment (Spadaro and Droby, 2015; Wisniewski et al., 2016). The disease causes light brown skin discoloration initially and ends with soft and wet rot, which quickly colonizes the entire berry (Franck et al., 2005). Blue-green colonies may appear on the fruit's surface, and the decayed fruit has a musty odor (Zoffoli and Latorre, 2011).

Sulfur dioxide (SO_2) is an effective treatment that is used to control the table grapes post-harvest decay during cold storage (Sanzani et al., 2012). The fungicide can control the germination and spread of *P. expansum* on the surface of the grapes (Sanzani et al., 2012). However, the use of SO_2 has some limitations (1) it causes surface bleaching for fresh grapes (de Oliveira et al., 2014), (2) it affects people who have sulfite allergies, and (3) restriction of chemical use in some countries affects grape producers. Therefore, scientists are currently searching for alternative control methods that are safe, effective, and environmentally friendly. Microbial biological control agents are among those getting more attention from researchers in recent years.

Several microorganisms (yeasts, bacteria, and fungi) have been reported for their potential to control post-harvest diseases in fruit and vegetables (Madbouly et al., 2020; Abo-Elyousr et al., 2021). Microorganisms isolated from the surface of fruits have applications due to the high survival rate on surfaces of fruits during treatment. Yeasts that naturally occur on the surface of fruits are useful antagonists for the control of post-harvest diseases. Yeasts are preferred for their ability to survive harsh environmental conditions and because they do not produce mycotoxins and allergies, and survive on a wide range of nutrients (Elisabeth et al., 2002).

The ascomycetous yeast *Pichia anomala* was first reported as having high anti-fungal activity by Boysen et al. (2000). Since then, numerous research on the use of yeast as a potential post-harvest bio-control have been conducted. Our previous research investigated that *P. anomala* has high anti-fungal activity against *P. expansum* in table grapes (Godana et al., 2020). We also determined that the yeast's pre-treatment with chitosan (1% w/v) enhances the yeast's antagonistic efficacy. Zhao et al. (2012) reported that the *P. anomala* (strain FY-102) isolated from the surface of apples has a high antagonistic effect against *Botryitis cinerea*. In addition to the control of post-harvest decay of table grapes, *P. anomala* has an outstanding contribution to the viticulture industry. It contributes positively to the wine aroma by the production of volatile compounds, mainly ethyl acetate. It also helps with early fermentation in the wine industry (Renouf et al., 2007). However, excessive use of *P. anomala* can spoil the wine due to there being too much acetic acid and ethyl acetate production (Plata et al., 2003).

In the last three decades, antagonistic yeast and other biological control agents have gained more attention (Wang et al., 2018). Different biological control agents (BCAs), bioactive compounds, food additives, and the mechanisms involved in biological control have been explored to explicate and develop bio-control products. Therefore, understanding the mechanisms of action of BCAs is imperative to improving viability and increasing their efficacy in disease control (Di Francesco et al., 2016).

Numerous reports show that yeasts have the potential to enhance the enzymatic activities and total phenolic compounds during post-harvest treatment in fruits and vegetables. For example, Mahunu et al. (2016) reported that *Pichia caribbica* with phytic acid can induce the PAL, POD, and CAT in apples which help the fruit to combat the blue mold disease. Other researchers also confirmed the use of yeast alone or in combination can significantly induce the major disease defense-related enzymes and phenolic compounds in post-harvest fruits and vegetables (Li and Tian, 2006; Al-Qurashi and Awad, 2015; Qin et al., 2015; Zhao et al., 2018; Abdelhai et al., 2019; Wang et al., 2019).

Our previous study showed a promising result that *P. anomala* could be an alternative post-harvest treatment instead of chemical fungicides to control post-harvest diseases of table grapes. However, the yeast pathogen control mechanism cannot thoroughly be investigated. Studying the yeast's effect on the fruit physiology, whether it boosts its defense ability is very important for commercializing these antagonistic yeasts in the bio-pesticide market. Therefore, our current study aimed to

understand the yeast control mechanisms, specifically (1) to determine changes in the enzymatic activities of *P. anomala* after being incubated in 1% chitosan (w/v), and (2) to ascertain the metabolic response of the enzymatic and non-enzymatic activities of table grapes after being treated by the yeast *P. anomala* induced with chitosan (1% w/v).

MATERIALS AND METHODS

Grapes

Table grapes (*Vitis vinifera* cv. Red Globe) were harvested from a vineyard located in Zhenjiang, Jiangsu, China. Fruits were taken to the research lab and sorted based on their color, size, ripeness, and free from mechanical damage. The sorted fruits were then surface disinfected with 0.2% (v/v) sodium hypochlorite (Tianjin Kaifeng Chemical Co., Ltd.) for 1 min.

Yeast

P. anomala (strain TL0903) was isolated from soil and preserved in the China General Microbiological Culture Collection Center No. 3616 and used for the experiment. The yeast has been preserved in nutrient yeast dextrose agar (NYDA) at 4°C after receiving from the culture center. The yeast was activated in nutrient yeast dextrose broth (NYDB) media before each experiment and was incubated in the rotary shaker (180 rpm) for 24 h at 28°C. The cells were centrifuged at 8000 × *g* for 6 min and washed three times with sterilized distilled water. The cells then adjusted to the required concentration using a hemocytometer (XB-K-250, Jianling Medical Device Co., Danyang, China).

Chitosan

Chitosan with 90% deacetylation was bought from Sangon Biotech Co., Ltd. (Shanghai, China).

Pathogen

Penicillium expansum was isolated from overripe grapes by our research group according to the method described by Dahiya et al. (2006). After isolation, the fungus was preserved on potato dextrose agar (PDA) media at 4°C. Before each experiment, the fungi were activated, and after 7 days of culture, fresh spore suspension was used. *P. expansum* spores were removed using a bacteriological loop and suspended in sterilized distilled water and thoroughly mixed for 30 min using a vortex. The spore concentration was adjusted to 1×10^5 spores/mL before each experiment.

Changes in Enzymatic Activities of *P. anomala* Induced With Chitosan

To determine the enzymatic activities of β-1,3-glucanase, catalase (CAT), malondialdehyde (MDA), *P. anomala* was cultured in NYDB media alone or NYDB media supplemented with 1% chitosan. The crude enzyme was extracted according to the methods described by Zhao et al. (2012). Briefly, the culture of yeast alone or incubated with chitosan (1% w/v) was washed three times. Then it was ground in liquid nitrogen and transferred to the 50 mL tubes. The CAT activity was determined according to the method described by Wang et al. (2018). Briefly, 10 mL of phosphate buffer and 10% trichloroacetic acid were added to the ground powder to determine the CAT and MDA activities, respectively. Then the crude extract was used for further analysis. To determine the CAT activity, 10 mL cold sodium phosphate buffer was added to 3 mL crude enzyme extract and centrifuged at 10000 × *g* for 5 min. Then, 0.5 ml of the mixture, 2 mL sodium phosphate buffer, and 0.5 mL hydrogen peroxide were used for the analysis. One unit was defined as the decrease in absorbance 240 nm of 0.01 protein in one minute and was expressed as U/mg protein.

The MDA content was determined according to the method described by Mahunu et al. (2016). Briefly, 2 mL of 0.5 thiobarbituric acid (TBA) in 15% trichloroacetic acid was added to a 1.5 mL crude extract. The mixture was then heated for 20 min at 95°C and then cooled in ice for 5 min. Finally, it was centrifuged at 12000 × *g* for 10 min and the absorbance was measure at 532 and 600 nm. The unit was expressed by μmoL/mg protein. The β-1,3-glucanase activity was analyzed according to the method described by Zhao et al. (2012). Briefly, the culture was collected and centrifuged at 7000 × *g* for 10 min at 4°C. Then, the supernatant was collected and filtered using a 0.45 μL filter membrane. Then 250 μL of crude extract was added to 250 μL of 0.2% laminarin (w/v) in potassium acetate buffer (50 mM, pH 5). The mixture was then incubated at 37°C for 1 h. Finally, 3,5 dinitrosalicylate was added, boiled for 5 min and the absorbance was measured at 500 nm. One unit was defined as the formation of 10 mg glucose by hydrolysis of laminarin in one hour, and the unit was expressed as U/mL supernatant. There were three replications in each treatment and each experiment was repeated two times for confirmation.

Analysis of Table Grapes Defense-Related Enzyme Activities After Being Treated by *P. anomala* Induced With Chitosan (1% w/v)

Crude Extraction

To assess the effect of *P. anomala* alone or induced with chitosan (1% w/v) on major disease defense-related enzymatic activities of table grapes, uniform wounds (3 mm deep × 3 mm diameter) were made at the center of each grape berries. Then, (1) 15 μL sterile distilled water, (2) 15 μL of the *P. anomala* suspension (10^8 cell/mL), (3) 15 μL of the *P. anomala* suspension (10^8 cell/mL) pretreated with chitosan (1% w/v) were pipetted into each wound. After 2 h, 15 μL *P. expansum* (1×10^5 spore/mL) was inoculated into each sample. The grapes were then wrapped with plastic film to keep high R.H. (95%) and incubated at 20°C for 3 days. Samples were taken every 24 h for three consecutive days. The wound tissues of five grapes were excised (6 mm deep) using a sterile cork borer. After that, 10 mL of sterile distilled water was added to 3 g of the excised tissue. Then, 50 mM phosphate buffer consisting of polyvinyl pyrrolidone (1%) and 1.33 mM was added to the sample. There were three replications in each treatment and each experiment was repeated two times for confirmation.

Polyphenol Oxidase (PPO) Activity

The PPO activity was determined according to Aquino-Bolaños and Mercado-Silva (2004). The crude enzyme extract (0.1 mL) was added to 2.9 mL sodium phosphate buffer (50 mM, pH 6.4, contains 0.1 mM catechol). Then, the samples were heated in a water bath (30°C) for 5 min. Changes in absorbance at 398 nm were recorded every 30 s for 3 min. The enzyme activity was expressed as unit mg/FW.

Phenylalanine Ammonia-Lyase (PAL) Activity

The PAL activity was determined according to the method used by Zhang et al. (2013). The crude enzyme (1 mL) was added to a 3 mL borate buffer (50 mM, pH 8.8, containing 10 mM phenylalanine). The solution was thoroughly mixed and heated (37°C for 60 min), and the absorbance was recorded at 290 nm. One PAL unit was defined as the formation of 1 μg of cinnamic acid equivalents per hour, and the specific activity was expressed as unit mg/FW.

Peroxidase (POD) Activity

The POD activity was determined according to the method described by Lurie et al. (1997). Crude enzyme extract (0.2 mL) was added to guaiacol 2.2 mL of 0.3% (50 mM sodium phosphate buffer, pH 6.4). The mixture was then incubated at 30°C for 5 min. The POD was measured at 470 nm every 30 s for 3 min. The enzyme activity was expressed as unit mg/FW.

Catalase (CAT) Activity

The CAT activity was determined according to the method described by Wang et al. (2004). In detail, 10 mL cold sodium phosphate buffer (100 mM, pH 7.8) was added to 3.0 ml of the crude enzyme extract. The mixture was then centrifuged at 1000 × *g* for 15 min. After that, 2 mL of sodium phosphate buffer (50 mM, pH 7.0), 0.5 mL enzyme extract, and 0.5 mL H_2O_2 (40 mM) were used to measure the H_2O_2 decomposition at 240 nm absorbance. The CAT enzyme activity was expressed in mg/FW, where one unit of catalase converts one μmol of H_2O_2 per min.

RT-qPCR for Determination of Defense-Related Genes Expression Levels

RNA was extracted from 2 g frozen table grape tissue (stored at −80°C) according to the Spin Column Plant Total RNA Purification Kit (Sangon Biotech, Shanghai, China). Both the purity and quantity were checked using a Spectrophotometer (Thermo Scientific, Fresno, CA, United States) at 260 and 280 nm. The concentration and integrity of RNA were evaluated using the RNA Nano 6000 Assay Kit of the Bioanalyzer 2100 system (Agilent Technologies, Santa Clara, CA, United States). The first-strand cDNA was synthesized from the RNA using the PrimeScript RT reagent kit with gDNA Eraser (Takara-Dalian, China) in PCR System. Specific primers were obtained from Sangon Biotech (Shanghai, China). The RT-qPCR was conducted with Bio-Rad CFX96 Real-Time PCR System (Applied Biosystems, United States) and the computer program set according to Youssef et al. (2020). The RT-qPCR was carried out using T.B. Green® Fast qPCR Mix (TAKARA BIO Inc., Shiga, Japan) and determined in ABI PRISM 7500 Real-Time PCR System (Applied Biosystems, United States) according to the manufacturer's instructions. The melting cycle was 95°C for 15 s, 60°C for 1 min, 95°C for 15 s, and 62°C for 15 s. Relative gene expression levels were calculated according to the method of $2^{-\Delta\Delta CT}$ (Livak and Schmittgen, 2001). The experiment was conducted twice, and there were three replications per treatment.

Non-enzymatic Assays

Sample Preparation

The treatments were prepared according to the procedures described above. Samples were then taken at 0, 24, 48, and 72 h for analysis. The wound tissues of table grapes were excised using a sterile cork borer, and 1.0 g of each sample was prepared in 10 mL of 70% ethanol (v/v). After that, the suspension was shaken in a rotary shaker for 2 h (120 rpm at 30°C). Finally, the extract was centrifuged at 1013 × *g* for 5 min, and the supernatant was reserved for further analysis. The suspension was used to determine the total phenolic compound and flavonoid contents (Vázquez et al., 2008).

Total Phenolic Content

The total phenolic content of table grapes was measured by spectrophotometry method using the Folin-Ciocalteu reagent (Swain and Hillis, 1959). Specifically, 1 mL extract, 9 mL double-distilled water, and 1 mL Folin-Ciocateau were added to a 25 mL volume flask. The mixture was then shaken for 5 min, and 10 mL Na_2CO_3 (7%) were added to the flask. Finally, double distilled water was added to the flask to bring the final volume to 25 mL and incubated for 90 min. Gallic acid at concentrations of 20, 40, 60, 80, and 100 mg/L were used as standard, and the absorption was measured at 750 nm. The results were expressed as mg of gallic acid equivalents (GAE) per 100 g dry weight (DW). The experiment was conducted twice, and there were three replications per treatment.

Total Flavonoid Content

The total flavonoid contents of table grapes were determined, according to Gurnani et al. (2016). Briefly, the reaction medium containing 250 μL of the ethanolic extract, $NaNO_2$ (5% w/v), $AlCl_3$ (10% w/v), and NaOH (4% w/v) was prepared, and absorption was measured at 425 nm against the blank. Quercetin at concentrations of 50, 100, 200, 300, 400, and 500 mg/L were used as standard. The results were expressed as mg quercetin equivalents (QE) per 100 g dry weight (DW). The experiment was conducted twice, and there were three replications per treatment.

Statistical Analysis

All collected data were from a representative experiment and all experiments were repeated at least twice. The Analysis of Variance (ANOVA) was carried out using Minitab Version 17 (Minitab LLC, State College, PA, United States). Tukey's test

was used for mean comparison, and $P < 0.05$ was considered statistically significant.

RESULTS

Changes in Enzymatic Activities of *P. anomala* Induced With Chitosan

The β-1,3-glucanase activity, CAT, and MDA content of *P. anomala* induced with 1% chitosan for 5 days are shown in **Figure 1**. As shown in the figure, the activity of β-1,3-glucanase increased with the storage time. A higher result was recorded for yeast incubated with chitosan as compared to the control. Incubation of *P. anomala* with 1% chitosan also significantly induced the activity of CAT as compared to the control. Even though the initial MDA accumulation of the yeast was the same, it showed significantly lower results for the yeast incubated with 1% chitosan. These results confirm that chitosan (1% w/v) can enhance the bio-control efficacy of *P. anomala*.

Analysis of Table Grapes Defense-Related Enzyme Activities After Being Treated by *P. anomala* Induced With Chitosan (1% w/v)

Polyphenoloxidase (PPO) Activity

The PPO activity of grapes treated with *P. anomala* and *P. anomala* supplemented with chitosan (1% w/v) stored at 20°C is shown in **Figure 2A**. In the first 24 h, there was no significant difference between *P. anomala* alone, and *P. anomala* supplemented with chitosan (1% w/v). However, after 24 h *P. anomala* supplemented with chitosan (1% w/v) showed the highest PPO activity compared to the other two treatments. The control group showed the lowest activity throughout the

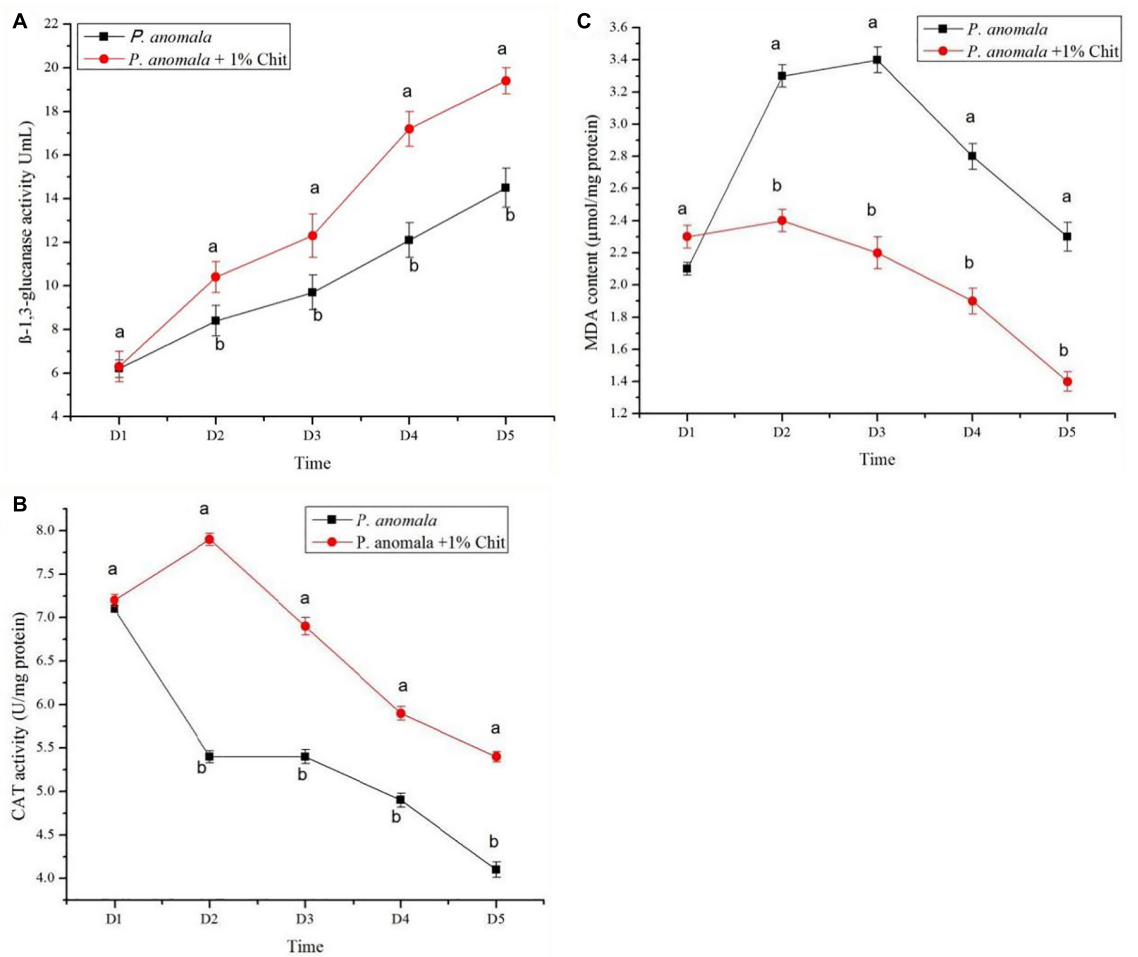

FIGURE 1 | The β-1,3-glucanase activity, CAT, and MDA content of *P. anomala* induced with 1% chitosan for 5 days are shown in Figure. **(A)** The activity of β-1,3-glucanase increased with the storage time. A higher result was recorded for yeast incubated with chitosan as comparedto the control. Incubation of *P. anomala* with 1% chitosan also significantly induced the activity of CAT as comparedto the control **(B)**. Even though the initial MDA accumulationof the yeast was the same, it showed significantly lower results for the yeast incubated with 1% chitosan **(C)**.

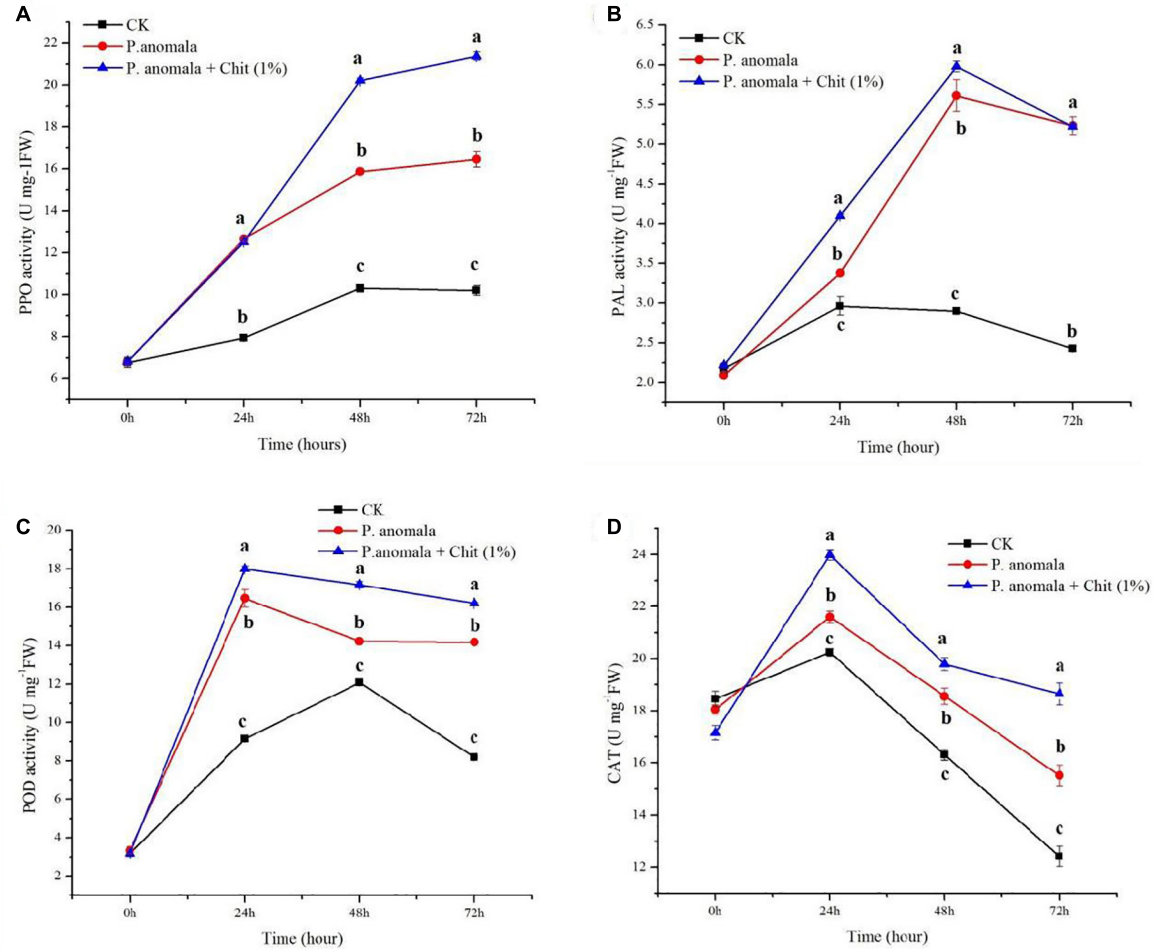

FIGURE 2 | Time course change of disease defense-related enzyme activities in grapes incubated at 20°C and 95% R.H for 3 days **(A)** PPO, **(B)** PAL, **(C)** POD, and **(D)** CAT. Treatments were as follows: **(A)** Control (double distilled water), **(B)** *P. anomala* alone (1×10^8), and **(C)** *P. anomala* enhanced with chitosan (1% w/v). Each treatment was replicated three times, and values with different letters are significantly different according to Tukey's mean comparison ($p < 0.05$) test.

storage period. This showed that the yeast could initiate PPO activity in grapes.

Phenylalanine Ammonia Lyase (PAL) Activity

P. anomala alone and *P. anomala* supplemented with chitosan (1% w/v) induced the PAL activity during the first 2 days of the storage period and decline after decline on day 3 (**Figure 2B**). PAL activity in grapes was highly induced for those treated by *P. anomala* supplemented with chitosan (1% w/v) compared to grapes treated with *P. anomala* alone the first 2 days. However, the PAL activity showed a similar result after 3 days of storage at 20°C. The control group showed the lowest PAL activity throughout the storage period. These suggest that *P. anomala* has a significant effect on inducing PAL activity during post-harvest storage.

Peroxidase (POD) Activity

The POD activity of grapes significantly increased in both treatments than the control during the storage period at 20°C (**Figure 2C**). For grapes treated with *P. anomala* alone and *P. anomala* supplemented with chitosan (1% w/v), the enzyme activity sharply increased on the first storage day and then declined. However, the control group showed an increase in POD activity until 48 h and then sharply declined. The control group showed the lowest enzyme activity, and grapes treated with *P. anomala* were supplemented with chitosan (1% w/v) and showed the highest enzyme activity throughout the storage period.

Catalase (CAT) Activity

The CAT activity of grapes treated with *P. anomala* alone and *P. anomala* supplemented with chitosan (1% w/v) is shown in **Figure 2D**. The CAT activity increased during the first day of storage and started to decline after 24 h of storage. The control group showed the lowest enzyme activity, and grapes treated with *P. anomala* supplemented with chitosan (1% w/v) showed the highest enzyme activity throughout the storage period. After 72 h of storage, the

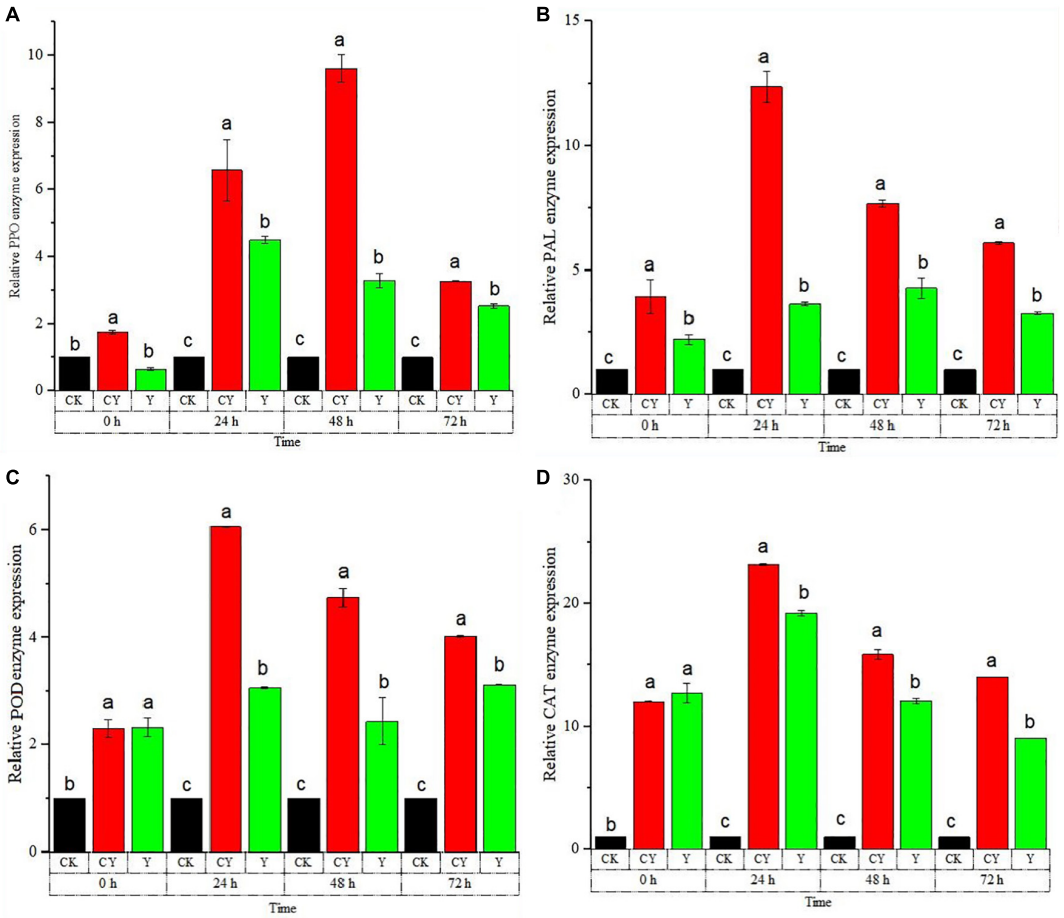

FIGURE 3 | Time course change of defense-related genes expression in table grapes. **(A)** polyphenol oxidase (*PPO*), **(B)** phenylalanine ammonia-lyase (*PAL*), **(C)** peroxidase (POD), and **(D)** catalase (*CAT*) enzymes. The results were obtained using RT-qPCR to determine relative gene expression levels of table grape berries incubated at 20°C from 0 to 72 h. Treatments: CK (Control) (sterile distilled water), CY (yeast incubated in 1% chitosan), and Y (Yeast alone). The results represent the mean of two independent experiments, each treatment with three replicates. Different letters on each bar indicate statistical significance at $p < 0.05$ using Tukey's mean separation test. 0 h means 1 h after the treatments were carried out.

CAT activity of grapes treated with *P. anomala* alone and the control group showed below the initial CAT activity (17 U mg/FW).

Effect *P. anomala* Induced With Chitosan on Defense-Related Enzyme Genes Expression Levels of Table Grapes

The RT-qPCR experiment was conducted to confirm the reliability of the activity of the defense-related enzymes discussed in section "Analysis of Table Grapes Defense-Related Enzyme Activities After Being Treated by *P. anomala* Induced With Chitosan (1% w/v)." The RT-qPCR of the five major defense-related enzymes shown in **Figure 3**. As shown in **Figure 3A**, the PPO enzyme gene expression was highest for table grapes treated with chitosan induced with chitosan (1% w/v) throughout the storage period.

On the second storage day, the highest expression level of PPO was recorded as around 9.45 fold that of the control group. The relative gene expression of the APX enzyme sharply rises the next day soon after storage, where it peaked 48 h after storage. The gene expression then started falling down the next day.

Throughout the storage period, grapes treated with *P. anomala* induced with chitosan showed the highest APX gene expression, which is a confirmatory finding for the previous results. The CHI enzyme gene expression is shown in **Figure 3C**. As shown in the figure, tables grapes treated with *P. anomala* induced with chitosan (1% w/v) showed the highest expression level compared to the yeast alone and the control group. The highest CHI expression was recorded 24 h after storage, which was about 4.05 fold of the control group.

On the third and fourth days, the CHI gene expression of table grapes treated with *P. anomala* was the same as the control group even though it showed a higher result on the second day. PAL enzyme's relative gene expression sharply rises the next day soon after storage, where it reached its peak point on the third day after storage. Throughout the storage period, grapes treated with *P. anomala* induced with chitosan (1% w/v) showed the

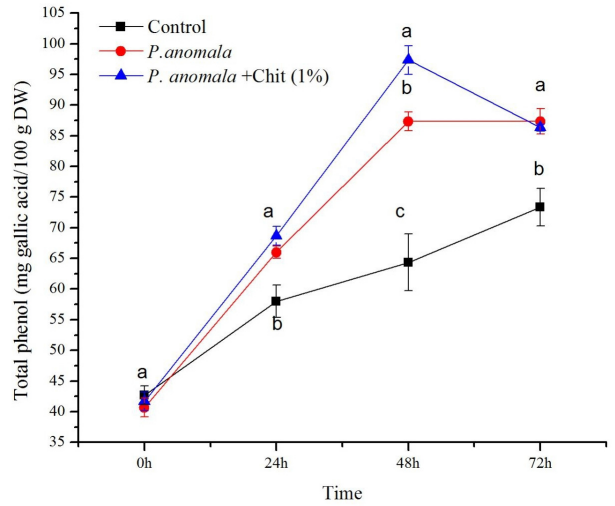

FIGURE 4 | Time course change of phenol content (mg gallic acid equivalents/100 g DW) extracts from table grape stored at 20°C. Treatments: CK (Control) (sterile distilled water), CY (*P. anomala* incubated in 1% chitosan), and Y (*P. anomala* alone). The results represent the mean of two independent experiments, each treatment with three replicates. Different letters on each bar indicate statistical significance at $p < 0.05$ using Tukey's mean separation test. 0 h means 1 h after the treatments were carried out.

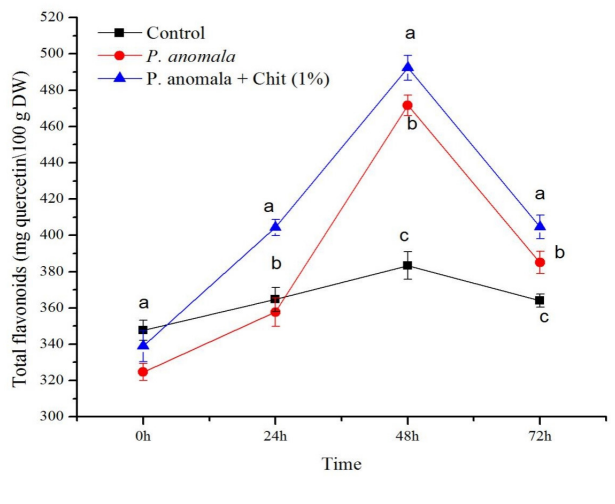

FIGURE 5 | Time course of flavonoid content (mg quercetin equivalents/100 g DW) extracts from table grape stored at 20°C. Treatments: CK (Control) (sterile distilled water), CY (*P. anomala* incubated in 1% chitosan), and Y (*P. anomala* alone). The results represent the mean of two independent experiments, each treatment with three replicates. Different letters on each bar indicate statistical significance at $p < 0.05$ using Tukey's mean separation test. 0 h means 1 h after the treatments were carried out.

highest PAL gene expression, which is a confirmatory finding for the previous results. The CAT enzyme's relative gene expression sharply rose, where it showed the highest results for table grapes treated with *P. anomala* induced with chitosan (1% w/v). The highest result was seen on the third day after storage for table grapes treated with *P. anomala* induced with chitosan, which was about 23.5 fold that of the control group. Throughout the storage period, grapes treated with *P. anomala* induced with chitosan showed the highest CAT gene expression, which is a confirmatory finding for the previous results.

In general, the above defense-related enzyme gene expression levels of table grapes were significantly up-regulated by *P. anomala* induced with chitosan (1% w/v), and the results verified the accuracy of enzyme activity experiments in section "Analysis of Table Grapes Defense-Related Enzyme Activities After Being Treated by *P. anomala* Induced With Chitosan (1% w/v)."

Non-enzymatic Assays

Total Phenolic Content

The total phenolic content of table grapes treated with *P. anomala* or *P. anomala* induced with chitosan (1% w/v) is shown in **Figure 4**. Grapes treated with *P. anomala* induced with chitosan showed the highest total phenolic content (ranged between 41.67 and 97.33 mg of gallic acid equivalents/100 g DW (GAE/100 g DW)) during the storage period. The highest total phenolic content was recorded at 48 h post-treatment, which was more than 1.5 fold than the control group. Grape tissue without any treatment (the control) showed the lowest total phenolic content (ranging between 42.67 and 73.33 GAE/100 g DW) during the storage period.

Total Flavonoid Content (TFC)

The TFC of grape tissues at a different time interval during the storage period is shown in **Figure 5**. Comparing the grape tissues treated with *P. anomala* induced with chitosan (1% w/v) with the control group, the TFC of the tissues treated with the yeast showed the highest (and ranged between 339 and 404.33 mg of quercetin equivalents/100 g DW (QE/100 g DW)) during the storage period. The highest TFC was recorded 48 h post-treatment, which was more than 1.02 fold compared to the control group. Grape tissues without any treatment (the control group) showed the lowest TFC (ranging between 347.67 and 364.67 QE/100 g DW) during the storage period.

DISCUSSION

Our previous research investigated whether chitosan (1% w/v) enhanced the bio-control efficacy of *P. anomala* against *P. expansum* both *in vitro* and *in vivo* (Godana et al., 2020). In the current study, we were interested in the mechanisms by which chitosan improved the bio-control efficacy of *P. anomala* against *P. expansum* in table grapes. The mechanism by which *P. anomala* suppresses the growth of *P. expansum* in the fruit is crucial for replacing the antagonistic yeasts with commercial fungicides.

The current study showed that incubation of *P. anomala* with 1% chitosan significantly increased the enzymatic activities of yeasts such as β-1,3-glucanase and CAT; and reduced the accumulation of MDA. Enzymes such as β-1,3-glucanase were found to increase the antagonistic efficacy of yeasts. In addition, the inducible enzyme degrades the cell wall of pathogens and

leads to cell lysis (Dahiya et al., 2006; Kang, 2012). Incubation of *P. anomala* with chitosan (1% w/v) also induced the CAT enzymatic activity, an enzyme that was determined to enhance the bio-control efficacy of other yeasts as well (Zhao et al., 2018). The CAT was found to be a good detoxification agent when plants are injured and accumulate a large number of reactive oxygen species (ROS) at the wound site, which leads to cell damage (An et al., 2012). The lowering of MDA content also lowers the oxidative damage to the yeast cells. The current result confirmed that the MDA content of the yeast cells incubated with 1% chitosan is lower compared to the control which improves the yeast bio-control performance.

When plants are attacked by pathogens, they enhance their defense mechanism through a broad spectrum of methods. Among them, the production of phenolic compounds, phytoalexins, and pathogenesis-related (PR) proteins helps to prevent pathogen invasion (Bowles, 1990). Pathogenesis-related proteins are disease defense enzymes that help control the rate of disease spread during infection (Deborah et al., 2001; Kumari and Vengadaramana, 2017). PAL, PPO, POD, and CAT are among the four crucial disease defense enzymes, and their activities are positively correlated with fruit disease resistance (Qin et al., 2015; Zhang et al., 2016; Youssef et al., 2020).

PPO can produce antimicrobial phenolic substances by the metabolism of phenols and oxidizing phenolic compounds into toxic quinones (Qin et al., 2015). Thus, it has a vital role in host plant defense mechanisms. Mahunu et al. (2016) reported that the increase in PPO activity reduced apples' blue mold disease. The current research also confirms that the use of *P. anomala* induced with chitosan significantly increased the PPO activity of table grapes, which significantly contribute to reduce the blue mold disease of table grapes caused by *P. expansum*.

PAL is a key and rate-limiting enzyme during the shikimic acid pathway in the phenolic metabolism during plant disease resistance. It plays a crucial role during lignin synthesis and accumulation. PAL is also actively involved in salicylic acid's biosynthesis, a hormone required for plant defense (Qin et al., 2015). PAL is responsible for the biosynthesis of p-coumaric acid derivatives, phytoalexin, and lignins that contribute to plant defense systems (Qin et al., 2003). In addition, it participates in the biosynthesis of the defense hormone salicylic acid, which is required for both local and systemic acquired resistance in plants (Dixon and Paiva, 1995).

Thus, the activity of PAL has a positive correlation with plant disease resistance. Our study investigated that the treatment of table grapes with *P. anomala* induced with chitosan (1% w/v) increased PAL activity. This shows that the antagonistic yeast suppresses the fungal growth by up-regulating the fruit disease defense enzymes and direct parasitism. Li and Tian (2006) also reported that the antagonistic yeast *Cryptococcus laurentii* up-regulated the PAL activity in the apple, which controlled the blue mold disease of the fruit.

Stimulation of ROS makes plant tissues vulnerable to fungal attack. POD and CAT are the main protective enzymes against ROS in plant tissues. POD is also noted to control the balance of H_2O_2 in the fruit's cell wall, which is essential for the cross-linking of phenolic compounds in response to several external stress factors such as injuries, pathogen attack, and environmental stress (Passardi et al., 2004). In our study, the treatment of grapes with *P. anomala* induced with chitosan (1% w/v) significantly increased both POD and CAT activity.

The RT-qPCR enables the reliable detection and measurement of the five main disease defense enzymes (PPO, PAL, POD, CHI, and CAT). Our study confirmed that treating table grapes with the yeast *P. anomala* alone or enhanced with chitosan up-regulated these enzymes. These further confirm that *P. anomala* alone or induced with chitosan (1% w/v) activate the defense mechanism of table grapes, up-regulate the expression of defense genes, and synthesize many other corresponding defense enzymes, thus improving the defense ability of table grapes against diseases.

Phenolic compounds are among the most important secondary metabolites that act as antioxidants in table grapes. They can strongly affect berry quality (color, flavor, astringency, and bitterness) and functional properties (Chamkha et al., 2003). Phenolic compounds can also increase the antimicrobial properties of table grapes (Champa et al., 2015). Raimbault et al. (2010) reported that higher enzymatic activity in pineapples leads to higher phenolic compound concentration during post-harvest storage. The availability of hydrogen peroxide, which is majorly affected by the POD enzyme, also affects the phenolic groups' cross-linking response to different external stresses (Passardi et al., 2004). In the current study, table grapes treated with *P. anomala* induced with chitosan showed the highest POD activity and highest total phenolic compound concentration, which supports previous studies by other researchers, which contribute to the fruit post-harvest shelf and help to mitigate both biotic and abiotic stresses during post-harvest storage. Al-Qurashi and Awad (2015) stated that table grapes' post-harvest treatment with 1% chitosan could increase the total phenolics and flavonoid level and increase POD activity. Higher accumulation of phenolic compounds in the fruit may also occur because of an increment of PAL enzyme when plants are exposed to biotic and abiotic stress such as high temperature, fungi, bacterial, and virus infections (Solecka and Kacperska, 2003).

Flavonoids are polyphenolic secondary metabolites that play different roles in many physiological activities, acting as phytoalexins and phytoanticipins in plant defense pathogens (Desta et al., 2016). In addition to their antimicrobial characteristics, flavonoids help our health during consumption and can reduce the risk of cancer, neurodegenerative diseases, heart disease, inflammation, aging, arthritis, and diabetes (Kumar and Pandey, 2013). The current study also confirms that post-harvest treatment of table grapes with *P. anomala* induced with chitosan can significantly increase the accumulation of total flavonoids in the fruit, which has a significant role, enabling the fruit to combat post-harvest diseases and other biotic and abiotic stresses.

CONCLUSION

Post-harvest treatment of table grapes with the antagonistic yeast *P. anom*aly alone or induced with chitosan (1% w/v) enhance the content and activities of PPO, POD, PAL, CAT, total phenol,

and flavonoid compounds. These findings contribute to knowledge of the mechanisms by which the antagonistic yeast enhances resistance against blue mold disease in table grapes. From the current study, it can be concluded that the yeast *P. anomala* enhanced with chitosan induced host resistance, which is directly related to enhancing the antioxidant system. This study will further enable future detailed investigation in the yeast pathogen control mechanisms to use yeasts as bio-pesticides.

DATA AVAILABILITY STATEMENT

The original contributions presented in the study are included in the article/supplementary material, further inquiries can be directed to the corresponding author.

AUTHOR CONTRIBUTIONS

EG: writing – original draft, methodology, data curation, and formal analysis. QY, XZ, and LZ: resources, supervision, validation, and visualization. HZ: funding acquisition, project administration, supervision, validation, writing – review, and editing. JL: methodology, writing – review, and editing. All authors contributed to the article and approved the submitted version.

FUNDING

This work was supported by the National Natural Science Foundation of China (32072276, 31901743, and 31971795).

REFERENCES

Abdelhai, M. H., Awad, F. N., Yang, Q., Mahunu, G. K., Godana, E. A., and Zhang, H. (2019). Enhancement the biocontrol efficacy of *Sporidiobolus pararoseus* Y16 against apple blue mold decay by glycine betaine and its mechanism. *Biol. Control.* 139:104079. doi: 10.1016/j.biocontrol.2019.104079

Abo-Elyousr, K. A. M., Al-Qurashi, A. D., and Almasoudi, N. M. (2021). Evaluation of the synergy between *Schwanniomyces vanrijiae* and propolis in the control of *Penicillium digitatum* on lemons. *Egypt. J. Biol. Pest Control* 31:66. doi: 10.1186/s41938-021-00415-4

Al-Qurashi, A. D., and Awad, M. A. (2015). Postharvest chitosan treatment affects quality, antioxidant capacity, antioxidant compounds and enzymes activities of 'El-Bayadi' table grapes after storage. *Sci. Hortic.* 197, 392–398. doi: 10.1016/j.scienta.2015.09.060

An, B., Li, B., Qin, G., and Tian, S. (2012). Exogenous calcium improves viability of biocontrol yeasts under heat stress by reducing ROS accumulation and oxidative damage of cellular protein. *Curr. Microbiol.* 65, 122–127. doi: 10.1007/s00284-012-0133-4

Aquino-Bolaños, E. N., and Mercado-Silva, E. (2004). Effects of polyphenol oxidase and per oxidase activity, phenolics and lignin content on the browning of cut jicama. *Postharvest Biol. Technol.* 33, 275–283. doi: 10.1016/j.postharvbio.2004.03.009

Bowles, D. J. (1990). Defense-related proteins in higher plants. *Annu. Rev. Biochem.* 59, 873–907. doi: 10.1146/annurev.bi.59.070190.004301

Boysen, M. E., Stina, B., and Johan, S. (2000). Effect of the biocontrol yeast *Pichia anomala* on interactions between *Penicillium roqueforti*, *Penicillium carneum*, and *Penicillium paneum* in moist grain under restricted air supply. *Postharvest Biol. Technol.* 19, 173–179. doi: 10.1016/S0925-5214(00)00086-7

Chamkha, M., Cathala, B., Cheynier, V., and Douillard, R. (2003). Phenolic Composition of Champagnes from Chardonnay and Pinot Noir Vintages. *J. Agric. Food Chem.* 51, 3179–3184. doi: 10.1021/jf021105j

Champa, W. A. H., Gill, M. I. S., Mahajan, B. V. C., and Arora, N. K. (2015). Preharvest salicylic acid treatments to improve quality and postharvest life of table grapes (*Vitis vinifera L.*) cv. Flame Seedless. *J. Food Sci. Technol.* 52, 3607–3616. doi: 10.1007/s13197-014-1422-7

Dahiya, N., Tewari, R., and Hoondal, G. S. (2006). Biotechnological aspects of chitinolytic enzymes: a review. *Appl. Microbiol. Biotechnol.* 71, 773–782. doi: 10.1007/s00253-005-0183-7

de Oliveira, V. C. E., Magnani, M., de Sales, C. V., Lima de Souza Pontes, A., Campos -Takaki, G. M., Montenegro Stamford, T. C., et al. (2014). Effects of post -harvest treatment using chitosan from *Mucor circinelloides* on fungal pathogenicity and quality of table grapes during storage. *Food Microbiol.* 44, 211–219. doi: 10.1016/j.fm.2014.06.007

Deborah, S. D., Palaniswami, A., Vidhyasekaran, P., and Velazhahan, R. (2001). Time-course study of the induction of defense enzymes, phenolics and lignin in rice in response to infection by pathogen and non-pathogen. *J. Plant Dis. Prot.* 108, 204–216.

Desta, K. T., Shin, S. C., Shim, J. H., Kim, G. S., Shin, H. C., and El-Aty, A. M. A. (2016). Flavonoid variations in pathogen-infected plants. *Front. Nat. Prod. Chem.* 2, 393–439. doi: 10.2174/9781681083599116020009

Di Francesco, A., Martini, C., and Mari, M. (2016). Biological control of postharvest diseases by microbial antagonists: how many mechanisms of action? *Eur. J. Plant Pathol.* 145, 711–717. doi: 10.1007/s10658-016-0867-0

Dixon, R. A., and Paiva, N. L. (1995). Stress-induced phenylpropanoid metabolism. *Plant Cell* 7, 1085–1097. doi: 10.2307/3870059

Elisabeth, F., Ulrika, D., Marianne, E. B., Karl-Johan, L., and Johan, S. (2002). Physiological characteristics of the biocontrol yeast *Pichia anomala* J121. *FEMS Yeast Res.* 2, 395–402. doi: 10.1016/S1567-1356(02)00098-3

Franck, J., Latorre, B. A., Torres, R., and Zoffoli, J. P. (2005). The effect of preharvest fungicide and postharvest sulfur dioxide use on postharvest decay of table grapes caused by *Penicillium expansum*. *Postharvest Biol. Technol.* 37, 20–30. doi: 10.1016/j.postharvbio.2005.02.011

Godana, E. A., Yang, Q., Wang, K., Zhang, H., Zhang, X., Zhao, L., et al. (2020). Bio-control activity of *Pichia anomala* supplemented with chitosan against *Penicillium expansum* in postharvest grapes and its possible inhibition mechanism. *LWT Food Sci. Technol.* 124:109188. doi: 10.1016/j.lwt.2020.109188

Gurnani, N., Gupta, M., Mehta, D., and Mehta, B. K. (2016). Chemical composition, total phenolic and flavonoid contents, and in vitro antimicrobial and antioxidant activities of crude extracts from red chilli seeds (*Capsicum frutescens L.*). *J. Taibah Univ. Sci.* 10, 462–470. doi: 10.1016/j.jtusci.2015.06.011

Madbouly, A., Abo Elyousr, K. A. M., and Mohamed Ismail, I. (2020). Biocontrol of *Monilinia fructigena,* causal agent of brown rot of apple fruit, by using endophytic yeasts. *Biol. Control* 144:104239. doi: 10.1016/j.biocontrol.2020.104239

Kang, T. (2012). Biological control of postharvest diseases of fruits and vegetables by microbial antagonists. *J. Nanjing Agric. Univ.* 40, 411–441. doi: 10.1146/annurev.phyto.40.120401.130158

Kumar, S., and Pandey, A. K. (2013). Chemistry and Biological Activities of Flavonoids: an Overview. *Sci. World J.* 2013:162750. doi: 10.1155/2013/162750

Kumari, Y. S., and Vengadaramana, A. (2017). Stimulation of Defense Enzymes in Tomato (*Solanum lycopersicum L.)* and Chilli (*Capsicum annuum L.*) in Response to Exogenous Application of Different Chemical Elicitors. *Univers. J. Plant Sci.* 5, 10–15. doi: 10.13189/ujps.2017.050102

Li, B., and Tian, S. (2006). Effects of trehalose on stress tolerance and biocontrol efficacy of *Cryptococcus laurentii*. *J. Appl. Microbiol.* 100, 854–861. doi: 10.1111/j.1365-2672.2006.02852.x

Livak, K. J., and Schmittgen, T. D. (2001). Analysis of Relative Gene Expression Data Using Real- Time Quantitative PCR and the $2^{-\Delta\Delta CT}$ Method. *Methods* 25, 402–408. doi: 10.1006/meth.2001.1262

Lurie, S., Fallik, E., Handros, A., and Shapira, R. (1997). The possible involvement of peroxidase in resistance to *Botrytis cinerea* in heat treated tomato fruit. *Physiol. Mol. Plant Pathol.* 50, 141–149. doi: 10.1006/pmpp.1996.0074

Mahunu, G. K., Zhang, H., Yang, Q., Zhang, X., Li, D., and Zhou, L. (2016). Improving the biocontrol efficacy of *Pichia caribbica* with phytic acid against postharvest blue mold and natural decay in apples. *Biol. Control.* 92, 172–180. doi: 10.1016/j.biocontrol.2015.10.012

Passardi, F., Penel, C., and Dunand, C. (2004). Performing the paradoxical: how plant peroxidases modify the cell wall. *Trends Plant Sci.* 9, 534–540. doi: 10.1016/j.tplants.2004.09.002

Plata, C., Millan, C., Mauricio, J. C., and Ortega, J. M. (2003). Formation of ethyl acetate and isoamyl acetate by various species of wine yeasts. *Food Microbiol.* 20, 217–224. doi: 10.1016/S0740-0020(02)00101-6

Qin, G. Z., Tian, S. P., Xu, Y., and Wan, Y. L. (2003). Enhancement of biocontrol efficacy of antagonistic yeasts by salicylic acid in sweet cherry fruit. *Physiol. Mol. Plant Pathol.* 62, 147–154. doi: 10.1016/S0885-5765(03)00046-8

Qin, X., Xiao, H., Xue, C., Yu, Z., Yang, R., Cai, Z., et al. (2015). Biocontrol of Gray Mold in Grapes with the Yeast *Hanseniaspora uvarum* alone and in Combination with Salicylic Acid or Sodium Bicarbonate. *Postharvest Biol. Technol.* 100, 160–167. doi: 10.1016/j.postharvbio.2014.09.010

Raimbault, A. K., Marie-Alphonsine, P. A., Horry, J. P., Francois-Haugrin, M., Romuald, K., and Soler, A. (2010). Polyphenol oxidase and peroxidase expression in four pineapple varieties (*Ananas comosus L.*) after a chilling injury. *J. Agric. Food Chem.* 59, 342–348. doi: 10.1021/jf102511z

Renouf, V., Claisse, O., and Lonvaud-Funel, A. (2007). Inventory and monitoring of wine microbial consortia. *Appl. Microbiol. Biotechnol.* 75, 149–164. doi: 10.1007/s00253-006-0798-3

Sanzani, S. M., Montemurro, C., Di Rienzo, V., Solfrizzo, M., and Ippolito, A. (2013). Genetic structure and natural variation associated with host of origin in *Penicillium expansum* strains causing blue mould. *Int. J. Food Microbiol.* 165, 111–120. doi: 10.1016/j.ijfoodmicro.2013.04.024

Sanzani, S. M., Reverberi, M., Punelli, M., Ippolito, A., and Fanelli, C. (2012). Study on the role of patulin on pathogenicity and virulence of *Penicillium expansum*. *Int. J. Food Microbiol.* 153, 323–331. doi: 10.1016/j.ijfoodmicro.2011.11.021

Sawicka, B. (2019). "Post-harvest Losses of Agricultural Produce," in *Zero Hunger, Encyclopedia of the UN Sustainable Development Goals*, eds W. Leal Filho, A. Azul, L. Brandli, P. Özuyar, and T. Wall (Cham: Springer). doi: 10.1007/978-3-319-69626-3_40-1

Solecka, D., and Kacperska, A. (2003). Phenylpropanoid deficiency affects the course of plant acclimation to cold. *Physiol. Plant.* 119, 253–262. doi: 10.1034/j.1399-3054.2003.00181.x

Spadaro, D., and Droby, S. (2015). Unraveling the mechanisms used by antagonistic yeast to control postharvest pathogens on fruit. *Acta Hortic.* 1144, 63–70. doi: 10.17660/actahortic.2016.1144.9

Swain, T., and Hillis, W. E. (1959). The phenolic constituents of *Prunus domestica*. I. - The quantitative analysis of phenolic constituents. *J. Sci. Food Agric.* 10, 63–68. doi: 10.1002/jsfa.2740100110

Vázquez, G., Fontenla, E., Santos, J., Freire, M. S., González-Álvarez, J., and Antorrena, G. (2008). Antioxidant activity and phenolic content of chestnut (*Castanea sativa*) shell and eucalyptus (*Eucalyptus globulus*) bark extracts. *Ind Crops Prod.* 28, 279–285. doi: 10.1016/j.indcrop.2008.03.003

Wang, M., Zhao, L., Zhang, X., Dhanasekaran, S., Abdelhai, M. H., Yang, Q., et al. (2019). Study on biocontrol of postharvest decay of table grapes caused by *Penicillium rubens* and the possible resistance mechanisms by *Yarrowia lipolytica*. *Biol. Control* 130, 110–117. doi: 10.1016/j.biocontrol.2018.11.004

Wang, Y., Li, Y., Xu, W., Zheng, X., Zhang, X., Abdelhai, M. H., et al. (2018). Exploring the effect of β-glucan on the biocontrol activity of *Cryptococcus podzolicus* against postharvest decay of apples and the possible mechanisms involved. *Biol. Control* 121, 14–22. doi: 10.1016/j.biocontrol.2018.02.001

Wang, Y. S., Tian, S. P., Xu, Y., Qin, G. Z., and Yao, H. (2004). Changes in the activities of proand anti-oxidant enzymes in peach fruit inoculated with *Cryptococcus laurentii* or *Penicillium expansum* at 0 or 20 °C. *Postharvest Biol. Technol.* 34, 21–28. doi: 10.1016/j.postharvbio.2004.04.003

Wisniewski, M., Droby, S., Norelli, J., Liu, J., and Schena, L. (2016). Alternative management technologies for postharvest disease control: the journey from simplicity to complexity. *Postharvest Biol. Technol.* 122, 3–10. doi: 10.1016/j.postharvbio.2016.05.012

Youssef, K., Roberto, S. R., Tiepo, A. N., Constantino, L. V., de Resende, J. T. V., and Abo-Elyousr, K. A. M. (2020). Salt Solution Treatments Trigger Antioxidant Defense Response against Gray Mold Disease in Table Grapes. *J. Fungi* 6: 179. doi: 10.3390/jof6030179

Zhang, C., Chen, K., and Wang, G. (2013). Combination of the biocontrol yeast *Cryptococcus laurenti*i with UV-C treatment for control of postharvest diseases of tomato fruit. *Biocontrol* 58, 269–281. doi: 10.3390/toxins9020066

Zhang, X., Li, Y., Wang, H., Gu, X., Zheng, X., Wang, Y., et al. (2016). Screening and Identification of Novel Ochratoxin A-Producing Fungi from Grapes. *Toxins* 8:333. doi: 10.3390/toxins8110333

Zhao, L., Sun, Y., Yang, D., Li, J., Gu, X., Zhang, X., et al. (2018). Effects of *Sporidiobolus pararoseus* Y16 on postharvest blue mold decay and the defense response of apples. *J. Food Qual.* 2018, 1–9. doi: 10.1155/2018/6731762

Zhao, Z., Zhang, H., Li, J., Cui, J., Zhang, X., and Ren, X. (2012). Enhancement of biocontrol efficacy of *Pichia carribbica* to postharvest diseases of strawberries by addition of trehalose to the growth medium. *Int. J. Mol. Sci.* 13, 3916–3932. doi: 10.3390/ijms13033916

Zoffoli, J. P., and Latorre, B. A. (2011). "Table grape (*Vitis vinifera* L.)," in *Postharvest Biology and Technology of Tropical and Subtropical Fruits: Cocona to Mango*, ed. E. M. Yahia (Oxford: Woodhead Publishing), 179–214. doi: 10.1533/9780857092885.179

Conflict of Interest: The authors declare that the research was conducted in the absence of any commercial or financial relationships that could be construed as a potential conflict of interest.

frontiers in Microbiology

REVIEW
published: 30 July 2021
doi: 10.3389/fmicb.2021.711092

A Comprehensive Review on the Impact of Edible Coatings, Essential Oils, and Their Nano Formulations on Postharvest Decay Anthracnose of Avocados, Mangoes, and Papayas

Dharini Sivakumar[1], Nurdan Tuna Gunes[2] and Gianfranco Romanazzi[3]*

[1] Phytochemical Food Network, Department of Crop Sciences, Tshwane University of Technology, Pretoria, South Africa, [2] Department of Horticulture, Faculty of Agriculture, Ankara University, Ankara, Turkey, [3] Department of Agricultural, Food and Environmental Sciences, Marche Polytechnic University, Ancona, Italy

OPEN ACCESS

Edited by:
Khamis Youssef, Agricultural Research Center, Egypt

Reviewed by:
Asgar Ali, University of Nottingham Malaysia Campus, Malaysia
Mohamed A. Mohamed, Agricultural Research Center, Egypt

***Correspondence:**
Dharini Sivakumar
SivakumarD@tut.ac.za

Specialty section:
This article was submitted to Food Microbiology, a section of the journal Frontiers in Microbiology

Received: *17 May 2021*
Accepted: *07 July 2021*
Published: *30 July 2021*

Citation:
Sivakumar D, Tuna Gunes N and Romanazzi G (2021) A Comprehensive Review on the Impact of Edible Coatings, Essential Oils, and Their Nano Formulations on Postharvest Decay Anthracnose of Avocados, Mangoes, and Papayas. Front. Microbiol. 12:711092. doi: 10.3389/fmicb.2021.711092

Subtropical fruit such as avocados (*Persea americana*), mangoes (*Mangifera indica* L.), and papayas (*Carica papaya* L.) are economically important in international trade and predominantly exported to European destinations. These fruits are highly consumed due to their health benefits. However, due to long-distance shipping and the time required to reach the retail department stores, postharvest losses, due to postharvest decay occurring during the supply chain, affect the fruit quality on arrival at the long-distance distribution points. Currently, the use of synthetic fungicide, Prochloraz®, is used at the packing line to reduce postharvest decay and retain the overall quality of mangoes and avocados. Due to the ban imposed on the use of synthetic fungicides on fresh fruit, several studies have focused on the development of alternative technologies to retain the overall quality during marketing. Among the developed alternative technologies for commercial adoption is the use of edible coatings, such as chitosan biocontrol agents and essential oil vapors. The objective of this review is to summarize and analyze the recent advances and trends in the use of these alternative postharvest treatments on anthracnose decay in avocados, mangoes, and papayas.

Keywords: chitosan, edible coatings, essential oil vapors, latent infections, biocontrol agents

INTRODUCTION

Avocados are an economically important fruit crop in South Africa, Israel, the United States, Mexico, Peru, Chile, Kenya, and Australia. Papayas and mangoes from Latin American countries, especially from Brazil, are exported in large volumes to the EU. The demand for avocado fruit is rapidly increasing in the last few years due to its global recognition as a "superfruit," based on nutritional facts and health benefits. The projection for the world avocado market by 2026 was to obtain an overall value of US$21.56 billion (Transparency Market Research Report, 2021).

Consumption of avocados has increased in countries; the United States, and the EU and Latin American countries together totaled 1,323,000 tons in 2019 (Transparency Market Research Report, 2021). In 2019, the world export of papayas and mangoes was 2,575,002 and 364,030 tons, which fetched US$3,552,922 and US$295,628,000, respectively (FAOSTAT, 2021).

The export of fruits to the long-distance markets is via refrigerated sea shipment. The entire marketing time frame includes approximately 30 days until it reaches the consumers. During transport, due to cold storage and shelf life at the retail outlet, fruits develop postharvest decay caused by anthracnose (*Colletotrichum gloeosporioides* Penz and Sacc), which is the most common postharvest fungal disease in avocados (Sanders et al., 2000), mangoes (Lima J. R. et al., 2013), and papayas (Dickman, 1994). *C. gloeosporioides* infects the fruit via direct penetration, remains quiescent, and causes latent infections (Swinburne, 1983; Siddiqui and Ali, 2014). The latency was broken when the fruit reaches the climacteric peak (Swinburne, 1983). In the ripe fruit, anthracnose symptoms manifest as sunken, dark-brown to black decay lesions; and in the presence of high humidity, prominent pinkish-orange spore masses appear on the lesions (Nelson, 2008). Fruits infected by postharvest fungal pathogens cause decay symptoms, thus affecting the fruit quality, which negatively affects the market value. *C. gloeosporioides* reportedly infects at an immature stage of the fruit and lives quiescently (Beno-Moualem and Prusky, 2000). Postharvest loss of papayas was reportedly 30–50% due to anthracnose (Bautista-Baños et al., 2013). Avocadoes, mangoes, and papayas are climacteric fruits. Changes occurring during fruit ripening, and ethylene emission activate the infection process, which negatively affects their quality, shelf life, and market value. The previous review written by Sivakumar and Bautista-Baños (2014) highlighted the need for a natural novel fungicide to replace the synthetic fungicide application at the postharvest stage due to higher levels of pesticide residues in the edible portion of the fruit, pathogens developing resistance to fungicides, and the influence of fungicides on environmental footprint. However, still, the synthetic non-systemic fungicide Prochloraz® {*N*-propyl-*N*-[2-(2,4,6-trichlorophenoxy) ethyl]-1*H*-imidazole-1-carboxamide} is applied at the packing line to control anthracnose decay in avocadoes, mangoes, and papayas (Swart et al., 2009; Henriod et al., 2016; Shimshoni et al., 2020). Although the exporting countries comply with the main trade regulations and the food safety requirements, the banning of Prochloraz® fungicide will occur in 2022 due to its hazardous toxicological properties. The major metabolite of 2,4,6-trichlorophenol has been listed as a human carcinogen (Group B2) by the US Environmental Protection Agency (EPA) (Shimshoni et al., 2020; EPA, 2021). The "Farm to Fork Strategy" plays a major role in the European Green Deal set out to reduce reliance on pesticides, increasing organic farming and providing sustainable diets to benefit consumers' health, which subsequently will help in reducing the medical care costs for treasury funds (EU COM, 2020).

Thus, investigations on numerous alternative postharvest treatments to control decay during the supply chain are ongoing to replace the application of Prochloraz® fungicide at the postharvest stage. Furthermore, chloride-based sanitizers used in the packing line can produce carcinogenic compounds such as chloramines, dichloramines, and trichloromethanes, which have hazardous effects (Schoeny, 2010). The chemicals used in alternative treatments must have minimum toxicological effects on humans, domestic animals, and the environment and must fall under the category of generally recognized as safe (GRAS) by the US Food and Drug Administration (US FDA) and the European Food Safety Authority (EFSA). In addition, the alternative postharvest treatments must also be able to trigger induced defense mechanism of the host (fruit) via its eliciting properties and antimicrobial properties without compromising the fruit quality (Romanazzi et al., 2016). Considering the above, this review summarizes and analyzes the recent advances and trends in the use of these alternative postharvest treatments on the control of anthracnose caused by *C. gloeosporioides* in subtropical climacteric fruits during marketing based on published research articles from 2014 to date.

EDIBLE COATINGS AND ADDITIVES

Chitosan, a biodegradable compound, is a polymeric compound of *N*-acetylglucosamine units joined by *b*-1,4-glycosidic links. Its production is by the deacetylation of chitin through the alkaline hydrolysis process of acetamide groups using NaOH or KOH (3.7%) at a temperature of 71°C (Gómez-Ríos et al., 2017). The chitosan was registered in the EU as a basic substance for plant protection use (Reg. EU 662014/563), especially in the application for organic agriculture and integrated pest management. Romanazzi et al. (2018) highlighted the contribution of chitosan in the management of postharvest decay of fresh fruit and vegetables due to its antimicrobial, eliciting, and film-forming activities. Rajestary et al. (2021) ran meta-analyses in which it were summarized as clear antimicrobial activity and decay control, while eliciting activity was often clarified and varied among the different studies for time and involved compounds. Romanazzi et al. (2018) showed a list of some of the available chitosan-based commercial products in countries such as Germany, the United States, the United Kingdom, Chile, New Zealand, Italy, Thailand, Poland, and China. Factors such as molecular weight of chitosan formulation, its concentration, method of application, and storage temperature of the fruit affect the efficacy of chitosan application on control of fruit decay (Velázquez-Del Valle et al., 2012). Marques et al. (2016) reported that chitosan, at concentrations of 1.0, 1.5, and 2.0%, inhibited the mycelial growth of *C. gloeosporioides* by 75, 86, and 90%, respectively; and at higher concentrations, 2.5 and 3.0%, showed a fungicidal effect by resulting in changes in conidial morphology. Marques et al. (2016) further reported that chitosan at concentrations of 1.5 and 2.0% completely arrested the germ tube formation and the germination process in *C. gloeosporioides*. Controlling the mycelial growth and the germination of *C. gloeosporioides* by chitosan demonstrates its fungicide potential. The electrostatic forces between its amino-protonated (NH^{2+}) groups and negative residues on cell surfaces of *C. gloeosporioides* (pathogen) were responsible for

the observed antifungal activity facilitated by chitosan (Elsabee and Abdou, 2013; Aloui et al., 2014). Commercial chitosan application (ChitoPlant®) at 1.5%, the formulation that dissolves in water, decreased anthracnose rot in avocados during a storage period of 28 days and after 5 days at marketing simulation conditions (Obianom et al., 2019). The mode of mechanism was attributed to the upregulation of phenylalanine ammonia-lyase, downregulation of lipoxygenase genes, and moderate retention of epicatechin content (90 mg kg^{-1} FW) in the skin probably due to delayed ripening and ethylene emission that had reduced the anthracnose decay (Obianom et al., 2019). Control of stem-end rot decay in commercial chitosan-coated (ChitoPlant® 1.5%) fruit was due to the upregulation of chitinase genes and higher superoxide dismutase activity (Obianom et al., 2019). Moreover, the non-toxic and antimicrobial properties and biodegradable nature of chitosan made it the most important natural biopolymer material for agriculture biotechnology. Conversely, avocados coated with carboxyl methylcellulose (1%) containing 2% of moringa leaf extract controlled the anthracnose decay by inhibiting the mycelial growth of *C. gloeosporioides* and maintaining the overall quality and shelf life of the fruits during marketing (Tesfay et al., 2017). Moringa leaf extract incorporated into carboxymethyl cellulose, exposed to gaseous ozone (O_3) treatments for 36 h and thereafter, stored at 10°C and 95% relative humidity (RH) for 21 days, extended the shelf life, and maintained the fruit quality of mangoes fruit ('Keitt') by reducing the decay (Bambalele et al., 2021). Avocado 'Maluma Hass' fruit treated with 1% carboxyl methylcellulose + 10% moringa extract maintained the postharvest quality of fruit stored for 3 weeks at 5.5°C and at the simulated retail shelf conditions for an additional 1 week (Kubheka et al., 2021). Fruits coated with edible coatings form a semi-permeable layer around the fruit and create a modified atmosphere (Ali et al., 2014), and this modifies the internal atmosphere of the fruit, which helped to reduce the decay incidence and severity as compared with the control fruits (Garcia and Davidov-Pardo, 2021). Modified atmospheres created by the coating around the fruit could have reduced the pH (lower) of the skin, which is unfavorable to decay-causing *C. gloeosporioides* (Yakoby et al., 2000). Ali et al. (2014) recommended the use of the ethanolic extract of propolis (1.5%) and gum arabic (10%) as a biofungicide for the control of anthracnose in papayas. In addition, the edible coatings reduce the rate of respiration, moisture loss, senescence, and weight loss due to the semi-permeable modified atmosphere layer on the fruit surface (Ali et al., 2014). **Table 1** summarizes the recent advances on edible coating and additives applied for subtropical fruits avocadoes and mangoes.

NANOMATERIAL ANTIFUNGAL PROPERTIES

Nanoparticles are considered effective fungicides to control fungal pathogens in crops due to their distinctive physical and chemical properties, which do not relate to their bulk properties (De la Rosa-García et al., 2018). The antifungal effects of the nanoparticles are due to the alternation of physicochemical properties (optical, catalytic, and electronic properties) associated with size (De la Rosa-García et al., 2018). Nanoparticles of zinc oxide (ZnO) were evaluated against *C. gloeosporioides* obtained from papayas and avocadoes (De la Rosa-García et al., 2018). ZnO nanoparticles inhibited the fungal growth of *C. gloeosporioides in vitro* by causing structural deformation by vacuolar expansion, swelling, and melanization in the spores and mycelia (De la Rosa-García et al., 2018). The mode of action of ZnO nanoparticles is due to the production of reactive oxygen species (ROS) in water suspensions (Applerot et al., 2010). ZnO is listed as GRAS by the US FDA (21CFR182.8991) (FDA, 2021). However, further toxicological studies on the migration of nanoparticles into the fruit and toxicological studies are required to ensure that fruits coated with nanoparticle formulations are safe for consumption.

NANOMATERIALS AND NANO-CHITOSAN COATING

Research on the incorporation of nanosized edible coatings, such as chitosan, with natural antimicrobials, such as essential oils, to improve fruit health, safety, and shelf life has become popular during the past 5 years. Nanosized chitosan particles are non-toxic, biodegradable, highly permeable through the biological membranes, and cost-effective and have a wide spectrum of antifungal activities, therefore regarded as a suitable natural agent for control of postharvest decay (Meena et al., 2020).

Chitosan coating with silver nanoparticle (chitosan-AgNP), having the size distribution from 10 to 15 nm, significantly inhibited the conidial germination and inhibited the anthracnose decay significantly in mango fruits. Incorporating the silver nanoparticle to chitosan formulation aided in the binding interaction and stabilization by helping the dispersion of the chitosan-AgNP composites in the formulation during application to improve the efficacy (Chowdappa et al., 2014).

However, the EU does not permit food products or packaging that possesses silver nanoparticles (AgNPs) without any authorization. Allowable limits, based on the EFSA (EFSA, 2011), must not exceed 0.05 mg L^{-1} in water and 0.05 mg kg^{-1} in food. This emphasizes that the testing for antimicrobial effectiveness should comply with the current regulations. Furthermore, incorporations of antimicrobials, such as essential oils, in edible coatings or films are commercially adoptable due to the cost-effectiveness of low volumes of essential oils, effective diffusion efficiency, and prolonged antimicrobial activity during marketing.

Within essential oils, the US FDA Regulatory Agency (FDA, 2021) considers thyme oil (TO) as GRAS. Nanostructured edible coatings based on chitosan (3%)–thyme essential oil (5%) nanoparticles showed a synergetic effect on the control of anthracnose in avocadoes (cv. Hass) by arresting the growth of *C. gloeosporioides* (Correa-Pacheco et al., 2017). The drawback of this study was that there was no comparison of the efficacy of the antifungal activity of chitosan nanoparticles-essential oil coating with the currently used commercial Prochloraz® fungicide, and it was not tested on the avocado cultivar Fuerte, which is

TABLE 1 | Recent advances on edible coating and additives applied for subtropical fruits avocado and mangoes.

Edible coatings	Findings and mode of action	References
Chitosan at concentrations 2.5 and 3.0%	Higher concentrations 2.5 and 3.0% showed fungicidal effect by resulting in changes in conidial morphology of *C. gloeosporioides*	Marques et al., 2016
Commercial chitosan application (ChitoPlant®) at 1.5% concentration	Up-regulation of phenylalanine ammonia-lyase and down-regulation of lipoxygenase genes and moderate retention of epicatechin content in avocados ('Hass')	Obianom et al., 2019
Carboxyl methylcellulose (1%) containing 2% ethanolic moringa leaf extract	Mycelial growth of *C. gloeosporioides*	Tesfay et al., 2017
Carboxyl methylcellulose (1%) containing 2% ethanolic moringa leaf extract, exposed to (O_3) before storage	Reduced the fruit decay and improved fruit quality of mango ('Keitt'). Exact mechanism not known	Bambalele et al., 2021
1% carboxyl methylcellulose + 10% moringa extract	Reduced the fruit decay and improved fruit quality of avocado Maluma Hass. Probably due to modification of the internal atmosphere causing the maintenance of a lower pH of the skin, which is unfavorable to *C. gloeosporioides* (Yakoby et al., 2000)	Yakoby et al., 2000; Garcia and Davidov-Pardo, 2021; Kubheka et al., 2021

highly susceptible to anthracnose decay. In addition, nano or microencapsulation of essential oils prevents the degradation of the active compounds and their stability during unfavorable environmental conditions, such as heat, oxygen, light, pressure, moisture, and pH (Majeed et al., 2015).

The efficacy of the chitosan nanoparticles-essential oil coating also depends on the release rate and migration of active components of essential oils from the edible coating matrix. Additional investigations are required on the influence of incorporation of chitosan nano formulation-TO on fruit quality by measuring the gas exchange barrier, water vapor transmission, tensile and transparent properties of the coatings, internal and external fruit quality, and organoleptic characteristics (Flores-López et al., 2016). Chitosan nanoparticle-essential oil coatings can affect the ripening pattern, flesh color, weight loss, fruit firmness, and degradation of phenolic compounds and antioxidant property of the subtropical fruits avocadoes, papayas, and mangoes. Furthermore, the inclusion of essential oils inside of chitosan nanoparticles helps in releasing and reducing the active compounds (Mohammadi et al., 2015).

In addition, chitosan nanomaterials contain functionalizing agents, such as Cu, Zn, and salicylic acid (SA), which were added to improve the upregulation of antioxidant-defense enzymes in the plant cells, regulate the plant cellular homeostasis, and provide protection against diseases (Saharan et al., 2015; Kumaraswamy et al., 2019). The Cu–chitosan nanoparticles were tested for postharvest application (Meena et al., 2020). The mode of action was due to induced protonation of amino groups of chitosan because of acidic pH that released Cu ions from chitosan nanostructures to perform the antifungal activity. The Cu^{2+} ions showed an antifungal activity by improving the production of highly reactive hydroxyl radicals that eventually harm the biomolecules of the fungal cells (Meena et al., 2020). Chitosan/nano-silica coating enhanced the activities of antioxidant enzymes (superoxide dismutase, catalase, and ascorbate peroxidase) and reduced the generation of superoxide anion (O^{2-}) and hydrogen peroxide (H_2O_2) (Song et al., 2016). Nitric oxide-releasing chitosan nanoparticles also reduced ethylene production and ROS and increased the antioxidant enzyme activity and antioxidant capacity in fruits (Ma et al., 2019).

Biopolymer chitosan is a suitable alternative to synthetic polymeric materials due to its biodegradable nature and negative impact on the environment. Chitosan and TiO_2 nanocomposite films maintained the quality of climacteric fruit by photodegradation of ethylene activity in the presence of UV light, which caused delayed fruit ripening (Kaewklin et al., 2018). Furthermore, a combination of 3% $CaCl_2$ and nano-chitosan improved the antioxidant capacity by improving the hydroxyl radical (•OH) scavenging capacity and possibly could have acted as "signalling compounds" triggering the increase in antioxidant activities (enzymatic and non-enzymatic) in tissues (Jin et al., 2012; Nguyen et al., 2020). **Table 2** summarizes the recent developments in nanomaterial antifungal properties.

ESSENTIAL OILS

Most essential oils are under the category of GRAS by the US FDA (FDA, 2021). Nanoemulsions of orange essential oil (*Citrus sinensis*) and xoconostle (*Opuntia oligacantha*) extract controlled anthracnose, increased the retention of fruit firmness in avocados, and improved the antioxidant activity due to the signaling effect of the active compounds of essential oils (Cenobio-Galindo et al., 2019). Furthermore, basil oil incorporated with beeswax coating increased shelf life and reduced anthracnose development in mango cv. Willard (Karunanayake et al., 2020). Rosemary pepper and Noni essential oils effectively controlled the *C. gloeosporioides* isolated from the papaya fruit (Dias et al., 2020). Noni essential oils totally inhibited conidial germination at 3,000 ppm, while rosemary pepper inhibited conidial germination at 5,000 ppm. The inhibition of mycelial growth of *C. gloeosporioides* occurred at 4,000- and 6,000-ppm concentrations with Noni and rosemary pepper essential oils (Dias et al., 2020). Savory oil with the active chemical compound carvacrol (71.2%) completely controlled the mycelial growth of *C. gloeosporioides* obtained

TABLE 2 | Summary of recent developments in nano materials antifungal properties.

Nano materials	Findings and mode of action	References
Nanoparticles of zinc oxide (ZnO)	Production of oxygen species (ROS) in water suspensions. Structural deformation by vacuolar expansion, swelling, and melanization in the spores and mycelia of *C. gloeosporioides*	Applerot et al., 2010; De la Rosa-García et al., 2018
Chitosan coating with silver nanoparticle (AgNP)	Incorporation of silver nanoparticle to chitosan formulation helped in binding interaction and stabilization to help dispersion of the chitosan-AgNP composites in the formulation improve the efficacy. Inhibited the conidial germination	Chowdappa et al., 2014
Chitosan-thyme essential oil nanoparticles	Chitosan nanoparticles at 3% and thyme oil at 5% showed fungicidal effect and reduced the anthracnose decay fruit cv. Hass	Correa-Pacheco et al., 2017
Cu–chitosan nanoparticles	The Cu^{2+} ions showed antifungal activity by improving the production of highly reactive hydroxyl radicals that eventually harm the biomolecules of the fungal cells	Meena et al., 2020
Chitosan/nano-silica coating	Enhanced the activities of antioxidant enzymes (superoxide dismutase, catalase, and ascorbate peroxidase) and reduced the generation of superoxide anion (O^{2-}) and hydrogen peroxide (H_2O_2)	Song et al., 2016
Nitric oxide-releasing chitosan nanoparticles	Reduced the ethylene production, reactive oxygen species, and increased the antioxidant enzyme activity and antioxidant capacity in fruits	Ma et al., 2019
Chitosan and TiO_2 nanocomposite films	Maintained the quality of climacteric fruit by photodegradation of ethylene activity in presence of UV light, which caused delayed fruit ripening	Kaewklin et al., 2018
Combination of 3% $CaCl_2$ and nano-chitosan	Chitosan improved the antioxidant capacity by improving the hydroxyl radical (•OH) scavenging capacity, and possibly could have acted as "signaling compounds" triggering the increase in increases in antioxidant activities (enzymatic and non-enzymatic) in tissues	Nguyen et al., 2020; Jin et al., 2017
Nano emulsions of orange essential oil (*Citrus sinensis*) and Xoconostle (*Opuntia oligacantha*) extract	Improved the antioxidant activity due to the signaling effect of active compounds of essential oils	Cenobio-Galindo et al., 2019

from the papaya fruit (Sarkosh et al., 2018). *C. gloeosporioides* isolated from mangoes was effectively controlled by thymol-based essential oil (Chillet et al., 2018). Essential oils also cause structural and functional damage in the microbial cell by affecting the membrane permeability, causing leakage of cellular constituents, and dissipating the H^+ and K^+ ion gradients (Sarkosh et al., 2018).

Obianom and Sivakumar (2018) illustrated that the incorporation of 0.1% (v/v) TO in half-strength Prochloraz® (reduced concentration) completely reduced the anthracnose rot in avocado cv. Fuerte. The incorporation of TO had induced the activity of defense enzymes and resulted in decay reduction (Obianom and Sivakumar, 2018). The growers prefer the TO application in the aqueous phase, as it is easy to implement on the packing line.

Spray-dried TO microencapsulated with modified starch/agave fructan microcapsules, 0.10 and 0.20 g filled in nylon bags (4 × 4 cm) (antifungal sachets), controlled the mycelial growth of *C. gloeosporioides* and reduced the anthracnose incidence in mangoes during storage in boxes, which were sealed with parafilm for 9 days at 20 ± 2°C (Esquivel-Chávez et al., 2021). Active components of TO together triggered the induced defense mechanism by upregulation of phenylalanine ammonia-lyase, chitinase, and β-1,3-glucanase enzymes in the fruit and exocarp while downregulating the lipoxygenase enzymes, which helped to retain a moderately higher concentration of epicatechin on the exocarp and delayed the fruit ripening (Bill et al., 2017). Furthermore, *C. gloeosporioides* isolated from the papaya fruit ('Sekaki') exposed to lemongrass oil vapor at a concentration of 28 μL L^{-1} containing geranial (45.6%) and neral (34.3%) as the major components for 18 h and stored for 9 days controlled the anthracnose decay due to fungicidal properties (Ali et al., 2015). **Table 3** summarizes the recent developments in application of essential oils volatile components on the control of postharvest decay in avocado, mango and papaya. In addition, the starch film incorporated with carvacrol (750 mg L^{-1}) and thymol (750 mg L^{-1}) in the starch film showed complete inhibition of *C. gloeosporioides* (*in vitro*) (Ochoa-Velasco et al., 2021). The synergetic effect of the chemical constituents of essential oil components is due to the increased phenolic compounds in the molecule structure and could have facilitated the binding of these compounds to the proteins, preferably the cell membrane of the pathogens, which could have facilitated the membrane disintegration and loss of cellular content (Ochoa-Velasco et al., 2021). Furthermore, an antimicrobial transparent flexible trilayer low-density polyethylene (LDPE) film containing organically modified layered double hydroxides (OLDHs) and plant bioactive TOTO showed a remarkable reduction in anthracnose disease events in Hass cultivar (Kesavan Pillai et al., 2020). The barrier and antifungal properties of nanocomposite film helped to release the volatile bioactive release in a controlled manner; thus, the synergistic effect of LDPE–OLDH–TO nanocomposite film can act as a prospective strategy to control anthracnose disease in avocados with modification of headspace gas composition (Kesavan Pillai et al., 2020).

TABLE 3 | Summary of recent developments in essential oils and incorporation of essential oils into wax or films on antifungal properties against *C. gloeosporioides*.

Essential oils	Findings and mode of action	References
Nano emulsions of orange essential oil (*Citrus sinensis*) and xoconostle *(Opuntia oligacantha)* extract	Controlled anthracnose, increased the retention of fruit firmness in avocados, and improved the antioxidant activity due to the signaling effect of the active compounds of essential oils.	Cenobio-Galindo et al., 2019
Basil oil incorporated with beeswax coating	Increased shelf life and reduced anthracnose development in mango cv. 'Willard.'	Karunanayake et al., 2020
Rosemary pepper and Noni essential oils	Controlled the *C. gloeosporioides* isolated from papaya fruit by inhibiting the conidial germination.	Dias et al., 2020
Savory oil with active chemical compound carvacrol (71.2%)	Controlled the mycelial growth of *C. gloeosporioides* obtained from papaya fruit. Essential oils caused structural and functional damage in the microbial cell by affecting the membrane permeability, causing leakage of cellular constituents, and dissipating the H^+ and K^+ ion gradients.	Sarkosh et al., 2018
Incorporation of 0.1% (v/v) thyme oil in half-strength Prochloraz® (reduced concentration)	Completely reduced the anthracnose rot in avocado cv. 'Fuerte.' The incorporation of thyme oil had induced the activity of defense enzymes and resulted in decay reduction.	Obianom and Sivakumar, 2018
Spray-dried thyme oil microencapsulated with modified starch/agave fructan microcapsules, 0.10 and 0.20 g filled in nylon bags (4 × 4 cm) (antifungal sachets)	Controlled the mycelial growth of *C. gloeosporioides* and reduced the anthracnose incidence in mangoes. Active components of thyme oil together triggered the induced defense mechanism; upregulation of phenylalanine ammonia-lyase, chitinase, and β-1,3-glucanase enzymes in the fruit and exocarp, while downregulating the lipoxygenase enzymes, moderately higher concentration of epicatechin on the exocarp; delayed fruit ripening.	Bill et al., 2017; Esquivel-Chávez et al., 2021
C. gloeosporioides isolated from papaya fruit ('Sekaki') exposed to lemon grass oil vapor at concentration of 28 $\mu g\ L^{-1}$ containing geranial (45.6%) and neral (34.3%) as the major components for 18 h and stored for 9 days	Controlled the anthracnose decay due to fungicidal properties.	Ali et al., 2015
Starch film incorporated with carvacrol (750 mg L−1) and thymol (750 mg L−1)	Inhibition of *C. gloeosporioides* (*in vitro*). The synergetic effect of the chemical constituents of essential oil components; due to the increased phenolic compounds in the molecule structure; membrane disintegration and loss of cellular content.	Ochoa-Velasco et al., 2021
Flexible trilayer low density polyethylene (LDPE) film containing organically modified layered double hydroxides (OLDH) and plant bioactive thyme oil (TO)	Reduction in anthracnose disease events in 'Hass' cultivar. The barrier and antifungal properties of nanocomposite film helped to release the volatile bioactive release in a controlled manner.	Kesavan Pillai et al., 2020

BIOCONTROL

The use of biocontrol agents is for the managing of postharvest decay of fruit as an alternative treatment to synthetic fungicides. The ideal antagonist should be able to survive adverse environmental conditions, should use an affordable growth substrate for mass production, should not infect the host plant, or should not produce metabolites that are toxic for consumers; it must be resistant to the commonly used pesticides and well suited with other chemical and physical postharvest treatments (Wilson and Wisniewski, 1989). The efficiency of biocontrol products could be improved during an integrated control strategy to reduce fungicide input (Govender et al., 2005). Biocontrol products, Biosave-100 and Biosave-110, were commercially used as a postharvest treatment especially for apples: Bio-Save [biocontrol agent (b.a) *Pseudomonas syringae*], Boni Protect (b.a *Aureobasidium pullulans*), Candifruit (b.a *Candida sake*), Nexy (b.a *Candida oleophila*), Pantovital (b.a *Pantoea agglomerans*), Shemer (b.a *Metschnikowia fructicola*), and Yield Plus (b.a i. *Cryptococcus albidus*) (Sharma et al., 2009; Spadaro and Droby, 2016; Janisiewicz and Jurick, 2017). However, commercial biocontrol products are limited to the control of anthracnose decay in avocados. Biocontrol agent *Debaryomyces nepalensis* completely controlled the anthracnose decay in mangoes at 1×10^7 cells mL^{-1} concentration at 15°C for 30 and 40 days (Konsue et al., 2020). Postharvest treatment with *D. nepalensis* reduced the anthracnose decay by delaying the ripening and senesce of the fruit caused due to an increase in cell membrane permeability and less lipid peroxidation (malondialdehyde content) than the control during storage (Konsue et al., 2020). The yeast, *Torulaspora indica* DMKU-RP31, controlled the controlling anthracnose and stem-end rot in mango fruits, and the volatiles produced by the yeast strain were responsible for the antifungal property (Konsue et al., 2020). Furthermore, dipping of the mangoes in *Metschnikowia pulcherrima* suspension (1.0×10^8 cfu mL^{-1}), SA solution (50 mg L^{-1}), or calcium chloride ($CaCl_2$) solution (1.0 g L^{-1}) reduced the anthracnose symptoms in fruit by inducing the defense-related enzymes phenylalanine ammonia-lyase, chitinase, and β-1,3-glucanase compared with the control treatment (Tian et al., 2018). Yeast *Meyerozyma caribbica* in sodium alginate coating controlled the anthracnose (*C. gloeosporioides* Pa14) in avocado

TABLE 4 | Summary of recent developments in biocontrol agent with antifungal properties against *Colletotrichum gloeosporioides* infecting mango and avocados.

Biocontrol agents	Findings	Mode of action	References
Yeast, *Torulaspora indica* DMKU-RP31	Controlled anthracnose *in* mango fruits	Antifungal volatiles but the components of volatiles not detected	Konsue et al., 2020
Combination of *Metschnikowia pulcherrima* suspension in, salicylic acid (SA) solution (50 mg L^{-1}), or calcium chloride ($CaCl_2$) solution (1 g L^{-1})	Reduced the anthracnose symptoms in the mango fruit	Inducing the defense-related enzymes phenylalanine ammonia-lyase, chitinase, and β-1,3-glucanase	Tian et al., 2018
Meyerozyma caribbica in sodium alginate coating	Controlled the anthracnose (*C. gloeosporioides* Pa14) in avocado fruit	Sodium alginate coating helped as a matrix to trap the yeast and the volatile compounds 1-butanol, 3-methyl- and phenethyl alcohol, and ethyl acetate to arrest the invasion of the pathogen	Iñiguez-Moreno et al., 2020
Cell free supernatant of *Bacillus atrophaeus* strain B5 harbors	Inhibited the mycelial growth and conidial germination of *C. gloeosporioides in vitro* and also reduced severity and incidence of anthracnose disease on avocado fruit	Expressed the biosynthesis of antibiotics mainly surfactin, bacillomycin, and iturin and probably could have shown antifungal activities against *C. gloeosporioides*	Guardado-Valdivia et al., 2018
Marine yeast *Debaryomyces hansenii* 1R11CB strain and marine bacteria *Stenotrophomonas rhizophila* KM02 strain	Reduced the decay incidence in mango ('Ataulfo')	Antagonists competing for nutrients such as glucose, sucrose, and fructose, colonizing the hyphae of *Colletotrichum* hyphae	Hernandez Montiel et al., 2017
Wickerhamomyces anomalus	Reduced the anthracnose incidence in avocado fruit	Mycoparasitism with *C. gloeosporioides* hyphae	Lima N. B. et al., 2013; Campos-Martínez et al., 2016

fruit (Iñiguez-Moreno et al., 2020). The sodium alginate coating helped as a matrix to trap the yeast and the volatile compounds, especially 1-butanol, 3-methyl- and phenethyl alcohol, and ethyl acetate, to arrest the invasion of the pathogen (Iñiguez-Moreno et al., 2020). The alcohols cause destruction of plasma membrane due to accelerated degeneration of protein molecules that eventually affect the metabolism and cell lysis (McDonnell and Russell, 1999). With ripening, the yeast population increased on the fruit surface and provided residual protection against anthracnose (Iñiguez-Moreno et al., 2020). Besides, *M. caribbica* also showed the mode of action due to competition for nutrients, biofilm development, and production of β-1,3-glucanase and chitinase enzymes (Iñiguez-Moreno et al., 2020).

Furthermore, cell-free supernatant of *Bacillus atrophaeus* strain B5 inhibited the mycelial growth and conidial germination of *C. gloeosporioides in vitro* and reduced the severity and incidence of anthracnose disease on avocado fruit. *B. atrophaeus* strain B5 harbors a gene that expressed the biosynthesis of antibiotics, mainly surfactin, bacillomycin, and iturin, which probably could have shown antifungal activities against *C. gloeosporioides* (Guardado-Valdivia et al., 2018). Inhibition of spore germination is vital to control the inoculum load at an early stage of decay development. The lipopeptides fengycins and iturins showed a higher antifungal activity than surfactin (Ongena and Jacques, 2008; Meena and Kanwar, 2015). Some lipopeptides (surfactin and other cyclic lipopeptides) were shown to elicit induced systemic resistance (ISR) in the host (Ongena and Jacques, 2008; Raaijmakers et al., 2010; Gond et al., 2015). Since the biocontrol agents do not fall under the category of GRAS compounds, the metabolites in the cell-free supernatants can be of great interest for the control of postharvest decay in avocado, mango, or papaya fruits (Guardado-Valdivia et al., 2018).

Marine yeast *Debaryomyces hansenii* 1R11CB strain and marine bacteria *Stenotrophomonas rhizophila* KM02 strain were identified as the suitable antagonistic agents to anthracnose (*C. gloeosporioides*) in mangoes ('Ataulfo') and reduced the decay incidence to 56 and 89%, respectively (Hernandez Montiel et al., 2017). The authors suggest that the possible mechanisms could be (i) antagonists competing for nutrients such as glucose, sucrose, and fructose with *C. gloeosporioides* due to their rapid growth rate, which affects the infection process of the pathogen by colonizing the hyphae of *Colletotrichum*; or (ii) by secreting chitinase to degrade β-glucan, mannoprotein, and chitin, respectively, of the cell wall components of *C. gloeosporioides* (Vero et al., 2013; Liu et al., 2016); or (iii) by inducing the host defense mechanism by triggering the antioxidants, peroxidase, catalase, and superoxide dismutase and of disease-defense enzyme phenylalanine ammonia-lyase, chitinase, and β-1,3-glucanase indirectly and preventing the entry of *C. gloeosporioides* (Wei et al., 2016; Wu et al., 2019). Furthermore, yeast *Wickerhamomyces anomalus* reduced the anthracnose (*C. gloeosporioides*) incidence in avocado fruit and provided effective protection against anthracnose (Campos-Martínez et al., 2016). *W. anomalus* showed mycoparasitism with *C. gloeosporioides* hyphae and caused the loss of turgor pressure and eventually yeast gaining entry into the fungal cells via cell walls (Lima N. B. et al., 2013; Campos-Martínez et al., 2016). **Table 4** summarizes the recent developments in biocontrol agent with antifungal properties against *C. gloeosporioides* infecting mangoes and avocados.

CONCLUDING REMARKS

Alternative treatments, edible coatings, films and additives, nanomaterials, essential oils, and biocontrol agents could be more effective during integrated combination via a "hurdle concept" due to their different mechanisms. The alternative products replacing the commercial synthetic fungicides should not affect the fruit quality or sensory properties of the fruit. In addition, during the application, the product should not affect the environment and other organisms that are agriculturally friendly. Furthermore, the practical application, reliability of the product, commercialization, registration, and cost-effectiveness of the treatments are important before recommending the treatments to the avocado, mango, and papaya industries.

AUTHOR CONTRIBUTIONS

All authors listed have made a substantial, direct and intellectual contribution to the work, and approved it for publication.

FUNDING

The SARChI Research Chair grant for Phytochemical Food Network to Improve Nutritional Quality for Consumers, supported by the NRF (National Research Foundation) grant number 98352, was gratefully acknowledged.

REFERENCES

Ali, A., Cheong, C. K., and Zahid, N. (2014). Composite effect of propolis and gum arabic to control postharvest anthracnose and maintain quality of papaya during storage. *Int. J. Agric. Biol.* 16, 1117–1122.

Ali, A., Wee Pheng, T., and Mustafa, M. A. (2015). Application of lemongrass oil in vapour phase for the effective control of anthracnose of 'Sekaki' papaya. *J. Appl. Microbiol.* 118, 1456–1464. doi: 10.1111/jam.12782

Aloui, H., Khwaldia, K., Licciardello, F., Mazzaglia, A., Muratore, G., Hamdi, M., et al. (2014). Efficacy of the combined application of chitosan and locust bean gum with different citrus essential oils to control postharvest spoilage caused by *Aspergillus flavus* in dates. *Int. J. Food Microbiol.* 170, 21–28. doi: 10.1016/j.ijfoodmicro.2013.10.017

Applerot, G., Abu-Mukh, R., Irzh, A., Charmet, J., Keppner, H., Laux, E., et al. (2010). Decorating parylene-coated glass with ZnO nanoparticles for antibacterial applications: a comparative study of sonochemical, microwave, and microwave-plasma coating routes. *ACS Appl. Mater. Inter.* 2, 1052–1059. doi: 10.1021/am900825h

Bambalele, N., Mditshwa, A., Tesfay, S. Z., and Magwaza, L. S. (2021). Moringa leaf extract infused into carboxymethyl cellulose edible coating combined with gaseous ozone as postharvest treatments maintain quality and extend shelf life of mango fruit. *Acta Hortic.* 1306, 225–232. doi: 10.17660/actahortic.2021.1306.28

Bautista-Baños, S., Sivakumar, D., Bello-Pérez, A., and VillanueVa, R. (2013). A review of the management alternatives for controlling fungi on papaya fruit during the postharvest supply chain. *Crop Prot.* 49, 8–20. doi: 10.1016/j.cropro.2013.02.011

Beno-Moualem, D., and Prusky, D. B. (2000). Early events during quiescent infection development by *Colletotrichum gloeosporioides* in unripe avocado fruits. *Phytopathology* 90, 553–559. doi: 10.1094/phyto.2000.90.5.553

Bill, M., Korsten, L., Remize, F., Glowacz, M., and Sivakumar, D. (2017). Effect of thyme oil vapours exposure on phenylalanine ammonia-lyase (PAL) and lipoxygenase (LOX) genes expression, and control of anthracnose in 'Hass' and 'Ryan' avocado fruit. *Sci. Hortic.* 224, 232–237. doi: 10.1016/j.scienta.2017.06.026

Campos-Martínez, A., Velázquez-del Valle, M. G., Flores-Moctezuma, H. E., Suárez-Rodríguez, R., Ramírez-Trujillo, J. A., et al. (2016). Antagonistic yeasts with potential to control Colletotrichum gloeosporioides (Penz.) Penz. & Sacc. and Colletotrichum acutatum J.H. Simmonds on avocado fruits. *Crop Prot.* 89, 101–104. doi: 10.1016/j.cropro.2016.07.001

Cenobio-Galindo, A. J., Juan, O., Abigail, R.-M., and María, L. C. (2019). Influence of bioactive compounds incorporated in a nanoemulsion as coating on avocado fruits (Persea americana) during postharvest storage: antioxidant activity. *Physicochem. Chang. Struct. Eval. Antioxid.* 8:500. doi: 10.3390/antiox8100500

Chillet, M., Minier, J., Ducrog, M., and Meile, J. C. (2018). Postharvest treatment of mango: potential use of essential oil with thymol to control anthracnose development. *Fruits* 73, 153–157. doi: 10.17660/th2018/73.3.2

Chowdappa, P., Shivakumar, G. C., Chethana, S., and Madhura, S. (2014). Antifungal activity of chitosan-silver nanoparticle composite against Colletotrichum gloeosporioides associated with mango anthracnose. *Afr. J. Microbiol. Res.* 8, 1803–1812. doi: 10.5897/ajmr2013.6584

EU COM (2020). *European Commission Brussels, 20.5.2020. Communication from the Commission to the European Parliament, the Council, the European Economic and Social Committee and the Committee of the Regions a Farm to Fork Strategy for a Fair, Healthy and Environmentally-Friendly Food System*. Available Online at: https://ec.europa.eu/info/sites/default/files/communication-annex-farm-fork-green-deal_en.pdf (accessed May 14, 2021).

Correa-Pacheco, Z. N., Bautista-Baños, S., Valle-Marquina, M. A., and Hernández-López, M. (2017). The effect of nanostructured chitosan and chitosan-thyme essential oil coatings on *Colletotrichum gloeosporioides* growth in vitro and on cv Hass avocado and fruit quality. *J. Phytopathol.* 165, 297–305. doi: 10.1111/jph.12562

De la Rosa-García, S. C., Martínez-Torres, P., Gómez-Cornelio, S., Corral-Aguado, M. A., Quintana, P., and Gómez-Ortíz, M. (2018). Antifungal activity of ZnO and MgO nanomaterials and their mixtures against *Colletotrichum gloeosporioides* strains from tropical fruit. *J. Nanomater.* 2018:3498527.

Dias, B. L., Costa, P. F., Dakin, M. S., de Souza Carlos Mou rao, D., Dias, F. R., de Sousa, R. R., et al. (2020). Control of papaya fruits anthracnose by essential oils of medicinal plants associated to different coatings. *J. Med. Plants Res.* 14, 239–246. doi: 10.5897/jmpr2019.6838

Dickman, M. B. (1994). "Papaya anthracnose," in *Compendium of Tropical Fruit Diseases*, eds R.C. Ploetz, G.A. Zentmyer, W.T. Nishijima, K.G. Rohrbach, and H.D. Ohr (Minneapolis, MN: American Phytopathological Society), 58–59.

EFSA (2011). European Food Safety Authority (EFSA) scientific committee. scientific opinion on guidance on the risk assessment of the application of nanoscience and nanotechnology in the food and feed chain. *EFSA J.* 9:2140. doi: 10.2903/j.efsa.2011.2140

Elsabee, M. Z., and Abdou, E. S. (2013). Chitosan based edible films and coatings: a review. *Mat. Sci. Eng. C* 33, 1819–1841. doi: 10.1016/j.msec.2013.01.010

EPA (2021). *United States Environmental Agency. Integrated Risk Information System (IRIS)*. Available Online at: https://cfpub.epa.gov/ncea/iris2/chemicalLanding.cfm?substance_nmbr=122. (accessed May 13, 2020).

Esquivel-Chávez, F., Colín-Chávez, C., Virgen-Ortiz, J. J., Martínez-Téllez, M. A., Avena-Bustillos, R. J., Peña-Madrigal, G., et al. (2021). Control of mango decay using antifungal sachets containing of thyme oil/modified starch/agave fructan microcapsules. *Future Foods* 3:100008. doi: 10.1016/j.fufo.2020.100008

FAOSTAT (2021). *Food and Agricultural Organization of the United Nations*. Available Online at: http://www.fao.org/faostat/en/#data/QC (accessed May 13, 2021)

FDA (2021). *United States Food & Drug Administration, CFR-Code of Federal Regulations Title 21*. Available Online at: https://www.accessdata.fda.gov/scripts/cdrh/cfdocs/cfcfr/CFRSearch.cfm?CFRPart=182&showFR=1 (accessed April 21, 2021)

Flores-López, M. L., Cerqueira, M. A., de Rodríguez, D. J., and Vincente, A. A. (2016). Perspectives on utilization of edible coatings and nano-laminate coatings for extension of postharvest storage of fruits and vegetables. *Food Eng. Rev.* 8, 292–305. doi: 10.1007/s12393-015-9135-x

Garcia, F., and Davidov-Pardo, G. (2021). Recent advances in the use of edible coatings for preservation of avocados: a review. *J. Food Sci.* 86, 6–15. doi: 10.1111/1750-3841.15540

Gómez-Ríos, D., Barrera-Zapata, R., and Ríos-Estepa, R. (2017). Comparison of process technologies for chitosan production from shrimp shell waste: a techno-economic approach using Aspen Plus®. *Food Bioprod. Process.* 103, 49–57. doi: 10.1016/j.fbp.2017.02.010

Gond, S. K., Bergen, M. S., Torres, M. S., and White, J. F. (2015). Endophytic Bacillus spp. produce antifungal lipopeptides and induce host defence gene expression in maize. *Microbiol. Res.* 172, 79–87. doi: 10.1016/j.micres.2014.11.004

Govender, V., Korsten, L., and Sivakumar, D. (2005). Semi-commercial evaluation of *Bacillus licheniformis* to control mango postharvest diseases in South Africa. *Postharvest Biol. Technol.* 38, 57–65. doi: 10.1016/j.postharvbio.2005.04.005

Guardado-Valdivia, L., Tovar-Pérez, E., Chacón-López, A., López-García, U., Gutiérrez-Martínez, P., Stoll, A., et al. (2018). Identification and characterization of a new *Bacillus atrophaeus* strain B5 as biocontrol agent of postharvest anthracnose disease in soursop (*Annona muricata*) and avocado (*Persea americana*). *Microbiol. Res.* 210, 26–32. doi: 10.1016/j.micres.2018.01.007

Henriod, R., Diczbalis, Y., Sole, D., Stice, K. N., and Tora, L. (2016). Investigation into various fungicides and alternative solutions for controlling postharvest diseases in papaya fruit. *Acta Hortic.* 1111, 113–118. doi: 10.17660/actahortic.2016.9789462611054.17

Hernandez Montiel, L. G., Zulueta Rodriguez, R., Angulo, C., Rueda Puente, E. O., Quiñonez Aguilar, E. E., and Galicia, R. (2017). Marine yeasts and bacteria as biological control agents against anthracnose on mango. *J. Phytopathol.* 165, 833–840. doi: 10.1111/jph.12623

Iñiguez-Moreno, M., Ragazzo-Sánchez, J. A., Barros-Castillo, J. C., Sandoval-Contreras, T., and Calderón-Santoyo, M. (2020). Sodium alginate coatings added with Meyerozyma caribbica: postharvest biocontrol of *Colletotrichum gloeosporioides* in avocado (Persea americana Mill. cv. Hass). *Postharvest Biol. Techol.* 163:111123. doi: 10.1016/j.postharvbio.2020.111123

Janisiewicz, W. J., and Jurick, W. M. (2017). "Sustainable approaches to control postharvest diseases of apples," in *Achieving Sustainable Cultivation of Apples*, ed. K. Evans (Washington: Burleigh Dodds Science Publishing), 307–336. doi: 10.19103/as.2016.0017.15

Jin, P., Wang, H., Zhang, Y., Huang, Y., Wang, L., and Zheng, Y. (2017). UV-C enhances resistance against gray mold decay caused by Botrytis cinerea in strawberry fruit. *Sci. Horticult.* 225, 106–111. doi: 10.1016/j.scienta.2017.06.062

Jin, P., Wu, X., Xu, F., Wang, X., Wang, J., and Zheng, Y. (2012). Enhancing antioxidant capacity and reducing decay of Chinese bayberries by essential oils. *J. Agric. Food Chem.* 60, 3769–3775. doi: 10.1021/jf300151n

Kaewklin, P., Siripatrawan, U., Suwanagul, A., and Lee, Y. S. (2018). Active packaging from chitosan-titanium dioxide nanocomposite film for prolonging storage life of tomato fruit. *Int. J. Biol. Macromol.* 112, 523–529. doi: 10.1016/j.ijbiomac.2018.01.124

Karunanayake, K. O. L. C., Liyanage, K. C. M., Jayakody, L. K. R. R., and Somaratne, S. (2020). Basil oil incorporated beeswax coating to increase shelf life and reduce anthracnose develop-ment in mango cv. Willard. *Ceylon J. Sci.* 49, 355–361. doi: 10.4038/cjs.v49i5.7802

Kesavan Pillai, Sivakumar, D., Sinha Ray, S., Obianom, P., Eggers, S., and Mhlabeni, T. (2020). "Active nanocomposite films based on low density polyethylene/organically modified layered double hydroxides/thyme oil to retain retail shelf life and quality of hass avocados [Conference presentation]," in *AIP Conference Proceedings*, (College Park, MD: American Institute of Physics).

Konsue, W., Dethoup, T., and Limtong, S. (2020). Biological control of fruit rot and anthracnose of postharvest mango by antagonistic yeasts from economic crops leaves. *Microorganisms* 8:317. doi: 10.3390/microorganisms8030317

Kubheka, S. F., Tesfay, S. Z., Mditshwa, A., and Magwaza, L. S. (2021). Efficacy of carboxymethyl cellulose and gum arabic edible coatings in combination with moringa leaf extract in improving postharvest quality of 'Maluma' avocado fruit. *Acta Hortic.* 1306, 293–300. doi: 10.17660/actahortic.2021.1306.37

Kumaraswamy, R. V., Kumari, S., Choudhary, R. C., Sharma, S. S., Pal, A., Raliya, R., et al. (2019). Salicylic acid functionalized chitosan nanoparticle: a sustainable biostimulant for plant. *Int. J. Biol. Macromol.* 123, 59–69. doi: 10.1016/j.ijbiomac.2018.10.202

Lima, J. R., Gondim, D. M. F., Oliveira, J. T. A., Oliveira, F. S. A., Gonçalves, L. R. B., and Viana, F. M. P. (2013). Use of killer yeast in the management of postharvest papaya anthracnose. *Postharvest Biol. Technol.* 83, 5–64.

Lima, N. B., de, A., Batista, M. V., De Morais, Jr., M. A., Barbosa, M. A. G., Michereff, S. J., et al. (2013). Five *Colletotrichum* species are responsible for mango anthracnose in northeastern Brazil. *Fungal Divers.* 61, 75–88. doi: 10.1007/s13225-013-0237-6

Liu, Y., Wang, R., Cao, Y., Chen, C., Bai, F., Xu, T., et al. (2016). Identification and antagonistic activity of endophytic bacterial strain Paenibacillus sp. 5 L8 isolated from the seeds of maize (*Zea mays* L. Jingke 968). *Ann. Microbiol.* 66, 653–660. doi: 10.1007/s13213-015-1150-x

Ma, Y., Fu, L., Hussain, Z., Huang, D., and Zhu, S. (2019). Enhancement of storability and antioxidant systems of sweet cherry fruit by nitric oxide-releasing chitosan nanoparticles (GSNO-CS NPs). *Food Chem.* 285, 10–21. doi: 10.1016/j.foodchem.2019.01.156

Majeed, H., Bian, Y., Ali, B., Jamil, A., Majeed, U., Khan, Q. F., et al. (2015). Essential oil encapsulations: uses, procedures, and trends. *RSC Adv.* 5, 58449–58463.

Marques, K. M., Galati, V. C., Fernandes, J. D. R., Guimarães, J. E. R., Silva, J. P., Mattiuz, B. H., et al. (2016). Use of chitosan for the control of postharvest anthracnose and quality in avocados. *Acta Hortic.* 1120, 225–232. doi: 10.17660/actahortic.2016.1120.34

McDonnell, G., and Russell, A. D. (1999). Antiseptics and disinfectants: activity, action, and resistance. *Clin. Microbiol. Rev.* 12, 147–179. doi: 10.1128/cmr.12.1.147

Meena, K. R., and Kanwar, S. S. (2015). Lipopeptides as antifungal and antibacterial agents: applications in food safety and therapeutics. *BioMed Res. Int.* 2015:473050.

Meena, M., Pilania, S., Pal, A., Mandhania, S., Bhushan, B., Kumar, S., et al. (2020). Cu-chitosan nano-net improves keeping quality of tomato by modulating physio-biochemical responses. *Sci. Rep.* 10:21914.

Mohammadi, A., Hashemi, M., and Hosseini, S. M. (2015). Postharvest treatment of nanochitosan-based coating loaded with *Zataria multiflora* essential oil improves antioxidant activity and extends shelf life of cucumber. *Innov. Food Sci. Emerg.* 33, 580–588. doi: 10.1016/j.ifset.2015.10.015

Nelson, S. (2008). *Anthracnose of Avocado. College of Tropical Agriculture and Human Resources (CTAHR) Publication, 1-6*. Available Online at: https://www.ctahr.hawaii.edu/oc/freepubs/pdf/pd-58.pdf. (accessed March 07, 2021)

Nguyen, V. T. B., Nguyen, D. H. H., and Nguyen, H. V. H. (2020). Combination effects of calcium chloride and nano-chitosan on the postharvest quality of strawberry (*Fragaria x ananassa* Duch.). *Postharvest Biol. Technol.* 162:111103. doi: 10.1016/j.postharvbio.2019.111103

Obianom, C., and Sivakumar, D. (2018). Differential response to combined Prochloraz and thyme oil drench treatment in avocados against the control of anthracnose and stem-end rot. *Phytoparasitica* 46, 273–281. doi: 10.1007/s12600-018-0663-9

Obianom, C., Romanazzi, G., and Sivakumar, D. (2019). Effects of chitosan treatment on avocado postharvest diseases and expression of phenylalanine ammonia-lyase, chitinase and lipoxygenase genes. *Postharvest Biol. Technol.* 147, 214–221. doi: 10.1016/j.postharvbio.2018.10.004

Ochoa-Velasco, C. E., Pérez-Pérez, J. C., Varillas-Torres, J. M., Navarro-Cruz, A. R., Hernández-Carranza, P., Munguía-Pérez, R., et al. (2021). Starch edible films/coatings added with carvacrol and thymol: in vitro and in vivo evaluation against *Colletotrichum gloeosporioides*. *Foods* 10:175. doi: 10.3390/foods10010175

Ongena, M., and Jacques, P. (2008). Bacillus lipopeptides: versatile weapons for plant disease biocontrol. *Trends Microbiol.* 16, 115–125. doi: 10.1016/j.tim.2007.12.009

Raaijmakers, J. M., De Bruijn, I., Nybroe, O., and Ongena, M. (2010). Natural functions of lipopeptides from Bacillus and Pseudomonas: more than surfactants and antibiotics. *FEMS Microbiol. Rev.* 34, 1037–1062. doi: 10.1111/j.1574-6976.2010.00221.x

Rajestary, S., Landi, L., and Romanazzi, G. (2021). Chitosan and postharvest decay of fresh fruit: meta-analysis of disease control and antimicrobial and eliciting activities. *Compr. Rev. Food Sci. Food Saf.* 20, 563–582. doi: 10.1111/1541-4337.12672

Romanazzi, G., Feliziani, E., and Sivakumar, D. (2018). Chitosan, a biopolymer with triple action on postharvest decay of fruit and vegetables: eliciting, antimicrobial and film-forming properties. *Front. Microbiol.* 9:2745.

Romanazzi, G., Sanzani, S. M., Bi, Y., Tian, S., Gutiérrez Martínez, P., and Alkan, N. (2016). Induced resistance to control postharvest decay of fruit and vegetables. *Postharvest Biol. Technol.* 122, 82–94. doi: 10.1016/j.postharvbio.2016.08.003

Saharan, V., Sharma, G., Yadav, M., Choudhary, M. K., Sharma, S. S., Pal, A., et al. (2015). Synthesis and in vitro antifungal efficacy of Cu–chitosan nanoparticles against pathogenic fungi of tomato. *Int. J. Biol. Macromol.* 75, 346–353. doi: 10.1016/j.ijbiomac.2015.01.027

Sanders, G. M., Korsten, L., and Wehner, F. C. (2000). Market survey of postharvest diseases and incidence of *Colletotrichum gloeosporioides* on avocado and mango fruit in South Africa. *Trop. Sci.* 40, 192–198.

Sarkosh, A., Schaffer, B., Vargas, A. I., Palmateer, A. J., Lopez, P., Soleymani, A., et al. (2018). Antifungal activity of five plant-extracted essential oils against anthracnose in papaya fruit. *Biol. Agric. Hortic.* 34, 18–26. doi: 10.1080/01448765.2017.1358667

Schoeny, R. (2010). Disinfection by-products: a question of balance. *Environ. Health Perspect.* 118, A466–A467.

Sharma, R. R., Singh, D., and Singh, R. (2009). Biological control of postharvest diseases of fruits and vegetables by microbial antagonists: a review. *Biol. Control* 50, 205–221. doi: 10.1016/j.biocontrol.2009.05.001

Shimshoni, J. A., Bommuraj, V., Chen, Y., Sperling, R., Barel, S., Feygenberg, O., et al. (2020). Postharvest fungicide for avocado fruits: antifungal efficacy and peel to pulp distribution kinetics. *Foods* 9:124. doi: 10.3390/foods9020124

Siddiqui, Y., and Ali, A. (2014). "*Colletotrichum gloeosporioides* (Anthracnose) (ED Bautista-Banos)," in *Post Harvest Decay: Control Strategies*, ed. S. Bautista-Banos. Amsterdam: Elsevier.

Sivakumar, D., and Bautista-Baños, S. (2014). A review on the use of essential oils for postharvest decay control and maintenance of fruit quality during storage. *Crop Prot.* 64, 27–37. doi: 10.1016/j.cropro.2014.05.012

Song, H., Yuan, W., Jin, P., Wang, W., Wang, X., Yang, L., et al. (2016). Effects of chitosan/nano-silica on postharvest quality and antioxidant capacity of loquat fruit during cold storage. *Postharvest Biol. Technol.* 119, 41–48. doi: 10.1016/j.postharvbio.2016.04.015

Spadaro, D., and Droby, S. (2016). Development of biocontrol products for postharvest diseases of fruit: the importance of elucidating the mechanisms of action of yeast antagonists. *Trends Food Sci. Technol.* 47, 39–49. doi: 10.1016/j.tifs.2015.11.003

Swart, S. H., Serfontein, J. J., Swart, G., and Labuschagne, C. (2009). Chemical control of post-harvest diseases of mango: the effect of fludioxonil and prochloraz on soft brown rot, stem-end rot and anthracnosE. *Acta Hortic.* 820, 503–510. doi: 10.17660/actahortic.2009.820.64

Swinburne, T. R. (1983). "Quiescent infections in post-harvest diseases," in *Post Harvest Pathology of Fruits and Vegetables*, ed. C. Dennis (London: Academic Press).

Tesfay, S. Z., Magwaza, L. S., Mbili, N., and Mditshwa, A. (2017). Carboxyl methylcellulose (CMC) containing moringa plant extracts as new postharvest organic edible coating for Avocado (*Persea americana* Mill.) fruit. *Sci. Hortic.* 226, 201–207. doi: 10.1016/j.scienta.2017.08.047

Tian, Y. Q., Li, W., Jiang, Z. T., Jing, M. M., and Shao, Y. Z. (2018). The preservation effect of Metschnikowia pulcherrima yeast on anthracnose of postharvest mango fruits and the possible mechanism. *Food Sci. Biotechnol.* 27, 95–105. doi: 10.1007/s10068-017-0213-0

Transparency Market Research Report (2021). *Global Avocado Market to Reach US$21.56 bn by 2026, Increasing Health Consciousness Among People to Promote Growth*. Available Online at: https://www.transparencymarketresearch.com/pressrelease/avocado-market.htm (accessed March 01, 2021)

Velázquez-Del Valle, M. G., Hernández-Lauzardo, A. N., Guerra-Sanchez, G., and Mariaca-Gaspar, G. I. (2012). Chitosan as an alternative to control phytopathogenic fungi on fruits and vegetables in Mexico. *Afr. J. Microbiol. Res.* 6, 6606–6611.

Vero, S., Garmendia, G., Belén González, M., Bentancur, O., and Wisniewski, M. (2013). Evaluation of yeasts obtained from Antarctic soil samples as biocontrol agents for the management of postharvest diseases of apple (Malus × domestica). *FEMS Yeast Res.* 13, 189–199. doi: 10.1111/1567-1364.12021

Wei, Y., Xu, M., Wu, H., Tu, S., Pan, L., and Tu, K. (2016). Defense response of cherry tomato at different maturity stages to combined treatment of hot air and *Cryptococcus laurentii*. *Postharvest Biol. Technol.* 117, 177–186. doi: 10.1016/j.postharvbio.2016.03.001

Wilson, C. L., and Wisniewski, M. E. (1989). Biological control of postharvest diseases of fruits and vegetables: an emerging technology. *Annu. Rev. Phytopathol.* 27, 425–441. doi: 10.1146/annurev.py.27.090189.002233

Wu, S., Zhen, C., Wang, K., and Gao, H. (2019). Effects of Bacillus subtilis CF-3 VOCs combined with heat treatment on the control of *Monilinia fructicola* in peaches and *Colletotrichum gloeosporioides* in litchi fruit. *J. Food Sci.* 84, 3418–3428. doi: 10.1111/1750-3841.14949

Yakoby, N., Kobiler, I., Dinoor, A., and Prusky, D. (2000). pH regulation of pectate-lyase secretion modulates the attack of *Colletotrichum gloeosporioides* on avocado fruits. *Appl. Environ Microb.* 66, 1026–1030. doi: 10.1128/aem.66.3.1026-1030.2000

Conflict of Interest: The authors declare that the research was conducted in the absence of any commercial or financial relationships that could be construed as a potential conflict of interest.

Publisher's Note: All claims expressed in this article are solely those of the authors and do not necessarily represent those of their affiliated organizations, or those of the publisher, the editors and the reviewers. Any product that may be evaluated in this article, or claim that may be made by its manufacturer, is not guaranteed or endorsed by the publisher.

frontiers in Microbiology

ORIGINAL RESEARCH
published: 05 August 2021
doi: 10.3389/fmicb.2021.709855

Functional and Genomic Analysis of *Rouxiella badensis* SER3 as a Novel Biocontrol Agent of Fungal Pathogens

*Luzmaria R. Morales-Cedeño[1], Sergio de los Santos-Villalobos[2] and Gustavo Santoyo[1]**

[1] *Instituto de Investigaciones Químico-Biológicas, Universidad Michoacana de San Nicolás de Hidalgo, Morelia, Mexico,*
[2] *Instituto Tecnológico de Sonora, Ciudad Obregón, Mexico*

In recent decades, various bacterial species have been characterized as biocontrol agents for plant crop diseases; however, only a few genera have been predominantly reported in the literature. Therefore, the identification of new antagonists against phytopathogens is essential for boosting sustainable food production systems. In this study, we evaluated the role of strain SER3 from the recently discovered *Rouxiella badensis* as a biocontrol agent. SER3 was isolated from the phyllosphere of decaying strawberry fruit (*Fragaria* × *ananassa*) and showed different grades of antagonism against 20 fungal pathogens of berries, based on confrontation assays, due to the action of its diffusible and volatile compounds. These fungal pathogens were isolated from decayed strawberry, blackberry, and blueberry fruit and were characterized through internal transcribed spacer (ITS) sequencing and homology searches, exhibiting similarity with well-known postharvest pathogens such as *Botrytis*, *Fusarium*, *Geotrichum*, *Mucor*, *Penicillium*, *Alternaria*, and *Botryosphaeria*. Koch's postulates were confirmed for most pathogens by reinfecting berry fruit. SER3 showed good capacity to inhibit the growth of *Botrytis cinerea* and *Fusarium brachygibbosum* in strawberry fruit, affecting mycelial development. To gain better understanding of the genetic and metabolic capacities of the SER3 strain, its draft genome was determined and was found to comprise a single chromosome of 5.08 Mb, 52.8% G + C content, and 4,545 protein-coding genes. Phylogenetic analysis indicated that the SER3 strain is affiliated with the *R. badensis* species, with an average nucleotide identity >96% and a genome-to-genome distance >70%. A comparison of the genomic properties of *R. badensis* SER3 and other close bacterial relatives showed several genes with potential functions in biocontrol activities, such as those encoding siderophores, non-ribosomal peptide synthetases, and polyketide synthases. This is the first study to demonstrate a novel role of the recently discovered *R. badensis* species (and any other species of the genus *Rouxiella*) as a biocontrol agent against postharvest fungal pathogens.

Keywords: genomic analysis, sustainable agriculture, fungal antagonism, postharvest disease, volatile organic compound

OPEN ACCESS

Edited by:
Khamis Youssef,
Agricultural Research Center, Egypt

Reviewed by:
Samir Jaoua,
Qatar University, Qatar
Chunpeng (Craig) Wan,
Jiangxi Agricultural University, China

****Correspondence:***
Gustavo Santoyo
gustavo.santoyo@umich.mx

Specialty section:
This article was submitted to Food Microbiology, a section of the journal Frontiers in Microbiology

Received: *14 May 2021*
Accepted: *12 July 2021*
Published: *05 August 2021*

Citation:
Morales-Cedeño LR, de los Santos-Villalobos S and Santoyo G (2021) Functional and Genomic Analysis of Rouxiella badensis SER3 as a Novel Biocontrol Agent of Fungal Pathogens. Front. Microbiol. 12:709855. doi: 10.3389/fmicb.2021.709855

INTRODUCTION

The demand for food is increasing worldwide, resulting in the requirement to produce it under eco-friendly systems to ensure food security (Allen and Prosperi, 2016). However, constant attack by fungal and oomycete phytopathogens reduces the yield and quality of crops, causing huge losses at different stages of the agricultural cycle (Dean et al., 2012; Kamoun et al., 2015). For example, *Botrytis cinerea* has been reported to infect more than 200 plant species and cause losses of more than €1 billion/annum globally (Romanazzi and Feliziani, 2014). Similarly, several species of the genus *Fusarium*, together with *Botrytis*, are among the top 10 pathogens worldwide that can cause serious yield losses in agriculture (Magan et al., 2010; Dean et al., 2012). Likewise, invasion by non-native species of phytopathogens owing to transportation and storage of vegetables and fruit is another factor that affects products postharvest (Fried et al., 2017).

Thus, an efficient alternative against crop infestation, which includes the use of antagonistic biological agents, has been developed to eliminate or reduce the use of pesticides in agriculture (Compant et al., 2005; Backer et al., 2018). One of the advantages of biological agents such as *Trichoderma* or bacteria is that they are safe and environment friendly (Elad, 2000; Wang et al., 2020). This group of beneficial microorganisms associated with plants has emerged as a viable, economical, and efficient alternative to control various pre- and postharvest diseases (Morales-Cedeño et al., 2021). Even antagonism in plant growth-promoting bacteria (PGPB) toward phytopathogens is considered an indirect mechanism to stimulate plant growth (Glick, 2012). Their mechanisms of antifungal action against fungal pathogens include the production of diffusible compounds [e.g., hydrolytic enzymes, siderophores, lipopeptides, phenazines, 1-aminocyclopropane-1-carboxylate (ACC) deaminase] or antibiotics and volatiles compounds (e.g., dimethyl disulfide, hydrogen cyanide, and others) (Hernández-León et al., 2015; Khan et al., 2018; Rojas-Solís et al., 2018). Multiple species of PGPB have been isolated and characterized based on their antagonism toward phytopathogens, including *Pseudomonas* spp. and *Bacillus* spp., among few other genera that are predominantly reported (Höfte and Altier, 2010; Santoyo et al., 2012; Islam et al., 2017). Thus, the search for new antagonistic bacterial species is essential to increase the possibility of developing new biofungicides for commercial application (Córdova-Albores et al., 2020).

In this study, we propose a novel ecological role for *Rouxiella badensis* strain SER3 as an antagonist of postharvest pathogens of berries. *R. badensis*, together with *Rouxiella silvae*, was recently proposed as a new bacterial species by Le Fléche-Matéos et al. (2017). Some genera phylogenetically close to *Rouxiella*, such as *Serratia* and *Rahnella*, have previously been described as antagonists and PGPB. For example, Koo and Cho (2009) isolated and characterized a strain of *Serratia* sp. SY5, which had the ability to stimulate the growth of maize seedlings under stressful conditions. In addition, Sun et al. (2020) observed that *Rahnella aquatilis* strain MEM40, isolated from the rhizosphere of a rice plant, showed plant growth promoter effects and antagonism against phytopathogens such as *Magnaporthe oryzae* and *F. graminearum*. The only report on the genus *Rouxiella* described its role as an inhibitor of human pathogenic bacterial growth, but this strain has not been fully characterized, and its taxonomic assignation remains at the genus level (Nam et al., 2020). The isolation of a possible *R. badensis* strain 70 (among other 43 isolated endophytic strains) as an antagonist of pathogenic bacteria and fungi has also been reported. However, the characterization of strain 70 was based only on a partial 16S rDNA sequence (1,023 bp); thus, elucidation of its taxonomic affiliation requires further analysis (Wang et al., 2019). Herein, we present the isolation and characterization of a novel ecological role of *R. badensis* as a biocontrol agent against 20 fungal phytopathogens of berries (*Fragaria* × *ananassa*, *Vaccinium* spp. var. Biloxi, *Rubus* subgenus *Eubatus*), also isolated and characterized in this study. Furthermore, the *R. badensis* SER3 genome was sequenced to support its taxonomic affiliation and mined for detecting biosynthetic gene clusters that could be involved in its biocontrol capabilities.

MATERIALS AND METHODS

Isolation and Characterization of Postharvest Fungal Pathogens

Endophytic fungal pathogens were isolated from berries, including strawberries (n = 33), blackberries (n = 36), and blueberries (n = 49), which were collected from commercial markets. Berry fruits were surface sterilized according to a previous study (Contreras et al., 2016). Briefly, berries were immersed in 70% ethanol for 30 s, then washed with sodium hypochlorite (NaOCI) solution (2.5% available Cl^-) for 5 min, and then rinsed with ethanol (70% v/v) for 30 s. Finally, the fruits were washed five times with sterile distilled water. Aliquots of sterile distilled water used in the final rinse were cultured on plates containing nutrient agar (NA) medium (Merck). The plates were examined for bacterial growth after incubation at 28°C for 4 days. The sterilized fruits were used in decaying experiments to isolate potentially endophytic fungal pathogens. Briefly, groups of 5–10 fruits (strawberries, blackberries, and blueberries) were placed in disinfected containers, closed, and kept in the dark at room temperature. Fruit weight and firmness were measured on days 1, 5, and 10 (until the growth of fungal mycelium was detected) with an analytical balance (Benchmark Scientific, Inc., Sayreville, NJ, United States) and a penetrometer (Model GY-1, Hangzhou Scientific Instruments), respectively. Koch's postulates of fungal endophytes were confirmed for most of the pathogens (except *Trichoderma*) as follows: berry fruits were sterilized as described above, placed inside sterile glass bottles, and inoculated with the spores obtained from each fungal culture ($\sim 1 \times 10^5$ spores/ml). Mycelial growth of fungi on the fruit was visualized after 5–10 days. Further characterization was performed to confirm fungal identity.

Genomic DNA was extracted from fungal isolates as per the protocol by Mahuku (2004), followed by polymerase chain reaction analysis to amplify the intergenic spacer (ITS) regions with the following primers: ITS4 (5′-TCCTCCGCTTATTGATATGC-3′)

and ITS5 (5′-GGAAGTAAAAGTCGTAACAAGG-3′) (Hernández-León et al., 2015). The amplified ITS regions of each of the 20 fungal isolates were sequenced at Macrogen, Seoul, South Korea. Sequences and most probable taxonomic affiliation were deposited in GenBank, and the accession numbers are shown in **Table 1**.

Isolation of SER3 and Confrontation Bioassays

Strain SER3 was isolated from the phyllosphere of strawberry fruit and selected for antagonism against the fungal pathogen *F. brachygibbosum* in a prescreening assay in dual culture (**Supplementary Figure 1**). The strain was grown at 30°C for 24 h on NA medium and maintained at 4°C.

Fungal antagonism by strain SER3 was evaluated as previously reported for Petri dish-based bioassays (Hernández-León et al., 2015). Briefly, SER3 was streaked onto potato dextrose agar (PDA) plates in a cross shape, and then, four mycelial plugs (6-mm diameter) from each of the 20 fungal isolates were deposited in the center of each quadrant. The plates were incubated in the dark at 30°C, and the mycelial growth diameter was measured on day 6.

The antifungal effects of the volatile compounds produced by strain SER3 were also evaluated in Petri plates. SER3 [100 μl, at $\sim 1 \times 10^6$ colony forming units (CFU)] was inoculated on one side of the divided Petri plates, and in the other sections, mycelial plugs of each studied fungus (6-mm diameter) were inoculated. The inoculated plates were incubated, and mycelial growth was measured as described above. Both experiments were independently performed in triplicate, and the inhibition percentage was calculated using the following formula:% growth inhibition = $[(Ac - Ab)/Ac] \times 100$, where Ac is the control mycelial area, and Ab is the mycelial area under treatment.

TABLE 1 | Fungal strains isolated from strawberries, blackberries and blueberries, with the closest identity based on the ITS sequence homology searches.

Strain	Closest Genbank species identity	Identity (%)	Access number	Source of isolation
62BCV	*Botrytis cinerea*	99.8	MN365049.1	Strawberries
62C	*Botrytis* sp.	99.4	MN365050.1	
4BF	*Fusarium brachygibbosum*	99.2	MN365015.1	
HBF	*Fusarium brachygibbosum*	98.3	MN365017.1	
FRB	*Geotrichum candidum*	98.3	MN394447.1	
1BF	*Mucor circinelloides*	99.1	MK880497.1	
22	*Mucor fragilis*	99	MN365051.1	
FRA	*Mucor fragilis*	99	MN364941.1	
1F	*Penicillium crustosum*	96.8	MN080331.1	
230	*Penicillium expansum*	99.6	MN393696.1	
5F	*Penicillium expansum*	99.6	MN080332.1	
4AF	*Trichoderma* sp.	98.8	MN365013.1	
2Z	*Alternaria alternata*	99	MN397936.1	Blackberries
7Z	*Geotrichum phurueaensis*	98	MN397937.1	
1A	*Alternaria alternata*	99.6	MK881030.1	Blueberries
3A	*Alternaria* sp.	99.4	MN393668.1	
4A	*Alternaria alternata*	96.2	MN410562.1	
6A	*Alternaria alternata*	97.3	MN365025.1	
5A	*Botryosphaeria rhodina*	99.4	MN364705.1	
1BOA	*Cladosporium* sp.	98.8	MN364646.1	

Fungal Growth Inhibition Bioassay on Strawberry Fruit and Microscopy Visualization

The strawberries were washed with running water and subsequently placed in a container with 70% ethanol for 1 min. The ethanol was decanted, and then, the berries were washed with 2.5% sodium hypochlorite for 1 min. This process was repeated three times, and finally, the strawberries were rinsed thrice with sterile deionized water.

Following the above procedure, strawberries were allowed to dry in a laminar flow hood, and an incision of approximately 3 mm length, width, and depth was made on each fruit with the tip of a sterile scalpel. Four treatments were performed, using the following: (i) sterile distilled water as the negative control; (ii) a mycelium plug, 7 mm in diameter, of the phytopathogen *B. cinerea* 62BCV or *F. brachygibbosum* 4BF as a positive control; and (iii) a bacterial suspension of SER3 (100 μl, $\sim 1 \times 10^6$ CFU) and a mycelium plug, 7 mm in diameter, of each phytopathogen; and (iv) the supernatants (100 μl) of strain SER3 obtained from nutrient broth after an overnight culture and the mycelium of the two studied phytopathogens grown for 24 h at 29°C. After treatment, the strawberries were placed in closed sterile plastic containers and maintained at room temperature for 3 days.

For microscopy visualization, strain SER3 was simultaneously striated with phytopathogenic fungi (*B. cinerea* 62BCV or *F. brachygibbosum* 4BF) in separate Petri dishes containing PDA. The bacteria were streaked on the cross-shaped dishes, and a 7-mm portion of the mycelium was deposited in the center of each quadrant, as previously mentioned. Subsequently, a mycelium sample was stained with lactophenol blue and safranin and visualized under a Velab VE-BC3 Plus optical microscope.

SER3 Genome Sequencing and Analysis

A single colony of strain SER3 was picked from a streaked NA plate (BD Bioxon), which was maintained at 30°C overnight. SER3 genomic DNA was extracted following standard protocols (Mahuku, 2004) and further purified using a Wizard® Genomic DNA Purification Kit (Promega, Fitchburg, WI, United States). The quality and quantity of the extracted DNA were evaluated with agarose gel electrophoresis and using a NanoDrop spectrophotometer (Thermo Scientific, Waltham, MA, United States), respectively. Genomic DNA from SER3 was sequenced commercially (MR DNA, Shallowater, TX, United States) by using the Illumina HiSeq technologies platform (2 × 300 bp). FastQC analysis, version 0.11.5, of the raw reads was employed to perform quality control (Andrews, 2010). Trimmomatic, version 0.32, was used to remove bases of low quality and adapter sequences (Bolger et al., 2014). Genome assembly was performed with contigs obtained through the PATRIC[1] genome

[1]https://www.patricbrc.org/

service and SPAdes assembler version 3.10.0 (Bankevich et al., 2012). The draft genome of SER3 was reordered according to the reference genome of *Rahnella aquatilis* KM12 (NCBI project accession number: ASM395610v2). PLACNETw was used to explore the presence of plasmids in the SER3 genome (Vielva et al., 2017).

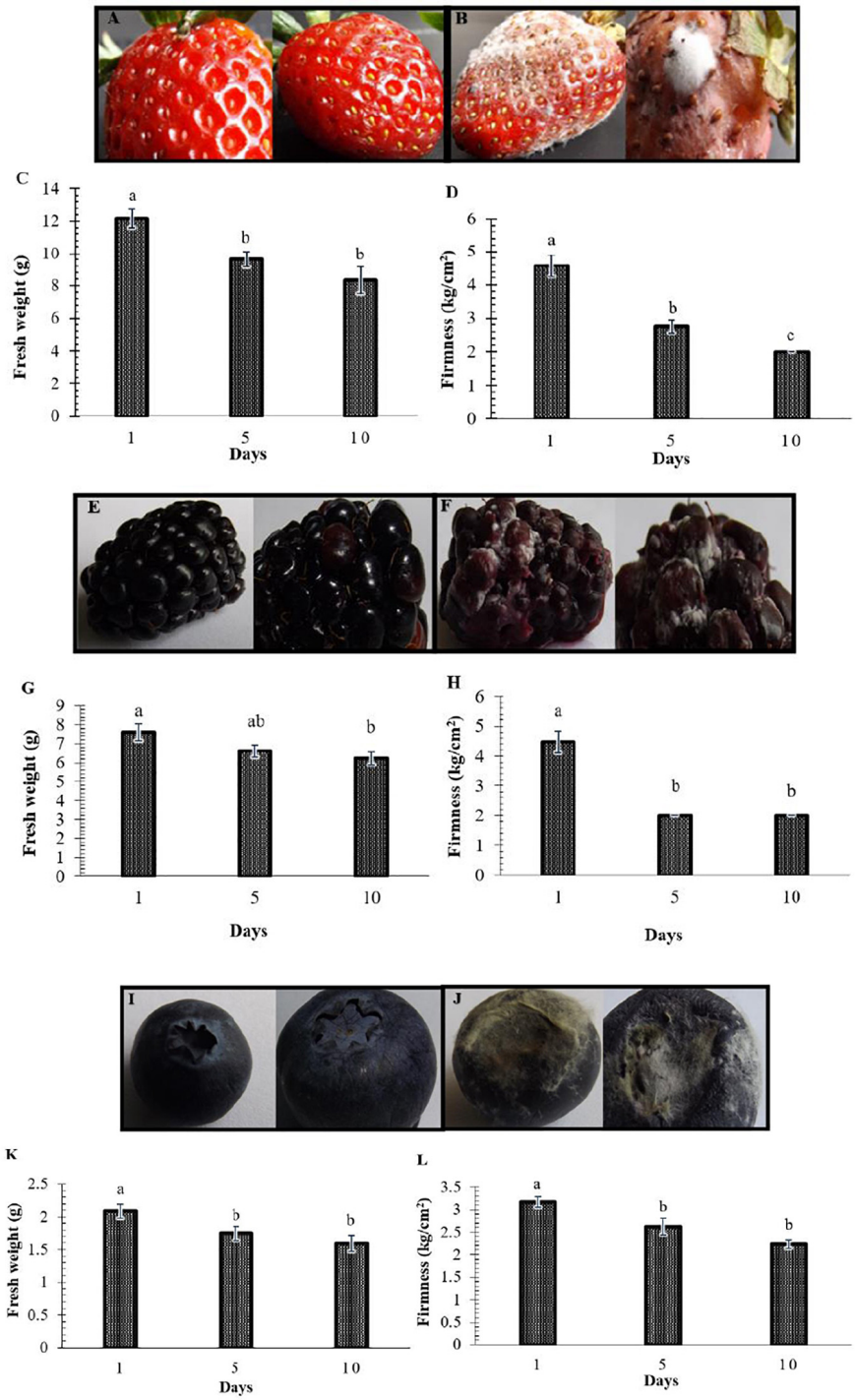

FIGURE 1 | Postharvest decay in berries represented by loss of weight and firmness. Representative fruit are shown in Panels **(A,B,E,F,I,J)**. **(A,E,I)** Fruit at the beginning of the study (control). **(B,F,J)** Fruit in decay on days 5 and 10. Panels **(C,G,K)** show the decrease in the weight of strawberries, blackberries, and blueberries, respectively. Panels **(D,H,L)** show the decline in firmness. Bars represent means ± standard deviation (n = 12). The letters indicate that the means differ significantly according to Duncan's multiple range test ($p < 0.05$).

Taxonomic Affiliation of Strain SER3

The 16S rRNA gene sequence was obtained from the genome and used in basic local alignment search tool (BLAST) homology searches to assign the possible taxonomic affiliation of strain SER3. After that, a genome-level approach was adopted, employing average nucleotide identity (ANI) > 95–96% (Yoon et al., 2017) and a genome-to-genome distance calculator (GGDC) > 70% (Meier-Kolthoff et al., 2013). This genome-level approach was based on strains having cutoff values for species delimitation established for the 16S rRNA gene (>98.7%) (Chun et al., 2018).

Phylogenomic Analysis of SER3

Phylogenomic relationships of *R. badensis* SER3 and the bacterial strains with high similarity according to ANI and GGDC values were analyzed using the REALPHY pipeline (Bertels et al., 2014). The neighbor-joining method was used for tree construction, and the nucleotide distance was measured using the Jukes–Cantor model. Furthermore, bootstrap analysis with 1,000 replications was performed.

Genome Annotation and Mining for Plant Growth-Promoting and Biocontrol Traits

The assembled genome was annotated using the Rapid Annotation of the Subsystem Technology (RAST) server[2]. Genome mining was performed by biosynthetic gene cluster (BGC) prediction using antiSMASH 4.0 (Blin et al., 2017) for *R. badensis* SER3 and other close bacterial genomes and manually

[2]http://rast.theseed.org/FIG/rast.cgi

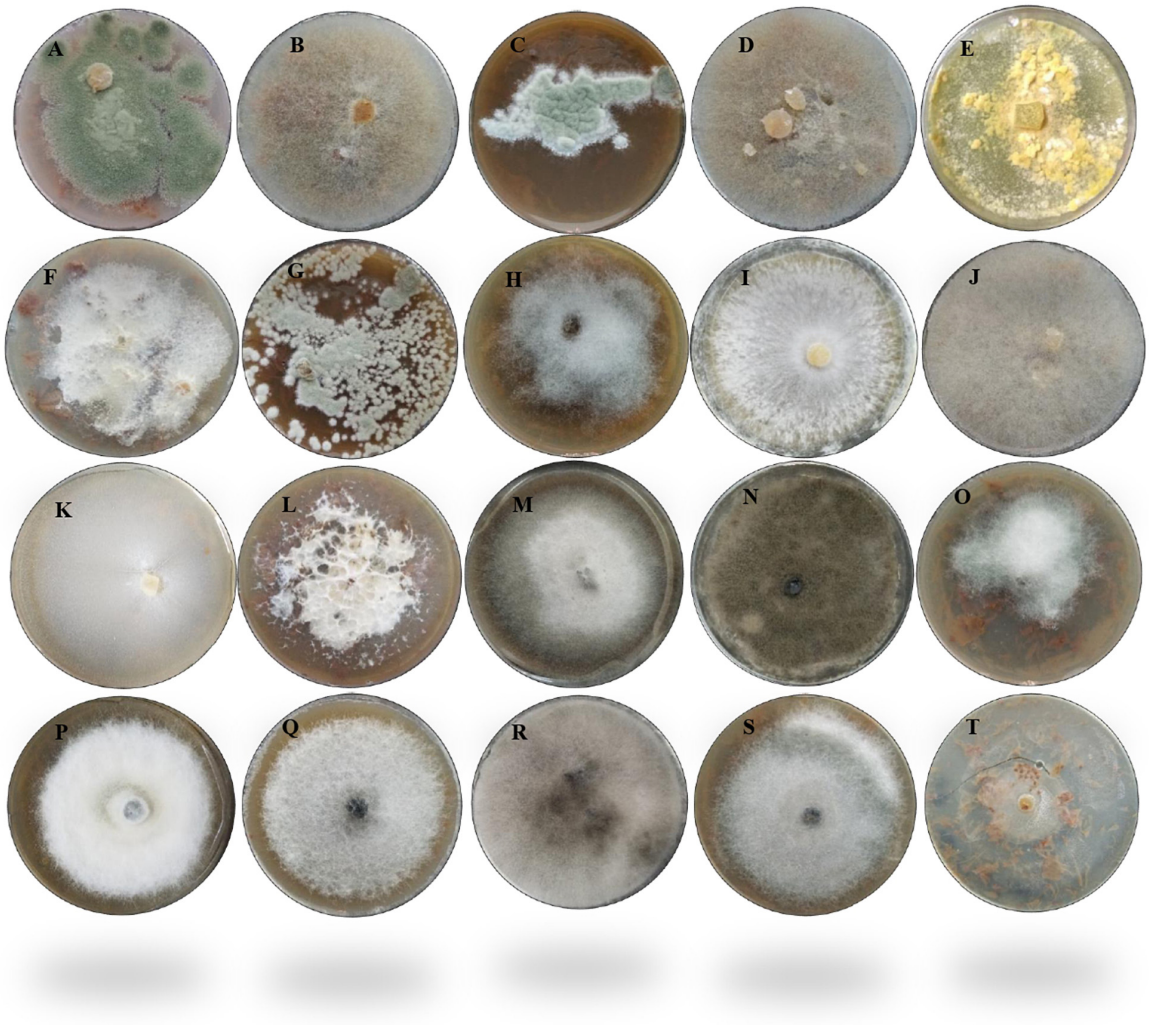

FIGURE 2 | Morphological appearance of the 20 fungal strains isolated from fruit berries. **(A)** *Penicillium crustosum*1F. **(B)** *Mucor circinelloides* 1BF. **(C)** *Penicillium expansum* 230. **(D)** *Mucor fragilis* 22. **(E)** *Trichoderma* sp. 4AF. **(F)** *Fusarium brachygibbosum* 4BF. **(G)** *Penicillium expansum* 5F. **(H)** *Botrytis* sp. 62C. **(I)** *Botrytis cinerea* 62BCV. **(J)** *Mucor fragilis* FRA. **(K)** *Geotrichum candidum* FRB. **(L)** *Fusarium brachygibbosum* HBF. **(M)** *Alternaria alternata* 1A. **(N)** *Cladosporium* sp. 1BOA. **(O)** *Alternaria alternata* 2Z. **(P)** *Alternaria* sp. 3A. **(Q)** *Alternaria alternata* 4A. **(R)** *Botryosphaeria rhodina* 5A. **(S)** *Alternaria alternata* 6A. **(T)** *Geotrichum phurueaensis* 7Z. The fungal growth was observed at different times, ranging from 5 to 8 days.

inspected from the annotations generated by the RAST server[3] (Aziz et al., 2008), specifically the RASTtk pipeline.

RESULTS

Isolation and Characterization of Postharvest Phytopathogens

In this study, the decay of berries over time showed a reduction in fresh weight and fruit firmness between days 5 and 10, consistent with the appearance of decaying symptoms caused by fungal pathogens (**Figure 1**). Following the decay, 20 berry fungi were isolated. **Figure 2** shows the morphological appearance of the isolated fungal strains. Sequencing of the ITS from the isolated fungi showed high homology with *B. cinerea*, *Botrytis* sp., *F. brachygibbosum*, *Geotrichum candidum*, *Geotrichum phurueaesis*, *Mucor circinelloides*, *Mucor fragilis*, *Penicillium crustosum*, *Penicillium expansum*, *Trichoderma* sp., *Alternaria alternata*, *Alternaria* sp., *Botryosphaeria rhodina*, and *Cladosporium* sp. (**Table 1**). To determine the infection rates of fungi, including those not reported as the main postharvest phytopathogens of berries, Koch's postulates were confirmed, thus corroborating their role in postharvest fungal infections (**Supplementary Figure 2**).

[3]http://rast.nmpdr.org

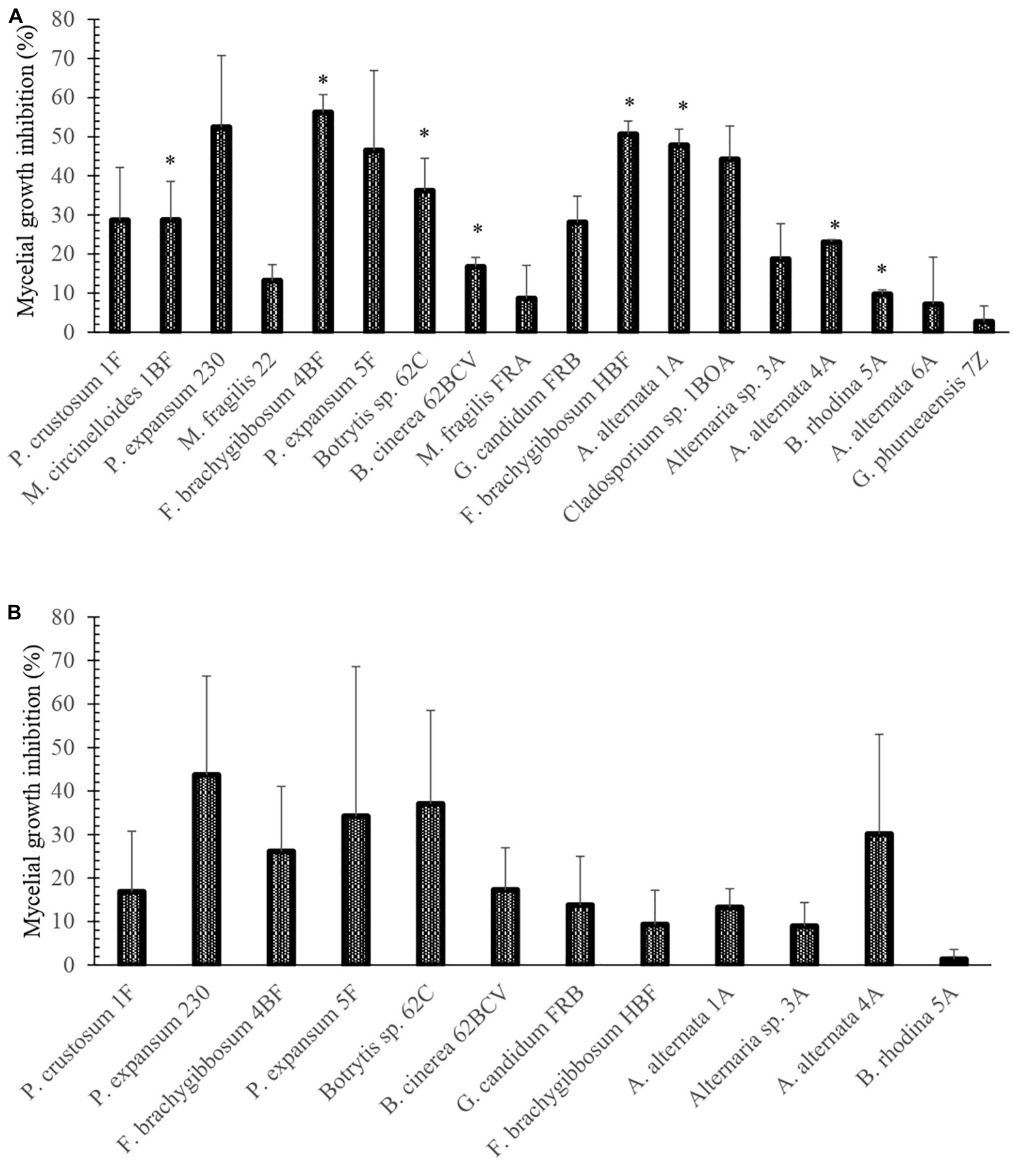

FIGURE 3 | Percentages of inhibition of fungi isolated from berries postharvest caused by **(A)** diffusible and **(B)** volatile compounds of the SER3 strain. The experiments were carried out independently three times. Bars represent mean ± SE. Asterisks indicate significant difference compared to the respective controls, using Student's *t*-test ($p < 0.05$).

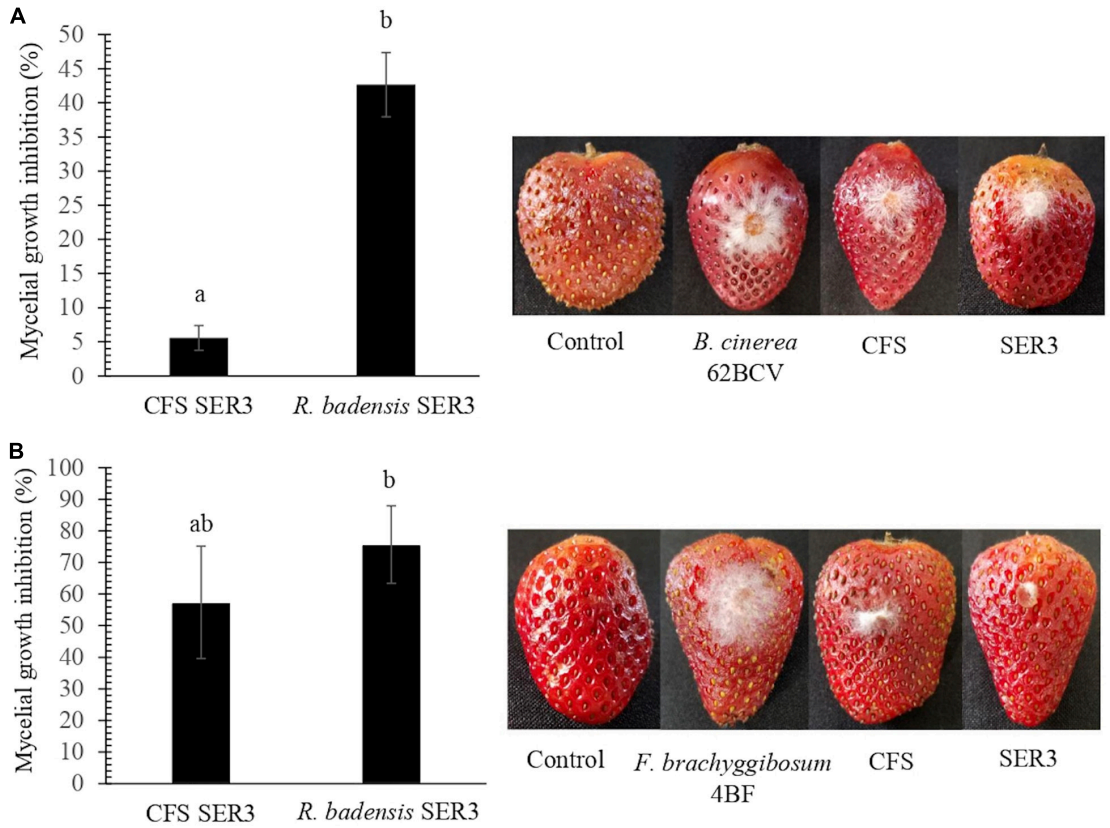

FIGURE 4 | Biocontrol effects of SER3 and its supernatant on strawberries. **(A)** Mycelial growth inhibition of *Botrytis cinerea* by the cell-free supernatant (CFS) and SER3. **(B)** Mycelial growth inhibition of *Fusarium brachyggibosum* by the CFS and SER3. Treatments consisted of sterile distilled water (control) and inoculation with pathogens, CFS from SER3, and cell suspensions of SER3. Experiments were independently performed three times, and bars represent mean ± SE ($n = 9$). Letters indicate significant difference, based on Duncan's multiple range test ($p < 0.05$).

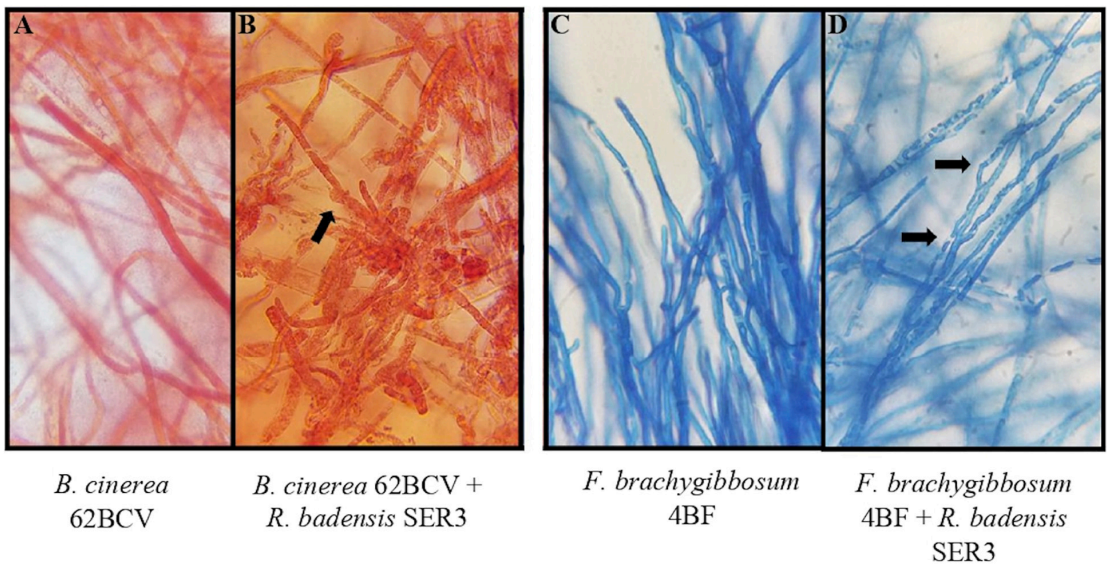

FIGURE 5 | Effect of SER3 on mycelial morphology of **(A,B)** *B. cinerea* and **(C,D)** *F. brachyggibosum*. Panels **(A,C)** represent the controls, Panels **(B,D)** show the interaction between the bacterial strain and each of the pathogens. Arrows indicate distortion of hyphae (×100 magnification).

Confrontation Assays

Once the growth and infection capacity of fungal phytopathogens was confirmed in strawberry and blueberry fruit, confrontation tests were performed using strain SER3. SER3 remarkably inhibited mycelial growth through the action of diffusible compounds against eight phytopathogens, such as *Alternaria alternata*, *Botryosphaeria rhodina*, *Mucor circinelloides*, *Botrytis* spp., *and Fusarium* spp. (**Figure 3A**). Although an inhibitory trend was observed in the growth of some phytopathogens by the action of volatile compounds from SER3, results showed that the inhibition was not significant (**Figure 3B**).

In vivo Phytopathogen Inhibition Assay Using Strain SER3

To evaluate the potential antagonism of strain SER3 against phytopathogens on fruit, two important postharvest phytopathogens (*B. cinerea* 62BCV and *Fusarium brachyggibosum* 4BF) were selected. **Figure 4** shows that SER3 produced significant mycelium growth inhibition of *B. cinerea* 62BCV through direct interaction (42.66%), while the cell-free supernatant (CFS) inhibited only 5.55% of phytopathogen growth. With *F. brachyggibosum* 4BF, mycelial growth was inhibited by 75.68%, while CFS restricted mycelial growth by 57.37%. Microscopic analysis of the mycelia of each fungal phytopathogen showed deformations and protrusions in their hyphae on application of the bacterial strain or the cell-free supernatant, whereas typical hyphae were observed in the control in the absence of strain SER3 or its CFS (**Figure 5**).

Genome Features of Strain SER3

To gain better understanding of the potential traits of strain SER3 involved in postharvest phytopathogen biocontrol, its genome was sequenced. The SER3 genome consisted of 47 contigs, and the quality of the assembly was evaluated with Quast[4], with approximately 5.08 Mb, a GC content of 52.8%, and 4,545 open reading frames, among other genes that code for ribosomal genes (**Table 2** and **Figure 6**). Similar numbers are also found in other *Rouxiella* genomes. The genome sequences were deposited in GenBank under the following accession numbers: NZ_CP049603.1; BioProject, PRJNA224116; and BioSample, SAMN14066751.

[4]http://quast.sourceforge.net/quast

TABLE 2 | Genome characteristics of strain SER3.

Size (Mb)	5.08
GC%	52.8%
Protein	4,545
rRNAs	4
tRNAs	61
Other RNA	6
Gene	4,684
Pseudogene	69
Scaffolds	1
Contigs	47
N50	255,898
L50	8

Taxonomic Affiliation of SER3

Based on the sequences of the 16S rRNA gene, SER3 showed 100% identity with the type strains of *R. badensis* DSM 100043^T (**Supplementary Figure 3**). A phylogenomic approach confirmed the close relationship with the *R. badensis* DSM 100043 type strain (**Figure 7**). Moreover, a comparison at the genomic level of strain SER3 through ANI > 95–96% and the GGDC > 70% also showed that it is strongly affiliated with *R. badensis* (**Table 3**).

Search for Biocontrol Gene Clusters in SER3 and Related Genomes

The antiSMASH program was used to determine the potential compounds involved in the postharvest biocontrol of phytopathogens by *R. badensis* SER3 and other closely related species, including two *R. badensis* strains (DSM 100043 and WG36), *Rhanella* spp., and *Serratia* spp. In the SER3 genome, biosynthetic gene clusters involved in siderophores (100%) and polyenes (77%) were observed. In addition, compounds such as thiopeptides, non-ribosomal peptide synthetases (NRPS), and polyketide synthases (PKS) were identified (**Table 4**). Similar biosynthetic clusters and percentages were observed in the other two *R. badensis* genomes analyzed, corroborating their close phylogenomic similarity. A 100% similarity was observed for siderophore biosynthetic clusters in *Rhanella* spp. and *Ewingella americana* CCUG 14506, and in *Obesumbacterium proteus* DSM 2777 and *Hafnia* spp. with a good similarity score (75%) in their respective genomes.

DISCUSSION

Berries (strawberries, blackberries, and blueberries) have a very short shelf life after harvest. Therefore, they must be immediately distributed for use, preferably under cold chain, which considerably hinders their international commercialization. High postharvest fruit losses due to phytopathogenic fungal diseases are related to high humidity levels, increased nutrients, low pH values, and low intrinsic resistance to postharvest decomposition and fungal diseases (Dukare et al., 2019). During the decomposition process, the fruit loses weight and decreases in firmness and quality, resulting in economic losses. In many instances, synthetic chemical compounds are used as coatings to avoid pathogen infections and extend their shelf life; however, toxic residues can be hazardous to human health, in addition to restricting the global commercialization of berries. Therefore, it is important to describe the phytopathogens that affect postharvest berries as well as to develop sustainable alternatives for their biological control (Abeer et al., 2013).

Here, 20 fungal strains were isolated from berries and characterized by ITS sequencing and homology searches. They showed similarity to *Botrytis* or *Fusarium*, among others. Previous reports have shown that several of these genera are phytopathogens that cause pre- and postharvest diseases in various crops, including strawberries (Dukare et al., 2019).

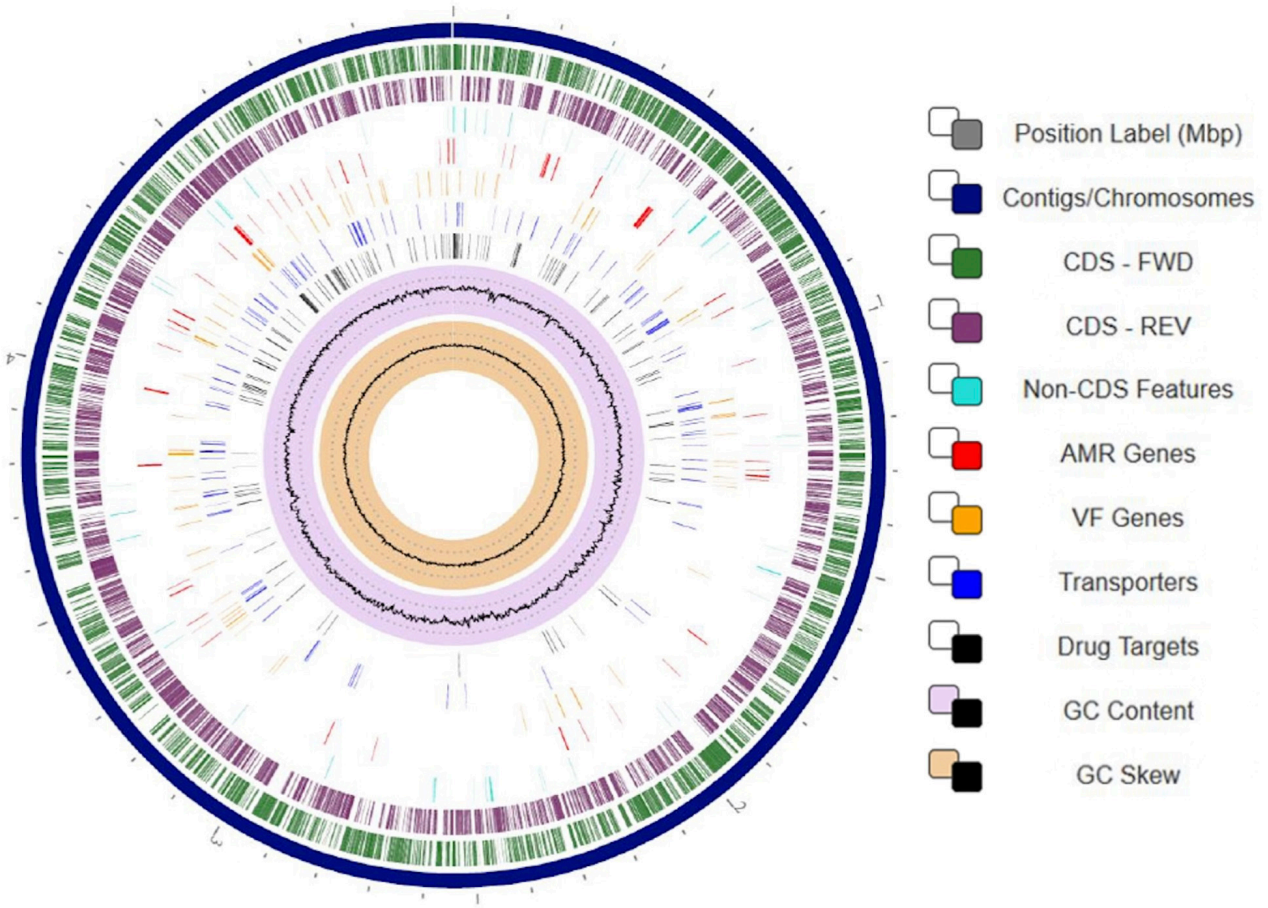

FIGURE 6 | Circular visualization of the *Rouxiella badensis* strain SER3 genome. Numbers represent megabases (Mbp). From outside to the center: 47 contigs were assembled to form a scaffold representing the chromosome (navy blue track). Genes on forward strand (green), genes on reverse strand (purple), non-CDS features (turquoise), resistance genes (red), virulence factor genes (orange), transporters (blue), drug targets (black), GC content (lilac and black), and GC skew (khaki and black). To display the circular viewer, we used genome annotation service from PATRIC (RAST tool kit).

In particular, *B. cinerea* can easily infect berries such as strawberry, blueberry, blackberry, raspberry, cranberry, and bilberry fruit, causing drastic losses after harvest (Leroux et al., 2002; Romanazzi and Feliziani, 2014; Petrasch et al., 2019). Another type of ascomycete fungus that causes damage to various crops is *Fusarium*, which is best known for affecting the roots and some aerial parts of plants, such as stems, and causes vascular browning, leaf epinasty, stunting, progressive wilting, defoliation, floral damage, and subsequent plant death (Dean et al., 2012). Herein, two strains with highly similar identity (98.3 and 99.2%) to *F. brachygibbosum* were isolated from strawberry fruit (**Table 1**). To our knowledge, *F. brachygibbosum* has not been reported as a fruit phytopathogen; therefore, this would be the first report as a postharvest pathogen in fruit such as strawberries. Further studies on the morphology of *F. brachygibbosum* and analysis of other molecular markers are being conducted by our research group to corroborate this hypothesis.

Other fungal genera found in berries were *Alternaria*, *Cladosporium*, *Geotrichum*, *Mucor*, and *Penicillium*, which have already been reported as causative agents of postharvest disease in these fruit (Koike et al., 2003; Tournas and Katsoudas, 2005; Gordon et al., 2016; López et al., 2016; Pastrana et al., 2017; Petrasch et al., 2019). It should be noted that fungi belonging to beneficial species such as *Trichoderma* have also been found in berries (Santoyo et al., 2021). In the present work, the strain *Trichoderma* sp. AF4 did not produce any apparent damage when reinoculated in strawberries and showed similar results as the uninoculated controls. Moreover, preliminary studies performed in our laboratory suggest that AF4 restricts the growth of some postharvest berry pathogens.

In agreement with the aforementioned studies, the fruit microbiome has been reported to contain not only pathogenic species but also microorganisms that can naturally help fight postharvest diseases, thus reducing losses through increased shelf life and fruit quality (Droby and Wisniewski, 2018). Consequently, we isolated the SER3 strain from the surface of a strawberry fruit, and it showed antifungal activity against *Fusarium* (**Supplementary Figure 1**). Furthermore, during activity evaluation, SER3 exhibited significant antagonism against the postharvest pathogens isolated herein. Moreover, the volatile

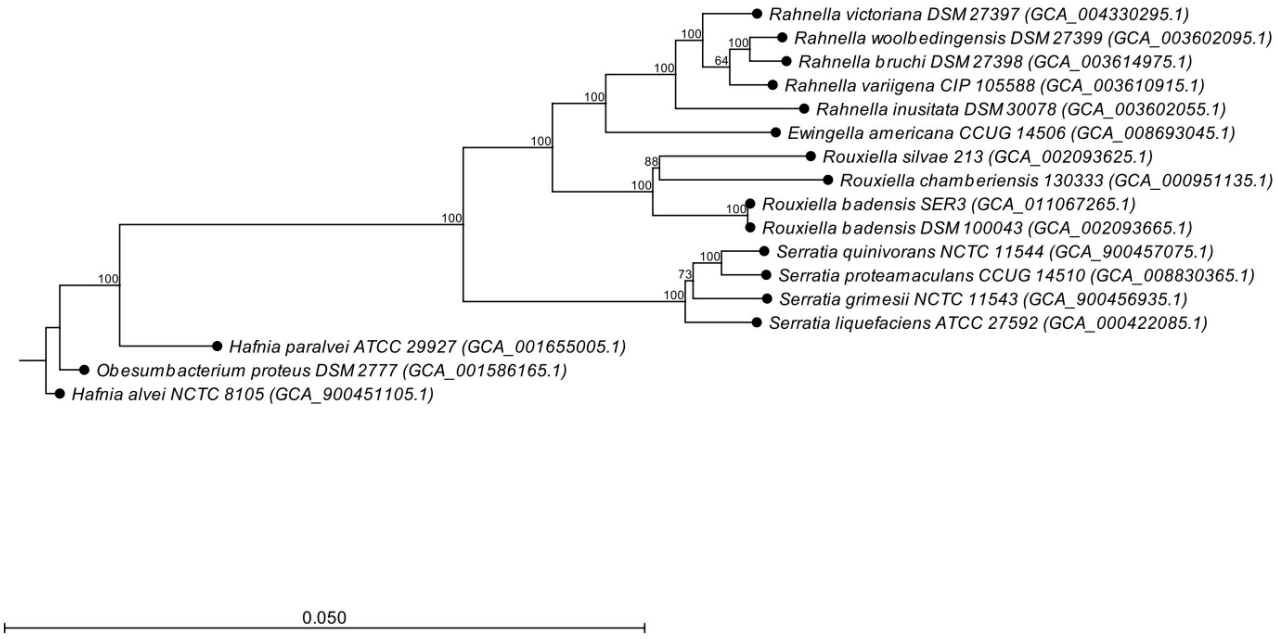

FIGURE 7 | Phylogenomic tree based on the whole genome sequence data of *Rouxiella badensis* strain SER3, including the relationship with other bacterial species. The phylogenetic tree was constructed using the neighbor-joining algorithm. Bootstrap analysis of 1,000 replications was performed and is expressed as a percentage. *Hafnia alvei* NCTC 8,105 was used as an outgroup.

compounds of SER3 also exhibited inhibition of mycelial growth, although to a lesser extent, with significant inhibition being observed only against two species, viz., *P. expansum* and *F. brachygibbosum*. These results suggested that SER3 antagonizes the phytopathogens through the action of diffusible (mainly) and volatile compounds, which is consistent with other studies showing similar mechanisms of action in other bacterial species (Hernández-León et al., 2015; Wallace et al., 2017). The inhibition of mycelial growth of postharvest phytopathogens was corroborated by *in vivo* tests on strawberry fruit using *B. cinerea* and *F. brachygibbosum*. Following the coinoculation of the SER3 strain and *B. cinerea* or *F. brachygibbosum*, the hyphae presented deformations and protrusions on the surface. This type of damage in the fungal pathogen hyphae has been observed in other studies and is associated with a reduction in fungal pathogenicity (Wallace et al., 2017; Emanuel et al., 2020).

TABLE 3 | OGRIs values obtained from the genome comparison of strain SER3 and closely related species.

Species/Strain	16S ≥98.7%	ANI ≥96%	GGDC ≥70%
Rouxiella badensis DSM 100043^T	100	99.69	98.20
Rahnella variigena CIP 105588^T	99.51	76.41	21.10
Obesumbacterium proteus DSM 2777^T	99.31	73.14	21.30
Hafnia paralvei ATCC 29927^T	99.31	72.56	20.40
Rouxiella chamberiensis 130333^T	99.31	80.56	23.80
Rahnella bruchi DSM 27398^T	99.31	76.23	20.90
Rahnella woolbedingensis DSM 27399^T	99.31	76.28	21.00
Rahnella inusitata DSM 30078^T	99.21	76.47	20.80
Rouxiella silvae 213^T	99.21	80.88	24.00
Serratia liquefaciens ATCC 27592^T	99.12	75.04	20.60
Serratia grimesii NBRC 13537^T	99.12	73.94	20.40
Ewingella americana ATCC 33852^T	99.12	76.81	21.30
Serratia proteamaculans CCUG 14510^T	99.12	74.66	20.20
Serratia quinivorans NCTC 11544^T	99.03	74.81	20.30
Rahnella victoriana DSM 27397^T	98.98	76.56	21.10
Hafnia alvei ATCC 13337^T	98.72	72.74	21.10

Given the relevant biocontrol properties of strain SER3, its genome was sequenced, and its taxonomic affiliation was assigned based on ANI and GGDC. Based on these parameters, SER3 was established to belong to the *R. badensis* species. *R. badensis* is a relatively new species described in 2017; it is a Gram-negative bacillus that forms whitish colonies, can grow optimally at 37°C, reduces nitrates, and produces acid from different sugars (Le Fléche-Matéos et al., 2017). To investigate the possible antifungal mechanism of *R. badensis* SER3, its genome was analyzed using the antiSMASH server (Blin et al., 2017), which led to the prediction of various antibiotic compounds and antifungal compounds such as siderophores, NRPS, and PKS. These three compounds are extracellular and are produced by a wide range of biocontrol bacterial species, such as *Bacillus* and *Pseudomonas*, and close relatives of *R. badensis*, such as *Rahnella aquatilis*, which have been characterized as antifungals (Calvo et al., 2007; Chen et al., 2007; Santoyo et al., 2012; Carmona-Hernandez et al., 2019). Likewise, NRPS and PKS are not exclusive to bacterial strains but can also be synthesized by phytopathogenic and beneficial fungi, such as *Trichoderma* (Mukherjee et al., 2012). Other compounds reported to have

TABLE 4 | AntiSMASH analysis and prediction of biosynthetic compounds in *R. badensis* SER3 and related bacterial genomes.

Bacterial species/strain	NRPS	Siderophore	Thiopeptide	Arylpolyene	T1PKS	T3PKS	transAT-PKS	Hserlactone	Redox-cofactor	transAT-PKS-like	thioamitides	Nrps-like	Terpene	Betalactone	RRE-containing	Ladderane	RiPP-like	Pyrrolnitrin
Rouxiella badensis SER3	38%	100%	14%	77%	+	18%	40%	+	13%	–	–	–	–	–	–	–	–	–
Rouxiella badensis DSM 100043	38%	100%	14%	72%	+	18%	40%	–	13%	–	–	–	–	–	–	–	–	–
Rouxiella badensis WG36	23%	100%	+	77%	+	12%	+	–	13%	+	–	–	–	–	–	–	–	–
Rouxiella silvae 213	–	–	14%	77%	–	–	–	–	+	–	+	20%	–	–	–	–	–	–
Rouxiella silvae Leaf50	38%	–	14%	77%	–	–	–	+	+	–	+	–	–	–	–	–	–	–
Rouxiella chamberiensis 130333	38%	–	14%	–	–	–	40%	+	+	–	–	–	100%	–	–	–	–	–
Rahnella bruchi DSM 27398	+	100%	14%	77%	–	–	–	+	–	–	–	–	–	+	13%	+	–	–
Rahnella woolbedingensis DSM 27399	–	100%	14%	77%	–	–	–	–	–	–	–	–	–	+	+	–	–	–
Rahnella inusitata DSM 30078	38%	100%	14%	66%	–	–	–	–	–	–	–	–	–	+	–	–	–	–
Rahnella variigena CIP 105588	–	100%	14%	72%	–	–	–	+	–	–	–	–	–	+	13%	–	–	–
Rahnella Victoriana DSM 27397	–	100%	14%	77%	–	–	–	2%	–	–	–	–	–	–	13%	–	–	–
Ewingella americana CCUG 14506	–	100%	14%	77%	–	–	–	–	–	–	–	–	–	+	–	–	+	–
Serratia liquefaciens ATCC 27592	57%	+	14%	83%	–	–	–	–	–	–	–	+	–	+	–	–	–	–
Serratia proteamaculans CCUG 14510	57%	+	–	73%	–	–	–	+	–	–	–	–	75%	+	–	–	–	–
Serratia quinivorans NCTC 11544	57%	+	+	77%	–	–	–	+	–	–	–	80%	–	+	–	–	–	–
Serratia grimesii NCTC 11543	57%	+	14%	77%	+	–	–	–	–	–	–	–	–	+	–	–	+	100%
Obesumbacterium proteus DSM 2777	–	75%	14%	–	–	–	–	+	–	–	–	–	–	+	–	–	–	–
Hafnia paralvei ATCC 29927	–	75%	14%	–	–	–	–	6%	–	–	–	–	–	+	–	–	–	–
Hafnia alvei NCTC 8105	–	75%	14%	+	–	–	–	+	–	–	–	–	–	+	–	–	–	–

been found in the *R. badensis* SER3 genome were a cluster of desferrioxamine-type siderophores (100% similarity), which are iron-chelating compounds (Boiteau et al., 2019) and can restrict the growth of pathogens (Kloepper et al., 1980; de los Santos-Villalobos et al., 2012). They have been reported in a wide range of biocontrol and plant growth promoter species (Crowley, 2006; Wang et al., 2020). Interestingly, the same compounds, such as siderophores, NRPS, and arylpolyene compounds, with similar percentages of identity were detected using antiSMASH in two other *R. badesis* genomes. Similarly, close relatives of *R. badensis*, such as *Rahnella*, also presented good similarity percentages with clusters for the synthesis of siderophores, thiopeptides, and arylpolyenes in their respective genomes. Other bacterial species, including those belonging to genera such as *Ewingella* (Roy Chowdhury et al., 2007), *Obesumbacterium* (Amin et al., 2014), and *Hafnia*, contain highly similar clusters for the synthesis of potential compounds, such as siderophores (100%). These results support the proven role of SER3 in the biocontrol of fungal pathogens and similar roles reported by Calvo et al. (2007) and Chen et al. (2007) in *Rahnella* and *Serratia* genera. To our knowledge, the potential role in the biocontrol of plant fungal pathogens has not been described for the rest of the bacterial species analyzed here with antiSMASH (**Table 4**).

CONCLUSION

In this study, a functional analysis of the biocontrol activities of the novel strain SER3 against postharvest pathogenic fungi of berries was performed, which showed a high genomic and phylogenetic identity with *R. badensis*. Thus, we propose a new ecological role for this species and other species of the genus *Rouxiella*. Notably, SER3 genome provides some indications of the antifungal modes of action; however, other mechanisms of biocontrol by *R. badensis* SER3 cannot be excluded, since other antifungal activities, such as the activity of lytic enzymes, have not been explored. In addition, antiSMASH analysis for other species analyzed in this study provides some clues of possible antagonistic action toward plant pathogens, although this hypothesis requires further investigation. Lastly, isolation of SER3 presents a new option in the biocontrol of postharvest pathogens of berries and provides new opportunities to investigate its role as a promoter of plant growth through direct mechanisms.

DATA AVAILABILITY STATEMENT

The datasets presented in this study can be found in online repositories. The names of the repository/repositories and accession number(s) can be found below: https://www.ncbi.nlm.nih.gov/genbank/, NZ_CP049603.1.

AUTHOR CONTRIBUTIONS

LRM-C conducted the experiments, analyzed the data, and prepared the figures and tables. SS-V and GS conceived and designed the experiments and analyzed the data. GS wrote the first draft of the manuscript. All authors contributed to manuscript revision, read, and approved the submitted version.

FUNDING

This work was supported by CONACYT-México (Propuesta A1-S-15956). LRM-C received a Ph.D. scholarship from CONACYT-México.

ACKNOWLEDGMENTS

We thank Julie Hernandez-Salmerón for excellent technical assistance with the genome assembly.

SUPPLEMENTARY MATERIAL

The Supplementary Material for this article can be found online at: https://www.frontiersin.org/articles/10.3389/fmicb.2021.709855/full#supplementary-material

Supplementary Figure 1 | Effect of diffusible compounds of SER3 following direct co-inoculation with the Fusarium pathogen. The bacterial strain was streaked onto plates in a cross shape, and mycelial plugs 4 mm in diameter were deposited at the center of the quadrants formed. Experiments were independently performed a minimum of three times. The plates were incubated, and mycelial growth was measured on day 3. The percentage of growth inhibition was measured as follows:% growth inhibition = [(Ac – Ab)/Ac] × 100, where Ac is the control mycelial area, and Ab is the mycelial area with treatment.

Supplementary Figure 2 | Koch's postulates. Berries were infected (n = 18) with spore solutions (1×10^5 spores/mL). Panel **(A)** shows blueberries inoculated with *Cladosporium sp*. 1BOA spores, while panel **(B)** shows strawberries inoculated with *Penicillium expansum* 230 spores, and panel **(C)** shows strawberries inoculated with *Mucor circinelloides* 1BF spores.

Supplementary Figure 3 | Phylogenetic tree based on the 16S ribosomal gene sequence of *Rouxiella badensis* strain SER3, including the relationship with other bacterial species (nucleotide sequence can be accessed in GenBank: CP049603). A phylogenetic tree was constructed using the maximum-likelihood algorithm. Bootstrap analysis of 1000 replications was performed and expressed as a percentage, and the most common enterobacteria were used as an outgroup.

REFERENCES

Abeer, H., Abd-Allah, E. F., Al-Obeed, R. S., Mridha, M. A. U., and Al-Huqail, A. A. (2013). Non-chemical strategies to control postharvest losses and extend the shelf life of table grape fruits. *Biol. Agric. Hortic.* 29, 82–90. doi: 10.1080/01448765.2013.763735

Allen, T., and Prosperi, P. (2016). Modeling Sustainable Food Systems. *Environ. Manage.* 57, 956–975. doi: 10.1007/s00267-016-0664-8

Amin, A. W., Anter, A. A., Ashoub, A. H., and El-Nuby, A. S. (2014). Evaluation of rhizobacteria as resistance inducers or bio-control agents for the control of Meloidogyne incognita in tomato. *Pak. J. Nematol.* 32, 211–221.

Andrews, S. (2010). *FastQC A Quality Control tool for High Throughput Sequence Data*. Available online at: http://www.bioinformatics.babraham.ac.uk/projects/fastqc

Aziz, R. K., Bartels, D., Best, A., DeJongh, M., Disz, T., Edwards, R. A., et al. (2008). The RAST Server: rapid annotations using subsystems technology. *BMC Genomics* 9:75. doi: 10.1186/1471-2164-9-75

Backer, R., Rokem, J. S., Ilangumaran, G., Lamont, J., Praslickova, D., Ricci, E., et al. (2018). Plant growth-promoting rhizobacteria: context, mechanisms of action, and roadmap to commercialization of biostimulants for sustainable agriculture. *Front. Plant Sci.* 871:1473. doi: 10.3389/fpls.2018.01473

Bankevich, A., Nurk, S., Antipov, D., Gurevich, A. A., Dvorkin, M., Kulikov, A. S., et al. (2012). SPAdes: a new genome assembly algorithm and its applications to single-cell sequencing. *J. Comput. Biol.* 19, 455–477. doi: 10.1089/cmb.2012.0021

Bertels, F., Silander, O. K., Pachkov, M., Rainey, P. B., and Van Nimwegen, E. (2014). Automated reconstruction of whole-genome phylogenies from short-sequence reads. *Mol. Biol. Evol.* 31, 1077–1088. doi: 10.1093/molbev/msu088

Blin, K., Wolf, T., Chevrette, M. G., Lu, X., Schwalen, C. J., Kautsar, S. A., et al. (2017). AntiSMASH 4.0 - improvements in chemistry prediction and gene cluster boundary identification. *Nucleic Acids Res.* 45, W36–W41. doi: 10.1093/nar/gkx319

Boiteau, R. M., Fansler, S. J., Farris, Y., Shaw, J. B., Koppenaal, D. W., Pasa-Tolic, L., et al. (2019). Siderophore profiling of co-habitating soil bacteria by ultra-high resolution mass spectrometry. *Metallomics* 11, 166–175. doi: 10.1039/c8mt00252e

Bolger, A. M., Lohse, M., and Usadel, B. (2014). Trimmomatic: a flexible trimmer for Illumina sequence data. *Bioinformatics* 30, 2114–2120. doi: 10.1093/bioinformatics/btu170

Calvo, J., Calvente, V., de Orellano, M. E., Benuzzi, D., and Sanz de Tosetti, M. I. (2007). Biological control of postharvest spoilage caused by Penicillium expansum and Botrytis cinerea in apple by using the bacterium Rahnella aquatilis. *Int. J. Food Microbiol.* 113, 251–257. doi: 10.1016/j.ijfoodmicro.2006.07.003

Carmona-Hernandez, S., Reyes-Pérez, J. J., Chiquito-Contreras, R. G., Rincon-Enriquez, G., Cerdan-Cabrera, C. R., and Hernandez-Montiel, L. G. (2019). Biocontrol of postharvest fruit fungal diseases by bacterial antagonists: a review. *Agronomy* 9:121. doi: 10.3390/agronomy9030121

Chen, F., Guo, Y. B., Wang, J. H., Li, J. Y., and Wang, H. M. (2007). Biological control of grape crown gall by Rahnella aquatilis HX2. *Plant Dis.* 91, 957–963. doi: 10.1094/PDIS-91-8-0957

Chun, J., Oren, A., Ventosa, A., Christensen, H., Arahal, D. R., da Costa, M. S., et al. (2018). Proposed minimal standards for the use of genome data for the taxonomy of prokaryotes. *Int. J. Syst. Evol. Microbiol.* 68, 1498–1513. doi: 10.1099/ijsem.0.002516

Compant, S., Duffy, B., Nowak, J., Clément, C., and Barka, E. A. (2005). Use of plant growth-promoting bacteria for biocontrol of plant diseases: principles, mechanisms of action, and future prospects. *Appl. Environ. Microbiol.* 71, 4951–4959. doi: 10.1128/AEM.71.9.4951-4959.2005

Contreras, M., Loeza, P. D., Villegas, J., Farias, R., and Santoyo, G. (2016). A glimpse of the endophytic bacterial diversity in roots of blackberry plants (Rubus fruticosus). *Genet. Mol. Res.* 15:gmr.15038542. doi: 10.4238/gmr.15038542

Córdova-Albores, L. C., Zelaya-Molina, L. X., Ávila-Alistac, N., Valenzuela-Ruíz, V., Cortés-Martínez, N. E., Parra-Cota, F. I., et al. (2020). Omics sciences potential on bioprospecting of biological control microbial agents: the case of the Mexican agro-biotechnology. *Rev. Mex. Fitopatol.* 39, 147–185. doi: 10.18781/r.mex.fit.2009-3

Crowley, D. E. (2006). "Microbial Siderophores in the plant rhizosphere,"in *Iron Nutrition in Plants and Rhizospheric Microorganisms*, eds L. L. Barton., and J. Abadia (Dordrecht: Springer), 169–198. doi: 10.1007/1-4020-4743-6_8

de los Santos-Villalobos, S., Barrera-Galicia, G. C., Miranda-Salcedo, M. A., and Peña-Cabriales, J. J. (2012). Burkholderia cepacia XXVI siderophore with biocontrol capacity against Colletotrichum gloeosporioides. *World J. Microbiol. Biotechnol.* 28, 2615–2623. doi: 10.1007/s11274-012-1071-9

Dean, R., Van Kan, J. A. L., Pretorius, Z. A., Hammond-Kosack, K. E., Di Pietro, A., Spanu, P. D., et al. (2012). The Top 10 fungal pathogens in molecular plant pathology. *Mol. Plant Pathol.* 13, 414–430. doi: 10.1111/j.1364-3703.2011.00783.x

Droby, S., and Wisniewski, M. (2018). The fruit microbiome: a new frontier for postharvest biocontrol and postharvest biology. *Postharvest Biol. Technol.* 140, 107–112. doi: 10.1016/j.postharvbio.2018.03.004

Dukare, A. S., Paul, S., Nambi, V. E., Gupta, R. K., Singh, R., Sharma, K., et al. (2019). Exploitation of microbial antagonists for the control of postharvest diseases of fruits: a review. *Crit. Rev. Food Sci. Nutr.* 68, 1498–1513. doi: 10.1080/10408398.2017.1417235

Elad, Y. (2000). Biological control of foliar pathogens by means of Trichoderma harzianum and potential modes of action. *Crop Prot.* 19, 709–714. doi: 10.1016/S0261-2194(00)00094-6

Emanuel, R. V., César Arturo, P. U., Lourdes Iveth, M. R., de la Cruz Homero, R., and Mauricio Nahuam, C. A. (2020). In vitro growth of Colletotrichum gloeosporioides is affected by butyl acetate, a compound produced during the co-culture of Trichoderma sp. and Bacillus subtilis. *3 Biotech* 10, 1–14. doi: 10.1007/s13205-020-02324-z

Fried, G., Chauvel, B., Reynaud, P., and Sache, I. (2017). "Decreases in Crop Production by Non-native Weeds, Pests, and Pathogens,"in *Impact of Biological Invasions on Ecosystem Services. Invading Nature - Springer Series in Invasion Ecology*, eds M. Vilà., and P. Hulme (Cham: Springer). doi: 10.1007/978-3-319-45121-3

Glick, B. R. (2012). Plant Growth-Promoting Bacteria : mechanisms and Applications. *Scientifica*. 2012:963401.

Gordon, T. R., Daugovish, O., Koike, S. T., Islas, C. M., Kirkpatrick, S. C., Yoshisato, J. A., et al. (2016). Options for Management of Fusarium Wilt of Strawberry in California. *Int. J. Fruit Sci.* 16, 160–168. doi: 10.1080/15538362.2016.1219294

Hernández-León, R., Rojas-Solís, D., Contreras-Pérez, M., del Orozco-Mosqueda, M. C., Macías-Rodríguez, L. I., Reyes-de la Cruz, H., et al. (2015). Characterization of the antifungal and plant growth-promoting effects of diffusible and volatile organic compounds produced by *Pseudomonas* fluorescens strains. *Biol. Control* 81, 83–92. doi: 10.1016/j.biocontrol.2014.11.011

Höfte, M., and Altier, N. (2010). Fluorescent pseudomonads as biocontrol agents for sustainable agricultural systems. *Res. Microbiol.* 161, 464–471. doi: 10.1016/j.resmic.2010.04.007

Islam, M. T., Rahman, M., Pandey, P., Jha, C. K., and Aeron, A. (2017). *Bacilli and Agrobiotechnology*. Berlin: Springer International Publishing. doi: 10.1007/978-3-319-44409-3.

Kamoun, S., Furzer, O., Jones, J. D. G., Judelson, H. S., Ali, G. S., Dalio, R. J. D., et al. (2015). The Top 10 oomycete pathogens in molecular plant pathology. *Mol. Plant Pathol.* 16, 413–434. doi: 10.1111/mpp.12190

Khan, N., Martínez-Hidalgo, P., Ice, T. A., Maymon, M., Humm, E. A., Nejat, N., et al. (2018). Antifungal activity of bacillus species against fusarium and analysis of the potential mechanisms used in biocontrol. *Front. Microbiol.* 9:2363. doi: 10.3389/fmicb.2018.02363

Kloepper, J. W., Leong, J., Teintze, M., and Schroth, M. N. (1980). *Pseudomonas* siderophores: a mechanism explaining disease-suppressive soils. *Curr. Microbiol.* 4, 317–320. doi: 10.1007/BF02602840

Koike, S. T., Vilchez, M. S., and Paulus, A. O. (2003). Fungal ecology of strawberry flower anthers and the saprobic role of Cladosporium cladosporioides in relation to fruit deformity problems. *HortScience* 38, 246–250. doi: 10.21273/hortsci.38.2.246

Koo, S. Y., and Cho, K. S. (2009). Isolation and characterization of a plant growth-promoting rhizobacterium, Serratia sp. SY5. *J. Microbiol. Biotechnol.* 19, 1431–1438.

Le Fléche-Matéos, A., Kügler, J. H., Hansen, S. H., Syldatk, C., Hausmann, R., Lomprez, F., et al. (2017). Rouxiella badensis sp. nov. and Rouxiella silvae sp. nov. isolated from peat bog soil and emendation description of the genus Rouxiella. *Int. J. Syst. Evol. Microbiol.* 67, 1255–1259. doi: 10.1099/ijsem.0.001794

Leroux, P., Fritz, R., Debieu, D., Albertini, C., Lanen, C., Bach, J., et al. (2002). Mechanisms of resistance to fungicides in field strains of Botrytis cinerea. *Pest Manag. Sci.* 58, 876–888. doi: 10.1002/ps.566

López, S. N., Sangorrín, M. P., and Pildain, M. B. (2016). Fruit rot of sweet cherries and raspberries caused by Penicillium crustosum and Mucor piriformis in

South Patagonia, Argentina. *Can. J. Plant Pathol.* 38, 511–516. doi: 10.1080/07060661.2016.1243582

Magan, N., Aldred, D., Mylona, K., and Lambert, R. J. W. (2010). Limiting mycotoxins in stored wheat. *Food Addit. Contam. Part A Chem. Anal. Control Expo. Risk Assess.* 27, 644–650. doi: 10.1080/19440040903514523

Mahuku, G. S. (2004). A simple extraction method suitable for PCR-based analysis of plant, fungal, and bacterial DNA. *Plant Mol. Biol. Report.* 22: 71–81. doi: 10.1007/bf02773351

Meier-Kolthoff, J. P., Auch, A. F., Klenk, H. P., and Göker, M. (2013). Genome sequence-based species delimitation with confidence intervals and improved distance functions. *BMC Bioinformatics* 14:60. doi: 10.1186/1471-2105-14-60

Morales-Cedeño, L. R., del Carmen Orozco-Mosqueda, M., Loeza-Lara, P. D., Parra-Cota, F. I., de los Santos-Villalobos, S., and Santoyo, G. (2021). Plant growth-promoting bacterial endophytes as biocontrol agents of pre- and post-harvest diseases: fundamentals, methods of application and future perspectives. *Microbiol. Res.* 242:126612. doi: 10.1016/j.micres.2020.126612

Mukherjee, P. K., Buensanteai, N., Moran-Diez, M. E., Druzhinina, I. S., and Kenerley, C. M. (2012). Functional analysis of non-ribosomal peptide synthetases (NRPSs) in Trichoderma virens reveals a polyketide synthase (PKS)/NRPS hybrid enzyme involved in the induced systemic resistance response in maize. *Microbiology* 158, 155–165. doi: 10.1099/mic.0.052159-0

Nam, Y. H., Hwang, B. S., Choi, A., and Chung, E. J. (2020). Isolation and characterization of strain Rouxiella sp. S1S-2 producing antibacterial compound. *Korean J. Microbiol.* 56, 152–159. doi: 10.7845/kjm.2020.0040

Pastrana, A. M., Kirkpatrick, S. C., Kong, M., Broome, J. C., and Gordon, T. R. (2017). Fusarium oxysporum f. sp. mori, a new forma specialis causing fusarium wilt of blackberry. *Plant Dis.* 101, 2066–2072. doi: 10.1094/PDIS-03-17-0428-RE

Petrasch, S., Knapp, S. J., van Kan, J. A. L., and Blanco-Ulate, B. (2019). Grey mould of strawberry, a devastating disease caused by the ubiquitous necrotrophic fungal pathogen Botrytis cinerea. *Mol. Plant Pathol.* 20, 877–892. doi: 10.1111/mpp.12794

Rojas-Solís, D., Zetter-Salmón, E., Contreras-Pérez, M., Rocha-Granados, M., del, C., Macías-Rodríguez, L., et al. (2018). *Pseudomonas* stutzeri E25 and *Stenotrophomonas* maltophilia CR71 endophytes produce antifungal volatile organic compounds and exhibit additive plant growth-promoting effects. *Biocatal. Agric. Biotechnol.* 13, 46–52. doi: 10.1016/j.bcab.2017.11.007

Romanazzi, G., and Feliziani, E. (2014). *Botrytis cinerea (Gray Mold)*. Amsterdam: Elsevier, doi: 10.1016/B978-0-12-411552-1.00004-1

Roy Chowdhury, P., Pay, J., and Braithwaite, M. (2007). Isolation, identification and ecology of Ewingella americana (the causal agent of internal stipe necrosis) from cultivated mushrooms in New Zealand. *Australas Plant Pathol.* 36, 424–428. doi: 10.1071/AP07045

Santoyo, G., del Orozco-Mosqueda, M. C., and Govindappa, M. (2012). Mechanisms of biocontrol and plant growth-promoting activity in soil bacterial species of Bacillus and *Pseudomonas*: a review. *Biocontrol Sci. Technol.* 22, 855–872. doi: 10.1080/09583157.2012.694413

Santoyo, G., Guzmán-Guzmán, P., Parra-Cota, F. I., de los Santos-Villalobos, S., del Carmen Orozco-Mosqueda, C., and Glick, B. R. (2021). Plant Growth Stimulation by Microbial Consortia. *Agronomy* 11:219. doi: 10.3390/AGRONOMY11020219

Sun, X., Ma, W., Xu, Y., Jin, X., and Ni, H. (2020). Complete Genome Sequence of Rahnella aquatilis MEM40, a Plant Growth-Promoting Rhizobacterium Isolated from Rice Rhizosphere Soil, with Antagonism against Magnaporthe oryzae and Fusarium graminearum. *Microbiol. Resour. Announc.* 9, e651–e620.

Tournas, V. H., and Katsoudas, E. (2005). Mould and yeast flora in fresh berries, grapes and citrus fruits. *Int. J. Food Microbiol.* 105, 11–17. doi: 10.1016/j.ijfoodmicro.2005.05.002

Vielva, L., De Toro, M., Lanza, V. F., and De La Cruz, F. (2017). PLACNETw: a web-based tool for plasmid reconstruction from bacterial genomes. *Bioinformatics* 33, 3796–3798. doi: 10.1093/bioinformatics/btx462

Wallace, R. L., Hirkala, D. L., and Nelson, L. M. (2017). Postharvest biological control of blue mold of apple by *Pseudomonas* fluorescens during commercial storage and potential modes of action. *Postharvest Biol. Technol.* 133, 1–11. doi: 10.1016/j.postharvbio.2017.07.003

Wang, S. S., Liu, J. M., Sun, J., Sun, Y. F., Liu, J. N., Jia, N., et al. (2019). Diversity of culture-independent bacteria and antimicrobial activity of culturable endophytic bacteria isolated from different Dendrobium stems. *Sci. Rep.* 9:10389. doi: 10.1038/s41598-019-46863-9

Wang, Z., Mei, X., Du, M., Chen, K., Jiang, M., Wang, K., et al. (2020). Potential modes of action of *Pseudomonas* fluorescens ZX during biocontrol of blue mold decay on postharvest citrus. *J. Sci. Food Agric.* 100, 744–754. doi: 10.1002/jsfa.10079

Yoon, S. H., Ha, S. M., Lim, J., Kwon, S., and Chun, J. (2017). A large-scale evaluation of algorithms to calculate average nucleotide identity. *Antonie van Leeuwenhoek* 110, 1281–1286. doi: 10.1007/s10482-017-0844-4 doi: 10.1007/s10482-017-0844-4

Conflict of Interest: The authors declare that the research was conducted in the absence of any commercial or financial relationships that could be construed as a potential conflict of interest.

Publisher's Note: All claims expressed in this article are solely those of the authors and do not necessarily represent those of their affiliated organizations, or those of the publisher, the editors and the reviewers. Any product that may be evaluated in this article, or claim that may be made by its manufacturer, is not guaranteed or endorsed by the publisher.

frontiers in Microbiology

ORIGINAL RESEARCH
published: 20 August 2021
doi: 10.3389/fmicb.2021.705329

Characteristics of Isolates of *Pseudomonas aeruginosa* and *Serratia marcescens* Associated With Post-harvest Fuzi (*Aconitum carmichaelii*) Rot and Their Novel Loop-Mediated Isothermal Amplification Detection Methods

*Meng Fu[1†], Xin Zhang[1†], Bei Chen[1], Mingzhu Li[1], Guoyan Zhang[2] and Langjun Cui[1]**

[1] The Key Laboratory of Medicinal Resources and Natural Pharmaceutical Chemistry, National Engineering Laboratory for Resource Development of Endangered Crude Drugs in Northwest China, The Ministry of Education, College of Life Sciences, Shaanxi Normal University, Xi'an, China, [2] Chenggu County Qunli Traditional Chinese Medicine Cooperative, Chenggu, China

Fuzi (the lateral root of *Aconitum carmichaelii* Debx.) is a traditional Chinese medicine that is cultivated in more than eight provinces in China. However, it can be easily devastated by post-harvest rot, causing huge losses. Therefore, it is extremely important that the primary causal pathogens of post-harvest Fuzi rot are identified and appropriate detection methods for them are developed to prevent and control losses. In this study, two bacterial strains (X1 and X2) were isolated from rotten post-harvest Fuzi. Based on their morphological, physiological, and biochemical characteristics, housekeeping gene homologies, and matrix-assisted laser desorption ionization/time-of-flight mass spectrometry (MALDI-TOF MS) results, these isolates were identified as *Pseudomonas aeruginosa* and *Serratia marcescens*. The pathogenicities of these isolates were confirmed by fulfilling Koch's postulates demonstrating that they were post-harvest Fuzi rot pathogens. Two loop-mediated isothermal amplification (LAMP) methods targeting the gyrase B subunit (*gyrB*) gene of *P. aeruginosa* and the phosphatidylinositol glycan C (*pigC*) gene of *S. marcescens* were successfully developed, and it was found that the target genes were highly specific to the two pathogens. These LAMP methods were used to detect *P. aeruginosa* and *S. marcescens* in 46 naturally occurring Fuzi and their associated rhizosphere soil samples of unknown etiology. The two bacterial assays were positive in some healthy and rotten samples and could be accomplished within 1 h at 65°C without the need for complicated, expensive instruments. To our knowledge, this is the first report of *P. aeruginosa* and *S. marcescens* causing post-harvest Fuzi rot. The newly developed methods are expected to have applications in point-of-care testing for the two pathogens under different Fuzi planting procedures and will significantly contribute to the control and prevention of Fuzi rot.

Keywords: *Aconitum carmichaelii* Debx., post-harvest, rot, *Pseudomonas aeruginosa*, *Serratia marcescens*, loop-mediated isothermal amplification

OPEN ACCESS

Edited by:
Sergio Ruffo Roberto, State University of Londrina, Brazil

Reviewed by:
Narayan Chandra Paul, Chonnam National University, South Korea
Khaled Abbas El-Tarabily, United Arab Emirates University, United Arab Emirates

****Correspondence:***
Langjun Cui
ljcui@snnu.edu.cn

† These authors have contributed equally to this work and share first authorship

Specialty section:
This article was submitted to Microbiotechnology, a section of the journal Frontiers in Microbiology

Received: *05 May 2021*
Accepted: *05 August 2021*
Published: *20 August 2021*

Citation:
Fu M, Zhang X, Chen B, Li M, Zhang G and Cui L (2021) Characteristics of Isolates of Pseudomonas aeruginosa and Serratia marcescens Associated With Post-harvest Fuzi (Aconitum carmichaelii) Rot and Their Novel Loop-Mediated Isothermal Amplification Detection Methods. Front. Microbiol. 12:705329. doi: 10.3389/fmicb.2021.705329

INTRODUCTION

Post-harvest diseases of crops are a significant issue worldwide, causing the loss of approximately 20–40% of global agricultural production (Roberto et al., 2019). Consequently, post-harvest processing, advanced disease detection, and disease prevention are extremely to minimize disease-induced damage in crops (Fang and Ramasamy, 2015). The most important post-harvest pathogens of most fruits, vegetables, and crops have now been identified and are detected using laboratory-based techniques including polymerase chain reaction (PCR), quantitative real-time PCR (qRT-PCR), immunofluorescence (IF), fluorescence *in situ* hybridization (FISH), enzyme-linked immunosorbent assay (ELISA), and loop-mediated isothermal amplification (LAMP) (Fang and Ramasamy, 2015). Each method has its advantages and limitations for disease detection, with powerful, inexpensive, and convenient methods being preferable.

Aconitum carmichaelii Debx. is a traditional Chinese medicinal plant (**Figures 1A,B**), the lateral root of which (known as Fuzi in Chinese) has been widely applied in Asia as an essential herbal drug for 2000 years. Fuzi has been used to treat various diseases, such as rheumatism, cardiovascular diseases, painful joints, syncope, and bronchial asthma (Xia et al., 2021). In the main planting regions in China, people also eat heat-cooked Fuzi in winter to prevent colds (Kao and Zhang, 2013). Due to its excellent therapeutic effects, there is a great demand for Fuzi in traditional Chinese medicine, with *A. carmichaeli* currently being cultivated in more than eight provinces in China, and the artificial planting regions having rapidly expanded in recent years. In the main planting regions of Hanzhong (Shaanxi Province) and Jiangyou (Sichuan Province), *A. carmichaelii* is often planted in the first November and harvested the following summer (from late June to early August). Under high temperature and humid conditions, post-harvest Fuzi is quickly decays within 12 h (**Figure 1C**), so harvested Fuzi is usually soaked in 20–30% Danba solution (main ingredient: $CaCl_2$) to prevent decay (Chen et al., 2020). However, this procedure can result in the various Fuzi processed products having high Danba residues, which further affects safe medication practices (Chen et al., 2020). Although low-temperature storage could prevent decay, it could increase the cost of the herb. Therefore, screening the available methods to prevent post-harvest Fuzi decay could minimize losses. However, the primary pathogens that cause post-harvest Fuzi decay and the appropriate detection methods for them are currently unknown.

In this study, *Pseudomonas aeruginosa* and *Serratia marcescens* were identified as causal pathogens of post-harvest Fuzi rot and novel LAMP methods were developed for their detection. It is hoped that these powerful methods will be convenient tools for detecting the two post-harvest Fuzi rot pathogen species, allowing companies to make more informed and timely decisions regarding their management.

MATERIALS AND METHODS

Isolation and Identification of the Post-harvest Pathogens

In July 2016, rotten and healthy post-harvest Fuzi materials were collected from Mianyang (Sichuan Province), Lijiang (Yunnan Province), and Hanzhong (Shaanxi Province) in China. Diseased tissue was excised from the rotten root and disinfected in 70% ethanol solution for 20 s, soaked in 0.1% NaOCl for 50 s, and rinsed in sterilized water three times. They were then cut with a sterilized blade, and a small block was taken from the inside of each sample and cultured on Luria-Bertani (LB) agar at 37°C. This resulted in 10 bacterial strains being isolated which were further cultured with LB liquid medium. Surface-sterilized healthy Fuzi were each inoculated with one of the isolate suspensions [10^8 colony-forming units (CFU)/mL] or distilled and deionized water (ddH_2O) as a blank control (n = 15 Fuzi per treatment consisting of three replicates). The inoculated Fuzi were then placed in a plant growth chamber (30°C and 70% relative humidity) for 15 days, and any apparent symptoms were recorded. When the visible rot zone beyond the wounded area on each Fuzi surface was more than 2 mm wide, it was scored as infected. The incidence of disease was calculated and expressed as a percentage (%), using the formula:

$$\text{Incidence of disease}(\%) = \text{Number of infected Fuzi} / \text{total number of Fuzi} \times 100\%.$$

It was found that only 2 of the 10 candidate bacterial isolates caused Fuzi rot. Therefore, these two strains were named X1 and X2. Then the two bacterial strains were re-isolated from the rotten root materials, and further confirmed based on the following detailed morphological and physiological analyses.

The morphological characteristics of isolates X1 and X2 were assessed using scanning electron microscopy, while their physiological and biochemical characteristics were analyzed according to Brenner et al. (2004) and the VITEK 2 COMPACT system (bioMérieux, Marcy-l'Étoile, France) based on Clinical and Laboratory Standards Institute guidelines.

Genomic DNA was extracted from isolates X1 and X2 using a bacterial genomic DNA extraction kit (Takara Bio Inc., Shiga, Japan) following the manufacturer's instructions. The 16S rRNA gene was then amplified using the universal bacterial primer pair 27F and 1492R (**Table 1**). The reaction system contained 12.5 μL of 2 × Taq PCR (Takara Bio Inc., Shiga, Japan), 1 μL of the F primer, 1 μL of the R primer, 20 ng of the DNA template, and enough ddH_2O to make a final volume of 20 μL. The PCR products were separated by agarose gel electrophoresis and purified with a commercial kit (Axygen, Union City, United States). The purified products were then sequenced by Sangon Biotech (Shanghai) Co., Ltd., and the sequences were aligned with the Nucleotide Basic Local Alignment Search

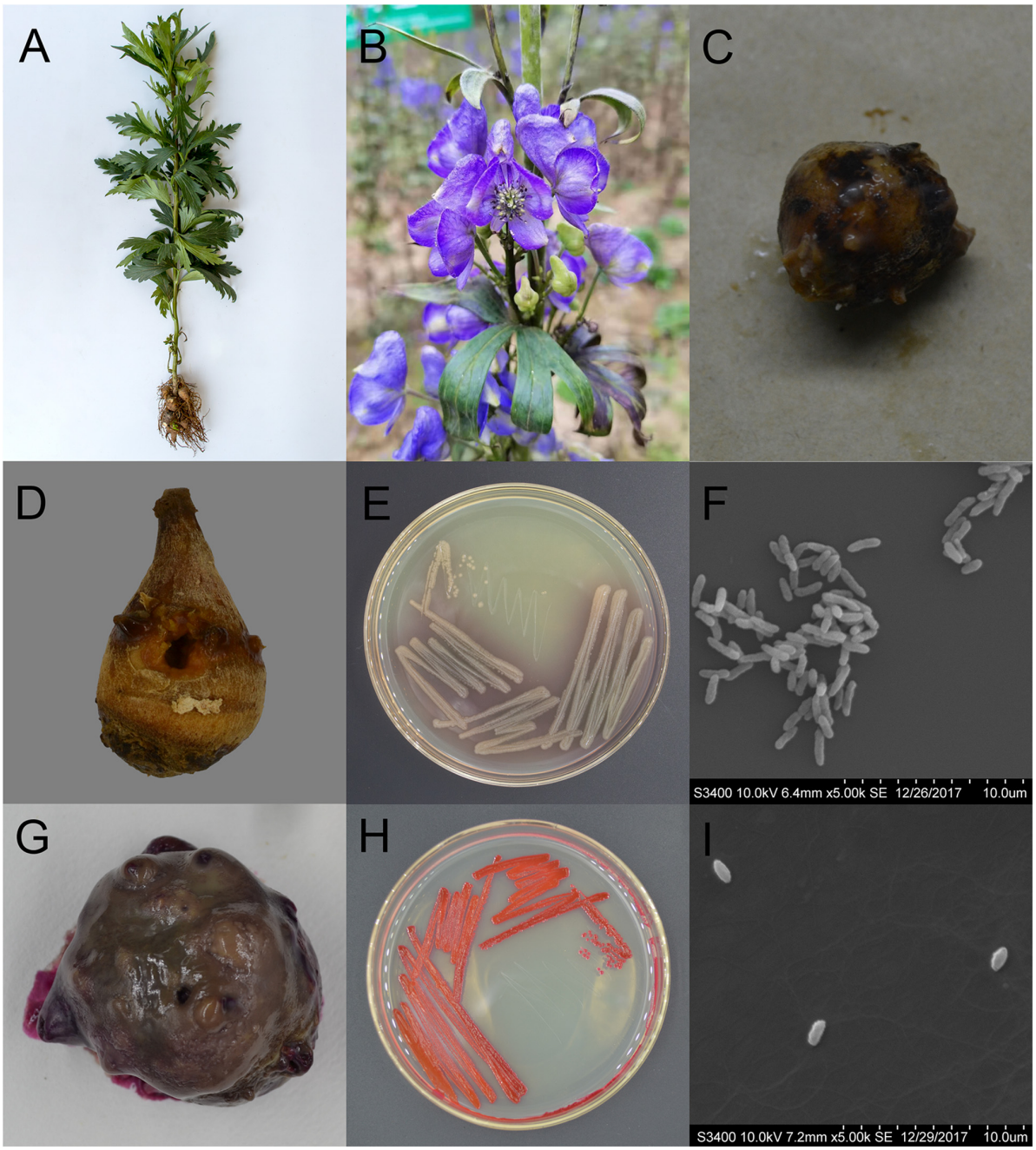

FIGURE 1 | Characteristics of *Aconitum carmichaelii* and the two isolated pathogens, Pseudomonas aeruginosa and Serratia marcescens. **(A)** *Aconitum carmichaelii* cultivars. **(B)** *Aconitum carmichaelii* flower. **(C)** Rotten Fuzi under natural conditions. **(D)** Rotten Fuzi inoculated with *Pseudomonas aeruginosa* X1. **(E)** The morphology of *Pseudomonas aeruginosa* X1 colonies on KB agar medium. **(F)** Cell of *Pseudomonas aeruginosa* X1 as observed by SEM at a magnification of ×5,000. **(G)** Rotten Fuzi inoculated with *Serratia marcescens* X2. **(H)** The morphology of *Serratia marcescens* X2 colonies on LB agar medium. **(I)** Cell of *Serratia marcescens* X2 as observed by SEM at a magnification of ×5,000.

Tool (BLASTN) online database. The housekeeping genes gyrase B subunit (*gyrB*) of X1 (Savli et al., 2003) and phosphatidylinositol glycan C (*pigC*) of X2 (Gillis et al., 2014) were amplified with relevant primers (**Table 1**) and sequenced. The 16S rRNA gene sequences and housekeeping gene sequences of closely related bacteria were then downloaded from the National Center for Biotechnology Information (NCBI),[1] and a phylogenetic tree was constructed using the neighbor-joining method and assembled in the MEGA 6.0 program.

[1]NCBI, www.ncbi.nlm.nih.gov.

TABLE 1 | Primer sets used for polymerase chain reaction (PCR) and the loop-mediated isothermal amplification (LAMP) assays.

	Name	Primers sequences	Annealing temperature
PCR primer	16S rDNA-27F	AGAGTTTGATCCTGGCTCAG	53°C
	16S rDNA-1492R	GGTTACCTTGTTACGACTT	
	gyrB-1F	CGACAATGGACGCGGTAT	55°C
	gyrB-1R	CCTTGGCTTCGTTGGGATT	
	pigC-F	AGCTGGAGCGGGAACTCA	58°C
	pigC-R	GCCGTCGAGAATCAAGGTGT	
LAMP primer	*gyrB*	**F3:** CAAGGTGTCCGGCGGCTT; **B3:** GGCTTGAAGTGAACTT CGGT; **FIP:** TTGTGGCGACGGATGGTCAG-CGGTGTGGGC GTCTCGG; **BIP:** GGTCTGGGAACAGGTCTACC-ATCGGTC TCGCCCACTTC; **LF:** TAGTTCATGGGACAGCGCGT; **LB:** GGC GTTCCGCAGTTCCCA;	Constant 65°C
	pigC	**F3:** GCGTTGAAGGCCCTGTTC; **B3:** GCAGGTAGCTGGGATC GTC; **FIP:** CAGAAGGCGCGCGATTCGG-GAGCGACACAGCG CACA; **BIP:** CAAAGCGACTTCAGCGCCTTC-CCAGCGCGGAA GACTCAA; **LF:**GGTGGGCAGGACGGTGAC; **LB:** TTCGAGTTCGGCGCCCGT	Constant 65°C

The identifications of the two isolates were further confirmed by VITEK® mass spectrometry (MS) based on matrix-assisted laser desorption ionization/time-of-flight (MALDI-TOF) technology (bioMérieux, Marcy-l'Étoile, France) following the manufacturer's recommendations. One colony of each isolate was directly spotted on the manufacturer's proprietary sample plates following the manufacturer's protocols and recommendations. α-Cyano-4-hydroxycinnamic acid matrix solution (1 μL; bioMérieux, Marcy-l'Étoile, France) was then applied to each sample and air-dried for 5 min at room temperature for crystallization. A total of three spots were analyzed on the VITEK MS system to identify the species of each isolate.

LAMP and PCR Primer Design and Reaction Systems

The specific LAMP primer sets of X1 and X2 were designed to target the housekeeping genes of *gyrB* and *pigC* using primer Explorer V5[2] and included two inner primers [forward inner primer (FIP) and backward inner primer (BIP)], two outer primers (forward primer F3 and backward primer B3), and two loop primers [loop forward primer (LF) and loop backward primer (LB)] (**Supplementary Figure 1** and **Table 1**). The PCR amplification primers were designed using the primer 5 software (**Table 1**). All primers were synthesized by Sangon Biotech (Shanghai) Co., Ltd., LAMP reactions were conducted according to Zhao et al. (2010). The optimized LAMP reaction mixture (25 μL) consisted of 1.5 × GelGreen® (Biomed, Beijing, China), 1 × ThermoPol® Reaction Buffer (New England Biolabs, Ipswich, United States), 8 mmol/L of $MgSO_4$, 1 mol/L of betaine (Sigma-Aldrich, St. Louis, United States), 1.6 mmol/L of each deoxynucleotide (dNTP), 0.2 μmol/L of each outer primer (F3 and B3), 0.4 μmol/L of each LF and LB primer, 0.8 μmol/L of each inner primer (FIP and BIP), 8 U of Bst DNA polymerase (New England Biolabs, Ipswich, United States), and 5 μL of DNA template. The LAMP reaction mixture was heated at 65°C for 60 min and the reaction was terminated by heating at 85°C for 5 min. The color of the solution, which was observed with the naked eye under blue light (470 nm), turned bright green in the presence of LAMP products and remained dark red in the absence of amplification. PCR reactions were conducted as described above. In addition, 3 μL of the products of both the LAMP reaction and PCR amplification were further detected on a standard 1% agarose gel.

[2]https://primerexplorer.jp/

LAMP Specificity and Sensitivity Tests

The two isolates X1 and X2, and the other closely related bacterial strains (**Supplementary Table 1**) were cultured with LB liquid medium. Their DNAs were then extracted and further used to test primer specificity. The DNAs of X1 and X2 were diluted to 20 ng/μL, 2 ng/μL, 200 pg/μL, 20 pg/μL, 2 pg/μL, 200 fg/μL, and 20 fg/μL, respectively, and used as templates for sensitivity testing. DNA extraction, PCR amplification, and LAMP were then carried out as described above.

Application of the LAMP Assays

A total of 46 healthy and rotten post-harvest Fuzi, and their associated rhizosphere soil samples were collected in Mianyang (Sichuan Province), Lijiang (Yunnan Province),

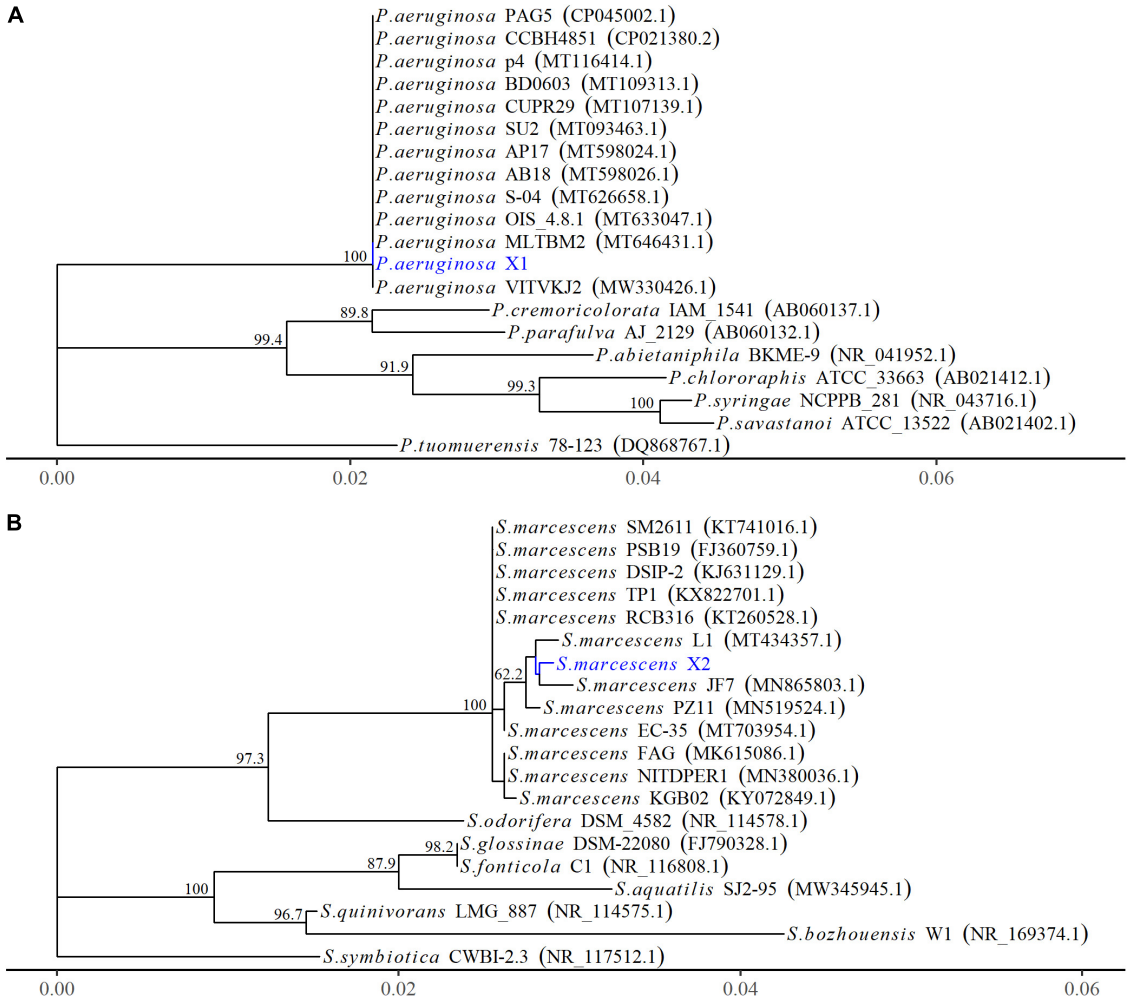

FIGURE 2 | The phylogenetic relationships of *Pseudomonas aeruginosa* and *Serratia marcescens* strains based on 16S rRNA gene. **(A)** The phylogenetic tree of *Pseudomonas aeruginosa* X1. **(B)** The phylogenetic tree of *Serratia marcescens* X2.The Phylogenetic tree was constructed using MEGA-X based on the maximum likelihood method, using the Kimura 2-parameter model. All bootstrap values > 50 from 1,000 replications are shown on the interior branch nodes. The sequences obtained in this study are in blue. GenBank accession number is provided next to the tick species name.

and Hanzhong (Shaanxi Province) (**Supplementary Table 3**). Both X1 and X2 were isolated and identified in sterilized Fuzi according to the above methods and in the rhizosphere soil samples using standard procedures. In addition, both sterilized Fuzi and soil DNAs were extracted with a commercial plant and soil genomic extraction kit (Tiangen, Beijing, China) and the two bacteria were detected in these samples using LAMP and PCR methods, as described above.

Statistical Analysis

All of the physiological and biochemical analyses, LAMP method establishment procedures, and sample assays were repeated at least four times. The data were analyzed through the chi-square test to determine whether the observations meet the theoretical expectations. The significance level when calculating the chi-square value is set to 0.05.

RESULTS

Identification and Characterization of Isolate X1

After 15 days inoculation, Fuzi inoculated with both ddH_2O and the 8 candidate bacterial isolates showed no rotten apparent symptoms. However, Fuzi inoculated with the two isolates X1 and X2 showed visible rotten symptoms, and the incidences of disease were 100% which were different significantly with the control groups [$X^2 = 15$, $X^2_{(df = 1,\ \alpha = 0{\cdot}05)} = 3.84$]. The Fuzi that were inoculated with isolate X1 showed symptoms that were identical to those observed in rotten post-harvest Fuzi, with the appearance of yellow lesions that were sunken and contained mucus (**Figure 1D**). Isolate X1 could grow well on King's B (KB) medium, with the individual colonies being smooth, round, and yellowish-green or blue-green on KB medium (**Figure 1E**), and the individual cells being short,

straight rods with dimensions of approximately 0.5–1.0 × 1.5–3.0 μm (**Figure 1F**). This bacterium could hydrolyze gelatin but not starch and could utilize mannitol but not maltose, xylose, γ-aminobutyrate, or ethylene glycol. The bacterium could also grow at temperatures up to 42°C but not at 46 or 4°C. Moreover, it could not grow in KB medium containing 8.5% NaCl. Analysis by the VITEK 2 COMPACT system indicated that L-malate, D-glucose, D-trehalose, xylitol, L-arabinose, acetate, and D-gluconate were assimilated, while erythritol, D-cellobiose, L-rhamnose, D-sorbitol, and sucrose were not assimilated by this bacterium.

The 16S rRNA gene of X1 was 1,378 bp in length (MW652657.1) and shared 100% identity with the other *P. aeruginosa* strains (MW.330426.1 and MT633047.1) (**Figure 2A**). Moreover, the housekeeping gene *gyrB* of X1 (MW691198) shared 100% identity with *P. aeruginosa* CP030910.1 and JUVT01000188.1. The MALDI-TOF MS results indicated that X1 was *P. aeruginosa* (confidence > 99.0%) (**Supplementary Figure 2A** and **Supplementary Table 2**). Therefore, based on the morphological and physiological observations, the phylogenetic analysis, and MALDI-TOF MS results, isolate X1 was classified as *P. aeruginosa*. Moreover, after X1 was reinoculated, it could lead to post-harvest Fuzi rot, and could be re-isolated from symptomatic Fuzi and had the same cultural, physiological, and biochemical characteristics as that inoculated.

Identification and Characterization of the Isolate X2

The Fuzi inoculated with isolate X2 also showed symptoms that were identical to those observed in rotten post-harvest Fuzi. Following inoculation with X2, red lesions appeared that were sunken, and the whole Fuzi was brown and soft (**Figure 1G**). The individual colonies were smooth, round, and red (or white) in color, and the individual cells were straight, round-ended rods with dimensions of 0.6–0.9 × 1.0–1.5 μm (**Figures 1H,I**). This bacterium could grow at temperatures of 37 and 40°C, but not 5°C. It could also grow in the presence of 7% (w/v) NaCl, but not 10% NaCl. It was able to assimilate L-malate, glycerol, D-galactose, gentiobiose, D-glucose, lactose, D-mannose, D-melibiose, sucrose, D-trehalose, L-arabinose, D-galacturonate, L-glutamate, D-xylose, citrate, glucuronate, and L-proline but could not assimilate D-cellobiose, erythritol, D-raffinose, D-melezitose, L-sorbose, L-rhamnose, D-turanose, or nitrate. The methyl red test was negative.

The 16S rRNA gene of X2 was 1,442 bp in length (MW652658.1) and showed 99.8% identity with the 16S rRNA genes from several other strains of *S. marcescens* identified by an NCBI BLAST query (MT434357.1 and MN519524.1) (**Figure 2B**). Moreover, the housekeeping gene *pigC* of X2 (MW691199) showed 99.8% identity with the *S. marcescens* strains (CP0313161.1 and AP019009.1). The MALDI-TOF MS results indicated that X2 was *S. marcescens* (confidence > 99.0%) (**Supplementary Figure 2B** and **Supplementary Table 2**). Therefore, based on the morphological and physiological observations, the phylogenetic analysis, and the MALDI-TOF MS results, isolate X2 was classified as *S. marcescens*. Moreover, after X2 was reinoculated, it could also lead to post-harvest Fuzi rot, and could be re-isolated from symptomatic Fuzi and had the same cultural, physiological, and biochemical characteristics as that inoculated.

Establishment of the LAMP-Based Methods

The specificities of the housekeeping genes and the LAMP primers were tested using genomic DNAs obtained from the two isolates X1 and X2, and the other closely related bacterial strains (**Supplementary Table 1**). Through conventional PCR, an 864-bp-long band from the housekeeping gene *gyrB* and a 1138-bp-long band from the housekeeping gene *pigC* were amplified in *P. aeruginosa* X1 (**Figure 3C**) and *S. marcescens* X2 (**Figure 3F**), respectively, but not in the other strains or the control (ddH_2O). Furthermore, bright green reaction products were only observed in the samples containing DNAs of *P. aeruginosa* X1 (**Figure 3A**) and *S. marcescens* X2 (**Figure 3D**). while dark red reaction products were observed for the other bacterial samples and the control. Finally, the electrophoresis results showed that the specific trapezoidal bands were only amplified in the samples of *P. aeruginosa* X1 (**Figure 3B**) and *S. marcescens* X2 (**Figure 3E**), and not in the other bacterial samples or the control. All of these results confirmed that the housekeeping gene *gyrB*, and *pigC*, and their target regions could discriminate the two bacteria from other closely related species.

The DNAs of the two bacterial isolates were serially diluted 10-fold from 20 ng/μL to 20 fg/μL, and used as DNA templates. After amplification, the reaction mixtures for *P. aeruginosa* X1 were bright green when the DNA concentration was more than 20 fg/μL (**Figure 4A**). The electrophoresis results further showed that when the DNA concentration was more than 20 fg/μL, there was a specific trapezoid strip, whereas when the DNA concentration was 20 fg/μL, no specific trapezoid strip was observed, which was consistent with the fluorescence detection results (**Figure 4B**). The sensitivity of PCR was 2 pg/μL for both *P. aeruginosa* X1 (**Figure 4C**) and *S. marcescens* X2 while the sensitivity of LAMP was 10- and 100-fold higher than this for each species, respectively (**Figures 4D–F**).

Application of LAMP and Comparison With Culture-Based Assays

A total of 46 naturally occurring Fuzi and their associated rhizosphere soil samples were evaluated using the LAMP assays to detect *P. aeruginosa* and *S. marcescens*. Among these, 13 of the Fuzi (**Figure 5A**) and 8 of the soil (**Figure 5B**) samples tested positive for *P. aeruginosa* in the LAMP assay. Similarly, 18 of the Fuzi (**Figure 6A**) and 11 of the soil (**Figure 6B**) samples tested positive in the *S. marcescens* assay. Moreover, *P. aeruginosa* could be isolated from four of Fuzi and three of the soil samples, and *S. marcescens* could be isolated from six of Fuzi and three of the soil samples (**Supplementary Table 3**).

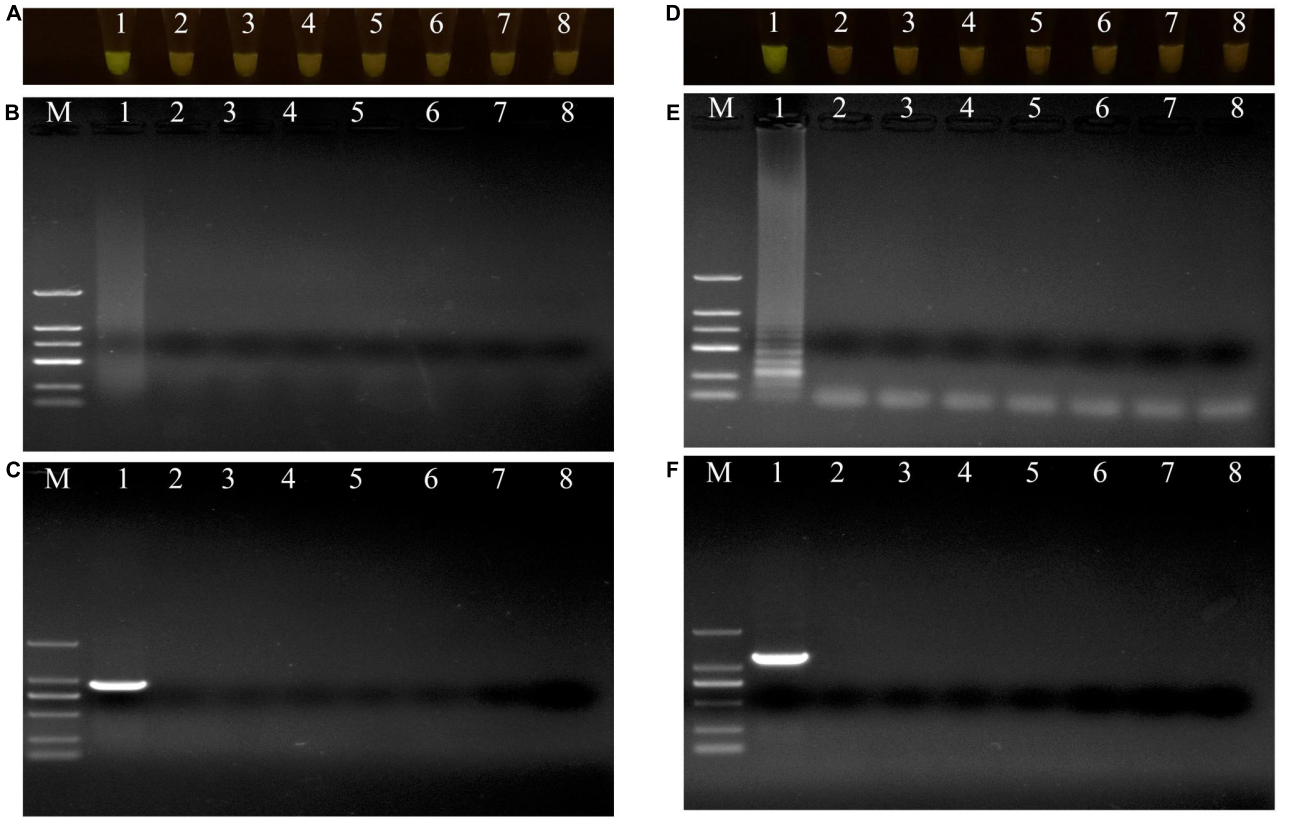

FIGURE 3 | Evaluations of specificity of loop-mediated isothermal amplification (LAMP) and polymerase chain reaction (PCR) assay. **(A–C)** Evaluation of specificity of LAMP and PCR assay for *Pseudomonas aeruginosa* X1 and the other close bacterial strains. Lane M: DNA marker DL2000; number 1–8: *Pseudomonas aeruginosa* X1, *Pseudomonas syringae* DC3000, *Pseudomonas putida* X13, *Pseudomonas psychrotolerans* 1.15631, *Pseudomonas nitroreducens* 1.1796, *Pseudomonas. toyotomiensis* 1.532, *Pseudomonas fluorescens* 1.4528, ddH_2O. **(D–F)** Evaluation of specificity of LAMP and PCR assay for *Serratia marcescens* X2 and the other close bacterial strains. Lane M: DNA marker DL2000; number 1–8: *Serratia marcescens* X2, *Serratia liquefaciens* BNCC 186068, *Serratia odorifera* Bio-67784, *Serratia plymuthica* 1.996, *Serratia fonticola* 1.995, *Serratia nematodiphla* 1.6853, *Serratia rubidaea* 1.10839, ddH_2O. **(A**,**D)** LAMP products visualized with gelgreen. Under daylight, positive reactions are shown by bright green color, and negative reactions are dark red color. **(B**,**E)** Determining the visual LAMP products by agarose gel electrophoresis. **(C**,**F)** Determining the PCR products by agarose gel electrophoresis.

DISCUSSION

In China's main planting regions of *A. carmichaelii*, post-harvest Fuzi rot can spread quickly, which can easily lead to devastation of the crop. Therefore, it is important that the main pathogens associated with post-harvest Fuzi rot are identified and suitable detection methods for them are developed to help establish economic methods for preventing such losses. In this study, two new pathogenic bacteria, *P. aeruginosa* X1 and *S. marcescens* X2, were isolated from rotten Fuzi and rapid and specific detection methods were established for them.

Both *P. aeruginosa* and *S. marcescens* can be found in many natural environments, including the atmosphere, the soil, plants, water, and hospitals (Besler and Little, 2017; Haddoudi et al., 2017; Chegini et al., 2020; Tan et al., 2020). Different strains of these species show diverse characteristics, with various strains having been proposed as pathogen/insect biocontrol agents, plant growth promotion bacteria (PGPBs) (Singh and Jha, 2016; Haddoudi et al., 2017; Kumawat et al., 2019; Al-Ghafri et al., 2020; Chandra et al., 2020; Turhan et al., 2020), and opportunistic human pathogens (Besler and Little, 2017; Tan et al., 2020). In particular, some *P. aeruginosa* strains show high intrinsic resistances to a range of antibiotics, resulting in significant morbidity and mortality rates (Chegini et al., 2020). In terms of plant diseases, several strains of *P. aeruginosa* can cause root rot in ginseng (*Panax ginseng*) (Gao et al., 2014), internal brown rot in stored onion (*Allium cepa*) bulbs (Abd-Alla et al., 2011), fruit rot in round melon (*Praecitrullus fistulosus*) (Mondal et al., 2012), and leaf disease in soybean (*Glycine max*) and lettuce (*Lactuca sativa*) (Plasencia-Márquez et al., 2017). Moreover, some strains of *S. marcescens* can induce lesions and necrosis in tobacco (*Nicotiana tabacum*) leaves, wilt virus in carrot (*Daucus carota*), yellow vine disease in sunflowers (*Helianthus* spp.), leaf chlorosis and necrotic spots in squash (*Cucurbita pepo* var. *styriaca*), leaf spot disease in industrial hemp (*Cannabis sativa*), soft rot in ginger (*Zingiber officinale*) rhizomes and many other diseases (Huang et al., 2020; Schappe et al., 2020). In this study, strains X1 and X2 were isolated from rotten post-harvest

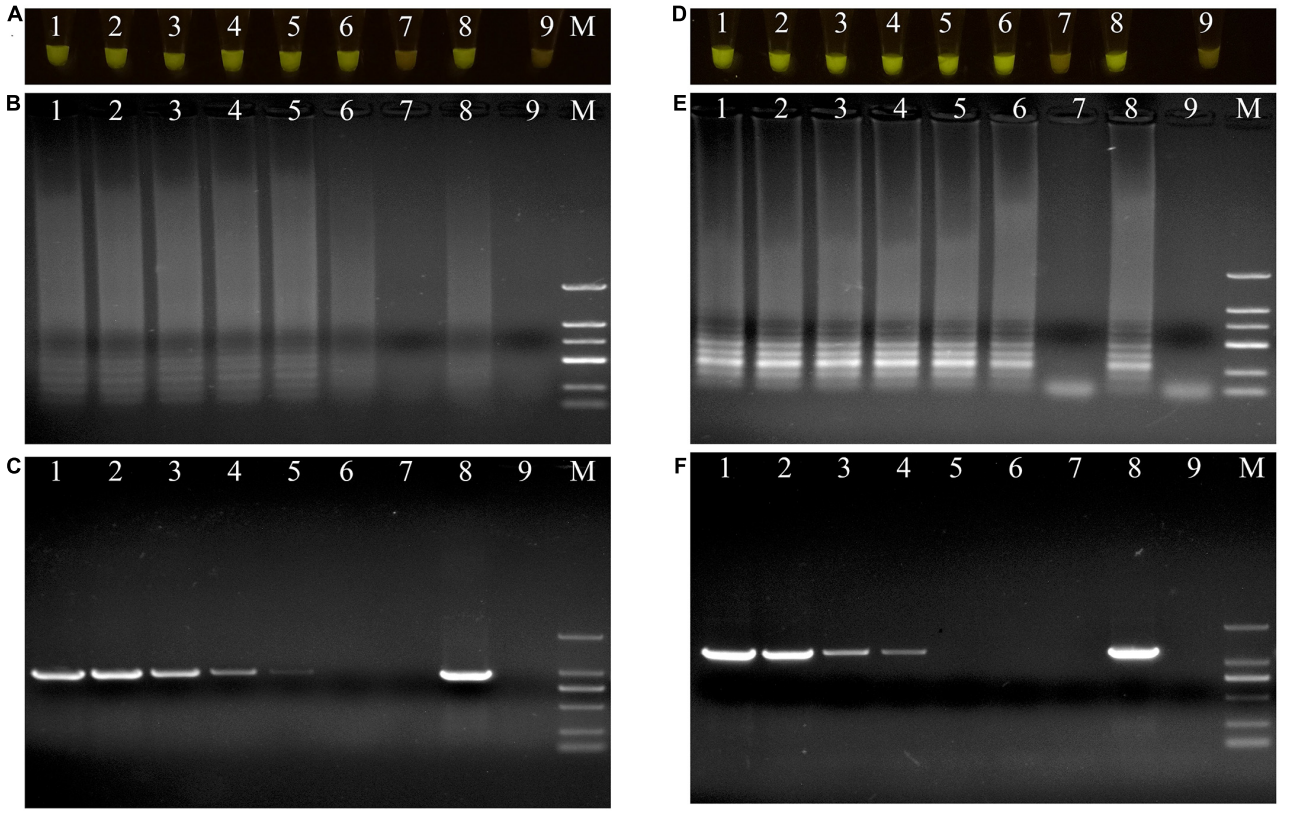

FIGURE 4 | Evaluations of sensitivity of loop-mediated isothermal amplification (LAMP) and polymerase chain reaction (PCR) assay. **(A–C)** Evaluation of sensitivity of LAMP and PCR assay for *Pseudomonas aeruginosa* X1. Lane M: DNA marker DL2000; number1–7: DNA at concentrations of 20 ng/μL, 2 ng/μL, 200 pg/μL, 20 pg/μL, 2 pg/μL, 200 fg/μL, and 20 fg/μL. number 8: positive control (*Pseudomonas aeruginosa* X1). number 9: ddH_2O. **(D–F)** Evaluation of sensitivity of LAMP and PCR assay for *Serratia marcescens* X2. Lane M: DNA marker DL2000; number 1–7: DNA at concentrations of 20 ng/μL, 2 ng/μL, 200 pg/μL, 20 pg/μL, 2 pg/μL, 200 fg/μL, and 20 fg/μL. number 8: positive control (*Serratia marcescens* X2). number 9: ddH_2O. **(A**,**D)** LAMP products visualized with gelgreen. Under daylight, positive reactions are shown by bright green color, and negative reactions are dark red color. **(B**,**E)** Determining the visual LAMP products by agarose gel electrophoresis. **(C**,**F)** Determining the PCR products by agarose gel electrophoresis.

Fuzi and were identified as *P. aeruginosa* and *S. marcescens*, respectively, based on their morphological, physiological, and biochemical characteristics, housekeeping gene homologies, and MALDI-TOF MS results. The pathogenicities of these isolates were confirmed by fulfilling Koch's postulates demonstrating they were post-harvest Fuzi rot pathogens. To our knowledge, this is the first report of *P. aeruginosa* and *S. marcescens* causing post-harvest Fuzi rot.

Although strains of both *P. aeruginosa* and *S. marcescens* strains can be PGPBs or pathogens of humans, animals, or plants, these species are not typical plant pathogens as they do not ordinarily cause visible damage to plants unless they are subjected to moderate to high temperatures and high moisture conditions. In this study, *P. aeruginosa* X1 and *S. marcescens* X2 were confirmed as post-harvest Fuzi rot pathogens. Other research has shown that the capacity of clinical isolates of *P. aeruginosa* to induce rot in vegetables was indistinguishable from that of agricultural isolates (Schroth et al., 2018). For instance, two clinical isolates from burn patients, *P. aeruginosa* PA13 and PA14, exhibited significant virulence in causing rot in all of the tested plants, especially on cucumber (*Cucumis sativus*), lettuce, potato (*Solanum tuberosum*), and tomato (*Solanum lycopersicum*) (Schroth et al., 2018). Moreover, *Serratia marcescens* YC16 isolated from rotten ginger has the potential to infect mammalian cells (Huang et al., 2020).

To date, detection methods for *P. aeruginosa* and *S. marcescens* have mainly focused on the human pathogen candidates. A number of methods have been used as diagnostic tools in clinical settings to identify *P. aeruginosa* in patient samples, such as culture-based assay, the high-throughput immunochemical method, the electrochemical detection method, and qRT-qPCR (Costaglioli et al., 2014; Alatraktchi et al., 2020; Montagut et al., 2020). However, the time and materials required for culture-based assays limit the number of samples that can be screened (Joyner et al., 2014), while the other methods are relatively difficult to operate, require expert technicians, and cannot provide real-time detection, making them less suitable for on-field testing and early warning systems (Fang and Ramasamy, 2015). Cost effective techniques based on LAMP have now emerged as substitutes for PCR because of their simplicity (only a heating block or water bath that is capable of maintaining a constant temperature of 60–65°C

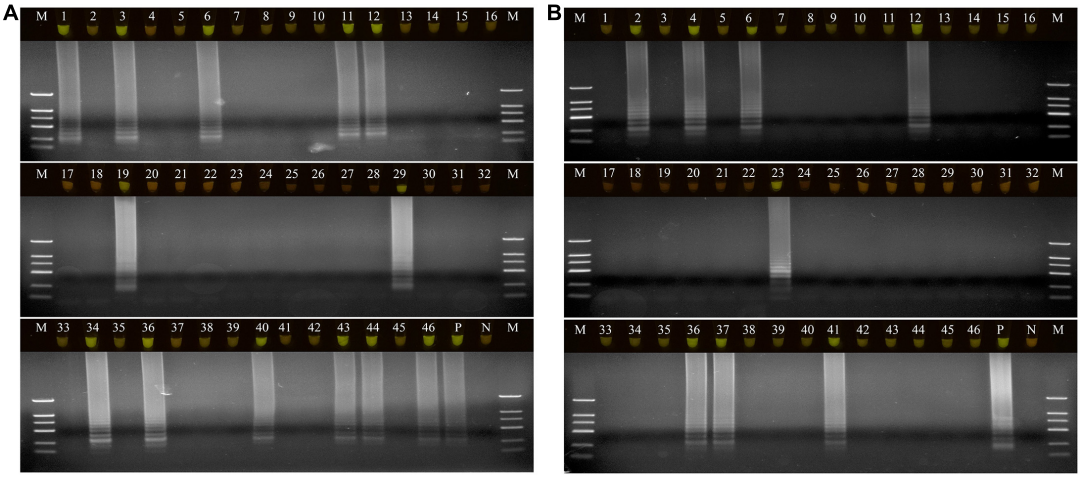

FIGURE 5 | The detection results of *Pseudomonas aeruginosa* by loop-mediated isothermal amplification (LAMP) in Fuzi and rhizosphere soil samples. **(A)** The detection results of *Pseudomonas aeruginosa* by LAMP in Fuzi samples. Lanes 1–46: different Fuzi samples. **(B)** The detection results of *Pseudomonas aeruginosa* by LAMP in Fuzi rhizosphere soil samples. Lanes 1–46: different Fuzi rhizosphere soil samples. **(Up)** LAMP products visualized with gelgreen. Under daylight, positive reactions are shown by bright green color, and negative reactions are dark red color. **(Down)** LAMP products determined by agarose gel electrophoresis. Lane M: DNA marker DL2000. Lane P: positive control (*Pseudomonas aeruginosa* X1). Lane N: negative control (ddH_2O).

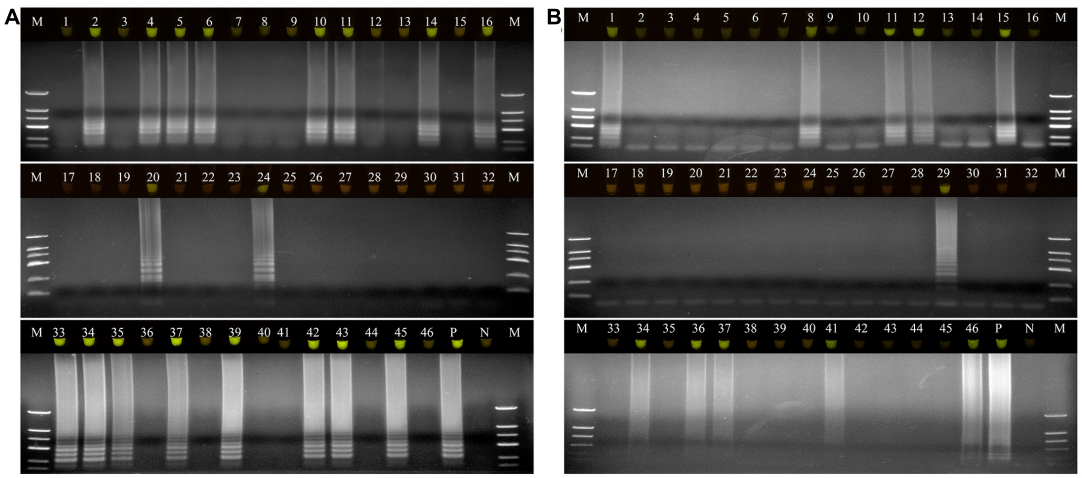

FIGURE 6 | The detection results of *Serratia marcescens* by loop-mediated isothermal amplification (LAMP) in Fuzi and rhizosphere soil samples. **(A)** The detection results of *Serratia marcescens* by LAMP in Fuzi samples. Lanes 1–46: different Fuzi samples. **(B)** The detection results of *Serratia marcescens* by LAMP in Fuzi rhizosphere soil samples. Lanes 1–46: different Fuzi rhizosphere soil samples. **(Up)** LAMP products visualized with gelgreen. Under daylight, positive reactions are shown by bright green color, and negative reactions are dark red color. **(Down)** LAMP products determined by agarose gel electrophoresis. Lane M: DNA marker DL2000. Lane P: positive control (*Serratia marcescens* X2). Lane N: negative control (ddH_2O).

is needed), rapidity, specificity, and sensitivity. For instance, Kim et al. (2016) developed a LAMP method to rapidly detect nosocomial carbapenem-resistant *P. aeruginosa* strains, using the β-lactamase genes bla_{VIM-2} and bla_{IMP-1} as targets, while Takano et al. (2019) established a novel LAMP method for assaying guiana extended-spectrum (GES) β-lactamase-producing *P. aeruginosa* strains in hospitalized patients through the detection of the gene bla_{GES}. In addition, Manajit et al. (2018) developed a uracil-DNA-glycosylase-supplemented loop-mediated isothermal amplification coupled with nanogold probe (UDG-LAMP-AuNP) method to specifically detect *P. aeruginosa* based on the extracytoplasmic function gene (*ecfX*). MALDI-TOF MS, qRT-PCR, repetitive element palindromic PCR, and next-generation sequencing methods have also been used to detect *S. marcescens* and identify potential environmental sources of infections (Iwaya et al., 2005; Joyner et al., 2014; Rödel et al., 2019; Yeo et al., 2019).

In the present study, two LAMP methods were successfully developed that targeted the genes *gyrB* of *P. aeruginosa*, and *pigC* of *S. marcescens*. The target genes and the LAMP methods were specific to these two pathogens, and LAMP methods had approximately a 10-fold higher sensitivity than conventional

PCR. The established LAMP methods were also used to detect *P. aeruginosa* and *S. marcescens* in 92 samples of unknown etiology, which included healthy and rotten Fuzi and their associated rhizospheric soil samples. The results showed that the two bacteria could be detected in several of the healthy Fuzi and their rhizospheric soil samples, indicating that they had colonized and survived in Fuzi and the soil but had not induced a rotten appearance. In the main planting regions of *A. carmichaelii*, Fuzi is harvested and directly used in culture without any washing or sterilizing procedures. Thus, it is likely that the Fuzi and/or soil act as "carriers" of *P. aeruginosa* or *S. marcescens* likely increasing the risk of *A. carmichaelii* infection with the two pathogens. In the growing season, live *A. carmichaelii* cultivars that are colonized by the two bacteria would show no disease symptoms due to the host defense mechanisms. However, the presence of these bacteria would result in drastic losses of the post-harvest Fuzi under high temperature and high moisture conditions. Other procedures, such as storage and transit, also represent potential sources of contamination by the two pathogens. Therefore, these agricultural practices should be examined as potential sources of *P. aeruginosa* and *S. marcescens*.

CONCLUSION

In conclusion, *P. aeruginosa* X1 and *S. marcescens* X2 were isolated, identified, and associated with post-harvest Fuzi rot and novel LAMP methods were developed for the detection of the two pathogens. The developed methods are rapid, convenient, efficient, specific, and sensitive, being able to be accomplished within 1 h at 65°C and not requiring any complex or expensive instruments. Thus, they represent very innovative, convenient, cheap, and rapid diagnostic tools. These methods are expected to provide point-of-care testing for the two pathogens under different Fuzi planting procedures, which will significantly contribute to the control and prevention of the Fuzi rot.

DATA AVAILABILITY STATEMENT

The datasets presented in this study can be found in online repositories. The names of the repository/repositories and accession number(s) can be found below: https://www.ncbi.nlm.nih.gov/, MW652657.1, MW652658.1, MW691198, and MW691199.

AUTHOR CONTRIBUTIONS

MF, XZ, and BC: formal analysis and writing. GZ: investigation. ML and LC: review, editing, and project administration. All authors have read and agreed to the published version of the manuscript.

FUNDING

This research was funded by the Science and Technology Benefit Program of the Ministry of Science and Technology (grant no. 2012GS610102), the Key Research and Development Program of Shaanxi Province (grant nos. 2019ZDLSF04-01-01, 2019SF-011, and 2020SF-326), and the Central University Innovation Team Project (grant no. GK202001006).

SUPPLEMENTARY MATERIAL

The Supplementary Material for this article can be found online at: https://www.frontiersin.org/articles/10.3389/fmicb.2021.705329/full#supplementary-material

REFERENCES

Abd-Alla, M. H., Mohamed, H., Bashandy, S. R., Ratering, S., and Schnell, S. (2011). First report of soft rot of onion bulbs in storage caused by *Pseudomonas aeruginosa* in Egypt. *J. Plant Interact.* 6, 229–238. doi: 10.1080/17429145.2010.535618

Alatraktchi, F. A., Svendsen, W. E., and Molin, S. (2020). Electrochemical detection of pyocyanin as a biomarker for *Pseudomonas aeruginosa*: a focused review. *Sensors* 20:5218. doi: 10.3390/s20185218

Al-Ghafri, H. M., Velazhahan, R., Shahid, M. S., and Al-Sadi, A. M. (2020). Antagonistic activity of *Pseudomonas aeruginosa* from compost against *Pythium aphanidermatum* and *Fusarium solani*. *Biocontrol Sci. Techn.* 30, 642–658. doi: 10.1080/09583157.2020.1750562

Besler, K. R., and Little, E. L. (2017). Diversity of *Serratia marcescens* strains associated with cucurbit yellow vine disease in Georgia. *Plant Dis.* 101, 129–136. doi: 10.1094/PDIS-05-16-0618-RE

Brenner, D. J., Krieg, N. R., Staley, J. T., and Garrity, G. M. (2004). Bergey's manual of systematic bacteriology (Second Edition). *Springer* 35, 799–811.

Chandra, H., Kumari, P., Bisht, R., Prasad, R., and Yadav, S. (2020). Plant growth promoting *Pseudomonas aeruginosa* from *Valeriana wallichii* displays antagonistic potential against three phytopathogenic fungi. *Mol. Bio. Rep.* 47, 6015–6026. doi: 10.1007/s11033-020-05676-0

Chegini, Z., Khoshbayan, A., Taati Moghadam, M., Farahani, I., and Shariati, A. (2020). Bacteriophage therapy against *Pseudomonas aeruginosa* biofilms: a review. *Ann. Clin. Microbiol. Antimicrob.* 19, 45–62. doi: 10.1186/s12941-020-00389-5

Chen, X., Wang, D. G., Feng, Z. P., Li, J. X., Zhang, G. Y., Liu, Z. C., et al. (2020). Establishment of a new method of processing *Aconiti Lateralis Radix Praeparata* based on Sini Decoction. Chin. *Tradit. Patent. Med.* 42, 1255–1261.

Costaglioli, P., Barthe, C., Fayon, M., Christoflour, N., Bui, S., Derlich, L., et al. (2014). Selection of *Pseudomonas aeruginosa* reference genes for RT-qPCR analysis from sputum of cystic fibrosis patients. *Mol. Cell Probe.* 28, 10–12. doi: 10.1016/j.mcp.2013.09.003

Fang, Y., and Ramasamy, R. R. (2015). Current and prospective methods for plant disease detection. *Biosensors* 5, 537–561. doi: 10.3390/bios5030537

Gao, J., Wang, Y., Wang, C. W., and Lu, B. H. (2014). First report of bacterial root rot of ginseng caused by *Pseudomonas aeruginosa* in China. *Plant Dis.* 98, 1577–1577. doi: 10.1094/PDIS-03-14-0276-PDN

Gillis, A., Rodríguez, M., and Santana, M. A. (2014). *Serratia marcescens* associated with bell pepper (*Capsicum annuum* L.) soft-rot disease under greenhouse conditions. *Eur. J. Plant Pathol.* 138, 1–8. doi: 10.1007/s10658-013-0300-x

Haddoudi, I., Sendi, Y., Batnini, M., Romdhane, S. B., Mhadhbi, H., and Mrabet, M. (2017). The bean rhizosphere *Pseudomonas aeruginosa* strain RZ9 strongly reduces *Fusarium culmorum* growth and infectiveness of plant roots. *Span. J. Agric. Res.* 15:e1003. doi: 10.5424/sjar/2017152-10595

Huang, K., Li, H. H., Pang, M., Zou, Y., Yang, D. L., and Zhang, W. L. (2020). *Serratia marcescens*: a key pathogen caused ginger rhizomes soft rot disease. *J. Plant Dis. Protec.* 127, 379–391. doi: 10.1007/s41348-020-00308-y

Iwaya, A., Nakagawa, S., Iwakura, N., Taneike, I., Kurihara, M., Kuwano, T., et al. (2005). Rapid and quantitative detection of blood *Serratia marcescens* by a real-time PCR assay: its clinical application and evaluation in a mouse infection model. *FEMS Microbiol. Lett.* 248, 163–170. doi: 10.1016/j.femsle.2005.05.041

Joyner, J., Wanless, D., Sinigalliano, C. D., and Lipp, E. K. (2014). Use of quantitative real-time PCR for direct detection of *Serratia marcescens* in marine and other aquatic environments. *Appl. Environ. Microbiol.* 80, 1679–1683. doi: 10.1128/AEM.02755-13

Kao, Y. P., and Zhang, H. W. (2013). Study on the safety and effectiveness of large-dose edible aconite. *Shaanxi J. Tradit. Chin. Med.* 34, 478–480.

Kim, H. J., Kim, H. S., Lee, J. M., Yoon, S. S., and Yong, D. (2016). Rapid detection of *Pseudomonas aeruginosa* and *Acinetobacter baumannii* harboring bla_{VIM-2}, bla_{IMP-1} and bla_{OXA-23} genes by using loop-mediated isothermal amplification methods. *Ann. Lab. Med.* 36, 15–22. doi: 10.3343/alm.2016.36.1.15

Kumawat, K. C., Sharma, P., Sirari, A., Singh, I., Gill, B. S., Singh, U., et al. (2019). Synergism of *Pseudomonas aeruginosa* (LSE-2) nodule endophyte with *Bradyrhizobium* sp. (LSBR-3) for improving plant growth, nutrient acquisition and soil health in soybean. *World J. Microb. Biot.* 35:47. doi: 10.1007/s11274-019-2622-0

Manajit, O., Longyant, S., Sithigorngul, P., and Chaivisuthangkura, P. (2018). Development of uracil-DNA-glycosylase-supplemented loop-mediated isothermal amplification coupled with nanogold probe (UDG-LAMP-AuNP) for specific detection of *Pseudomonas aeruginosa*. *Mol. Med. Rep.* 17, 5734–5743. doi: 10.3892/mmr.2018.8557

Mondal, K. K., Mani, C., Singh, J., Dave, S. R., Tipre, D. R., and Kurmar, A. (2012). Fruit rot of tinda caused by *Pseudomonas aeruginosa*-a new report from India. *Plant Dis.* 96, 141–141. doi: 10.1094/PDIS-05-11-0404

Montagut, E. J., Vilaplana, L., Martin-Gomez, M., and Marco, M. P. (2020). High-throughput immunochemical method to assess the 2-heptyl-4-quinolone quorum sensing molecule as a potential biomarker of *Pseudomonas aeruginosa* infections. *ACS Infect Dis.* 6, 3237–3246. doi: 10.1021/acsinfecdis.0c00604

Plasencia-Márquez, O., Corzo-López, M., Martínez Zubiaur, Y., Rivero, D., Devescovi, G., and Venturi, V. (2017). First report of soybean (*Glycine max*) disease caused by *Pseudomonas aeruginosa* in Cuba. *Plant Dis.* 101:11.

Roberto, S. R., Youssef, K., Hashim, A. F., and Ippolito, A. (2019). Nanomaterials as alternative control means against postharvest diseases in fruit crops. *Nanomaterials* 9:1752. doi: 10.3390/nano9121752

Rödel, J., Mellmann, A., Stein, C., Alexi, M., Kipp, F., Edel, B., et al. (2019). Use of MALDI-TOF mass spectrometry to detect nosocomial outbreaks of *Serratia marcescens* and *Citrobacter freundii*. *Eur. J. Clin. Microbiol. Infect. Dis.* 38, 581–591. doi: 10.1007/s10096-018-03462-2

Savli, H., Karadenizli, A., Kolayli, F., Gundes, S., Ozbek, U., and Vahaboglu, H. (2003). Expression stability of six housekeeping genes: a proposal for resistance gene quantification studies of *Pseudomonas aeruginosa* by real-time quantitative RT-PCR. *J. Med. Microbiol.* 52, 403–408. doi: 10.1099/jmm.0.05132-0

Schappe, T., Ritchie, D. F., and Thiessen, L. D. (2020). First report of *Serratia marcescens* causing a leaf spot disease on industrial hemp (*Cannabis sativa* L.). *Plant Dis.* 104, 1248–1249. doi: 10.1094/PDIS-04-19-0782-PDN

Schroth, M. N., Cho, J. J., Green, S. K., and Kominos, S. D. (2018). Epidemiology of *Pseudomonas aeruginosa* in agricultural areas. *J. Med. Microbiol.* 67, 1191–1201. doi: 10.1099/jmm.0.000758

Singh, R. P., and Jha, P. N. (2016). The multifarious PGPR *Serratia marcescens* CDP-13 augments induced systemic resistance and enhanced salinity tolerance of wheat (*Triticum aestivum* L.). *PLoS One* 11:e0155026. doi: 10.1371/journal.pone.0155026

Takano, C., Seki, M., Kim, D. W., Gardner, H., Mclaughlin, R. E., Kilgore, P. E., et al. (2019). Development of a novel loop-mediated isothermal amplification method to detect guiana extended-spectrum (GES) β-lactamase genes in *Pseudomonas aeruginosa*. *Front. Microbiol.* 10:25. doi: 10.3389/fmicb.2019.00025

Tan, D. G., Fu, L. L., Sun, X. P., Xu, L., and Zhang, J. M. (2020). Genetic analysis and immunoelectron microscopy of wild and mutant strains of the rubber tree endophytic bacterium *Serratia marcescens* strain ITBB B5-1 reveal key roles of a macrovesicle in storage and secretion of prodigiosin. *J. Agric. Food Chem.* 68, 5606–5615. doi: 10.1021/acs.jafc.0c00078

Turhan, E., Kiran, S., Ates, Ç, Ates, O., Kusvuran, S., and Ellialtioglu, S. S. (2020). Ameliorative effects of inoculation with *Serratia marcescens* and grafting on growth of eggplant seedlings under salt stress. *J. Plant Nutr.* 43, 594–603. doi: 10.1080/01904167.2019.1690662

Xia, F., Wang, L., Chen, J., Fu, M., Wang, G., Yan, Y., et al. (2021). Variations of microbial community in *Aconitum carmichaeli* Debx. rhizosphere soil in a short-term continuous cropping system. *J. Microbiol.* 59, 481–490. doi: 10.1007/s12275-021-0515-z

Yeo, K. T., Octavia, S., Lim, K., Lin, C., Lin, R., Thoon, K. C., et al. (2019). *Serratia marcescens* in the neonatal intensive care unit: a cluster investigation using molecular methods. *J. Infect. Public Heal.* 13, 1006–1011. doi: 10.1016/j.jiph.2019.12.003

Zhao, X., Wang, L., Chu, J., Li, Y., Li, Y., Xu, Z., et al. (2010). Development and application of a rapid and simple loop-mediated isothermal amplification method for food-borne *Salmonella* detection. *Food Sci. Biotechnol.* 19, 1655–1659. doi: 10.1007/s10068-010-0234-4

Conflict of Interest: The authors declare that the research was conducted in the absence of any commercial or financial relationships that could be construed as a potential conflict of interest.

Publisher's Note: All claims expressed in this article are solely those of the authors and do not necessarily represent those of their affiliated organizations, or those of the publisher, the editors and the reviewers. Any product that may be evaluated in this article, or claim that may be made by its manufacturer, is not guaranteed or endorsed by the publisher.

frontiers in Microbiology

ORIGINAL RESEARCH
published: 27 August 2021
doi: 10.3389/fmicb.2021.729014

Dynamic Microbiome Changes Reveal the Effect of 1-Methylcyclopropene Treatment on Reducing Post-harvest Fruit Decay in "Doyenne du Comice" Pear

*Yang Zhang[1], Congcong Gao[1], Md. Mahidul Islam Masum[2], Yudou Cheng[1], Chuangqi Wei[1], Yeqing Guan[1] and Junfeng Guan[1]**

[1] Plant Genetic Engineering Center of Hebei Province, Institute of Biotechnology and Food Science, Hebei Academy of Agriculture and Forestry Sciences, Shijiazhuang, China, [2] Department of Plant Pathology, Bangabandhu Sheikh Mujibur Rahman Agricultural University, Gazipur, Bangladesh

Pathogen-induced decay is one of the most common causes of fruit loss, resulting in substantial economic loss and posing a health risk to humans. As an ethylene action inhibitor, 1-methylcyclopropene (1-MCP) can significantly reduce fruit decay, but its effect on fruit pathogens remains unclear. Herein, the change in microbial community structure was analyzed using the high-throughput sequencing technology, and characteristics related to fruit quality were determined after 1-MCP (1.0 Ml L^{-1}) treatment in "Doyenne du Comiceis" pear fruit during storage at ambient temperature. Overall, 1-MCP was highly effective in reducing disease incidence and induced multiple changes of the fungal and bacterial microbiota. At day 15, the microbial diversity of fungi or bacteria was reduced significantly in the control fruit (non-treated with 1-MCP), which had the most severe decay incidence. For fungi, in addition to *Alternaria* being the most abundant in both 1-MCP treatment (59.89%) and control (40.18%), the abundances of *Botryosphaeria* (16.75%), *Penicillium* (8.81%), and *Fusarium* (6.47%) increased significantly with the extension of storage time. They became the primary pathogens to cause fruit decay in control, but they were markedly decreased in 1-MCP treatment, resulting in reduced disease incidence. For bacteria, the abundance of *Gluconobacter* (50.89%) increased dramatically at day 15 in the control fruit, showing that it also played a crucial role in fruit decay. In addition, *Botryosphaeria*, *Fusarium* fungi, and *Massilia*, *Kineococcus* bacteria were identified as biomarkers to distinguish 1-MCP treatment and control using Random Forest analysis. The redundancy analysis (RDA) result showed that the amount of *Botryosphaeria*, *Penicillium*, and *Fusarium* were positively correlated with disease incidence and respiration rate of pear fruits while negatively correlated with fruit firmness. This investigation is the first comprehensive analysis of the microbiome response to 1-MCP treatment in post-harvest pear fruit, and reveals the relationship between fruit decay and microbial composition in pear fruit.

Keywords: microbiome, 1-MCP, pear, fruit quality, decay

OPEN ACCESS

Edited by:
Khamis Youssef, Agricultural Research Center, Egypt

Reviewed by:
Dov Bernard Prusky, Agricultural Research Organization (ARO), Israel
Debdulal Banerjee, Vidyasagar University, India

****Correspondence:***
Junfeng Guan
junfeng-guan@263.net

Specialty section:
This article was submitted to Food Microbiology, a section of the journal Frontiers in Microbiology

Received: *22 June 2021*
Accepted: *02 August 2021*
Published: *27 August 2021*

Citation:
Zhang Y, Gao C, Masum MMI, Cheng Y, Wei C, Guan Y and Guan J (2021) Dynamic Microbiome Changes Reveal the Effect of 1-Methylcyclopropene Treatment on Reducing Post-harvest Fruit Decay in "Doyenne du Comice" Pear. Front. Microbiol. 12:729014. doi: 10.3389/fmicb.2021.729014

INTRODUCTION

As one of the three deciduous fruit trees, pear is an important fruit crop grown throughout the temperate zone. *Pyrus communis* L. cv. "Doyenne du Comice" is very popular among consumers because of its gorgeous appearance, rich fragrance, soft and juicy flesh, high commodity value, and health care value (López et al., 2001). However, the fruit decay caused by pathogenic agents has seriously limited the post-harvest shelf life.

Pathogen-induced decay is the most crucial reason for post-harvest fruit loss among many other factors such as environmental conditions, sprouting, quality loss, and overripening (Sommer, 1985; Buchholz et al., 2018). Disease losses in pears are mainly caused by fungi, including blue mold caused by *Penicillium expansum*, gray mold caused by *Botrytis cinerea*, bitter rot caused by *Glomerella cingulate*, and Mucor rot caused by *Mucor piriformis* (Mari et al., 2003; Sardella et al., 2016; Luciano-Rosario et al., 2020). In recent years, there has been an increasing number of reports of fungal infections in pears on different cultivars worldwide. The interactions between pathogens, including fungi and bacteria, and plants have been extensively studied, but much remains to be explored about the diversity of fruit microbiome during post-harvest storage, especially the pathogens causing fruit decay (Willersinn et al., 2015; Buchholz et al., 2018).

To date, various chemical and physical methods have been used to maintain the quality of fruits and to reduce the damage of pathogens (Wassermann et al., 2019; Aslam et al., 2020). By competing with ethylene for binding receptors, 1-methylcyclopropene (1-MCP), as an ethylene action inhibitor, delays ethylene-mediated physiological and biochemical responses related to fruit ripening. Thus, 1-MCP has been widely used to store and preserve fruits and vegetables as a new fresh-keeping agent (Jiang et al., 2004; Khan and Singh, 2007; Zhang et al., 2012; Li et al., 2013). Several reports have shown that 1-MCP reduces fruit decay in various fruits under proper concentration (Dou et al., 2005; Xu et al., 2017; Min et al., 2018). However, these studies mainly focused on the inhibition effect of 1-MCP on some particular pathogens or diseases; the impact of 1-MCP on the microbial diversity of post-harvest fruits remains unclear. Therefore, we anticipate that this study will contribute to a deeper understanding of 1-MCP using post-harvest fruit storage.

Initially, the effect of fresh-keeping agents on fruit microorganisms was studied using traditional approaches, such as pathogen isolation, colony counts of bacteria and molds, and denaturing gradient gel electrophoresis (DGGE) technology (Sheffield et al., 1989; Feroz et al., 2016; Lin et al., 2018). However, these methods required re-culturing microorganisms in a nutrient medium, which led to the loss of many slow-growing but important microorganisms. The microbiome can greatly delineate the composition, structure, and diversity of microbial populations in various environments. The development of DNA sequencing technology has made the microbiome an efficient and direct means to explore biological diversity in post-harvest fruit (Droby and Wisniewski, 2018; Zhang et al., 2020; Taîbi et al., 2021).

In the present study, we have performed a DNA metabarcoding approach to investigate the fruit microbiome changes induced by 1-MCP treatment in post-harvest pear storage. Furthermore, the relationship among the disease incidence, fruit quality, physiological characteristics, and microbial composition was also demonstrated after the 1-MCP treatment in the pear fruit.

MATERIALS AND METHODS

Material Collection and Treatments

The "Doyenne du Comice" pear (*P. communis* L.) fruits were harvested at maturity stage (July 2020) from an orchard of Shenzhou City (115.490266°E, 38.05122°N), Hebei Province, China, and transported to the Lab directly. Fruits with similar weight (about 120 g per fruit) were randomly divided into two groups: one was treated with 1.0 μl L^{-1} 1-MCP (SmartFresh, AgroFresh, United States) at 25°C for 14 h and another was set as control (CK) without 1-MCP. Then, the fruits were stored at 25 ± 0.5°C and relative humidity of 90 ± 5% for 0, 5, 10, and 15 days. The treatments were marked as CK0d, CK5d, CK10d, and CK15d, representing fruits stored for 0, 5, 10, and 15 days in the control group, while MCP0d, MCP5d, MCP10d, and MCP15d represent fruits stored for 0, 5, 10, and 15 days in 1-MCP treated group, respectively.

Analysis of Microbial Diversity

DNA Extraction and Illumina Sequencing

For sampling, four pieces of fruit tissue, including pulp and peel (about 40 g, 1 cm thick) were symmetrically taken from each fruit, and the samples were homogenized with a blender. Total microbial DNA was extracted from the fruit homogenate. Each treatment contained five replicates, and each replicate had five fruits. The 16S rRNA genes V4–V5 region was amplified with the primers 799F (5′-AAC MGG ATT AGA TAC CCK G-3′) and 1193R (5′-ACG TCA TCC CCA CCT TCC-3′). The ITS1 region of the fungal community was amplified with the primer ITS1F (5′-CTT GGT CAT TTA GAG GAA GTA A-3′) and ITS2 (5′-GCT GCG TTC TTC ATC GAT GC-3′). The PCR products were sequenced on an Illumina MiSeq/NovaSeq platform at Personal Biotechnology, Shanghai, China.

Sequence Analysis

After the barcode sequence was removed, sequence denoising was carried out according to the QIIME 2 DADA2 analysis process (Bolyen et al., 2019). The number of amplicon sequence variants (ASVs) at each of the seven taxonomic levels including domain, phylum, class, order, family, genus, and species was counted according to the results of taxonomic annotations, and the flower plot was performed by the genes cloud tools, a free online platform for data analysis[1]. Taxonomic composition was analyzed after all samples were adjusted to the same sequencing depth, and microbial dynamics at each taxonomic level were shown. Biomarker identification was analyzed by using Random

[1]https://www.genescloud.cn

Forest with the function of "classify-samples-ncv" in Q2-sample-classifier. Correlations of fungi and bacteria were performed by the gene cloud tools. Relationship among fruit quality, physiological characteristics, and microbial community diversity was analyzed using redundancy analysis (RDA) and plotted by the gene cloud tools.

Fungi Isolation and Identification

A small piece of fruit tissue was cut off from the diseased spot, soaked in 70% alcohol for 30 s, washed with sterile water three times, and then placed on the PDA medium. After 3–5 days of incubation at 25°C, mycelium was picked from the edge of the colony and transferred to a fresh PDA medium for purification. After two or three times of purification, a single pure colony was obtained as no contamination of other fungi was detected under a microscope (OLYMPUS BX51, Japan). The purified colonies were inoculated in PDA inclined medium for 2 days and then stored at 4°C for further use.

Based on the isolation of four strains of pathogenic fungi, 0.1 g of activated fungal hyphae was taken and ground into powder with liquid nitrogen. Total fungal DNA was extracted using the fungal genomic DNA rapid extraction kit (Sangon Biotech, Shanghai) according to the instructions. DNA samples were amplified with primers of ITS1/ITS4 and sequenced by Sangon Biotech (Shanghai). The obtained sequences were BLAST at NCBI to complete fungal identification.

Fungal Membrane Integrity Determined by Fluorescence Microscope

Fungal membrane integrity was performed according to the method described by Li and Tian (2006). Fungal spores were treated with 1.0 $\mu l\ L^{-1}$ 1-MCP for 14 h, and stained with 10 $\mu g\ ml^{-1}$ of propidium iodide (PI) (Sangon Biotech, Shanghai) for 10 min at 30°C in the dark. The spores were observed and photographed using a microscope (OLYMPUS BX51, Japan), equipped with a luciferin rhodonine filter set (OLYMPUS U-RFL-T, Japan). The fungal membrane integrity rate (MIR) was calculated by the following formula: MIR = [1 − (the number of red spores/the number of total spores)] × 100%.

Disease Incidence

Disease incidence was calculated as the ratio of the number of fruits with visible disease spots to the total number of fruit ($n = 30$). Each treatment had five replicates.

Assessment of Fruit Quality and Physiological Characteristics

Fruit Quality

Fruit quality including firmness, soluble solid content (SSC), and titratable acidity (TA) were measured as our previous study (Cheng et al., 2019). For firmness, pear fruit was peeled about 1-mm thick at the equator and was determined with a handheld firmness meter (GY-4, Tuopu, China). SSC was measured using a PAL-1 handheld digital saccharimeter (ATGAO, Japan). TA was measured using the method of acid–base titration. Each treatment was conducted in triplication, and each replication consists of five fruits.

Respiration Rate and Ethylene Production Rate

The respiration rate was analyzed using an infrared CO_2 analyzer (HWF-1A, Kexi Instruments, China), and the ethylene content was analyzed using a gas chromatograph (GC-9790II, Fuli Instruments, China) and calculated to ethylene production rate. Each treatment had three replicates and 10 fruits per replication.

Weight Loss Ratio

The weight loss ratio of pear fruit was calculated by comparing the fruit weight at each time point after treatment with that at day 0. Each treatment had three replicates with 10 fruits per replicate.

Statistical Analysis

The graphs were generated by using the GraphPad Prism 8 software (GraphPad Inc., CA, United States). The significant differences between treatments were tested by two-way analysis of variance (ANOVA), and differences were considered to be significant at $p < 0.05$ (*), $p < 0.01$ (**), and $p < 0.001$ (***). In addition, sequence data analyses were performed using QIIME 2 and R packages (v4.0.3).

RESULTS

1-Methylcyclopropene Reduced Decay of Pear Fruit

To determine the effect of 1-MCP in resistance to fruit disease, the disease incidence of fruit decay was compared between 1-MCP treatment and CK after 0, 5, 10, and 15 days of storage. As shown in **Figure 1A**, many hyphae were observed on the surface of the fruits in the CK group, but few in the 1-MCP treatment group after 10 and 15 days of storage, indicating that fruits treated differently showed different resistance to pathogens. Further results showed that there was no significant difference in disease incidence at day 5 between the 1-MCP group and the control group, while there was a significant difference ($p < 0.01$) at day 10 and a very significant difference ($p < 0.001$) at day 15 (**Figure 1B**).

1-Methylcyclopropene Affected Microbial Diversity in Pear Fruit

Number of Amplicon Sequence Variants

In order to show the effect of 1-MCP on the microbial diversity in fruit, we compared the number of ASVs with different treatments (**Supplementary Table 1**). As shown in **Supplementary Figure 1**, the number of ASVs of both fungi and bacteria in CK at day 15 (CK15d) was much smaller than that in other treatments, indicating that some dominant species of fungi or bacteria affected the microbial diversity in CK at day 15.

Taxonomic Composition of Fruit Microorganisms

The dominant microorganisms are much more likely to be the pathogens causing fruit decay. Therefore, the 10 most abundant fungal or bacterial taxa were analyzed at the levels of

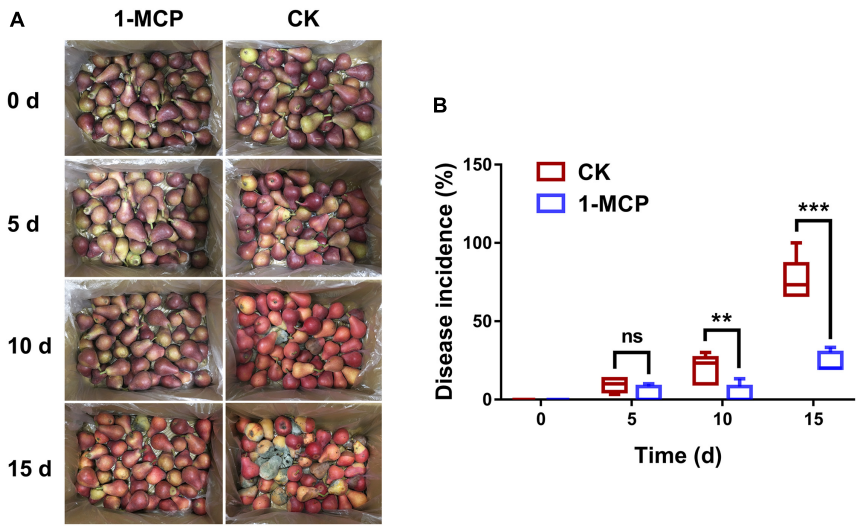

FIGURE 1 | Pear (*Pyrus communis* L.cv. "Doyenne du Comice") fruit decay was reduced by 1.0 μl L^{-1} 1-methylcyclopropene (MCP) during storage. **(A)** Symptoms of pear decay during storage. **(B)** Disease incidence of pear fruit during storage. The disease incidence rate was calculated using the formula as the number of fruits with visible disease spots/the total number of fruits × 100. Each treatment had five replicates. The asterisk represents the significance between the different treatments (**$p < 0.01$; ***$p < 0.001$).

phylum, class, order, family, and genus (**Figures 2**, **3**). The same sequencing scale was used for subsequent analysis to compare the dynamic changes of fungi or bacteria in different treatments.

For fungi, *Ascomycota* and *Basidiomycota* were superior in all samples at the phylum level. Interestingly, in contrast to the 1-MCP treatment group, the abundance of *Ascomycetes* in the control group increased over time, while the abundance of *Basidiomycetes* decreased, indicating that *Ascomycetes* became the dominant pathogen causing the fruit decay and that 1-MCP had a significant effect on the fungal microbiota in pear fruit. At the class level, *Dothideomycetes* (63.66%), *Sordariomycetes* (19.73%), and *Eurotiomycetes* (8.82%) increased significantly in CK15d, while *Tremellomycetes* decreased over time. *Pleosporales* (41.70%), *Dothideales* (5.07%), *Hypocreales* (19.71%), *Eurotiales* (8.81%), and *Botryosphaeriales* (16.75%) were the most common order in CK15d, while *Pleosporales* (63.63%), *Capnodiales* (4.39%), *Dothideales* (2.69%), and *Filobasidiales* (3.24%) were abundant in MCP15d. At the family level, *Pleosporaceae* (40.18%), *Aureobasidiaceae* (5.07%), *Nectriaceae* (19.68%), *Botryosphaeriaceae* (16.75%), and *Aspergillaceae* (8.81%) were the most abundant fungal group in CK15d, while *Pleosporaceae* (59.89%), *Aureobasidiaceae* (2.68%), *Filobasidiaceae* (3.24%), and *Didymellaceae* (3.58%) were in MCP15d. At the genus level, *Alternaria* (40.18%), *Aureobasidium* (5.05%), *Botryosphaeria* (16.75%), *Penicillium* (8.81%), and *Fusarium* (6.47%) accounted for the largest proportion in CK15d, while *Alternaria* (59.89%), *Aureobasidium* (2.68%), *Filobasidium* (3.07%), and *Didymella* (2.69%) accounted for MCP15d. In particular, *Alternaria*, *Botryosphaeria*, *Penicillium*, and *Fusarium* increased significantly in CK15d compared with CK0d, indicating that these fungi were likely to be the major pathogens that caused fruit decay.

For bacteria, *Proteobacteria* was the overwhelming majority at phylum level across all samples, while *Firmicutes* and *Bacteroidetes* were squeezed out after 15 days of storage. At class level, *Gammaproteobacteria* (25.72%) and *Alphaproteobacteria* (70.92%) occupied the prominent positions in CK15d, while *Gammaproteobacteria* (42.02%), *Alphaproteobacteria* (39.33%), *Clostridia* (6.25%), and *Actinobacteria* (6.38%) remained abundant in MCP15d. At order level, *Acetobacterales* (70.33%) and *Enterobacteriales* (24.84%) squeezed *Betaproteobacteriales* (0.76%) out of competition in CK15d, while *Betaproteobacteriales* (30.32%) remained abundant in MCP15d even though *Acetobacterales* (27.88%) increased considerably. Similarly, the family *Acetobacteraceae* (70.33%) and *Enterobacteriaceae* (24.84%) increased significantly in CK15d, while *Burkholderiaceae* (30.09%), *Acetobacteraceae* (27.87%), and *Enterobacteriaceae* (7.77%) were the most prevalent bacterial groups in MCP15d. In CK15d, *Gluconobacter* (50.89%) was the dominant bacterial taxonomic community at the genus level, whereas in MCP15d, *Gluconobacter* (26.99%) and *Massilia* (18.71%) were the most common, indicating that 1-MCP induced multiple changes in bacterial microbiota in pear fruit.

Biomarker Identification Associated With 1-Methylcyclopropene-Treated Pear Fruit

Random Forest algorithm is a well-known and powerful machine learning algorithm based on the decision tree, and it is particularly well suited to microbial community data, which often presents discrete and discontinuous distributions (Breiman, 2001). In this study, Random Forest was used to analyze the biomarkers of intergroup differences between 1-MCP treatment and control at the genus level. As shown in **Figure 4**, the top 20 most important genera are listed, and their abundance distribution is plotted as a heat map, which could be considered as the biomarkers of each corresponding

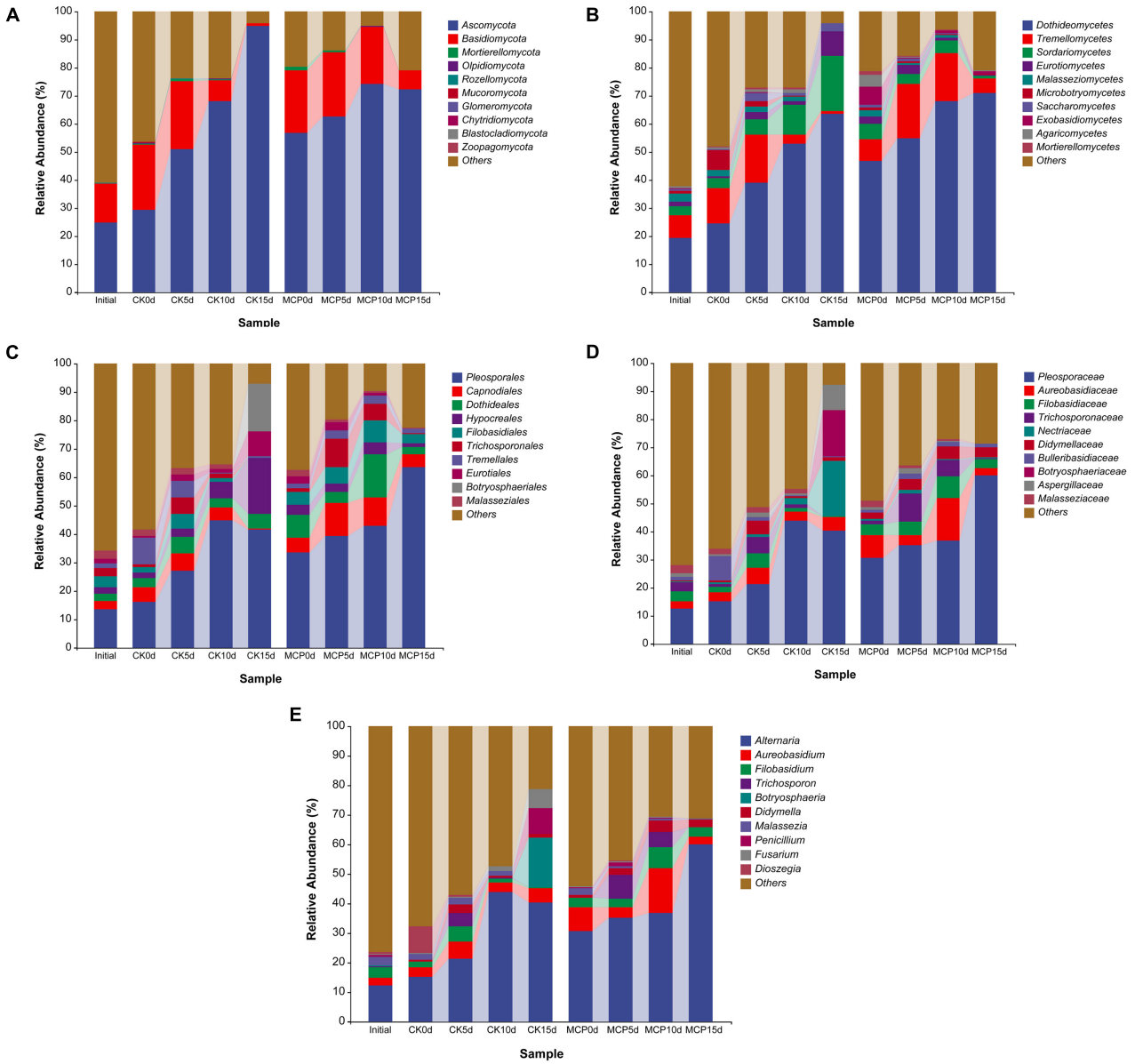

FIGURE 2 | Taxonomic composition of fungi at phylum **(A)**, class **(B)**, order **(C)**, family **(D)**, and genus **(E)** levels. Pear (*Pyrus communis* L. cv. "Doyenne du Comice") fruits were treated with or without 1.0 μl L^{-1} of 1-MCP during storage. Fruits were stored at 25 ± 0.5°C and relative humidity of 90 ± 5% for 0, 5, 10, and 15 days. The treatments were marked as CK0d, CK5d, CK10d, and CK15d, representing fruit stored for 0, 5, 10, and 15 days in the control group, while MCP0d, MCP5d, MCP10d, and MCP15d represent fruits stored for 0, 5, 10, and 15 days in the 1-MCP-treated group, respectively.

treatment. *Botryosphaeria* and *Fusarium* were presumably the biomarkers of CK15d, implying that these two fungi were critical in distinguishing between applications with or without 1-MCP treatment after 15 days of storage. The bacterial genera *Massilia* and *Kineococcus* were the crucial biomarkers to distinguish between CK15d and MCP15d.

Correlations of Fungi and Bacteria

To explore functional relationships between microorganisms, we analyzed the correlations of the 10 most abundant bacteria and fungi at the genus level (**Supplementary Figure 2**). The results revealed a positive or negative relationship between specific bacteria and fungi, suggesting that they were functionally synergetic or antagonistic. The bacteria *Aquabacterium* and *Asticcacaulis*, in particular, were strongly positively correlated with a correlation coefficient of 0.86 ($p < 0.05$), while *Lactobacillus* and *Muribaculaceae* came in second with a correlation coefficient of 0.83. There were also positive correlation coefficients between bacteria and fungi such as *Gluconobacter* and *Botryosphaeria* (0.62), *Asticcacaulis* and *Malassezia* (0.50), and *Pseudomonas* and *Didymella* (0.50). On the other hand, we found that *Alternaria* and *Gluconobacter*

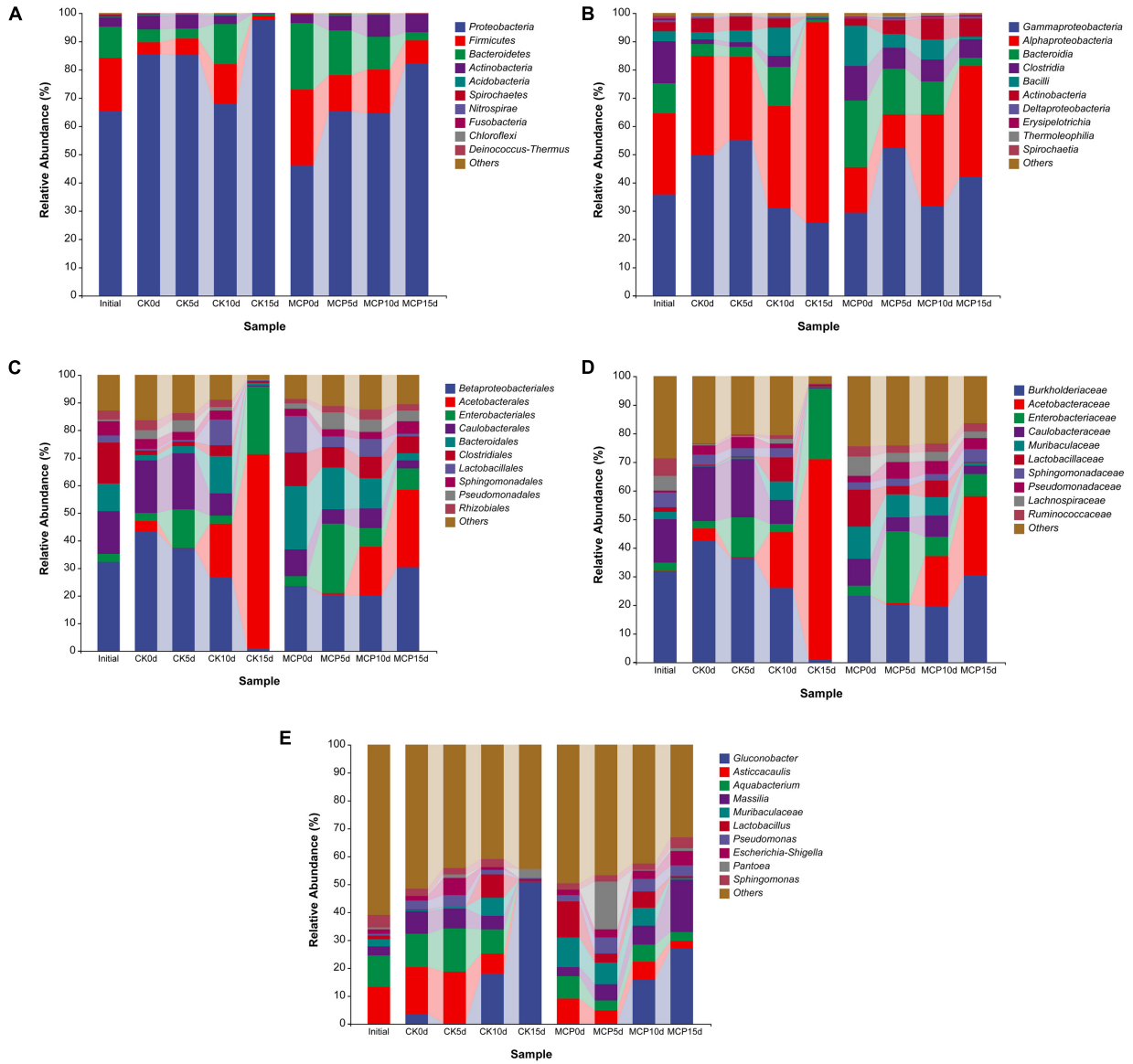

FIGURE 3 | Taxonomic composition of bacteria at phylum **(A)**, class **(B)**, order **(C)**, family **(D)**, and genus **(E)** levels. Pear (*Pyrus communis* L. cv. "Doyenne du Comice") fruits were treated with or without 1.0 μl L^{-1} of 1-MCP during storage. Fruits were stored at 25 ± 0.5°C and relative humidity of 90 ± 5% for 0, 5, 10, and 15 days. The treatments were marked as CK0d, CK5d, CK10d, and CK15d, representing fruit stored for 0, 5, 10, and 15 days in the control group, while MCP0d, MCP5d, MCP10d, and MCP15d represent fruits stored for 0, 5, 10, and 15 days in the 1-MCP-treated group, respectively.

were found to negatively correlate with other fungi or bacteria, indicating that they were closely related to fruit decay. Indeed, *Alternaria* showed negative correlations with *Malassezia* (−0.52) and *Asticcacaulis* (−0.4), and *Gluconobacter* was negatively correlated with *Aquabacterium* (−0.49), *Asticcacaulis* (−0.47), and *Sphingomonas* (−0.4).

Effect of 1-Methylcyclopropene on Fungal Membrane Integrity Rate

To determine the effect of 1.0 μl L^{-1} 1-MCP on fungal membrane integrity, the spores with damaged cell membranes were stained with PI and observed using the fluorescence microscope. Sterile water was used as a negative control and carbendazim, a broad spectrum of fungicide, was served as a positive control. The antifungal effect of 1-MCP was confirmed by comparing 1-MCP treatment and the negative control, and the efficiency of the assay was verified by comparing 1-MCP treatment or the negative control to the positive control. After 14 h of incubation under various treatments, the MIR of *Penicillium* spores was 96.3% in the negative control, 90.7% in 1-MCP treatment, and 66.7% in the positive control (**Supplementary Figure 3**). There was no significant difference of MIR between the negative control and 1-MCP treatment, while

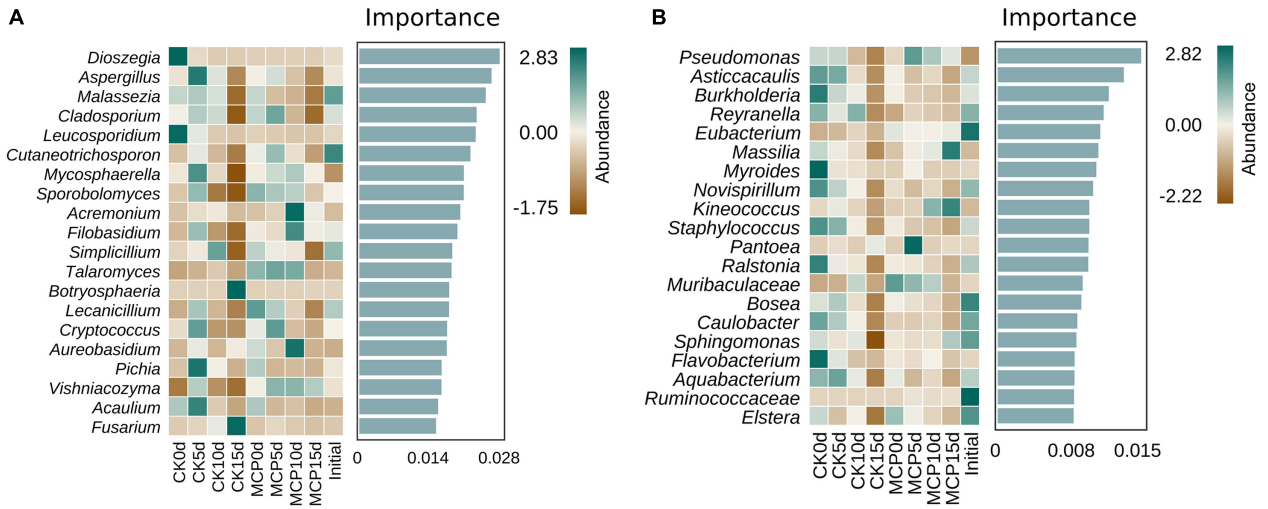

FIGURE 4 | Random forest analysis of fungi **(A)** and bacteria **(B)** in pear (*Pyrus communis* L.cv. "Doyenne du Comice") fruit after treatment with or without 1-MCP during storage. The horizontal axis of the histogram shows the importance of species to the classifier model, and the vertical axis is the taxon name of fungi or bacteria at the genus level. The heat map shows the abundance distribution of these genera in each group. Five-fold cross-validation was used. Results from the Random Forest analysis showed that *Botryosphaeria* and *Fusarium* were presumably the fungal biomarkers, and *Massilia* and *Kineococcus* were the bacterial biomarkers of CK15d, indicating that these organisms were critical in distinguishing between applications with or without 1-MCP treatment after 15 days of storage.

there was a significant difference between 1-MCP treatment and the positive control. For *Fusarium*, the MIR was determined as 98.7% in the negative control, 97.3% in 1-MCP treatment, and 83% in the positive control. Similarly, there was no significant difference of MIR between the negative control and 1-MCP treatment, while there was significant difference between 1-MCP treatment and the positive control. For *Alternaria*, the MIR was determined as 70.7% in the negative control, 66.7% in 1-MCP treatment, and 68% in the positive control. No significant difference in MIR was observed among them. These results suggest that 1.0 μl L^{-1} of 1-MCP had little effect on the fungal membrane integrity.

Relationship Among Fruit Quality, Physiological Characteristics, and Microbial Community Diversity

Fruit firmness, SSC, TA, respiration rate, ethylene production rate, and weight loss ratio were investigated to reveal the relationship among fruit quality, physiological characteristics, and microbial community diversity. The results showed that the firmness was higher in 1-MCP treated pear than in CK storage (**Figure 5A**), while SSC had no significant difference (**Figure 5B**). Similarly, 1-MCP-treated fruit showed significantly higher TA than CK during storage (**Figure 5C**). The respiration rate of post-harvest pear fruits was inhibited considerably by 1-MCP on days 5, 10, and 15, suggesting that 1-MCP could reduce the nutrient loss of pear fruit (**Figure 5D**). Simultaneously, 1-MCP greatly reduced ethylene production on days 5 and 10 but bursts on day 15, resulting in a slower fruit ripening (**Figure 5E**). The ethylene production rate decreased significantly in CK on day 15 due to the excessive decay of the fruit. After 15 days of storage, the weight of the fruit had lost 13.3% in the control group, but just 3.9% in the 1-MCP-treated group (**Figure 5F**).

Redundancy analysis was performed to explore the relationship among disease incidence, fruit quality, physiological characteristics, and microbial community following 1-MCP treatment. As shown in **Figure 6**, the abundance of three pathogens that cause fruit rot, including *Botryosphaeria*, *Penicillium*, and *Fusarium*, were positively correlated with disease incidence and respiration rate but negatively correlated with firmness.

DISCUSSION

As a specific inhibitor of ethylene receptor, 1-MCP can bind to ethylene receptor in plant cells, thereby preventing ethylene-dependent responses such as fruit ripening and senescence and, thus, extending shelf-life and maintaining fruit quality (Hassan and Mahfouz, 2010). Several studies have shown that 1-MCP can effectively reduce post-harvest fruit decay. For instance, 1-MCP may help preserve tomato fruit by reducing fruit decay caused by *Alternaria alternata*, *B. cinerea*, and *Fusarium* spp. (Su and Gubler, 2012). In jujubes, 1-MCP effectively suppressed the growth of blue mold-induced fruit rot and significantly reduced the incidence of natural decay (Zhang et al., 2012). To examine the effect of 1-MCP on the decay of d'Anjou pear fruit, the application of 1-MCP was found to reduce bull's-eye rot, *Phacidiopycnis* rot, stem end gray mold at 300 nl L^{-1}, and snow-mold rot at 30 nl L^{-1} (Spotts et al., 2007). Another study found that 1-MCP treatment significantly reduced post-harvest decay of peach fruit and that disease development was reduced when inoculated with *P. expansum* (Liu et al., 2005). In apples, the effect of 1-MCP treatment on post-harvest gray mold and its possible

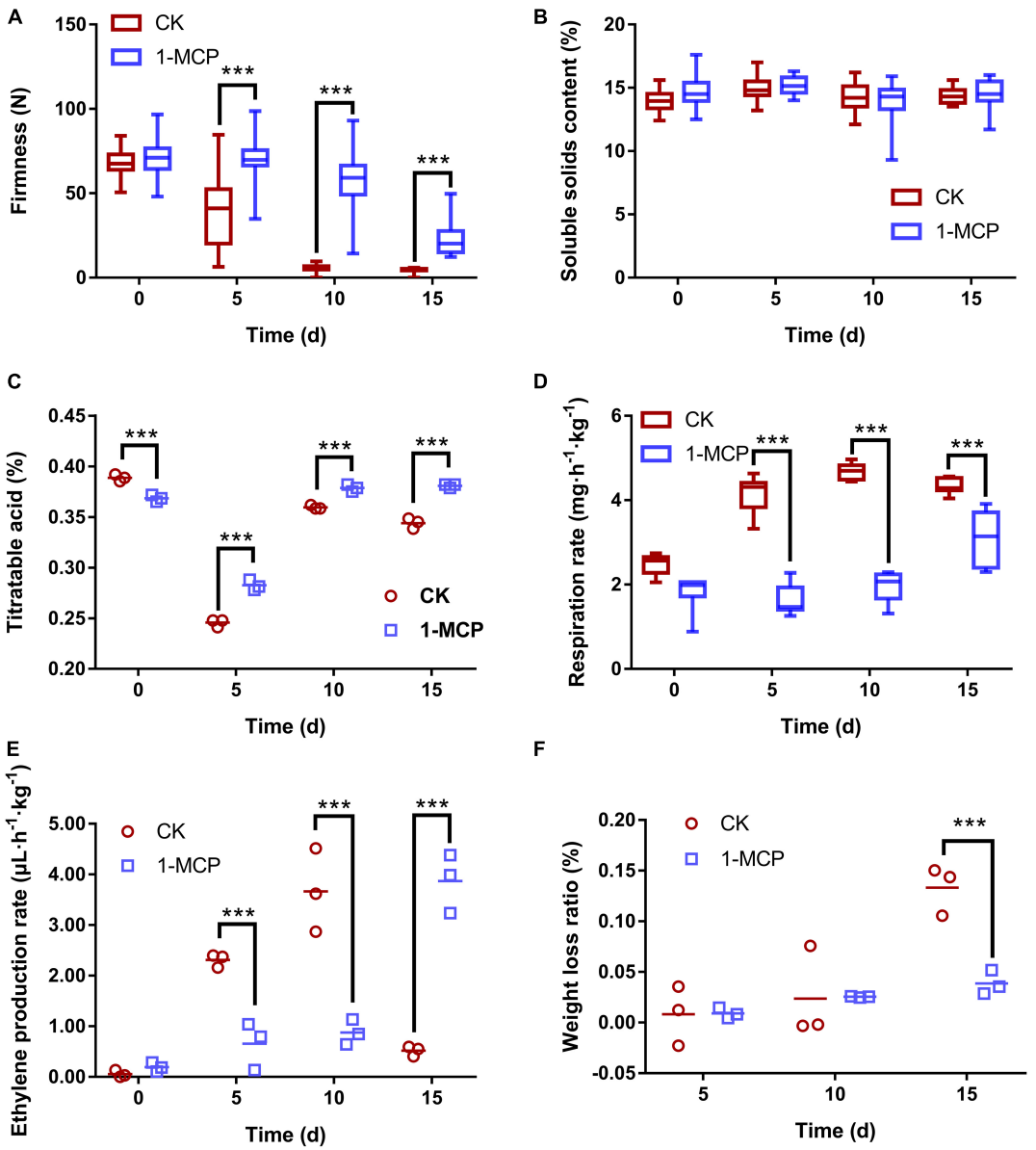

FIGURE 5 | Changes in pear (*Pyrus communis* L.cv. "Doyenne du Comice") fruit in firmness **(A)**, soluble solids content **(B)**, titratable acidity (TA) **(C)**, respiration rate **(D)**, ethylene production rate **(E)**, and weight loss ratio **(F)** with/without 1-MCP treatment. The asterisk denotes the significance of difference among treatments (***$p < 0.001$).

mechanisms were investigated (Zhou et al., 2016). In the current research, 1-MCP substantially reduced the disease incidence of pear (*P. communis* L.cv. "Doyenne du Comice") by increasing disease resistance, demonstrating that it had a remarkable capacity to mitigate post-harvest diseases of pear fruit.

The next-generation Illumina-based sequencing was used in this study to explore the microbial community of pear fruit treated with or without 1-MCP for 0–15 days of storage. Many fungi and bacteria associated with fruit decay were detected, and their abundance varied among different treatments (**Figures 2**, **3**). In our research, we found the two most common phyla, *Ascomycota* and *Basidiomycota*, in fungi associated with pear fruit samples, both of which are known to cause post-harvest fruit diseases (Ren et al., 2019b; Wassermann et al., 2019; Zambounis et al., 2020). The class *Dothideomycetes* was the most abundant class in both treatments and its abundance increased with the storage time in the present research, which is in line with the studies of endophytic mycobiota in "Jingbai" pear and microbial communities associated with apple and blackcurrant fruits (Vepštaitė-Monstavičė et al., 2018; Ren et al., 2019a). Several families in the *Pleosporales* order of fungi have infected living plants and caused serious plant diseases (Zhang et al., 2009; Wang et al., 2020). *Pleosporaceae* is the largest family in *Pleosporales*, which was characterized as the most

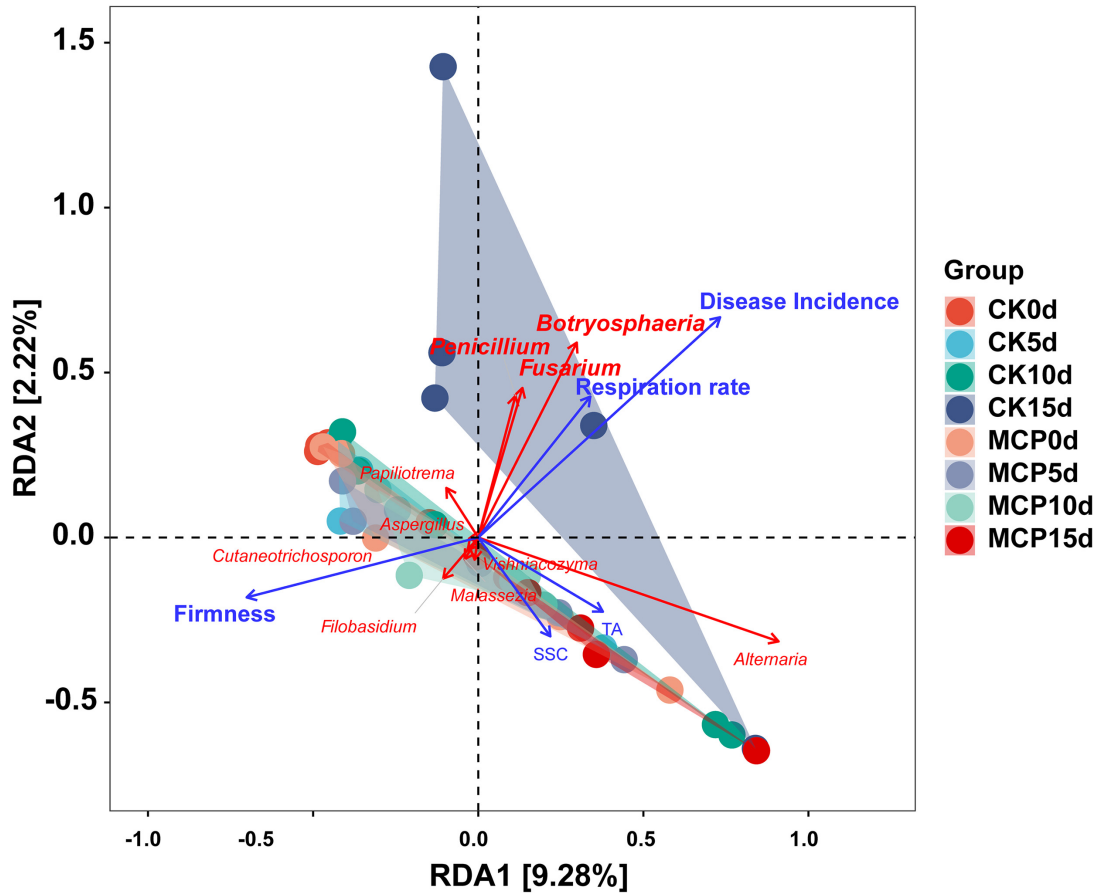

FIGURE 6 | Redundancy analysis (RDA) ordination graph for pear (*Pyrus communis* L.cv. "Doyenne du Comice") fruit quality, physiological characteristics, and fungal community diversity. Ten most abundant fungal genera (red arrows) and four fruit quality factors (blue arrows) including disease incidence, firmness, soluble solid content (SSC), TA, and respiration rate were plotted. Angles between species and fruit quality factors represent the positive and negative correlation between them (acute angle: positive correlation; obtuse angle: negative correlation; right angles: no correlation). This result indicates the important effect of *Botryosphaeria*, *Penicillium* and *Fusarium* on disease incidence, respiration rate, and firmness during the ripening of fruit.

abundant family in this study. Members of this family have been reported as plant parasites or saprobes occurring on plant leaves, stems, or fruits (Ariyawansa et al., 2015). At genus level, fungi such as *Alternaria*, *Botryosphaeria*, *Penicillium*, and *Fusarium* were found to grow significantly during storage in this study, which have been detected in a variety of diseased fruits in previous studies (Campenhout et al., 2017; Parveen et al., 2018; Zhao X. et al., 2019; Chen et al., 2020). In comparison with 1-MCP-treated group, *Botryosphaeria* and *Penicillium* were found highly abundant in the control group after 15 days of storage, indicating that 1-MCP may alleviate the disease caused by *Botryosphaeria* and *Penicillium*. The growth patterns of most dominant microorganisms indicated that their abundance increased with the extension of storage time. The main reason for this growth pattern is that the decay-causing pathogens constantly proliferated in the fruit.

Moreover, a high number of *Proteobacteria* were found in many orchard samples including fruits, bark, leaves, and rootstocks by metagenomics (Martins et al., 2013; Liu et al., 2018; Wassermann et al., 2019; Jo et al., 2020). *Proteobacteria* are usually classified into five groups based on rRNA sequences, which are denoted by the Greek letters α, β, γ, δ, and ε. In the present study, two classes of proteobacteria such as *Alphaproteobacteria* and *Gammaproteobacteria* were found to be more prevalent across all the samples (**Figure 4**), which is consistent with recent studies indicating that bacteria in this taxon are closely related to plant disease (Zhang et al., 2018; Wang et al., 2019). In the current study, the abundance of family *Acetobacteraceae* increased significantly both in control and 1-MCP treatment, indicating that the members in this family played an important role in fruit decay. Further results showed that the *Gluconobacter* genus, an important member of the family *Acetobacteraceae*, increased significantly after 15 days of storage. In accordance with the present results, previous studies have demonstrated that genus *Gluconobacter* were closely related to the fruit decay in apple, pear, and apricot (Van Keer et al., 1981; Liu et al., 2020). However, Bevardi, Frece (Bevardi et al., 2013) reported the biocontrol abilities of *Gluconobacter oxydans* strain isolated from the apple surface against post-harvest infecting fungus *P. expansum*. Current research indicates that members of

this genus may grow on the surface of pears as an antagonistic or saprophytic bacterium, but more isolation and identification studies are required to validate this hypothesis.

Biomarker discovery is one of the most important means being used for reflecting the lifestyle and disease of various hosts (Di Paola et al., 2011; Segata et al., 2011; Zhimo et al., 2021). It has been proven that Random Forest can effectively, stably, and accurately classify microbial community samples (Yatsunenko et al., 2012; Chen et al., 2021). *Botryosphaeria* and *Fusarium* were identified as biomarkers in this study to distinguish between 1-MCP treatment and untreated control pear fruits. Notably, members of these two fungal genera have been reported as the pathogens that cause fruit decay in a variety of fruits (Rittenburg, 1983; Garibaldi et al., 2012; Sever et al., 2012; Tang et al., 2012; Zhao X. et al., 2019; Zhao Z.Y. et al., 2019).

Furthermore, correlation matrix revealed a few positive and negative correlation patterns among the dominant fungal and bacterial genera. *Lactobacillus* and *Muribaculaceae* were found highly correlated in the microbial community of pear, which seemed to be consistent with other research that found *Lactobacillus plantarum* restored the gut microbiota imbalance by manipulating relative abundances of certain bacteria in *Muribaculaceae* (Gao et al., 2021). *Gluconobacter* and *Botryosphaeria* were also found to be correlated during the process of fruit decay, indicating that these pathogens could coexist and may be functionally related (Tournas and Katsoudas, 2012). In addition, there were several negative correlation patterns among the microbes, for instance, *Alternaria* and *Malassezia*, *Alternaria* and *Asticcacaulis*, *Gluconobacter* and *Aquabacterium*, *Gluconobacter* and *Asticcacaulis*, and *Gluconobacter* and *Sphingomonas*, which may be due to the high abundance of *Alternaria* and *Gluconobacter* inhibiting the growth of other microorganisms.

In order to show the effect of 1-MCP on fungi, fluorescence staining experiment was conducted to determine the membrane damage of spores caused by 1-MCP. The results showed that 1.0 μl L^{-1} of 1-MCP had little effect on the integrity of fungal cell membrane, suggesting that 1-MCP does not inhibit the development of fungi by damaging cell integrity of spores. Several studies have shown that 1-MCP decreased fruit firmness during storage but was delayed (Villarreal et al., 2010; Moises et al., 2017; Cheng et al., 2019), which has also been confirmed by the present findings (**Figure 5**). Fruit softening is closely related to the activities of cell wall hydrolases, such as polygalacturonase (PG), pectin methyl esterase (PME), and β-galactosidase (β-Gal). It has been reported that 1-MCP significantly lessened the fruit decay by reducing the activities of PG, PME, and β-Gal (Zhang et al., 2019). Therefore, 1-MCP is likely to minimize fruit decay by inactivating the pectinase activity in fruit, maintaining high fruit hardness, and preventing pathogen infection, rather than inhibiting pathogens directly. The RDA findings in this study obviously revealed the relationship between fruit quality and microbial community after 1-MCP treatment. *Botryosphaeria*, *Penicillium*, and *Fusarium* were shown to be positively correlated with disease incidence and respiration rate, and negatively correlated with fruit firmness (**Figure 6**), suggesting that these fungal genera are involved in fruit decay and quality change during storage.

CONCLUSION

Findings in this study suggest that 1-MCP treatment effectively reduced the disease incidence and induced multiple changes in fungal and bacterial microbiota in "Doyenne du Comice" pear fruit. In contrast to the control, decay-causing fungi such as *Botryosphaeria*, *Penicillium*, and *Fusarium* were suppressed by 1-MCP treatment and their quantity was positively correlated with TA and respiration rate but negatively correlated with fruit firmness. Thus, this study investigated the microbiome responses to 1-MCP during storage and revealed a relationship between fruit decay and microbial composition in "Doyenne du Comice" pear fruit.

DATA AVAILABILITY STATEMENT

The datasets generated for this study can be found in the Sequence Read Archive (Accession: PRJNA739857).

AUTHOR CONTRIBUTIONS

YZ and CG performed the experiments and analyzed the data. JG designed the study and provided the funding. YZ, MM, and JG wrote the manuscript. YC, CW, and YG did the visualization and reviewed the manuscript. All authors read and approved the final manuscript.

FUNDING

This research was supported by Talents Construction Project of Science and Technology Innovation, Hebei Academy of Agriculture and Forestry Sciences (HAAFS), Hebei Postdoctoral Science Foundation (B2021003034), and Agriculture Science and Technology Innovation Project of HAAFS (2019-2-1).

SUPPLEMENTARY MATERIAL

The Supplementary Material for this article can be found online at: https://www.frontiersin.org/articles/10.3389/fmicb.2021.729014/full#supplementary-material

REFERENCES

Ariyawansa, H. A., Thambugala, K. M., Manamgoda, D. S., Jayawardena, R., Camporesi, E., Boonmee, S., et al. (2015). Towards a natural classification and backbone tree for *Pleosporaceae*. *Fungal Divers.* 71, 85–139.

Aslam, R., Alam, M. S., and Saeed, P. A. (2020). Sanitization potential of ozone and its role in postharvest quality management of fruits and vegetables. *Food Eng. Rev.* 12, 48–67. doi: 10.1007/s12393-019-09204-0

Bevardi, M., Frece, J., Mesarek, D., Bošnir, J., Mrvčić, J., Delaš, F., et al. (2013). Antifungal and antipatulin activity of *Gluconobacter oxydans* isolated from

apple surface. *Arch. Ind. Hygiene Toxicol.* 64, 279–284. doi: 10.2478/10004-1254-64-2013-2308

Bolyen, E., Rideout, J. R., Dillon, M. R., Bokulich, N. A., Abnet, C. C., Al-Ghalith, G. A., et al. (2019). Reproducible, interactive, scalable and extensible microbiome data science using QIIME 2. *Nat. Biotechnol.* 37, 852–857.

Breiman, L. (2001). Random forests. *Mach. Learn.* 45, 5–32.

Buchholz, F., Kostić, T., Sessitsch, A., and Mitter, B. (2018). The potential of plant microbiota in reducing postharvest food loss. *Microb. Biotechnol.* 11, 971–975. doi: 10.1111/1751-7915.13252

Campenhout, J. V., Hemelrijck, W. V., Grammen, C., and Bylemans, D. (2017). First report of *Botryosphaeria dothidea* in Belgium causing fruit rot on pear. *Plant Dis.* 101:1672. doi: 10.1094/pdis-01-17-0112-pdn

Chen, X., Teng, L., Dan, H., et al. (2020). Occurrence of black leaf spot caused by *Alternaria alternata* on Korla fragrant pear in Xinjiang of China. *J. Plant Pathol.* 102:265. doi: 10.1007/s42161-019-00406-3

Chen, Y.-H., Xue, F., Yu, S.-F., Li, X.-S., Liu, L., Jia, Y.-Y., et al. (2021). Gut microbiota dysbiosis in depressed women: the association of symptom severity and microbiota function. *J. Affect. Disorders* 282, 391–400. doi: 10.1016/j.jad.2020.12.143

Cheng, Y., Liu, L., Feng, Y., Dong, Y., and Guan, J. (2019). Effects of 1-MCP on fruit quality and core browning in 'Yali' pear during cold storage. *Sci. Hortic.* 243, 350–356. doi: 10.1016/j.scienta.2018.08.041

Di Paola, M., De Filippo, C., Cavalieri, D., Ramazzotti, M., Poullet, J. B., Massart, S., et al. (2011). PP90 Impact of diet in shaping gut microbiota revealed by a comparative study in children from Europe and rural Africa. *Digest. Liver Dis.* 43, S445–S446.

Dou, H., Jones, S., and Ritenour, M. (2005). Influence of 1-MCP application and concentration on post-harvest peel disorders and incidence of decay in citrus fruit. *J. Horticult. Sci. Biotechnol.* 80, 786–792. doi: 10.1080/14620316.2005.11512015

Droby, S., and Wisniewski, M. (2018). The fruit microbiome: a new frontier for postharvest biocontrol and postharvest biology. *Postharvest. Biol. Technol.* 140, 107–112. doi: 10.1016/j.postharvbio.2018.03.004

Feroz, F., Shimizu, H., Nishioka, T., Mori, M., and Sakagami, Y. (2016). Bacterial and fungal counts of dried and semi-dried foods collected from Dhaka, Bangladesh, and their reduction methods. *Biocontrol. Sci.* 21, 243–251. doi: 10.4265/bio.21.243

Gao, Y., Liu, Y., Ma, F., Sun, M., Song, Y., Xu, D., et al. (2021). Lactobacillus plantarum Y44 alleviates oxidative stress by regulating gut microbiota and colonic barrier function in Balb/C mice with subcutaneous d-galactose injection. *Food Funct.* 12, 373–386. doi: 10.1039/d0fo02794d

Garibaldi, A., Bertetti, D., Poli, A., and Gullino, M. L. (2012). First report of fruit rot in pear caused by *Botryosphaeria dothidea* in Italy. *Plant Dis.* 96, 910–910. doi: 10.1094/pdis-02-12-0130-pdn

Hassan, F. A. S., and Mahfouz, S. A. (2010). Effect of 1-methylcyclopropene (1-MCP) treatment on sweet basil leaf senescence and ethylene production during shelf-life. *Postharvest Biol. Technol.* 55, 61–65. doi: 10.1016/j.postharvbio.2009.07.008

Jiang, W., Zhang, M., He, J., and Zhou, L. (2004). Regulation of 1-MCP-treated banana fruit quality by exogenous ethylene and temperature. *Food Sci. Technol. Int.* 10, 15–20. doi: 10.1177/1082013204042189

Jo, Y., Back, C.-G., Choi, H., and Cho, W. K. (2020). Comparative microbiome study of mummified peach fruits by metagenomics and metatranscriptomics. *Plants* 9:1052. doi: 10.3390/plants9081052

Khan, A. S., and Singh, Z. (2007). 1-MCP regulates ethylene biosynthesis and fruit softening during ripening of 'Tegan Blue' plum. *Postharvest. Biol. Technol.* 43, 298–306. doi: 10.1016/j.postharvbio.2006.10.005

Li, B. Q., and Tian, S. P. (2006). Effects of trehalose on stress tolerance and biocontrol efficacy of *Cryptococcus laurentii*. *J. Appl. Microbiol.* 100, 854–861. doi: 10.1111/j.1365-2672.2006.02852.x

Li, F., Zhang, X., Song, B., Li, J., Shang, Z., and Guan, J. (2013). Combined effects of 1-MCP and MAP on the fruit quality of pear (*Pyrus bretschneideri* Reld cv. Laiyang) during cold storage. *Sci. Hortic.* 2013, 544–551. doi: 10.1016/j.scienta.2013.10.018

Lin, S., Taylor, N. J., and Peduto Hand, F. (2018). Identification and characterization of fungal pathogens causing fruit rot of deciduous holly. *Plant Dis.* 102, 2430–2445. doi: 10.1094/pdis-02-18-0372-re

Liu, H., Jiang, W., Zhou, L., Wang, B., and Luo, Y. (2005). The effects of 1-methylcyclopropene on peach fruit *(Prunus persica* L. cv. Jiubao) ripening and disease resistance. *Int. J. Food Sci. Technol.* 40, 1–7. doi: 10.1111/j.1365-2621.2004.00905.x

Liu, J., Abdelfattah, A., Norelli, J., Burchard, E., Schena, L., Droby, S., et al. (2018). Apple endophytic microbiota of different rootstock/scion combinations suggests a genotype-specific influence. *Microbiome* 6:18.

Liu, X., Lin, Y., Lu, Z., et al. (2020). Diversity of endophytic bacteria in nectarine and apricot and isolation, identification of soft rot pathogen. *J. Food Sci. Technol.* 38, 37–45.

López, M. L., Miró, R., and Graell, J. (2001). Quality and aroma production of Doyenne du Comice pears in relation to harvest date and storage atmosphere. *Food Sci. Technol. Int.* 7, 493–500. doi: 10.1106/flwj-18cn-8tr9-480g

Luciano-Rosario, D., Keller, N. P., and Jurick, W. M. II (2020). *Penicillium expansum*:biology, omics, and management tools for a global postharvest pathogen causing blue mould of pome fruit. *Mol. Plant Pathol.* 21, 1391–1404. doi: 10.1111/mpp.12990

Mari, M., Bertolini, P., and Pratella, G. C. (2003). Non-conventional methods for the control of post-harvest pear diseases. *J. Appl. Microbiol.* 94, 761–766. doi: 10.1046/j.1365-2672.2003.01920.x

Martins, G., Lauga, B., Miot-Sertier, C., Mercier, A., Lonvaud, A., Soulas, M. L., et al. (2013). Characterization of epiphytic bacterial communities from grapes, leaves, bark and soil of grapevine plants grown, and their relations. *PLoS One* 8:e73013. doi: 10.1371/journal.pone.0073013

Min, D., Li, F., Zhang, X., Shu, P., Cui, X., Dong, L., et al. (2018). Effect of methyl salicylate in combination with 1-methylcyclopropene on postharvest quality and decay caused by *Botrytis cinerea* in tomato fruit. *J. Sci. Food Agric.* 98, 3815–3822. doi: 10.1002/jsfa.8895

Moises, Z., Kang-Mo, K., Jung, K. M., and Mosbah, M. K. (2017). Influence of 1-Methylcyclopropene treatment on postharvest quality of four scab (*Venturia inaequalis*)-resistant apple cultivars. *J. Food Qual.* 2017, 1–12. doi: 10.1155/2017/5951041

Parveen, S., Wani, A. H., Bhat, M. Y., Wani, T. A., and Malik, A. R. (2018). First report of *Penicillium glaucum* Link causing *Penicillium* rot of pear fruits *Pyrus communis* L. in Jammu and Kashmir, India. *Braz. J. Biol. Sci.* 4, 265–272. doi: 10.21472/bjbs.040805

Ren, F., Dong, W., Sun, H., and Yan, D.-H. (2019a). Endophytic mycobiota of Jingbai pear trees in north China. *Forests* 10:260. doi: 10.3390/f10030260

Ren, F., Dong, W., and Yan, D. H. (2019b). Organs, cultivars, soil, and fruit properties affect structure of endophytic mycobiota of Pinggu peach trees. *Microorganisms* 7:322. doi: 10.3390/microorganisms7090322

Rittenburg, L. H. (1983). Peach fruit rots caused by *Botryosphaeria* spp. and *Glomerella cingulata*. *Plant Dis.* 67, 449–450. doi: 10.1094/pd-67-449

Sardella, D., Muscat, A., Brincat, J.-P., Gatt, R., Decelis, S., and Valdramdis, V. (2016). A comprehensive review of the pear fungal diseases. *Int. J. Fruit Sci.* 16, 351–377. doi: 10.1080/15538362.2016.1178621

Segata, N., Izard, J., Waldron, L., Gevers, D., Miropolsky, L., Garrett, W. S., et al. (2011). Metagenomic biomarker discovery and explanation. *Genome Biol.* 12:R60.

Sever, Z., Ivić, D., Kos, T., and Miličević, T. (2012). Identification of *Fusarium* species isolated from stored apple fruit in Croatia. *Arh. Hig. Rada. Toksikol.* 63, 463–470. doi: 10.2478/10004-1254-63-2012-2227

Sheffield, V. C., Cox, D. R., Lerman, L. S., and Myers, R. M. (1989). Attachment of a 40-base-pair G+C-rich sequence (GC-clamp) to genomic DNA fragments by the polymerase chain reaction results in improved detection of single-base changes. *Proc. Natl. Acad. Sci. U.S.A.* 86, 232–236. doi: 10.1073/pnas.86.1.232

Sommer, N. F. (1985). Role of controlled environments in suppression of postharvest diseases. *Can. J. Plant Pathol.* 7, 331–339. doi: 10.1080/07060668509501700

Spotts, R. A., Sholberg, P. L., Randall, P., Serdani, M., and Chen, P. M. (2007). Effects of 1-MCP and hexanal on decay of d'Anjou pear fruit in long-term cold storage. *Postharvest. Biol. Technol.* 44, 101–106. doi: 10.1016/j.postharvbio.2006.12.003

Su, H., and Gubler, W. D. (2012). Effect of 1-methylcyclopropene (1-MCP) on reducing postharvest decay in tomatoes (*Solanum lycopersicum* L.). *Postharvest. Biol. Techno.* 64, 133–137. doi: 10.1016/j.postharvbio.2011.06.005

Taîbi, A., Rivallan, R., Broussolle, V., Pallet, D., Lortal, S., Meile, J.-C., et al. (2021). Terroir is the main driver of the epiphytic bacterial and fungal communities

of mango carposphere in Reunion island. *Front. Microbiol.* 11:e619226. doi: 10.3389/fmicb.2020.619226

Tang, W., Ding, Z., Zhou, Z. Q., Wang, Y. Z., and Guo, L. Y. (2012). Phylogenetic and pathogenic analyses show that the causal agent of apple ring rot in china is *Botryosphaeria dothidea*. *Plant Dis.* 96, 486–496. doi: 10.1094/pdis-08-11-0635

Tournas, V. H., and Katsoudas, E. (2012). "Microbiology of apples and apple products and related health hazards," in *Apples: Nutrition, Consumption and Health*, eds S. J. Cordoba and F. A. Delgado (New York, NY: Nova Science Publishers Inc), 79–106.

Van Keer, C., Vanden Abeele, P., Swings, J., Gossele, F., and de Ley, J. (1981). *Acetic acid bacteria* as causal agents of browning and rot of apples and pears. *Zentralbl. Bakteriol. Parasitenkd. Hyg. Abt. 1 Orig. Reihe C* 2, 197–204. doi: 10.1016/s0721-9571(81)80040-3

Vepštaitė-Monstavičė, I., Lukša, J., Stanevičienė, R., Strazdaitė-Žielienė, Ž, Yurchenko, V., Serva, S., et al. (2018). Distribution of apple and blackcurrant microbiota in Lithuania and the Czech Republic. *Microbiol. Res.* 206, 1–8. doi: 10.1016/j.micres.2017.09.004

Villarreal, N. M., Bustamante, C. A., Civello, P. M., and Martínez, G. A. (2010). Effect of ethylene and 1-MCP treatments on strawberry fruit ripening. *J. Sci. Food Agr.* 2010, 683–689. doi: 10.1002/jsfa.3868

Wang, M., Eyre, A. W., Thon, M. R., Oh, Y., and Dean, R. A. (2020). Dynamic changes in the microbiome of rice during shoot and root growth derived from seeds. *Front. Microbiol.* 11:559728. doi: 10.3389/fmicb.2020.559728

Wang, X., Liu, S., Chen, M., Yu, C., Zhao, Y., Yang, H., et al. (2019). Low temperature (15 °C) reduces bacterial diversity and prolongs the preservation time of *Volvariella volvacea*. *Microorganisms* 7:475. doi: 10.3390/microorganisms7100475

Wassermann, B., Kusstatscher, P., and Berg, G. (2019). Microbiome response to hot water treatment and potential synergy with biological control on stored apples. *Front. Microbiol.* 10:e02502. doi: 10.3389/fmicb.2019.02502

Willersinn, C., Mack, G., Mouron, P., Keiser, A., and Siegrist, M. (2015). Quantity and quality of food losses along the Swiss potato supply chain: stepwise investigation and the influence of quality standards on losses. *Waste Manage.* 46, 120–132.

Xu, X., Lei, H., Ma, X., Lai, T., Song, H., and Shi, X. (2017). Antifungal activity of 1-methylcyclopropene (1-MCP) against anthracnose (*Colletotrichum gloeosporioides*) in postharvest mango fruit and its possible mechanisms of action. *Int. J. Food Microbiol.* 2017, 1–6. doi: 10.1016/j.ijfoodmicro.2016.10.002

Yatsunenko, T., Rey, F. E., Manary, M. J., Trehan, I., Dominguez-Bello, M. G., Contreras, M., et al. (2012). Human gut microbiome viewed across age and geography. *Nature* 486, 222–227. doi: 10.1038/nature11053

Zambounis, A., Ganopoulos, I., Tsaftaris, A., Valasiadis, D., and Madesis, P. (2020). Metagenomics analysis of fungal communities associated with postharvest diseases in pear fruits under the effect of management practices. *Arch. Microbiol.* 202, 2391–2400. doi: 10.1007/s00203-020-01960-6

Zhang, J., Wang, E. T., Singh, R. P., Guo, C., Shang, Y., Chen, J., et al. (2018). Grape berry surface bacterial microbiome: impact from the varieties and clones in the same vineyard from central China. *J. Appl. Microbiol.* 2018, 204–214. doi: 10.1111/jam.14124

Zhang, Q., Dai, W., Jin, X., and Li, J. (2019). Calcium chloride and 1-methylcyclopropene treatments delay postharvest and reduce decay of New Queen melon. *Sci. Rep.* 9:13563.

Zhang, Q., Shi, W., Zhou, B., Du, H., Xi, L., Zou, M., et al. (2020). Variable characteristics of microbial communities on the surface of sweet cherries under different storage conditions. *Postharvest. Biol. Technol.* 173:111408. doi: 10.1016/j.postharvbio.2020.111408

Zhang, Y., Schoch, C. L., Fournier, J., Crous, P. W., de Gruyter, J., Woudenberg, J. H. C., et al. (2009). Multi-locus phylogeny of *Pleosporales*: a taxonomic, ecological and evolutionary re-evaluation. *Stud. Mycol.* 64, 85–102. doi: 10.3114/sim.2009.64.04

Zhang, Z., Tian, S., Zhu, Z., Xu, Y., and Qin, G. (2012). Effects of 1-methylcyclopropene (1-MCP) on ripening and resistance of jujube (*Zizyphus jujuba* cv. Huping) fruit against postharvest disease. *LWT Food Sci. Technol.* 45, 13–19. doi: 10.1016/j.lwt.2011.07.030

Zhao, X., Chen, M., Pan, L., Fu, Q., Chen, J. Y., and Xiang, M. L. (2019). First report of fruit rot on 'Cuiguan' pear caused by *Fusarium proliferatum* in China. *Plant Dis.* 104, 1554–1555. doi: 10.1094/pdis-04-19-0875-pdn

Zhao, Z. Y., Liu, Y. Y., Yang, J. H., Yang, X. L., and Wang, J. H. (2019). First report of *Fusarium lateritium* causing fruit rot of yellow peach (*Amygdalus persica*) in China. *New Dis. Rep.* 39:6. doi: 10.5197/j.2044-0588.2019.039.006

Zhimo, V. Y., Kumar, A., Biasi, A., Salim, S., Feygenberg, O., Toamy, M. A., et al. (2021). Compositional shifts in the strawberry fruit microbiome in response to near-harvest application of *Metschnikowia fructicola*, a yeast biocontrol agent. *Postharvest. Biol. Technol.* 175:111469. doi: 10.1016/j.postharvbio.2021.111469

Zhou, X. W., Zhou, H. L., Shi, Y. L., Tang, Y. P., and Meng, N. (2016). Mechanism of 1-MCP-induced resistance to grey mold in postharvest apples. *Modern Food Sci. Technol.* 32, 211–219.

Conflict of Interest: The authors declare that the research was conducted in the absence of any commercial or financial relationships that could be construed as a potential conflict of interest.

Publisher's Note: All claims expressed in this article are solely those of the authors and do not necessarily represent those of their affiliated organizations, or those of the publisher, the editors and the reviewers. Any product that may be evaluated in this article, or claim that may be made by its manufacturer, is not guaranteed or endorsed by the publisher.

frontiers in Microbiology

ORIGINAL RESEARCH
published: 01 September 2021
doi: 10.3389/fmicb.2021.720372

Sodium Hydrosulfide Induces Resistance Against *Penicillium expansum* in Apples by Regulating Hydrogen Peroxide and Nitric Oxide Activation of Phenylpropanoid Metabolism

*Huiwen Deng[1], Bin Wang[2], Yongxiang Liu[2], Li Ma[2], Yuanyuan Zong[2], Dov Prusky[2,3] and Yang Bi[2]**

[1] College of Horticulture, Gansu Agricultural University, Lanzhou, China, [2] College of Food Science and Engineering, Gansu Agricultural University, Lanzhou, China, [3] Department of Postharvest Science of Fresh Produce, Agricultural Research Organization (ARO), Volcani Center, Rishon LeZion, Israel

OPEN ACCESS

Edited by:
Khamis Youssef, Agricultural Research Center, Egypt

Reviewed by:
Kamal A. M. Abo-Elyousr, Assiut University, Egypt
Lintle Mohase, University of the Free State, South Africa

***Correspondence:**
Yang Bi
biyang@gsau.edu.cn

Specialty section:
This article was submitted to Food Microbiology, a section of the journal Frontiers in Microbiology

Received: *04 June 2021*
Accepted: *30 July 2021*
Published: *01 September 2021*

Citation:
Deng H, Wang B, Liu Y, Ma L, Zong Y, Prusky D and Bi Y (2021) Sodium Hydrosulfide Induces Resistance Against Penicillium expansum in Apples by Regulating Hydrogen Peroxide and Nitric Oxide Activation of Phenylpropanoid Metabolism. Front. Microbiol. 12:720372. doi: 10.3389/fmicb.2021.720372

As a multifunctional signaling molecule, hydrogen sulfide (H_2S) has been reported to induce plant responses to a variety of abiotic stresses. However, there are no reports on H_2S treatment inducing resistance in apples against *Penicillium expansum*, a biotic factor, and its possible mechanism of action. In this study, fumigating apples with 5 mM sodium hydrosulfide (NaHS), the exogenous donor of H_2S, for 12 h reduced the diameter of lesions in fruit colonized by *P. expansum*. NaHS treatment markedly promoted the synthesis of endogenous H_2S, hydrogen peroxide (H_2O_2), and nitrogen oxide (NO). *In vivo* NaHS treatment enhanced the activities of phenylalanine ammonia-lyase, cinnamate 4-hydroxylase, *p*-coumarate:coenzyme A ligase isoenzymes, caffeoyl-CoA-O-methyltransferase, caffeic acid-O-methyltransferase, ferulic acid-5-hydroxylase, cinnamyl-CoA reductase, and cinnamyl-alcohol dehydrogenase. The treatment also facilitated the production of specific phenolic acids, such as cinnamic acid, *p*-coumaric acid, caffeic acid, ferulic acid, and sinapic acid; total phenolic compounds; *p*-coumaryl alcohol; coniferyl alcohol; sinapyl alcohol; and lignin. NaHS treatment induced resistance against *P. expansum* in apples through H_2O_2- and NO-mediated activation of phenylpropanoid metabolism.

Keywords: apple fruit, NaHS, *Penicillium expansum*, induced resistance, signaling molecule, phenylpropanoid metabolism

INTRODUCTION

Penicillium expansum is a critical pathogen that can cause blue mold in various temperate fruits (Errampalli, 2014), resulting not only in fruit rot but also in the accumulation of patulin in the fruit, which presents a potential safety hazard (Yu et al., 2020). Although *P. expansum* can be effectively controlled by the fungicides pyrimethanil and thiabendazole (Ghosh et al., 2006; Sugar and Basile, 2008), pesticide residues remain on the fruit after storage and pose a risk to human health and the

pathogens can possible develop resistance to them. Moreover, there may be registration difficulties (Romanazzi et al., 2016). These reasons make it necessary to exploit new alternative strategies for preventing postharvest diseases.

Induced resistance is a novel, valid approach that has been applied to control postharvest diseases of fruit and vegetables by triggering natural resistance using elicitors and increasing host resistance against pathogens (Bi et al., 2020). Hydrogen sulfide (H_2S) is a signaling molecule that is extensively found in plants and has a protective function in stress responses (Yamasaki and Cohen, 2016). Studies have shown that exogenous H_2S and NaHS treatments potentially enhance plant resistance against various biological or abiotic stresses (Wang, 2012; Guo et al., 2016). NaHS treatment significantly inhibits the decay of fresh-cut pears caused by *P. expansum* and *Aspergillus niger* (Hu K. D. et al., 2014); alleviates fresh-cut sweet potato rot induced by *Geotrichum candidum*, *Mucor rouxianus*, and *Rhizopus nigricans* (Tang et al., 2014); and sustains a lower rot index in strawberry fruit (Hu et al., 2012). Other studies have indicated that NaHS treatment improves the activity of L-cysteine desulfhydrase (LCD) in *Arabidopsis thaliana* and promotes the generation of endogenous H_2S, which regulates the downstream synthesis of salicylic acid, a signal molecule (Shi et al., 2015); reduces the activity of phenylalanine ammonia-lyase; enhances the activity of ascorbate peroxidase, catalase, and peroxidase; and eliminates excessive reactive oxygen species, all of which preserves the stability of the cell membrane (Hu K. D. et al., 2014). Previous molecular analyses revealed that the delayed postharvest senescence of apples caused by H_2S was linked to the suppression of the genes involved in ethylene biosynthesis (*MdACS1*, *MdACS3*, *MdACO1*, and *MdACO2*) and signal transduction (*MdETR1*, *MdERS1*, *MdERS2*, *MdERF3*, *MdERF4*, and *MdERF5*); these results supported the proposed counteractive role of H_2S in ethylene biosynthesis and signaling (Ziogas et al., 2018). However, H_2S treatment in the present work induces the resistance of apples to *P. expansum*, and its mechanism of action has not been investigated yet.

The objectives of this study were to evaluate the effect of NaHS treatment on the colonization pattern of *P. expansum* in treated apples and analyze the possible mechanism of action by evaluating the levels of H_2S, hydrogen peroxide (H_2O_2), and nitrogen oxide (NO) and the activation of the enzymatic products of phenylpropanoid metabolism.

MATERIALS AND METHODS

Materials

Apples (*Malus domestica* Borkh cv. Delicious) were picked from a state-owned orchard in the Tiaoshan farm in Jingtai County, Gansu Province, China. The fruits selected were of similar size and without any defects. A total of 360 fruits were randomly divided into two groups. Each group included three replicates of 60 fruits. They were placed in transport boxes (45 apples per box), delivered to the laboratory on the day of harvesting, and maintained in cold storage (4°C ± 2°C; RH, 55–65%). *P. expansum* T01 was donated by Professor Tian Shipping of the Institute of Botany, Chinese Academy of Sciences, and preserved on potato dextrose agar at 25°C. NaHS (AR 68%) was bought from Shanghai Macklin Biochemical Technology Co., Ltd. HPLC-grade standards were purchased from Nanjing Yuanzhi Biotechnology Co., Ltd.

NaHS Treatment

Following previous screening study protocols (Li D. et al., 2016), a 5-mM solution of NaHS was prepared using distilled water. Accordingly, 50 ml of 5 mM NaHS solution was placed in a 90-mm-diameter container that was then placed in a 13-L desiccator. NaHS treatment was conducted following the method of Li D. et al. (2016) with appropriate modifications. The fruits were placed in ambient temperature (22°C ± 2°C; RH, 55–60%) for approximately 24 h and washed twice to remove dirt, after which they were dipped in 0.1% (v/v) sodium hypochlorite for 2 min. The fruits were washed again with tap water and dried at ambient temperature (22°C ± 2°C; RH, 55–60%) for 2 h. Then, the fruits were fumigated with NaHS solutions in a desiccator for 12 h with distilled water acting as control. All treated fruits were placed in a carton and stored at ambient temperature (22°C ± 2°C; RH, 55–60%). Overall, 48 fruits were randomly selected for each treatment with three replicates.

Inoculation

The spore suspension was prepared according to the method of Tahir et al. (2015). Herein, 5 ml of sterile water was added to a 5-day-old culture plate of *P. expansum* and the spores were scraped off and filtered through four layers of germ-free gauze to obtain a suspension of 1×10^6 spores/ml.

Inoculation and measurement of lesion diameters were conducted as per the method of Li S. E. et al. (2019). All fruits were disinfected using 75% ethanol, and four uniform piercings were made using a sterilized nail (3 mm × 3 mm). After 24 h of treatment, 20 μl of the prepared spore suspension was inoculated into the wound. The fruits were dried and then placed at ambient temperature (22°C ± 2°C; RH, 55–60%). Lesion diameters were measured at 3, 4, 5, 6, and 7 days after inoculation. The longest and shortest diameters of the lesion area were determined by the crossover method and the average was taken as the lesion diameter. Three replicates of 12 randomly selected fruits per treatment method were examined.

Sampling

Sampling was performed as per the method of Ge et al. (2017). After 0, 2, 4, 6, 8, and 10 days of treatment, the test and control fruits were peeled, and using a stainless steel knife, approximately 2.0 g of fresh tissue was collected from 2 to 3 mm below the epidermis at the equatorial part for each fruit. The samples were then pulverized into powder after adding liquid nitrogen and stored at −80°C in 50 ml centrifuge tubes.

Endogenous H_2S, NO, and H_2O_2 Content Assays

Endogenous H_2S content was determined following the method of Sekiya et al. (1982) with appropriate modifications. Frozen

tissue powder (1 g) was homogenized in 1 ml of 50 mM PBS (pH = 6.8) extracting solution, including 100 mM EDTA-Na_2 and 200 mM ascorbic acid. The homogenate (1 ml) was placed in 0.5 ml of 1 M HCl to release H_2S, which was absorbed by 0.5 ml of 1% (w/v) zinc acetate. After allowing the reaction to occur for 30 min, 0.3 ml of 5 mM dimethyl-p-phenylenediamine dihydrochloride dissolved in 3.5 mM H_2SO_4 was added, followed by 0.3 ml of 50 mM $NH_4Fe(SO_4)_2$ in 100 mM H_2SO_4. The absorbance was measured at 667 nm after incubating for 15 min at ambient temperature (22°C ± 2°C). Results are presented on a fresh weight basis, and the endogenous H_2S content was represented as mol kg^{-1}.

Nitrogen oxide content was determined using a kit from the Suzhou Keming Biotechnology Co., Ltd., following the protocols of the manufacturer. Frozen tissue powder (0.5 g) was placed in 1 ml of extracting solution, and then centrifuged at 10,000 × *g* for 15 min at 4°C. The reaction system included 100 μl of the supernatant and 50 μl of reagents 1 and 2, respectively. After incubating at ambient temperature (22°C ± 2°C; RH, 55–60%) for 15 min, the absorbance was measured at 550 nm, with extracting solution as a control. Results are expressed on a fresh weight basis, and the NO content was expressed as mmol kg^{-1}.

H_2O_2 content was measured using the method of Prochazkova et al. (2001) with appropriate modifications. Frozen tissue powder (1 g) was homogenized in 1 ml of cooled acetone and centrifuged at 10,000 × *g* for 40 min at 4°C. The reaction system included 1 ml of the supernatant, 100 μl of 20% titanium tetrachloride solution (v/v), and 200 μl of ammonia solution. It was homogenized for 5 min and centrifuged at 10,000 × *g* for 15 min at 4°C. The sediment was washed four times with cooled acetone and dissolved in 1.5 ml of 1 mM H_2SO_4. Absorbance was measured at 410 nm. Results are represented on a fresh weight basis, and the H_2O_2 content was represented as mmol kg^{-1}.

Measurement of Enzyme Activity

The activity of phenylalanine ammonia-lyase (PAL) was assayed following the method of Koukol and Conne (1961) with appropriate modifications. Frozen tissue powder (2 g) was homogenized in 2 ml of 0.1 M sodium borate buffer (pH = 8.8), including 5 mM β-mercaptoethanol (BME), 2 mM EDTA, and 4% polyvinylpyrrolidone (PVP) for PAL. The homogenates were centrifuged at 10,000 × *g* for 40 min at 4°C and the supernatant was used as a crude enzyme extract. The reaction system included 3 ml of buffer solution, 500 μl of L-phenylalanine, and 500 μl of crude enzyme extract. These were incubated for 1 h at 40°C, and the reaction was terminated by adding 200 μl of 6 M HCl. Absorbance was measured at 290 nm and PAL activity was represented as U mg^{-1} protein.

The activities of cinnamate 4-hydroxylase (C4H) and *p*-coumarate:coenzyme A ligase isoenzymes (4CL) were determined using the method of Voo et al. (1995) with appropriate modifications. Frozen tissue powder (2 g) was placed in 2 ml of extracting solution containing 5 mM BME, 4 mM $MgCl_2$, 50 mM Tris–HCl, 10% glycerinum, 10 μM Leupeptin, 1 mM PMSF, 5 mM ascorbic acid, and 0.15% PVP to crude extracts of C4H and 4CL enzymes. The C4H reaction system included 2 ml of 0.05 M Tris–HCl (pH = 8.9) containing 2 μM *trans*-cinnamic acid, 2 μM $NADPNa_2$, 5 μM D-glucose 6-phosphate disodium salt, and 800 μl of crude enzyme extract. The reaction system of 4CL included 150 μl of 75 mM $MgCl_2$, 150 μl of 1 μM CoA, 150 μl of 80 M ATP, 150 μl of 20 mM *p*-coumaric acid, and 500 μl of crude enzymes extract. The absorbance of C4H and 4CL were measured at 340 and 333 nm, respectively, and the activities of C4H and 4CL were expressed as U mg^{-1} protein.

The activities of caffeoyl-CoA-O-methyltransferase (CCoAOMT), caffeic acid-O-methyltransferase (COMT), ferulic acid-5-hydroxylase (F5H), and cinnamyl-CoA reductase (CCR) were measured using the enzyme-linked immunosorbent assay (Shanghai Enzyme-Linked Biotechnology Co., Ltd.) according to the protocols of the manufacturer. Crude enzyme extractions containing frozen tissue powder (0.5 g) were homogenized in 4.5 ml of 0.01 M PBS (pH = 7.2) extracting solution for CCoAOMT, COMT, F5H, and CCR. The reaction system included 40 μl sample dilution and 10 μl crude enzymes were incubated for 30 min at 37°C, rinsed five times with washing liquid, and dried. Afterward, 50 μl of enzyme standard reagent was added, incubated for 30 min at 37°C, and rinsed five times again. Then, 50 μl chromogenic agent A and 50 μl chromogenic agent B were added, mixed, and incubated in the dark for 10 min at 25°C. Finally, 50 μl of termination solution was added. Absorbance was measured at 450 nm, and the amounts of CCoAOMT, COMT, F5H, and CCR were expressed as U mg^{-1} protein.

The activity of cinnamyl-alcohol dehydrogenase (CAD) was determined following the method of Goffner et al. (1992) with appropriate modifications. Frozen tissue powder (2 g) was placed in 2 ml of 0.2 M Tris–HCl (pH = 7.5) extracting solution for CAD crude enzyme extraction. The reaction system included 1 ml of 2 mM NADP, 1.4 ml of 1 mM *trans*-cinnamic acid, and 600 μl of crude enzyme. The mixture was incubated for 30 min at 37°C, and then the reaction was terminated by adding 200 μl of 1 M HCl. Absorbance was measured at 340 nm and the activity of CAD was expressed as U mg^{-1} protein.

Protein Content Assay

The protein content was determined following the method of Bradford (1976) using bovine serum albumin as standard.

Quantification of Phenolic Acid and Lignin Monomer Content

Phenolic acid and lignin monomer contents were determined using the method of Fuad and Imad (2015) with appropriate modifications. Frozen tissue powder (3 g) was homogenized in 2 ml of methanol (75%, v/v). Ultrasonic extraction was carried out for 1 h at ambient temperature (22°C ± 2°C; RH, 55–60%). The homogenates were centrifuged at 10,000 × *g* for 40 min, and 3 ml of the supernatant was evaporated for 5 h at 40°C in a low-temperature rotary evaporator. The concentrate was redissolved in 1 ml of mobile phase and filtered through a 0.22-μm microporous membrane for HPLC analysis. A Waters Symmetry® C18 (4.6 × 250 mm, 5 μm) column (Ultra-fast Liquid chromatography from ACQUITY Arc, Waters, United States)

was used with a quadruple gradient. The elution velocity was 0.8 ml min^{-1} and the injection volume was 5 μl. Sinapic acid and caffeic acid were assayed at 325 nm. Ferulic acid, *p*-coumaric acid, cinnamic acid, *p*-coumaryl alcohol, sinapyl alcohol, and coniferyl alcohol were assayed at 322, 310, 276, 322, 273, and 263 nm, respectively. The content of phenolic acids and *p*-coumaryl alcohol, sinapyl alcohol, and coniferyl alcohol was calculated using peak time and peak area of the mixture of sample as a standard curve. Results are represented on a fresh weight basis, and the monomer content was expressed as mg kg^{-1}.

Analysis of Total Phenolic Compounds and Lignin Contents

The amount of total phenolic compounds was assayed using the method of Chen et al. (2015) with appropriate modifications. Frozen tissue powder (1 g) was placed in 10 ml of 0.5% acetic acid 70% acetone extracting solution and incubated in the dark for 24 h. The homogenates were centrifuged at 10,000 × *g* for 40 min at 4°C. The reaction system included 1 ml of extracting solution, 2 ml of Folin–Ciocalteu reagent (1:10 dilution), and 2 ml of 7.5% (w/v) sodium carbonate. It was incubated for 5 min at 50°C with methanol as control. Absorbance was measured at 760 nm, and the content of total phenolic compounds was evaluated using a gallic acid standard curve. Results are represented on a fresh weight basis, and the total phenolic compound content was expressed as g kg^{-1}.

The amount of lignin was measured following the method of Morrisson (1972) with appropriate modification. Frozen tissue powder (3 g) was placed in 5 ml of 95% ethanol and centrifuged at 10,000 × *g* for 10 min at 4°C. The sediment was rinsed thrice with 95% ethanol and thrice with ethanol:normal hexane = 1:2 (v/v) and then dried. The reaction system included the precipitate and 1 ml of 25% acetyl bromide glacial acetic acid solution, and it was incubated in a 70°C water bath for 30 min. The reaction was stopped by adding 1 ml of 2 M NaOH, after which 2 ml of glacial acetic acid and 200 μl of 7.5 M hydroxylamine hydrochloric acid were added. The homogenates were centrifuged at 10,000 × *g* for 25 min at 4°C. Glacial acetic acid was added to 20 μl of supernatant to bring the total volume to 5 ml. Absorbance was assayed at 280 nm. Lignin content was represented as OD_{280} kg^{-1}.

Statistical Analysis

All experiments were performed at least thrice. Results were represented as mean ± standard error (Origin 8.5). The difference between treatments was analyzed using ANOVA and SPSS 18.0 (SPSS Inc., Chicago, IL, United States) for Duncan's multiple range test at the 5% level.

RESULTS

Effect of NaHS on *P. expansum* Colonization and Increased Endogenous H_2S, NO, and H_2O_2 Content

The lesion diameter is an important indicator reflecting resistance of fruit. NaHS treatment reduced lesion diameter of apple fruit, which decreased by 32.25% compared with the control at 4 days of treatment ($P < 0.05$) (**Figure 1**).

NaHS treatment enhanced the endogenous H_2S level in fruit after 2 days of treatment (**Figure 2A**). Moreover, the level of endogenous NO in the NaHS-treated fruit increased after 2 days of treatment, which was 26.39 and 27.86% higher than that in the control at 2 and 6 days of treatment, respectively (**Figure 2B**). The H_2O_2 content increased in the NaHS-treated fruit after 2 days of treatment and peaked at 4 days of treatment, which was 74.29% higher than that of the control. At 6 days of treatment, compared with the control, the H_2O_2 content increased by 64.08% in the treated fruit (**Figure 2C**). Taken together, the results indicate that NaHS treatment of apples facilitated the generation of endogenous H_2S, NO, and H_2O_2.

NaHS Treatment Activated the Phenylpropanoid Pathway and Phenolic Compound Accumulation

The activities of key enzymes involved in phenylpropanoid metabolism are critical for regulating fungal colonization

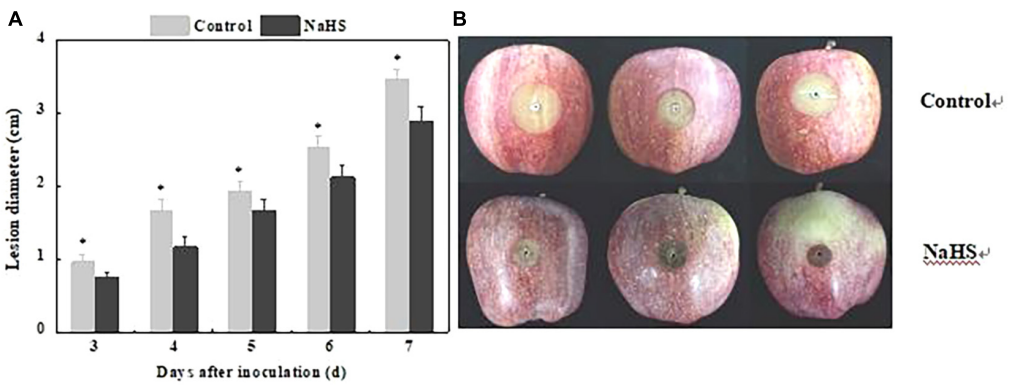

FIGURE 1 | Inhibition of *Penicillium expansum*-induced decay in apples by NaHS. The bars represent the standard error of the mean (±SE). The lesion diameter **(A)** and representative photographs were taken after 5 days **(B)**. *Significant differences at $P < 0.05$.

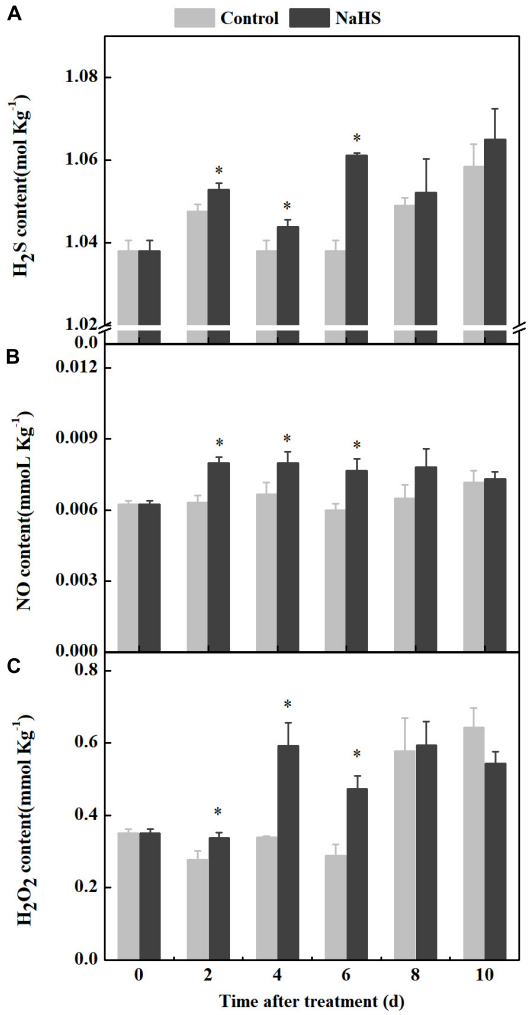

FIGURE 2 | Changes in endogenous H_2S, NO, and H_2O_2 contents in apples after NaHS treatment. H_2S **(A)**, NO **(B)**, and H_2O_2 **(C)**. The light gray and black bars represent the control and NaHS treatments, respectively. The bars represent the standard error of the mean (± SE). *Significant differences at $P < 0.05$.

(**Figure 3**). NaHS treatment enhanced the activities of PAL, C4H, 4CL, COMT, F5H, CCoAOMT, CCR, and CAD in apples compared with the control. Among them, the maximum change was found in the activity of PAL, which was 158% higher in the NaHS-treated fruit compared with the control at 6 days of treatment (**Figure 3A**), while the minimum change was 4CL activity, which was 31.0% higher in the treated fruit compared with the control at 4 days of treatment(**Figure 3C**).

Phenolic acids are mainly generated by the phenylpropanoid pathway. The contents of *p*-coumaric, sinapic, ferulic, and caffeic acid in fruits were increased by NaHS treatment after 2 days of treatment. The content of *p*-coumaric acid in the NaHS-treated fruit was 51.0% higher than that in the control at 8 days of treatment. Compared with the control, the range of changes in the sinapic, ferulic, and caffeic acid content of the treated fruit was around 15% during storage. In addition, the cinnamic acid content fluctuated in the two groups during storage. The total content of phenolic compounds in the treated fruits increased after 2 days of treatment compared with the control (**Figure 4F**). These results indicated that NaHS treatment affected phenylpropanoid pathway by altering the contents of five phenolic acids and the total phenolic compound content.

NaHS Treatment Promoted the Synthesis of Lignin Monomers and Lignin

Lignin is composed of *p*-coumaryl, sinapyl, and coniferyl alcohols, which all belonged to monolignols. The contents of *p*-coumaryl, sinapyl, and coniferyl alcohols in the fruit increased and consisted of the process of wound healing, while the NaHS treatment enhanced the accumulation of these compounds. At 6 days of treatment, the contents of *p*-coumaryl and sinapyl alcohols increased by 45 and 39% compared with the control, respectively (**Figures 5A,C**). At 8 days of treatment, the content of coniferyl alcohol in the NaHS-treated fruit was 25% higher than that in the control (**Figure 5B**). Moreover, the peak of lignin content was found at 4 days of treatment in the treated fruit, which was earlier and higher compared with the control (**Figure 5D**). These results indicated that the NaHS treatment enhanced the accumulation of *p*-coumaryl alcohol, sinapyl alcohol, coniferyl alcohol, and lignin in fruits.

DISCUSSION

In this study, we have described a new mechanism by which NaHS treatment promotes the generation of endogenous H_2S, NO, and H_2O_2 in apples, thus modulating the mechanism of host resistance (**Figure 2**). These results are similar to the observations that NaHS increases the contents of endogenous H_2O_2 and NO in wheat (Karpets et al., 2020) and H_2S and NO in tomato seedlings (Liang et al., 2018). NaHS is used as a postharvest treatment to delay senescence in kiwifruits (Zhu et al., 2014), mulberries (Hu H. et al., 2014), and strawberries (Hu et al., 2012). At 1 ppm, H_2S has no negative effects on human health, and the enzymes in the human body can detoxify H_2S by oxidizing it to harmless sulfate (Wang, 2012).

NaHS is an exogenous H_2S donor that dissociates into Na^+ and HS^- when dissolved in water; HS^- then combines with H^+ to generate H_2S (Hosoki et al., 1997). L-cysteine and D-cysteine desulfhydrase are important enzymes for endogenous H_2S generation and are activated by exogenous H_2S in plants (Hu H. et al., 2014). L/D-CD can degrade cysteine into H_2S, pyruvate, and ammonium (Wang, 2012). Endogenous H_2S activates nitrate reductase (NR), which turns NAD(P)H and nitrate into NAD^+ and H_2O. Nitrite is unstable and rapidly decomposes to form NO (Besson-Bard et al., 2008; Liang et al., 2018). In addition, H_2S can activate NADPH oxidase (NOX), which forms O_2^- by transferring electrons, which then produces H_2O_2 *via* superoxide dismutase (SOD) (Karpets et al., 2020). Therefore, we infer that NaHS promotes endogenous H_2S production by activating L/D-CD activity. H_2S accelerates the formation of H_2O_2 by activating NOX and SOD, resulting in induced resistance. As a signal molecule, H_2O_2 activates NR and facilitates the synthesis

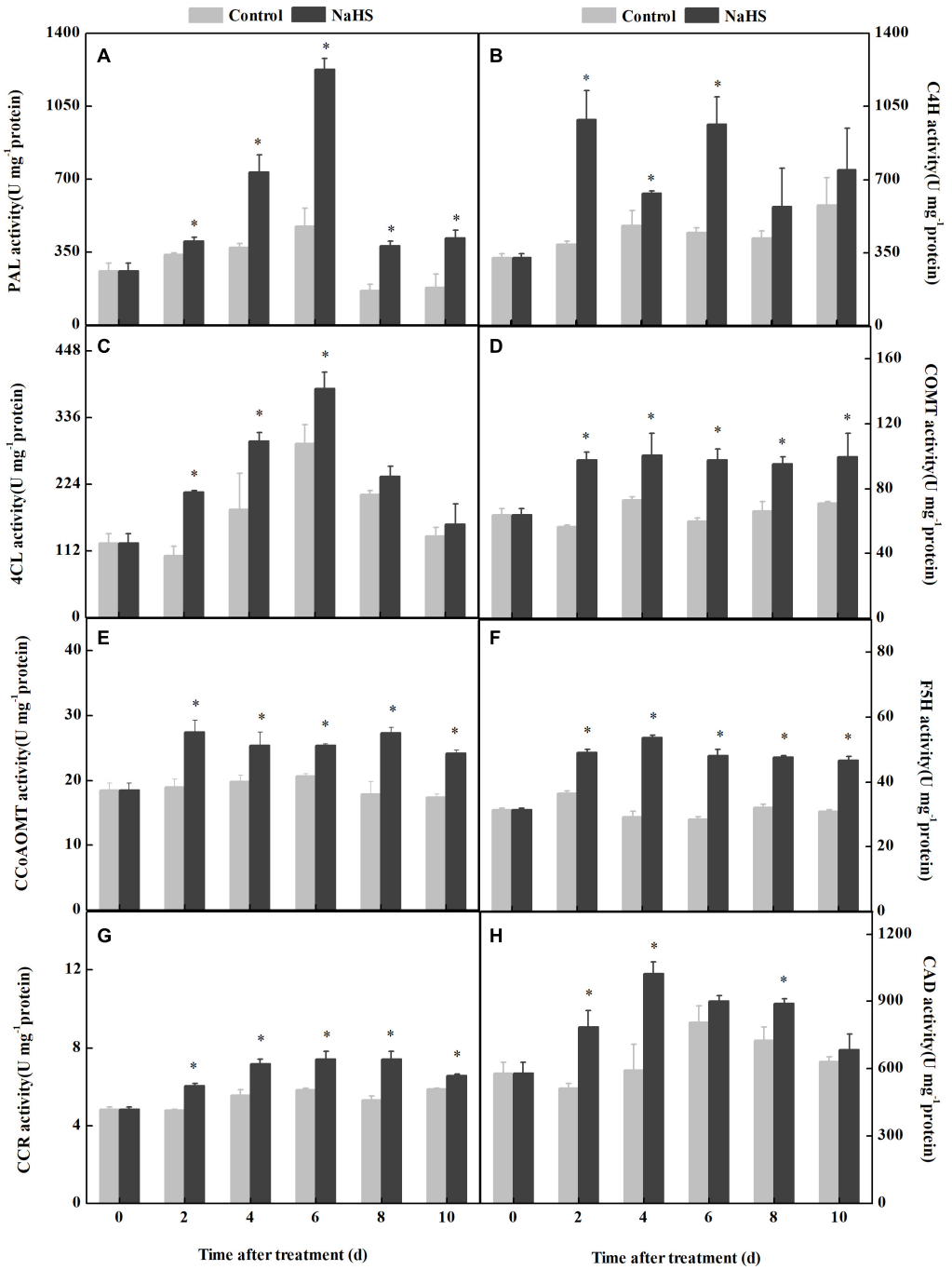

FIGURE 3 | Changes in the activity of the key enzyme of the phenylpropanoid pathway in apples after NaHS treatment. PAL **(A)**, C4H **(B)**, 4CL **(C)**, COMT **(D)**, CCoAOMT **(E)**, F5H **(F)**, CCR **(G)**, and CAD **(H)**. The light gray and black bars represent the control and NaHS treatments, respectively. The bars represent the standard error of the mean (± SE). *Significant differences at $P < 0.05$.

of endogenous NO. The potential mechanism of NaHS in promoting the production of endogenous H_2S, NO, and H_2O_2 remains to be identified.

The possibility that NaHS modulates H_2O_2 raised the question of whether it will also modulate the phenylpropanoid pathway in apples. Phenylpropanoid metabolism, which generates phenolic acids and monolignols, plays a vital role in inducing stress resistance against biotic factors. Phenolic acids have shown antifungal and antioxidant activity (Romanazzi et al., 2016). PAL is a crucial enzyme in the phenylpropanoid metabolism, catalyzing the conversion of L-phenylalanine into cinnamic acid (Deng and Lu, 2017). C4H catalyzes the synthesis of *p*-coumaric

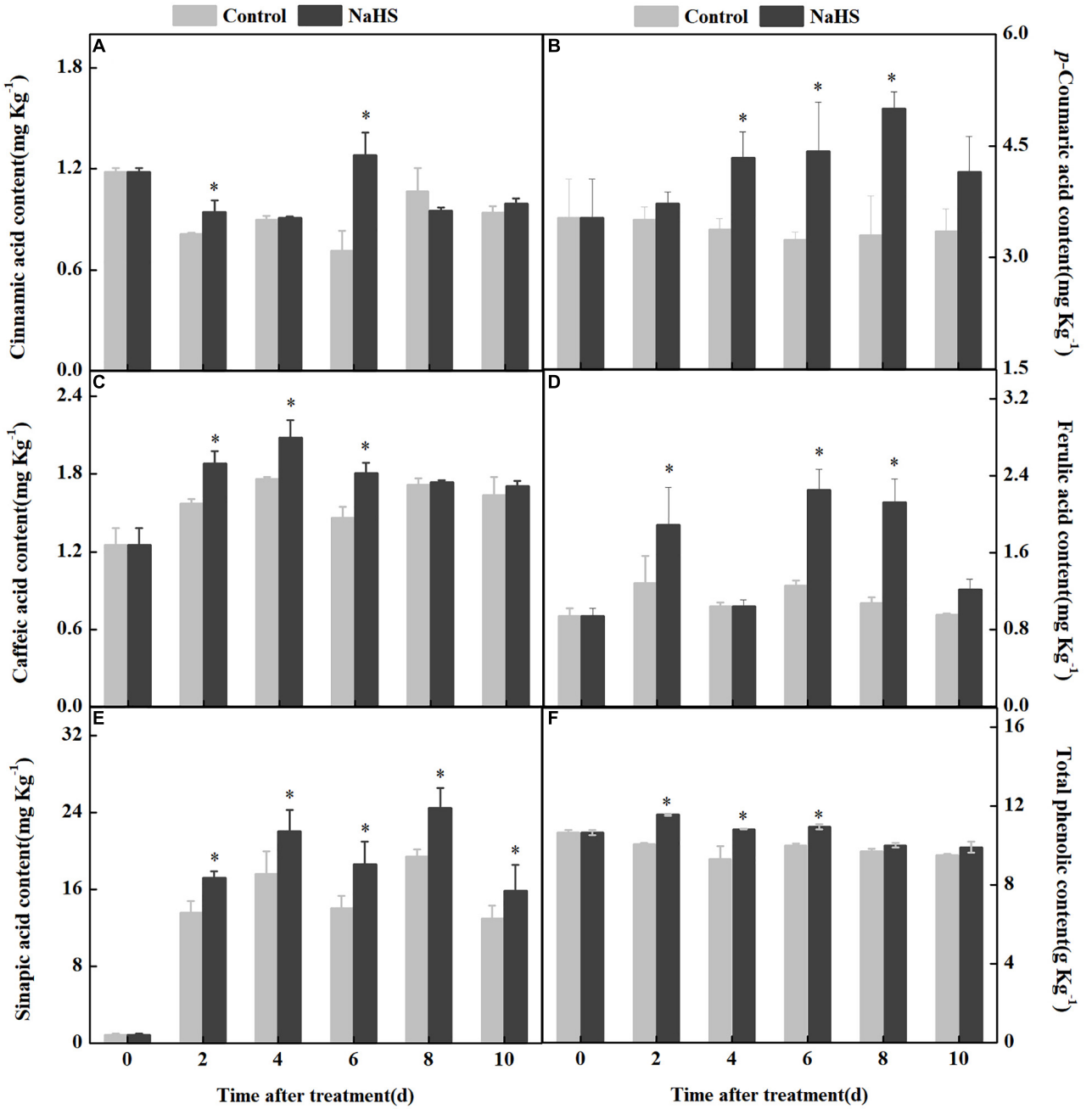

FIGURE 4 | Changes in the content of five phenolic acids and total phenolic compounds in apples after NaHS treatment. Cinnamic acid **(A)**, *p*-coumaric acid **(B)**, caffeic acid **(C)**, ferulic acid **(D)**, sinapic acid **(E)**, and total phenolic compounds **(F)**. The light gray and black bars represent the control and NaHS treatments, respectively. The bars represent the standard error of the mean (± SE). *Significant differences at $P < 0.05$.

acid from cinnamic acid and caffeic acid from *p*-coumaric acid. Sinapic acid is produced from caffeic acid by COMT and F5H (Arrieta-Baez and Stark, 2006; Vogt, 2010). In this study, we identified that NaHS treatment markedly enhanced the activities of PAL, C4H, 4CL, COMT, and F5H (**Figures 3A–D,F**) and accelerated the synthesis of cinnamic, *p*-coumaric, ferulic acid, and total phenolic compounds in apples (**Figure 4**). These results were similar to those where H_2S treatment in *Linum album* roots increases PAL activity and accelerates the accumulation of ferulic acid and total phenolic compounds (Fakhari et al., 2019). Given that H_2S promoted the synthesis of NO and H_2O_2, it is understandable that it also activated the phenylpropanoid pathway (Fakhari et al., 2019). A previous study showed that the gene expression and activity of PAL, C4H, and 4CL were upregulated by NO and that it elevated the generation of total phenolic and lignin in peach (Li G. J. et al., 2016). In addition,

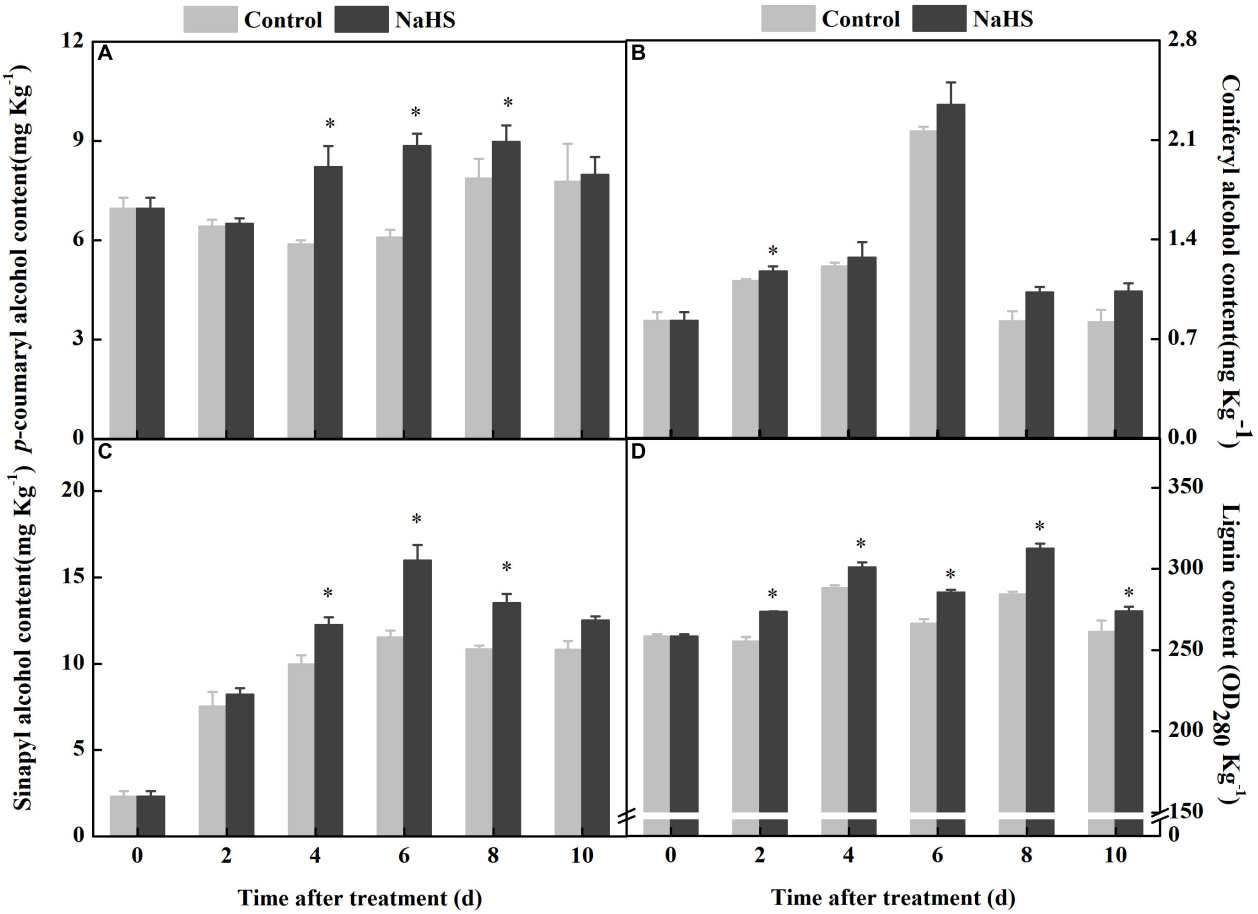

FIGURE 5 | Changes in the content of *p*-coumaryl alcohol, coniferyl alcohol, sinapyl alcohol, and lignin in apples after NaHS treatment. *p*-Coumaryl alcohol **(A)**, coniferyl alcohol **(B)**, sinapyl alcohol **(C)**, and lignin **(D)**. The light gray and black bars represent the control and NaHS treatments, respectively. The bars represent the standard error of the mean (± SE). *Significant differences at $P < 0.05$.

H_2O_2 activates PAL, C4H, and 4CL; promotes the synthesis of lignin; and accelerates the lignification process in bamboo shoot (Li D. et al., 2019). Therefore, we infer that H_2S, NO, and H_2O_2 could serve as signal molecules to activate the phenylpropanoid pathway in the apple system.

p-Coumaric acid is a significant bridge connecting the phenylpropanoid and lignin pathways. Lignin is primarily composed of coniferyl, *p*-coumaroyl, and sinapyl alcohol, which are generated from *p*-coumaroyl-CoA, feruloyl-CoA, and sinapaldehyde, respectively, by an enzyme cascade of CCR and CAD or CCR (Vanholme et al., 2010). They undergo oxidative crosslinking to form guaiacyl lignin, syringyl lignin, and parahydroxyphenyl lignin, respectively (Zhao and Dixon, 2011; Chezem and Clay, 2016). The present study indicated that NaHS treatment improves the activities of CCoAOMT, F5H, COMT, CCR, and CAD (**Figures 3D–H**) and promotes the accumulation of *p*-coumaryl, coniferyl, sinapyl alcohols, and lignin in apples (**Figure 5**). It has been reported that NO not only activates PAL, C4H, and 4CL but also increases the content of lignin in muskmelon (Yan et al., 2019). In addition, H_2O_2 improves the synthesis of lignin in bamboo shoots (Li D. et al., 2019). Therefore, we speculate that H_2S promotes the synthesis of phenolic acids, increases enzyme activity in lignin synthesis, and accelerates the accumulation of lignin and monolignols that could contribute to the enhanced resistance against the pathogen *P. expansum*.

CONCLUSION

Penicillium expansum is a wound pathogen, and enhanced phenylpropanoid metabolic activation in apples may contribute to the prevention of *P. expansum* colonization. NaHS treatment enabled the generation of endogenous H_2S, NO, and H_2O_2 in apples. Moreover, NaHS supported the activities of PAL, C4H, 4CL, COMT, F5H, CCoAOMT, CCR, and CAD and induced the accumulation of cinnamic, *p*-coumaric, caffeic, ferulic, and sinapic acids and total phenolic compounds. NaHS treatment also accelerated the accumulation of *p*-coumaryl, coniferyl, and sinapyl alcohols and lignin. Given that NaHS fumigation on apples is safe for human consumption, this treatment could

be considered as a possible postharvest treatment to induce resistance against *P. expansum* in apples.

DATA AVAILABILITY STATEMENT

The raw data supporting the conclusions of this article will be made available by the authors, without undue reservation.

AUTHOR CONTRIBUTIONS

HD wrote the manuscript. YB reviewed and edited the manuscript and was the project administrator and supervisor. BW carried out data curation and investigation. YL analyzed the data. LM provided experiment assistance. YZ and DP edited and organized the manuscript. All authors contributed to the article and approved the submitted version.

FUNDING

This work was supported by the National Natural Science Foundation of China (31861143046).

SUPPLEMENTARY MATERIAL

The Supplementary Material for this article can be found online at: https://www.frontiersin.org/articles/10.3389/fmicb.2021.720372/full#supplementary-material

REFERENCES

Arrieta-Baez, D., and Stark, R. E. (2006). Modeling suberization with peroxidase-catalyzed polymeriz-etion of hydroxy-cinnamic acids: Cross-coupling and dimerization reactions. *Phytochemistry* 67, 743–753. doi: 10.1016/j.phytochem.2006.01.026

Besson-Bard, A., Pugin, A., and Wendehenne, D. (2008). New insights into nitric oxide signaling in plants. *Annu. Rev. Plant Biol.* 59, 21–39. doi: 10.1146/annurev.arplant.59.032607.092

Bi, Y., Xue, H. L., and Wang, J. J. (2020). "Induced resistance in fruits and vegetables by elicitors to control postharvest diseases," in *Postharvest pathology of fresh horticultural produce*, eds L. Palou and J. L. Smilanick (Dordrecht: CRC Press), 798–803.

Bradford, M. M. (1976). A rapid and sensitive method for the quantitation of microgram quantities of protein utilizing the principle of protein-dye binding.Anal. *Biochem* 72, 248–254. doi: 10.1016/0003-2697(76)90527-3

Chen, L. Y., Cheng, C. W., and Liang, J. Y. (2015). Effect of esterification condensation on the folin-ciocalteu method for the quantitative measurement of total phenols. *Food Chem.* 170, 10–15. doi: 10.1016/j.foodchem.2014.08.038

Chezem, W. R., and Clay, N. K. (2016). Regulation of plant secondary metabolism and associated specialized cell development by MYBs and bHLHs. *Phytochemistry* 131, 26–43. doi: 10.1016/j.phytochem.2016.08.006

Deng, Y., and Lu, S. (2017). Biosynthesis and Regulation of Phenylpropanoids in Plants. *Crit. Rev. Plant Sci.* 36, 257–290. doi: 10.1080/07352689.2017.1402852

Errampalli, D. (2014). *Penicillium expansum* (Blue Mold). *Postharvest Decay* 2014, 189–231. doi: 10.1016/B978-0-12-411552-1.00006-5

Fakhari, S., Sharifi, M., De, Michele, R., Ghanati, F., Safaie, N., et al. (2019). Hydrogen sulfide directs metabolic flux towards the lignan biosynthesis in *linum album* hairy roots. *Plant Physiol. Biochem.* 135, 359–371. doi: 10.1016/j.plaphy.2018.12.015

Fuad, A. R., and Imad, O. (2015). Development and validation of an HPLC-UV method for determination of eight phenolic compounds in date palms. *J. AOAC Int.* 98, 1335–1339. doi: 10.5740/jaoacint.15-010

Ge, Y. H., Wei, M. L., Li, C. Y., Chen, Y. R., Lv, J. Y., and Li, J. R. (2017). Effect of acibenzolar-S-methyl on energy metabolism and blue mould of 'Nanguo' pear fruit. *Sci. Hortic.* 225, 221–225. doi: 10.1016/j.scienta.2017.07.012

Ghosh, A., Pirgozliev, S., Errampalli, D., Wainman, L., and Stokes, S. (2006). Effect of preharvest application of pyrimethanil and calcium chloride for the control of postharvest blue mold and gray mold of apples.Can. *J. Plant Pathol.* 28, 350–350.

Goffner, D., Joffroy, I., Grima-Pettenati, J., Halpin, C., Knight, M. E., Schuch, W., et al. (1992). Purification and characterization of isoforms of cinnamyl alcohol denydrogenase from Eucalyptus xylem. *Planta.* 188, 48–53. doi: 10.1007/BF01160711

Guo, H. M., Xiao, T. Y., Zhou, H., Xie, Y. J., and Shen, W. B. (2016). Hydrogen sulfide: a versatile regulator of environmental stress in plants. *Acta Physiol. Plant.* 38, 1–13. doi: 10.1007/s11738-015-2038-x

Hosoki, R., Matsuki, N., and Kimura, H. (1997). The possible role of hydrogen sulfide as an endogenous smooth muscle relaxant in synergy with Nitric Oxide. *Biochem. Biophys. Res. Commun.* 237, 527–531. doi: 10.1006/bbrc.1997.6878

Hu, H., Shen, W., and Li, P. (2014). Effects of hydrogen sulphide on quality and antioxidant capacity of mulberry fruit. *Int. J. Food Sci. Technol.* 49, 399–409. doi: 10.1111/ijfs.12313

Hu, K. D., Wang, Q., Hu, L. Y., Gao, S. P., Wu, J., Li, Y. H., et al. (2014). Hydrogen sulfifide prolongs postharvest storage of fresh-cut pears (*Pyrus pyrifolia*) by alleviation of oxidative damage and inhibition of fungal growth. *PLoS One* 9:e85524. doi: 10.1371/journal.pone.0085524

Hu, L. Y., Hu, S. L., Wu, J., Li, Y. H., Zheng, J. L., Liu, J., et al. (2012). Hydrogen sulfide prolongs postharvest shelf life of strawberry and plays an antioxidative role in fruits. *J. Agric. Food Chem.* 60, 8684–8693. doi: 10.1021/jf300728h

Karpets, Y. V., Kolupaev, Y. E., Lugovaya, A. A., Shvidenko, N. V., and Yastreb, T. O. (2020). Functional interaction of ROS and nitric oxide during induction of heat resistance of wheat seedlings by hydrogen sulfide donor. *Russ. J. Plant Physiol.* 67, 653–660. doi: 10.1134/S1021443720030140

Koukol, J., and Conne, E. (1961). The metabolism of aromatic compounds in higher plants. IV. Purification and properties of the phenylalanine deaminase of *Hordeum vulgare*. *J. Biol. Chem.* 236, 2692–2698. doi: 10.1016/S0021-9258(18)96962-96960

Li, D., Limwachiranon, J., Li, L., Du, R., and Luo, Z. S. (2016). Involvement of energy metabolism to chilling tolerance induced by hydrogen sulfide in cold-stored banana fruit. *Food Chem.* 208, 272–278. doi: 10.1016/j.foodchem.2016.03.113

Li, D., Limwachiranon, J., Li, L., Zhang, L., Xu, Y. Q., and Luo, Z. S. (2019). Hydrogen peroxide accelerated the lignification process of bamboo shoots by activating the phenylpropanoid pathway and programmed cell death in postharvest storage. *Postharvest Biol. Technol.* 153, 79–86. doi: 10.1016/j.postharvbio.2019.03.012

Li, G. J., Zhu, S. H., Wu, W. X., Zhang, C., Peng, Y., Wang, Q. G., et al. (2016). Exogenous nitric oxide induces disease resistance against monilinia fructicola through activating the phenylpropanoid pathway in peach fruit. *J. Sci. Food Agric* 2016:8146. doi: 10.1002/jsfa.8146

Li, S. E., Jiang, H., Wang, Y., Liang, L., Prusky, D., Yan, J., et al. (2019). Effect of benzothiadiazole treatment on improving the mitochondrial energy metabolism involved in induced resistance of apple fruit during postharvest storage. *Food Chem.* 302:125288. doi: 10.1016/j.foodchem.2019.125288

Liang, Y. L., Zheng, P., Li, S., Li, K. Z., and Xu, H. N. (2018). Nitrate reductase-dependent NO production is involved in H_2S-induced nitrate stress tolerance in tomato via activation of antioxidant enzymes. *Sci. Hort.* 229, 207–214. doi: 10.1016/j.scienta.2017.10.044

Morrisson, I. M. (1972). A semi-micro method from the determination of lignin and its use in predicting the digestibility of forage crops. *J. Agric. Food Chem.* 23, 455–463. doi: 10.1002/jsfa.2740230405

Prochazkova, D., Sairam, R. K., Srivastava, G. C., and Singh, D. V. (2001). Oxidative stress and antioxidant activity as the basis of senescence

in maize leaves. *Plant Sci.* 161, 765–771. doi: 10.1016/s0168-9452(01)00462-9

Romanazzi, G., Sanzani, S. M., Bi, Y., Tian, S. P., Martínez, P. G., and Alkan, N. (2016). Induced resistance to control postharvest decay of fruit and vegetables.Postharvest Biol. *Technol.* 122, 82–94. doi: 10.1016/j.postharvbio.2016.08.003

Sekiya, J., Schmidt, A., Wilson, L. G., and Filner, P. (1982). Emission of hydrogen-sulfifide by leaf tissue in response to L-cysteine. *Plant Physiol.* 70, 430–436. doi: 10.1104/pp.70.2.430

Shi, H. T., Ye, T. T., Han, N., Bian, H. W., Liu, X. D., and Chan, Z. L. (2015). Hydrogen sulfide regulates abiotic stress tolerance and biotic stress resistance in *arabidopsis*.J. *Integr. Plant Biol.* 57, 628–640. doi: 10.1111/jipb.12302

Sugar, D., and Basile, S. R. (2008). Timing and sequence of postharvest fungicide and biocontrol agent applications for control of pear decay. *Postharvest Biol. Technol.* 49, 107–112. doi: 10.1016/j.postharvbio.2007.12.008

Tahir, I. I., Nybom, H., Ahmadi-Afzadi, M., Røen, K., Sehic, J., and Røen, D. (2015). Susceptibility to blue mold caused by *Penicillium expansum* in apple cultivars adapted to a cool climate. *Eur. J. Hortic. Sci.* 80, 117–127. doi: 10.17660/eJHS.2015/80.3.4

Tang, J., Hu, K. D., Hu, L. Y., Li, Y. H., and Zhang, H. (2014). Hydrogen sulfide acts as a fungicide to alleviate senescence and decay in fresh-cut sweetpotato. *HortScience* 49, 938–943. doi: 10.21273/HORTSCI.49.7.938

Vanholme, R., Demedts, B., Morreel, K., Ralph, J., and Boerjan, W. (2010). Lignin biosynthesis and structure.J. *Plant Biochem. Physiol.* 153, 895–905. doi: 10.1104/pp.110.155119

Vogt, T. (2010). Phenylpropanoid Biosynthesis. *Mole. Plant.* 3, 2–20. doi: 10.1093/mp/ssp106

Voo, K. S., Whetten, R. W., O'Malley, D. M., and Sederoff, R. R. (1995). 4-Coumarate: Coenzyme A ligase from loblolly pine xylem (isolation, characterization, and complementary DNA cloning). *Plant Physiol.* 108, 85–97. doi: 10.1104/pp.108.1.85

Wang, R. (2012). Physiological implications of hydrogen sulfide: a whiff exploration that blossomed. *Physiol. Rev.* 92, 791–896. doi: 10.1152/physrev.00017.2011

Yamasaki, H., and Cohen, M. F. (2016). Biological consilience of hydrogen sulfide and nitric oxide in plants: gases of primordial earth linking plant, microbial and animal physiologies. *Nitric Oxide.* 55, 91–100. doi: 10.1016/j.niox.2016.04.002

Yan, B. W., Zhang, Z., Zhang, P., Zhu, X., Jing, Y. Y., Wei, J., et al. (2019). Nitric oxide enhances resistance against black spot disease in muskmelon and the possible mechanisms involved. *Sci. Hortic.* 256:108650. doi: 10.1016/j.scienta.2019.108650

Yu, L. L., Qiao, N. Z., Zhao, J., Zhao, J. X., Zhang, H., Tian, F., et al. (2020). Postharvest control of *Penicillium expansum* in fruits: A review. *Food Biosci.* 36:100633. doi: 10.1016/j.fbio.2020.100633

Zhao, Q., and Dixon, R. A. (2011). Transcriptional networks for lignin biosynthesis: more complex than we thought? *Trends Plant Sci.* 16, 227–233. doi: 10.1016/j.tplants.2010.12.005

Zhu, L., Wang, W., Shi, J., Zhang, W., Shen, Y., Du, H., et al. (2014). Hydrogen sulfideextends the postharvest life and enhances antioxidant activity of kiwifruit duringstorage. *J. Sci. Food Agr.* 94, 2699–2704. doi: 10.1002/jsfa.6613

Ziogas, V., Molassiotis, A., Fotopoulos, V., and Tanou, G. (2018). Hydrogen sulfide: A potent tool in postharvest fruit biology and possible mechanism of action. *Front. Plant Sci.* 9:1375. doi: 10.3389/fpls.2018.01375

Conflict of Interest: The authors declare that the research was conducted in the absence of any commercial or financial relationships that could be construed as a potential conflict of interest.

Publisher's Note: All claims expressed in this article are solely those of the authors and do not necessarily represent those of their affiliated organizations, or those of the publisher, the editors and the reviewers. Any product that may be evaluated in this article, or claim that may be made by its manufacturer, is not guaranteed or endorsed by the publisher.

frontiers in Microbiology

ORIGINAL RESEARCH
published: 04 January 2022
doi: 10.3389/fmicb.2021.808938

Isolation and Characterization of *Bacillus velezensis* Strain P2-1 for Biocontrol of Apple Postharvest Decay Caused by *Botryosphaeria dothidea*

Hongbo Yuan[1†], Bingke Shi[1†], Li Wang[1,2†], Tianxiang Huang[1], Zengqiang Zhou[1], Hui Hou[1] and Hongtao Tu[1*]*

[1] Zhengzhou Fruit Research Institute, Chinese Academy of Agricultural Sciences, Zhengzhou, China, [2] Key Lab of Horticultural Plant Biology, Ministry of Education, and College of Plant Science and Technology, Huazhong Agricultural University, Wuhan, China

OPEN ACCESS

Edited by:
Khamis Youssef,
Agricultural Research Center, Egypt

Reviewed by:
Chao-an Long,
Huazhong Agricultural University, China
Filippo De Curtis,
Università degli Studi del Molise, Italy
Sen Lian,
Qingdao Agricultural University, China

***Correspondence:**
Hui Hou
houhui@caas.cn
Hongtao Tu
tuhongtao@caas.cn

[†] These authors have contributed equally to this work

Specialty section:
This article was submitted to Food Microbiology, a section of the journal Frontiers in Microbiology

Received: 04 November 2021
Accepted: 10 December 2021
Published: 04 January 2022

Citation:
Yuan H, Shi B, Wang L, Huang T, Zhou Z, Hou H and Tu H (2022) Isolation and Characterization of Bacillus velezensis Strain P2-1 for Biocontrol of Apple Postharvest Decay Caused by Botryosphaeria dothidea. Front. Microbiol. 12:808938. doi: 10.3389/fmicb.2021.808938

Botryosphaeria dothidea causes apple ring rot, which is among the most prevalent postharvest diseases of apples and causes significant economic loss during storage. In this study, we investigated the biocontrol activity and possible mechanism of *Bacillus velezensis* strain P2-1 isolated from apple branches against *B. dothidea* in postharvest apple fruit. The results showed strain P2-1, one of the 80 different endophytic bacterial strains from apple branches, exhibited strong inhibitory effects against *B. dothidea* growth and resulted in hyphal deformity. *B. velezensis* P2-1 treatment significantly reduced the ring rot caused by *B. dothidea*. Additionally, the supernatant of strain P2-1 exhibited antifungal activity against *B. dothidea*. Re-isolation assay indicated the capability of strain P2-1 to colonize and survive in apple fruit. PCR and qRT-PCR assays revealed that strain P2-1 harbored the gene clusters required for biosynthesis of antifungal lipopeptides and polyketides. Strain P2-1 treatment significantly enhanced the expression levels of pathogenesis-related genes (*MdPR1* and *MdPR5*) but did not significantly affect apple fruit qualities (measured in fruit firmness, titratable acid, ascorbic acid, and soluble sugar). Thus, our results suggest that *B. velezensis* strain P2-1 is a biocontrol agent against *B. dothidea*-induced apple postharvest decay. It acts partially by inhibiting mycelial growth of *B. dothidea*, secreting antifungal substances, and inducing apple defense responses.

Keywords: apple ring rot, *Botryosphaeria dothidea*, *Bacillus velezensis*, biological control, postharvest quality

INTRODUCTION

Apple ring rot, caused by *Botryosphaeria dothidea*, is one of the most prevalent postharvest diseases affecting apples. It results in significant yield and quality losses during storage (Tang et al., 2012; Jurick et al., 2013; Zhang et al., 2016; Huang et al., 2021). Additionally, *B. dothidea* can infect apple tree branches or trunks during their growth stage, causing stem canker and tree death (Phillips et al., 2005; Xue et al., 2021). Apple ring rot caused by *B. dothidea* is difficult to control due to the latent infection characteristic (Liu et al., 2011). This disease is primarily controlled through the use of fungicides but environmental and food safety concerns severely limit their use. Furthermore,

several fungicide-resistant isolates of *B. dothidea* have been frequently reported in recent years as a result of the long-term use of pesticides (An et al., 2016; dos Santos et al., 2019; Wang L. et al., 2021). Therefore, alternative and environmentally friendly methods of controlling this disease are urgently needed.

Biological control of apple ring rot disease with endophytes is an alternative method with friendly and non-toxic characteristics. A wide range of microorganisms, including *Streptomyces rochei, Meyerozyma guilliermondii*, and *Bacillus* spp., have been identified as effective in the biological control of apple ring rot disease (Chen et al., 2016; Zhang et al., 2016; Huang et al., 2021). For example, yeast *M. guilliermondii* strain Y-1 isolated from grape skins demonstrated antifungal activity against *B. dothidea* by inhibiting spore germination and mycelial growth. Furthermore, strain Y-1 was found to be capable of inducing a series of defense responses and confer host resistance (Huang et al., 2021). By stimulating a series of defense mechanisms, *S. rochei* strain A-1, isolated from healthy apple fruit can effectively inhibit postharvest decay of apples caused *by B. dothidea* (Yong et al., 2014; Zhang et al., 2016). *Bacillus* spp. is a species that has been isolated and studied extensively as a biological control agent. At present, *Bacillus* spp. including *B. subtilis* strain 9407 and *B. amyloliquefaciens* strain PG12 have been reported to possess antagonistic activity against *B. dothidea* (Chen et al., 2016; Fan et al., 2017). Several strains of *B. velezensis* have also been reported to act as biocontrol agents, preventing plant diseases and promoting plant growth. For instance, *B. velezensis* strain ZW-10 exhibited activity against the *Magnaporthe oryzae*, via secondary metabolites (Chen et al., 2020). It has been reported that *B. velezensis* strain 83 from the mango tree phyllosphere is capable of controlling anthracnose and promoting plant growth (Balderas-Ruíz et al., 2020). *B. velezensis* strain HC6 showed antimicrobial activity against the *Listeria monocytogenes*, by producing lipopeptide surfactin (Liu et al., 2020). Recent reports indicated that *B. velezensis* strains Lle-9 and D4 possessed antifungal activity against a variety of pathogenic fungi, including *B. dothidea* (Khan et al., 2020; Liu et al., 2021). However, whether *B. velezensis* is effective against *B. dothidea* in apples and the underlying mechanisms remain unknown.

In this study, 80 bacterial isolates were obtained from the branches of apple variety "Kitanosach," which were highly resistant to *B. dothidea*. Among them, a *B. velezensis* strain P2-1 exhibited strong inhibition activity against the growth of *B. dothidea* and apple postharvest decay caused by *B. dothidea*. Furthermore, *B. velezensis* strain P2-1 was capable to suppress apple ring rot caused by a fungicide-resistant strain. Additionally, the ability of *B. velezensis* strain P2-1 to colonize apple fruit wounds was assessed and the possible biocontrol mechanism of strain P2-1 against *B. dothidea* was explored.

MATERIALS AND METHODS

Pathogenic Fungal Isolates

The pathogens *B. dothidea*, *Valsa mali*, *V. pyri,* and *Colletotrichum gloeosporioides* strains were used in this study and stored at Zhengzhou Fruit Research Institute, Chinese Academy of Agricultural Sciences, Zhengzhou, China (Wang L. et al., 2021; Yuan et al., 2021). *B. dothidea* strain Bd220 is a carbendazim-sensitive isolate, while *B. dothidea* strain Bd7 is a carbendazim-resistant isolate bearing an E198A point mutation in the *ß*–tubulin gene (GAG-GCG) (Wang L. et al., 2021). The fungal strains used in this study were cultured in potato dextrose agar (PDA) (Potato extracts 200 g L^{-1}, Glucose 2 g L^{-1}, Agar 15 g L^{-1}) and grow at 25°C.

Isolation of Endophytic Bacteria Strains

One-year-old branches (about 1 cm in diameter) without any disease symptoms were collected from apple tree (variety named "Kitanosach") for endophytic bacteria isolation at Zhengzhou, Henan province, China in July 2021. "Kitanosach" is a high resistant variety to *B. dothidea* (Hou et al., 2017). The endophytic bacteria were isolated according to a previous study with some modifications (Yuan et al., 2021). In brief, the bark of apple branches was peeled off and cut into small pieces (5 mm × 5 mm) and put into 75% ethyl alcohol for 1 min. The small pieces were then placed into 1% sodium hypochlorite for 5 min. After disinfection, the small pieces were washed with sterilized ddH_2O five times and put onto sterilized filter paper to absorb water. Subsequently, the small pieces were transferred to 1 mL of ddH_2O containing a 0.2 cm-diameter steel ball, and shaking the tube for 1 min at 4,000 rpm in a grinder (SCIENTZ-48, Ningbo city, China). Next, 100 μL of supernatant was put onto NA medium (Peptone 10 g L^{-1}, Beef extract 3 g L^{-1}, Sodium chloride 5 g L^{-1}, Agar 15 g L^{-1}). The plates were incubated at 25°C for 2–3 days, after which emerged bacteria colonies were sub-cultured onto new plates. After purification, the endophytic bacteria were used to test the antifungal activity against *B. dothidea*.

Dual Culture Test for Screening Potential Biocontrol Bacterium

In total, 80 different endophytic bacteria strains were isolated from the branches of a healthy apple tree and were screened for antagonistic activity against *B. dothidea* strain Bd220 by dual culture test based on a pervious study with some modifications (Yuan et al., 2021). Briefly, endophyte bacteria isolates were cultivated overnight in LB broth (Peptone 10 g L^{-1}, Yeast extract 5 g L^{-1}, Sodium chloride 10 g L^{-1}) at 200 rpm, 28°C and 3 μL of bacteria were placed at each side 2 cm from the center on PDA medium on Petri dishes. Meanwhile, a mycelial plug (5 mm in diameter) of the tested pathogenic fungi was inoculated at the center of PDA plate. Plates were incubated at 25°C for 6 days. Then, the colony diameter of the pathogenic fungal isolate was measured using vernier calipers. The negative control was just inoculated with the pathogenic fungal isolate. The test was carried out three times, and each treatment had three replicates. Inhibition = (colony diameter of control-colony diameter of treated)/(colony diameter of control) × 100%. After the preliminary screening, the antagonistic strains were further tested antifungal activity against *V. mali*, *C. gloeosporioides* and *V. pyri* strains.

An ultra-depth three-dimensional microscope (KEYENCE, Japan) was used to assess the morphological characteristics of hyphae at 2 days of dual culture. Three replicates were analyzed per treatment, with a minimum of 10 hyphae per replicate. The assay was repeated two times.

Antagonistic Strain Identification

The endophytic bacteria strain P2-1 was identified via morphological and molecular identification. The physiological and biochemical characters of strain P2-1 were carried out according to a previous report (Holt et al., 1994). For molecular identification, total DNA of P2-1 isolate was extracted with a DNA extraction kit (Omega, Guangdong, China), and the 16S rDNA, *gyrA* and *ropB* sequences were amplified with appropriate primers in **Supplementary Table 1** (Rooney et al., 2009; Fan H. et al., 2016). All PCR reactions were conducted in a reaction containing 1.5 μL of 10 × Taq buffer, 1 μL of 2.5 mM dNTPs, 1 μL of 100 mM Mg^{2+}, 0.25 μL of 5 U μL^{-1} Taq DNA polymerase, 0.25 μL of each primer (10 μM), 1 μL of 10 ng μL^{-1} bacteria DNA, and ddH_2O to a final 20 μL volume. Thermo cycler settings were: 3 min at 94°C; 30 cycles of 94°C for 30 s, 56°C for 30 s, and 72°C for 50 s; 72°C for 5 min. PCR products were sequenced by Bgi Genomics Co., Ltd., Beijing, China, and the resultant sequences were blasted against the NCBI nucleotide collection database. Highly homologous sequences were selected for multiple sequence alignment with the MEGA 7.0 software. A phylogenetic tree was constructed via a Neighbor-Joining approach, with 1,000 replicate Bootstrap analyses being used to calculate node support.

Assessment of Supernatant of Antagonistic Strain on *Botryosphaeria dothidea* Mycelial Growth

A bacterial colony of strain P2-1 was added to the 100 mL of LB broth in a shaker at 200 rpm for 2 days at 28°C. The samples were then centrifuged for 10 min at 5,000 rpm and the obtained supernatant was passed through a filter with a 0.22 μm pore size to remove remaining bacterial cells and get the supernatant. PDA medium was mixed with different supernatant volumes to yield PDA, containing 1, 2, 5, or 10% supernatant. Each plate was inoculated with a *B. dothidea* plug (5 mm in diameter). *B. dothidea* colony diameters were measured after a 6-day inoculation period, with untreated PDA medium serving as a control. This assay was repeated three times, with three replicates each time.

Biocontrol Activity of *Bacillus velezensis* Strain P2-1 Against *Botryosphaeria dothidea* in Apple Fruit

The activity of strain P2-1 against *B. dothidea* in apple fruit (Gala) was determined according to a previous report (Huang et al., 2021). In brief, two wounds (3 mm deep and 5 mm wide) were punctured with a sterile borer. Each wound was treated with 40 μL of strain P2-1 cell suspension (1×10^8 CFU mL^{-1}) or supernatant. Sterile water or fungicide carbendazim (0.8 g L^{-1}) (Tianjin Hanbang Plant Protective Agent Co., Ltd., Tianjing, China) treated apples were used as negative and positive controls, respectively. Following the 24 h of incubation at 25°C with a relative humidity of 85%, the apple fruit wounds were inoculated with *B. dothidea* mycelial plugs. Disease lesion length was measured using vernier calipers at 3 and 5 days post inoculation (dpi). The assays were repeated three times, with 10 inoculation sites per experiment. Disease incidence was calculated as follows: number of disease sites/total number of inoculation sites × 100%.

Colonization of *Bacillus velezensis* Strain P2-1 in Apple Fruit Wounds

Apple fruits (Gala) wounds were punctured with a sterile borer, according to the same procedure mentioned above, following the application of 40 μL of strain P2-1 cell suspension (1×10^8 CFU mL^{-1}) to each wound. The fruits were then incubated at 20°C. We collected the wounded tissue (about 0.6 g) at 0 (3 h after inoculation), 1, 2, 3, 4, 5, and 6 days post inoculation, respectively. The wounded tissue was then ground by using a grinder as the same procedure mentioned above. Serial 10-fold dilution was prepared and each dilution (0.1 mL) was put onto NA medium on Petri dishes. After 2 days of incubation at 28°C, the plates were counted for bacterial colonies. The experiment was repeated twice, with three replicates each time.

Efficacy of *Bacillus velezensis* Strain P2-1in Reducing Apple Fruit Natural Decay Development

Healthy apple fruits (Gala) were harvested from an orchard in Xinxiang, Henan province, China, which contained over 10-year-old trees that were severely infected with *B. dothidea*. Apple fruits were inoculated with strain P2-1, by dipping them for 2 min in the cell suspension (1×10^8 CFU mL^{-1}) or sterile distilled water and then dried. The treated fruits were kept in a transparent plastic box at 20°C with a relative humidity of 85%. The number of fruits with rot disease was weekly recorded. The experiment was repeated twice and each treatment consisted of three replicates, with ten fruit samples in each replicate. The percentage of disease incidence was calculated as follows: Number of rotted fruits/total number of fruits × 100%.

Effects of *Bacillus velezensis* Strain P2-1 on Postharvest Quality Parameters of Apple

To assess the effect of strain P2-1 on the postharvest quality of apple fruits (Gala), freshly harvested fruits were treated and stored as previously described. Four parameters were determined: (i) fruit firmness, (ii) ascorbic acid content, (iii) titratable acid content, and (iv) soluble sugar content. The firmness of each apple was determined at three points along the equatorial region, using the GY-1 Texture Analyzer equipped with a 5 mm diameter flat probe (TOP, Beijing, China). Ascorbic acid was measured according to a previous study (Özden and Bayindirli, 2002). Titratable acid concentrations were determined by titration with 0.1 N NaOH to a pH of 8.1 (Wright and Kader, 1997). Soluble sugar was assessed using the fehling reagent titration method (Guo et al., 2019).

Detection of Antibiotic Biosynthesis Genes in *Bacillus velezensis* Strain P2-1

The total genomic DNA of strain P2-1 was extracted using a DNA extraction kit (Omega, Guangdong, China). Specific genes associated with the biosynthesis of an individual antibiotic in bacteria were amplified using the primers indicated in **Supplementary Table 1**. The PCR products were then electrophoretically separated and sequenced. qRT-PCR was used to assess the expression levels of antibiotic biosynthesis genes in strain P2-1. The total RNA was extracted using the RNA extraction kit (Omega, Guangdong, China) from 2-day-old cultures (grown in LB broth). The Prime Script^{TM} RT Reagent Kit (Omega, Guangdong, China) was used to synthesize first-strand cDNA from 1 μg of total RNA. qRT-PCR was performed using a Light Cycler® 96 PCR Detection System (Roche, Germany) with a ChemoHS qPCR kit (Monad, Suzhou, China) following the manufacturer's protocol. **Supplementary Table 1** includes the primers for qRT-PCR. The 16S ribosomal RNA gene was used as a reference gene (Yu et al., 2015), and relative gene expression was normalized using the $2^{-\Delta\Delta Ct}$ method (Livak and Schmittgen, 2001). All of the experiments were carried out twice, with at least three biological replicates each time.

Effect of *Bacillus velezensis* Strain P2-1 on Induction of Defense-Related Gene Expression

Healthy apple fruits (Gala) were evenly sprayed with strain P2-1 cell suspension (1×10^8 CFU mL^{-1}) for total RNA extraction. As a control, sterile distilled water treatment was used. Total RNA was extracted at 0, 24, and 48 h post inoculation (hpi), using RNA extraction kit (Omega, Guangdong, China). The transcript levels of pathogenesis-related protein (*PR*) genes *MdPR1* and *MdPR5* were measured with specific primers in **Supplementary Table 1**. Elongation factor 1-a (*EF1a*) was used as a reference gene. This assay was repeated two times, with three replicates each time.

RESULTS

Isolation and Screening of Antagonistic Bacteria

In a previous work, we tested 189 apple germplasms for resistance to *B. dothidea* and discovered that two varieties, "Kitanosach" and "Qinguan," demonstrated great resistance to ring rot disease caused by *B. dothidea* (Hou et al., 2017). In this study, endophytic bacterial strains were isolated from the bark of branches of "Kitanosach." In total, 80 bacterial isolates were obtained and screened in the dual culture test for potential antagonistic activity against *B. dothidea*. Only three strains exhibited significant antagonistic activity against *B. dothidea*, with strain P2-1 showing enhanced inhibition of approximately 73.3% of *B. dothidea* mycelial growth (**Figure 1A** and **Table 1**). The inhibition zone of *B. dothidea* mycelial growth by strain P2-1 was of 8.6 mm. The antagonistic effect of strain P2-1 on *B. dothidea* hyphae characteristics was further assessed by microscopic observations. The results indicated that, in comparison to normal hyphae, *B. dothidea* hyphae after antagonism with the strain P2-1 exhibited abnormal stretching with deformity and a protoplast-like ball at the end of hyphae (**Figure 1B**). Further statistic results showed a significantly smaller average hyphal diameter of *B. dothidea* under the stress of strain P2-1 than that of control (**Figure 1C**).

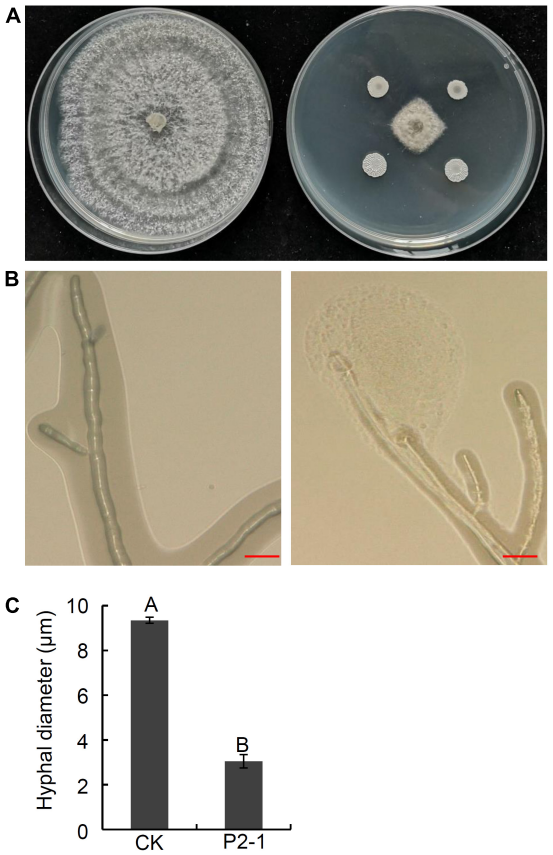

FIGURE 1 | Inhibition of strain P2-1 on hyphal growth of *B. dothidea*. **(A)** Antifungal activity of strain P2-1 against *B. dothidea*. Left: *B. dothidea* CK; Right: *B. dothidea* at the present of strain P2-1. The pictures were taken at 6 days after inoculation. **(B)** Effect of strain P2-1 on hyphal morphology of *B. dothidea*. Left: *B. dothidea* CK; Right: *B. dothidea* at the present of strain P2-1. The picture was taken at 2 days after antagonism with strain P2-1 using an ultra-depth three-dimensional microscope. Bar = 20 μm. **(C)** Hyhal diameter of *B. dothidea* after antagonism with strain P2-1. Values are means ± SD from three replicates. Different letters indicate significant differences between different treatments according to Student's *t*-test ($P < 0.01$).

TABLE 1 | The inhibition of strain P2-1 against phytopathogenic fungi.

Phytopathogenic fungi	Inhibition (%)
Botryosphaeria dothidea	73.3 ± 2.4
Valsa mali	73.2 ± 1.0
Colletotrichum gloeosporioides	65.3 ± 1.3
Valsa pyri	65.2 ± 3.3

Data represents the mean ± SD of three biological replicates.

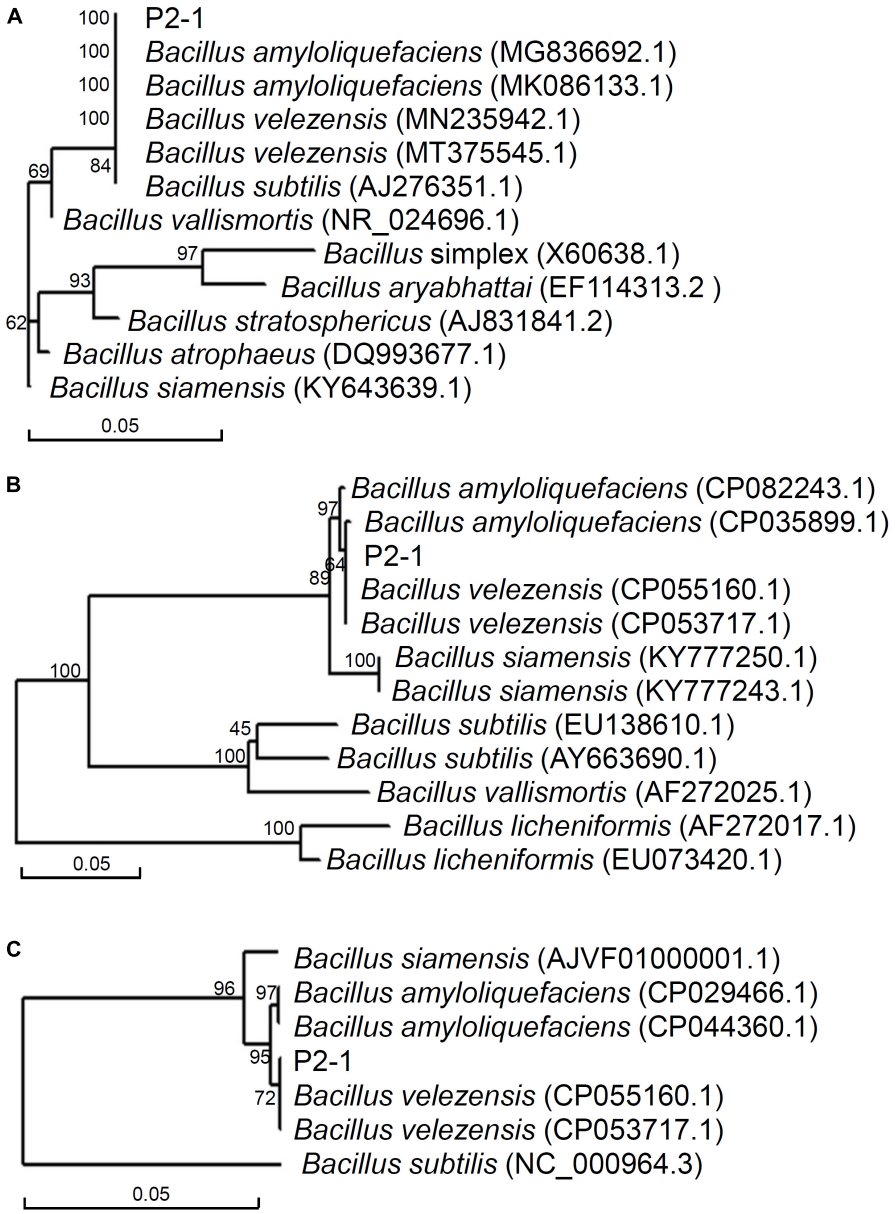

FIGURE 2 | Phylogenetic analysis of strain P2-1 and its relatives based on 16 S rDNA **(A)**, *gyrA* **(B)**, and *ropB* **(C)**.

In addition, strain P2-1 was able to significantly inhibit the three other important fruit pathogens *V. mali*, *C. gloeosporioides,* and *V. pyri*, with respective inhibition of 73.2, 65.3, and 65.2% (**Table 1**). These results indicated that strain P2-1 possessed broad-spectrum antagonistic activity *in vitro*.

Identifying the Bacterial Strain P2-1

The results of biochemical and physiological testing of strain P2-1 are summarized in **Supplementary Table 2**. The bacterium strain P2-1 was identified as a gram-positive strain. Positive results were obtained for VP, citrate, methyl red, V-general, nitrate reductase, starch hydrolysis, and gelatin liquefaction tests (**Supplementary Table 2**). Strain P2-1 could grow on media containing glucose, xylose, or mannitol as a carbon source. These features were similar to those found in *Bacillus* sp.

Partial 16 S rDNA sequence from strain P2-1 was amplified and used to construct a phylogenetic tree with closely related sequences. It was shown that strain P2-1 shared a branch with *B. velezensis*, *B. amyloliquefaciens,* and *B. subtilis* strains (**Figure 2A**). To further identify the species of strain P2-1, phylogenetic trees based on partial *gyrA* and *ropB* sequences were similarly constructed. The results indicated that strain P2-1 was most closely related to *B. velezensis* (**Figures 2B,C**). Therefore, strain P2-1 was identified as *B. velezensis* (16S rDNA accession number: OL314749; gyrA accession number: OL345592; ropB accession number: OL345593).

Efficacy of *Bacillus velezensis* Strain P2-1 in Controlling Ring Rot Caused by *Botryosphaeria dothidea* in Apple

To investigate the efficacy of strain P2-1 strain in controlling the apple ring rot associated with *B. dothidea*, apple fruits were treated with strain P2-1 cell suspension and inoculated with *B. dothidea*. Three days after *B. dothidea* inoculation, the control apple fruits developed a brown lesion around the inoculation site, whereas the apple fruits treated with strain P2-1 cell suspension showed almost no disease symptom (**Figure 3A**). At 5 days post *B. dothidea* inoculation, strain P2-1 cell suspension still exhibited significant inhibition activity against disease development (**Figure 3A**). The disease incidence was reduced to 56.7%, compared to the control treated fruit (which was equivalent to 98.3%) (**Figure 3B**). As a positive control, apple fruits treated with carbendazim remained disease-free (**Figure 3A**). Additionally, when apple fruits were treated with strain P2-1 cell suspension, the average lesion diameter was significantly reduced when compared to the control (**Figure 3C**). Thus, these findings indicated that a suspension of P2-1 cells was capable of suppressing the incidence and severity of apple ring rot caused by *B. dothidea*.

Bacillus velezensis Strain P2-1 Supernatant Mediated Suppression of *Botryosphaeria dothidea*

To determine whether strain P2-1 supernatant also possessed antagonistic activity against *B. dothidea,* we collected supernatant of strain P2-1 and added it into PDA medium to yield PDA containing 1, 2, 5, or 10% of strain P2-1 supernatant. The dual culture assay revealed that strain P2-1 supernatant suppressed *B. dothidea* mycelial growth significantly (**Figures 4A,B**). The inhibition of *B. dothidea* by 1, 2, 5 and 10% of strain P2-1 supernatant was 37.8, 73.2, 79.3, and 89.0%, respectively (**Figure 4C**).

Additionally, the efficiency of strain P2-1 supernatant was studied in preventing ring rot triggered by *B. dothidea* in apple fruit. The results showed that strain P2-1 supernatant significantly reduced *B. dothidea*-caused apple ring rot disease. When compared to the control, strain P2-1 supernatant dramatically reduced disease incidence and average lesion diameter (**Figures 4D,E**). These findings suggested that the strain P2-1 supernatant has antifungal efficacy toward *B. dothidea*.

Bacillus velezensis Strain P2-1 Mediated Suppression of Carbendazim-Resistance Isolate of *Botryosphaeria dothidea*

To further test whether strain P2-1 had an antagonistic potential for fungicide-resistance isolate of *B. dothidea*, Bd7, a carbendazim-resistance isolate (**Supplementary Figure 1**; Wang L. et al., 2021), was antagonized with strain P2-1 bacterial suspension or supernatant. The strain P2-1 cell suspension and supernatant greatly reduced Bd7 mycelial growth in a dual culture study (**Supplementary Table 3**).

We also investigated the efficacy of strain P2-1 cell suspension in suppressing ring rot, caused by carbendazim-resistance isolate Bd7 in apple fruit. Strain P2-1 cell suspension dramatically reduced the incidence of disease and average lesion width in apple fruits, infected with Bd7 isolate (**Figure 5**).

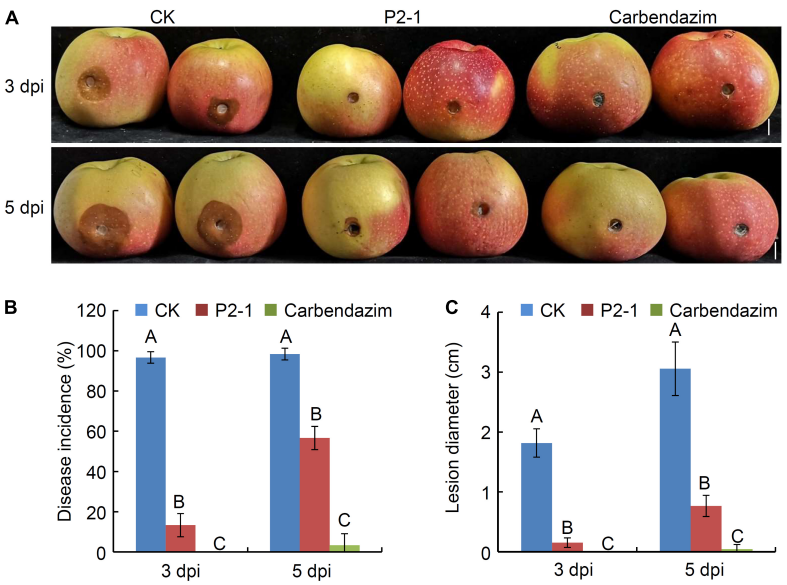

FIGURE 3 | Suppression of *B. velezensis* strain P2-1 cell suspension on apple ring rot caused by *B. dothidea*. **(A)** Strain P2-1 cell suspension antagonized apple ring rot. Treatment with sterile distilled water or carbendazim was used as the negative and positive control, respectively. Bar = 1 cm. **(B)** Statistical analysis of the disease incidence. **(C)** Statistical analysis of disease lesion diameter. Each data represents the mean ± SD of three replicates. Disease lesion length and disease incidence were measured at 3 and 5 days post inoculation (dpi), respectively. Letters above the bars indicate statistical significance and different letters indicate significant different means ($p < 0.01$) based on Student's *t*-test.

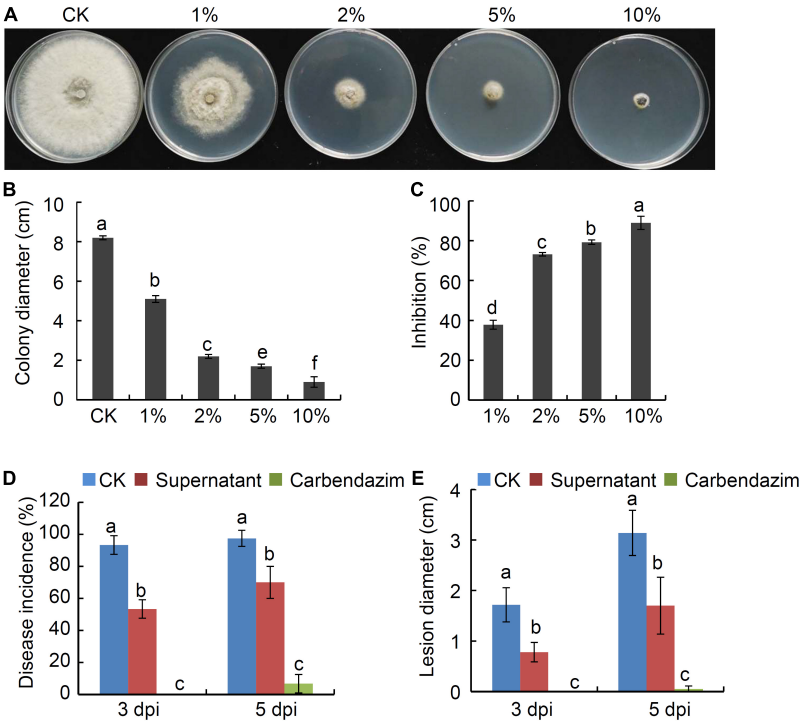

FIGURE 4 | Suppression of *B. velezensis* strain P2-1 supernatant on *B. dothidea*. **(A)** Inhibition of strain P2-1 supernatant on mycelial growth of *B. dothidea*. **(B)** Statistical analysis of colony diameter. **(C)** Inhibition rate of strain P2-1 supernatant on mycelial growth *B. dothidea*. **(D)** Effect of strain P2-1 supernatant on apple ring rot disease incidence. **(E)** Effect of strain P2-1 supernatant on apple ring rot disease lesion diameter. Each data represents the mean ± SD of three replicates. Letters above the bars indicate statistical significance and different letters indicate significant different means ($p < 0.05$) based on Student's *t*-test.

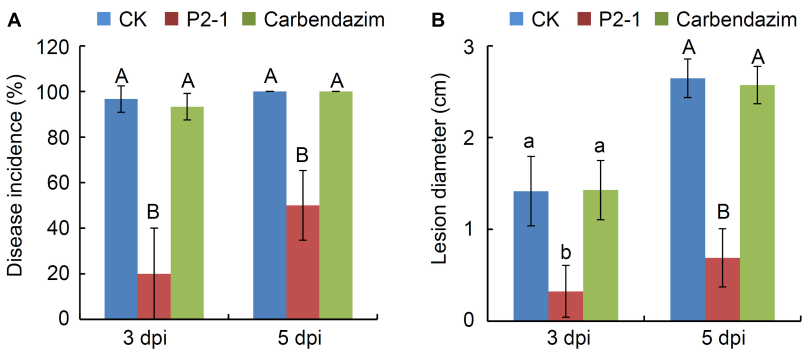

FIGURE 5 | Effect of *B. velezensis* strain P2-1 cell suspension on apple ring rot caused by carbendazim-resistant isolate Bd7. **(A)** Effect of strain P2-1 cell suspension on apple ring rot disease incidence. Treatment with sterile distilled water or carbendazim was used as the negative control. **(B)** Effect of strain P2-1 cell suspension on apple ring rot disease lesion diameter. Each data represents the mean ± SD of three replicates. Letters above the bars indicate statistical significance and different lower case and upper case letters indicate significant different means at $p < 0.05$ and $p < 0.01$ based on Student's *t*-test, respectively.

These findings revealed that strain P2-1 was capable of suppressing apple ring rot disease caused by the carbendazim-resistance isolate.

Colonization of *Bacillus velezensis* Strain P2-1 in Apple Fruit Wounds

We studied the population dynamics of strain P2-1 in apple fruit. Statistical results showed that the number of strain P2-1 colonies in inoculated apple fruit were 1.19×10^7 CFU/wound at 0 dpi, and rapidly increased to 4.66×10^7 CFU at 1 dpi (**Figure 6**). The population of strain P2-1 colonies reached a small peak with the population 6.61×10^8 CFU at 3 dpi, and declined slightly at 4 dpi. Following that, the number of strain P2-1 slightly increased or decreased but remained typically consistent during the subsequent storage time. At 10 dpi, the population of strain P2-1 remained higher (9.93×10^8 CFU) than the initial number (**Figure 6**). These results indicated the capability of strain P2-1 to successfully colonize in apple wounds.

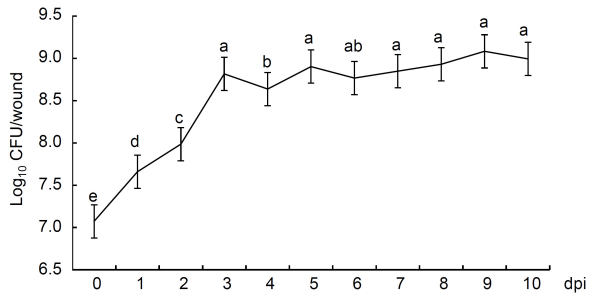

FIGURE 6 | Population dynamics of *B. velezensis* strain P2-1 in wounds of apple fruit. The colonies were counted and population densities were expressed as $\log_{10}$ CFU/wound. Each data represents the mean ± SD of three biological replicates. Different letters indicate significant differences between different treatments according to Student's *t*-test ($P < 0.05$).

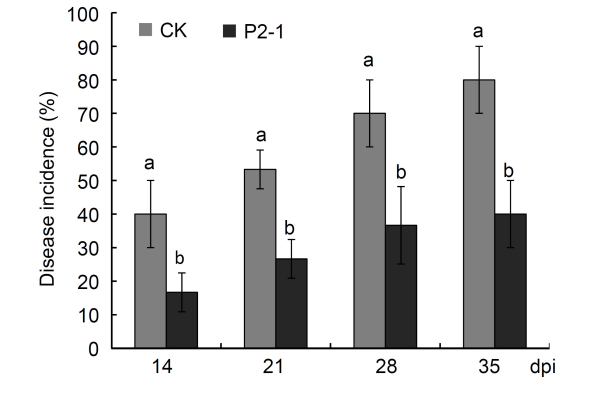

FIGURE 7 | Disease incidence of natural decay in apple fruits treated with *B. velezensis* strain P2-1 cell suspension after harvest. Each data represents the mean ± SD of three biological replicates at each time point. Different letters indicate significant differences between different treatments according to Student's *t*-test ($P < 0.05$).

Efficacy of *Bacillus velezensis* Strain P2-1 for Reducing Apple Fruit Natural Decay

Apples were treated with strain P2-1 cell suspension after harvest to examine the influence of strain P2-1 on apple decay during the postharvest period. Statistical results showed that strain P2-1 treatment significantly reduced the incidence of disease as compared to the control treatment during 35 days storage period (**Figure 7**). At 28 days and thereafter, the disease incidence of control treatment was more than 70%, while the disease incidence of strain P2-1 treatment remained less than 40% (**Figure 7**), suggesting that strain P2-1 was effective toward control of apple postharvest decay.

Effects of *Bacillus velezensis* Strain P2-1 on Postharvest Quality Parameters of Apple

To assess the impact of antagonistic strain P2-1 on apple postharvest quality, four criteria were tested: (i) fruit firmness, (ii) ascorbic acid, (iii) titratable acid, and (iv) soluble sugar. The results indicated that strain P2-1 had no obvious influence on fruit firmness, ascorbic acid, titratable acid, or soluble sugar in apples (**Table 2**). This indicated that strain P2-1 had no significant influence on the postharvest quality of apple.

TABLE 2 | Effects of *B. velezensis* strain P2-1 on postharvest quality parameters of apple.

Treatment	Firmness (N)	Ascorbic acid (mg/100 g)	Titratable acid (%)	Soluble sugar (%)
CK	31.62 ± 0.09	3.87 ± 0.58	0.19 ± 0.01	10.41 ± 0.37
P2-1	32.06 ± 0.94	3.68 ± 0.26	0.21 ± 0.01	11.05 ± 0.56

Data represents the mean ± SD of three biological replicates. The samples treated with sterile distilled water were used as CK.

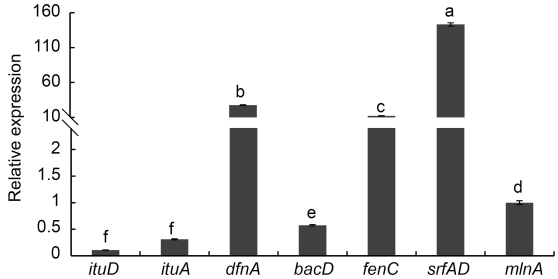

FIGURE 8 | Analysis of antibiotic biosynthesis genes expression from *B. velezensis* strain P2-1 using qRT-PCR. Relative expression was determined by comparing *mlnA*, arbitrarily set to 1. Each data represents the mean ± SD of three biological replicates at each time point. Different letters indicate significant differences between different treatments according to Student's *t*-test ($P < 0.05$).

Analysis of Antibiotic Biosynthesis Genes From *Bacillus velezensis* Strain P2-1

Bacillus species are found to harbor numerous clusters of the genes involved in the synthesis of antifungal polyketides and lipopeptides. The PCR assays showed that the expected size of PCR products was obtained from strain P2-1 using specific primers (**Supplementary Figure 2**). Sequencing analysis results confirmed the involvement of eight genes in the lipopeptide biosynthesis including *ituD*, *ituA*, *srfAD*, *bacA*, *mlnA*, *bacA/B*, *bmyA*, and *dfnA*. Additionally, **Figure 8** indicated that seven genes were expressed in strain P2-1, and *srfAD* and *dfnA* were expressed at a higher level upon comparison with other genes. The expression of *bymA* gene was not detected.

Effect of *Bacillus velezensis* Strain P2-1 on Pathogenesis-Related Gene Expression in Apple Fruit

To examine the expression of *PR* genes in response to strain P2-1 treatment, apple fruits were equally sprayed with strain P2-1 cell suspension and the levels of *MdPR1* and *MdPR5* genes were determined using qRT-PCR. The results indicated that strain P2-1 treatment considerably increased *MdPR1* and *MdPR5*

expression when compared to the control. *MdPR1* transcript levels in strain P2-1-treated apple fruit reached their peak at 48 hpi, and they were 8.9-fold higher than in the control fruit (**Figure 9A**). The pattern of *MdPR5* gene expression was identical to that of *MdPR1*. *MdPR5* transcript levels were 5.4-fold greater in strain P2-1-treated apple fruit compared to the control (**Figure 9B**). This result indicated that strain P2-1 treatment could activate *PR* genes expression in apple fruit.

DISCUSSION

B. dothidea-caused ring rot is a serious postharvest disease that has an impact on global apple crop supplies. However, due to the latent infection characteristic, it is difficult to control this disease with chemical fungicides (Liu et al., 2011). Endophyte-based biocontrol of apple ring rot disease has emerged as a viable alternative to chemical fungicides in recent years (Chen et al., 2016; Zhang et al., 2016; Huang et al., 2021). In this study, we demonstrated that the use of *B. velezensis* strain P2-1 effectively reduced the width of apple ring rot lesions and the incidence of postharvest disease caused by *B. dothidea*, implying that this strain constitutes a promising resource for biocontrol of *B. dothidea* caused apple postharvest decay. In addition, *B. velezensis* strain P2-1 possessed broad-spectrum antagonistic activity against plant pathogens, which is consistent with previous studies (Khan et al., 2020; Liu et al., 2021).

Many plant phytopathogens, including *B. dothidea*, have been discovered to be resistant to fungicides (Zhou and Wang, 2001; Fan F. et al., 2016; Wang L. et al., 2021), which is one of the emerging challenges in plant disease management strategies. In recent research, we investigated the carbendazim sensitivity of *B. dothidea* isolates from apple orchards from nine Chinese provinces and discovered carbendazim-resistant isolates in three of them (Wang L. et al., 2021). An et al. (2016) also identified thiophanate-methyl resistant isolates in China. These findings encouraged us to emphasize the efficiency of endophytes in controlling fungicide-resistant *B. dothidea* isolates. Our results revealed that *B. velezensis* strain P2-1 cell suspension and supernatant could significantly inhibit the mycelial growth of carbendazim-resistant isolate. Moreover, *B. velezensis* strain P2-1 was found to be able to significantly suppress the apple ring rot disease caused by carbendazim-resistance isolate. This is the first report on the use of endophytes to prevent carbendazim resistance in *B. dothidea* isolates.

The ability of biocontrol agents to colonize and survive in host tissue is critical for their practical application. *B. velezensis* strain P2-1 was an endophytic bacterium isolated from the branches of apple. In addition, we could re-isolate strain P2-1 from the treated apple fruits. The population of strain P2-1 colonies reached a small peak at 3 dpi, which was 55.5-fold greater than the population at 0 dpi, and remained high throughout the subsequent storage period. The rapid growth of strain P2-1 in apple fruit wounds is necessary for its colonization and the production of antagonistic metabolites. When apple fruits were treated with strain P2-1, the natural decay disease incidence was greatly reduced as compared to the control treatment during storage. These findings indicate that *B. velezensis* strain P2-1 could colonize apple fruit well and was effective in preventing apple postharvest decay caused by *B. dothidea*.

Numerous strategies by which *Bacillus* spp. acts as a biocontrol agent against plant diseases have been described (Chen et al., 2016, 2020; Fan et al., 2017; Balderas-Ruíz et al., 2020; Liu et al., 2020). After antagonism with the *B. velezensis* strain P2-1, *B. dothidea* hyphae exhibited aberrant stretching, thin deformation, and a protoplast-like ball at the hyphae's end (**Figure 1B**), which has been previously reported in *Botrytis cinerea* response to *B. velezensis* strain QSE-21 (Xu et al., 2021). Further research revealed that the supernatant of strain P2-1 exhibited potent antifungal activity toward *B. dothidea*, implying that the supernatant included antimicrobial substances. We confirmed that strain P2-1 harbored numerous gene clusters involved in the synthesis of antifungal lipopeptides and polyketides, such as *ituD*, *ituA*, *srfAD*, *bacA*, *mlnA*, *bacA/B*, *bmyA*, and *dfnA*. This finding is consistent with the previous studies conducted on other *Bacillus* species (Athukorala et al., 2009; Kim et al., 2017). We then examined the degree of expression of antibiotic biosynthesis genes and discovered that *srfAD* and *dfnA* were expressed at a higher level than other genes.

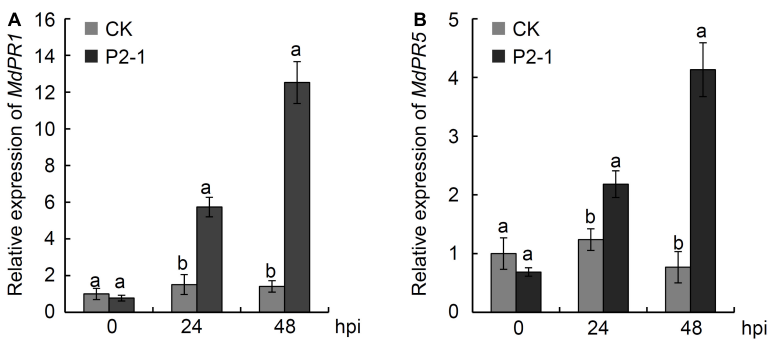

FIGURE 9 | qRT-PCR assay for *MdPR1* gene **(A)** and *MdPR5* gene **(B)** expression in apple fruit induced by *B. velezensis* strain P2-1. Each data represents the mean ± SD of three biological replicates at each time point. Different letters indicate significant differences between different treatments according to Student's *t*-test ($P < 0.05$).

This suggested that *srfAD* and *dfnA* in strain P2-1 may play an important role in antifungal activity against *B. dothidea*.

Biocontrol agents induced disease resistance is an effective method against plant diseases. Previous studies have mentioned that *Bacillus* spp. could enhance resistance against pathogens in fruits by inducing the transcription of defense-associated genes or enzymes (Waewthongrak et al., 2014; Wu et al., 2017; Huang et al., 2021; Wang F. et al., 2021). We also found a similar report that *B. velezensis* strain P2-1 treatment strongly elicited the *PR1* and *PR5* expressions in apple fruit.

The effect of fruit quality is one of the most important criteria in determining whether biocontrol agents may be used in the postharvest process in practice (Liu et al., 2010; Sun et al., 2017). Although some microorganisms have been identified as potential biocontrol agents against *B. dothidea* caused apple postharvest decay (Zhang et al., 2016; Huang et al., 2021), influence of antagonistic strains on the postharvest quality of apple has not yet been evaluated. In the present study, we noticed that *B. velezensis* strain P2-1 had no significant influence on the postharvest quality of apple fruit, which suggested the commercialization potential of *B. velezensis* strain P2-1, to control apple postharvest decay caused by *B. dothidea*.

CONCLUSION

B. velezensis strain P2-1, isolated from apple branches, can successfully prevent apple postharvest decay caused by *B. dothidea* during storage, hence preserving postharvest quality. *B. velezensis* strain P2-1 harbored numerous clusters of the genes that are involved in the synthesis of antifungal lipopeptides and polyketides. Moreover, *B. velezensis* strain P2-1 treatment strongly induced *PR* genes expression in apple fruit. Overall, our research has identified a viable biocontrol agent for *B. dothidea*-induced apple postharvest decay and sheds light on the interaction mechanism between the biocontrol agent and pathogenic fungi.

DATA AVAILABILITY STATEMENT

The original contributions presented in the study are included in the article/**Supplementary Material**, further inquiries can be directed to the corresponding author/s.

AUTHOR CONTRIBUTIONS

HY designed the research and wrote the manuscript. HY, BS, and LW performed the experiments with helps from TH, ZZ, and HH. HY and HH analyzed the data. HT provided the funding. All authors contributed to the article and approved the submitted version.

FUNDING

This work was obtained the financial support of the National Key R&D Program of China (No. 2017YFE0135600) and Central Public-Interest Scientific Institution Basal Research Fund (No. ZGS202110).

SUPPLEMENTARY MATERIAL

The Supplementary Material for this article can be found online at: https://www.frontiersin.org/articles/10.3389/fmicb.2021.808938/full#supplementary-material

Supplementary Figure 1 | Test the carbendazim sensitivity of *B. dothidea* isolates. *B. dothidea* isolate Bd7 was used to value the carbendazim sensitivity. Carbendazim-sensitive isolate Bd220 was used as a negative control. The picture was taken at 5 dpi.

Supplementary Figure 2 | PCR analysis of antibiotic biosynthesis genes from *B. velezensis* strain P2-1. M, Trans 2K DNA ladder, 1, *ituD*; 2, *ituA*; 3, *srfA*; 4, *baeA*; 5, *mlnA*; 6, *bacA/B*; 7, *bmyA*; 8, *dfnA*.

REFERENCES

An, J., Guo, L., Zhu, X., and Song, Y. (2016). Susceptibility of *Botryosphaeria dothidea* to tebuconazole and thiophanate-methyl. *Plant Prod.* 42, 187–191. doi: 10.3969/j.issn.0529-1542.2016.02.034

Athukorala, S. N., Fernando, W. D., and Rashid, K. Y. (2009). Identification of antifungal antibiotics of *Bacillus* species isolated from different microhabitats using polymerase chain reaction and MALDI-TOF mass spectrometry. *Can. J. Microbiol.* 55, 1021–1032. doi: 10.1139/W09-067

Balderas-Ruíz, K. A., Bustos, P., Santamaria, R. I., González, V., Cristiano-Fajardo, S. A., Barrera-Ortíz, S., et al. (2020). *Bacillus velezensis* 83 a bacterial strain from mango phyllosphere, useful for biological control and plant growth promotion. *AMB Express* 10, 1–19. doi: 10.1186/s13568-020-01101-8

Chen, X., Zhang, Y., Fu, X., Li, Y., and Wang, Q. (2016). Isolation and characterization of *Bacillus amyloliquefaciens* PG12 for the biological control of apple ring rot. *Postharvest Biol. Technol.* 115, 113–121. doi: 10.1016/j.postharvbio.2015.12.021

Chen, Z., Zhao, L., Chen, W., Dong, Y., Yang, C., Li, C., et al. (2020). Isolation and evaluation of *Bacillus velezensis* ZW-10 as a potential biological control agent against *Magnaporthe oryzae*. *Biotechnol. Biotechnol. Equip.* 34, 714–724. doi: 10.1080/13102818.2020.1803766

dos Santos, K. M., Tsuji, S. S., Câmara, M. P. S., Michereff, S. J., and Lopes, U. P. (2019). Sensitivity to methyl benzimidazole carbamate fungicides of *Botryosphaeriaceae* species from mango orchards in the Northeast of Brazil. *Eur. J. Plant Pathol.* 153, 209–222. doi: 10.1007/s10658-018-1556-y

Fan, F., Li, N., Li, G., and Luo, C. (2016). Occurrence of fungicide resistance in *Botrytis cinerea* from greenhouse tomato in Hubei Province, China. *Plant Dis.* 100, 2414–2421. doi: 10.1094/PDIS-03-16-0395-RE

Fan, H., Ru, J., Zhang, Y., Wang, Q., and Li, Y. (2017). Fengycin produced by *Bacillus subtilis* 9407 plays a major role in the biocontrol of apple ring rot disease. *Microbiol. Res.* 199, 89–97. doi: 10.1016/j.micres.2017.03.004

Fan, H., Zeng, L., Yang, P., Guo, Z., and Bai, T. (2016). First report of banana soft rot caused by *Klebsiella variicola* in China. *Plant Dis.* 100:517. doi: 10.1094/PDIS-05-15-0586-PDN

Guo, L., Luo, J., Pang, R., Wang, R., Huang, Y., Qiao, C., et al. (2019). Gene expression related to sugar content during storage of Kiwifruit under room temperature with CPPU treatment. *Acta Agric.* 34, 40–45.

Holt, J. G., Krieg, N. R., Sneath, P. H., Staley, J. T., and Williams, S. T. (1994). *Bergey's Manual of Determinative Bacteriology*, 9th Edn. Baltimore, MD: William & Wilkins.

Hou, H., Zhang, H., Zhou, Z., Wang, L., Yan, Z., and Wang, S. (2017). Evaluation of resistance to apple ring rot in *Malus* germplasms. *Acta Hortic. Sin.* 44:1559. doi: 10.16420/j.issn.0513-353x.2017-0286

Huang, Y., Sun, C., Guan, X., Lian, S., Li, B., and Wang, C. (2021). Biocontrol efficiency of *Meyerozyma guilliermondii* Y-1 against apple postharvest decay caused by *Botryosphaeria dothidea* and the possible mechanisms of action. *Int. J. Food Microbiol.* 338:108957. doi: 10.1016/j.ijfoodmicro.2020.108957

Jurick, W. M. II, Vico, I., Gaskins, V. L., Janisiewicz, W. J., and Peter, K. A. (2013). First report of *Botryosphaeria dothidea* causing white rot on apple fruit in Maryland. *Plant Dis.* 97:999. doi: 10.1094/PDIS-01-13-0053-PDN

Khan, M. S., Gao, J., Chen, X., Zhang, M., Yang, F., Du, Y., et al. (2020). The endophytic *Bacteria Bacillus velezensis* Lle-9, isolated from *Lilium leucanthum*, harbors antifungal activity and plant growth-promoting effects. *J. Microbiol. Biotechnol.* 30, 668–680. doi: 10.4014/jmb.1910.10021

Kim, Y., Balaraju, K., and Jeon, Y. (2017). Biological characteristics of *Bacillus amyloliquefaciens* AK-0 and suppression of ginseng root rot caused by *Cylindrocarpon destructans*. *J. Appl. Microbiol.* 122, 166–179. doi: 10.1111/jam.13325

Liu, H. M., Guo, J. H., Cheng, Y. J., Luo, L., Liu, P., Wang, B. Q., et al. (2010). Control of gray mold of grape by *Hanseniaspora uvarum* and its effects on postharvest quality parameters. *Ann. Microbiol.* 60, 31–35. doi: 10.1007/s13213-010-0018-3

Liu, R., Li, J., Zhang, F., Zheng, D., Chang, Y., Xu, L., et al. (2021). Biocontrol activity of *Bacillus velezensis* D4 against apple Valsa canker. *Biol. Control* 163:104760. doi: 10.1016/j.biocontrol.2021.104760

Liu, Y., Chen, Z., Liu, Y., Wang, X., Luo, C., Nie, Y., et al. (2011). Enhancing bioefficacy of *Bacillus subtilis* with sodium bicarbonate for the control of ring rot in pear during storage. *Biol. Control* 57, 110–117. doi: 10.1016/j.biocontrol.2011.01.008

Liu, Y., Teng, K., Wang, T., Dong, E., Zhang, M., Tao, Y., et al. (2020). Antimicrobial *Bacillus velezensis* HC6: production of three kinds of lipopeptides and biocontrol potential in maize. *J. Appl. Microbiol.* 128, 242–254. doi: 10.1111/jam.14459

Livak, K. J., and Schmittgen, T. D. (2001). Analysis of relative gene expression data using real-time quantitative PCR and the $2^{-\Delta\Delta\ CT}$ method. *Methods* 25, 402–408. doi: 10.1006/meth.2001.1262

Özden, C., and Bayindirli, L. (2002). Effects of combinational use of controlled atmosphere, cold storage and edible coating applications on shelf life and quality attributes of green peppers. *Eur. Food Res. Technol.* 214, 320–326. doi: 10.1007/s00217-001-0448-z

Phillips, A. J. L., Rumbos, I. C., Alves, A., and Correia, A. (2005). Morphology and phylogeny of *Botryosphaeria dothidea* causing fruit rot of olives. *Mycopathologia* 159, 433–439. doi: 10.1007/s11046-005-0256-2

Rooney, A. P., Price, N. P., Ehrhardt, C., Swezey, J. L., and Bannan, J. D. (2009). Phylogeny and molecular taxonomy of the *Bacillus subtilis* species complex and description of *Bacillus subtilis* subsp. *inaquosorum* subsp. nov. *Int. J. Syst. Evol. Microbiol.* 59, 2429–2436. doi: 10.1099/ijs.0.009126-0

Sun, P., Cui, J., Jia, X., and Wang, W. (2017). Isolation and characterization of *Bacillus amyloliquefaciens* L-1 for biocontrol of pear ring rot. *Hortic. Plant J.* 3, 183–189. doi: 10.1016/j.hpj.2017.10.004

Tang, W., Ding, Z., Zhou, Z. Q., Wang, Y. Z., and Guo, L. Y. (2012). Phylogenetic and pathogenic analyses show that the causal agent of apple ring rot in China is *Botryosphaeria dothidea*. *Plant Dis.* 96, 486–496. doi: 10.1094/pdis-08-11-0635

Waewthongrak, W., Leelasuphakul, W., and Mccollum, G. (2014). Cyclic lipopeptides from *Bacillus subtilis* ABS–S14 elicit defense-related gene expression in citrus fruit. *PLoS One* 9:e109386. doi: 10.1371/journal.pone.0109386

Wang, F., Xiao, J., Zhang, Y., Li, R., Liu, L., and Deng, J. (2021). Biocontrol ability and action mechanism of *Bacillus halotolerans* against *Botrytis cinerea* causing grey mould in postharvest strawberry fruit. *Postharvest Biol. Technol.* 174:111456. doi: 10.1016/j.postharvbio.2020.111456

Wang, L., Tu, H., Hou, H., Zhou, Z., Yuan, H., Luo, C., et al. (2021). Occurrence and detection of carbendazim-resistance in *Botryosphaeria dothidea* from apple orchards in China. *Plant Dis*. doi: 10.1094/pdis-06-20-1204-re [Epub ahead of print].

Wright, K. P., and Kader, A. A. (1997). Effect of controlled-atmosphere storage on the quality and carotenoid content of sliced persimmons and peaches. *Postharvest Biol. Technol.* 10, 89–97. doi: 10.1016/S0925-5214(96)00062-2

Wu, Y., Lin, H., Lin, Y., Shi, J., Xue, S., Hung, Y.-C., et al. (2017). Effects of biocontrol bacteria *Bacillus amyloliquefaciens* LY-1 culture broth on quality attributes and storability of harvested litchi fruit. *Postharvest Biol. Technol.* 132, 81–87. doi: 10.1016/j.postharvbio.2017.05.021

Xu, Y., Wang, L., Liang, W., and Liu, M. (2021). Biocontrol potential of endophytic *Bacillus velezensis* strain QSE-21 against postharvest grey mould of fruit. *Biol. Control* 161:104711. doi: 10.1016/j.biocontrol.2021.104711

Xue, D., Liu, J., Li, B.-H., Xu, X., Liu, N., Lian, S., et al. (2021). Effect of rainfall and temperature on perithecium production of *Botryosphaeria dothidea* on cankered apple branches. *Phytopathology* 111, 982–989. doi: 10.1094/phyto-07-20-0262-r

Yong, D., Wang, C., Li, G., and Li, B. (2014). Control efficiency of endophytic actinomycetes A-1 against apple fruit ring rot and its influence on the activity of defense-related enzymes. *Acta Phytophys. Sin.* 41, 335–341. doi: 10.13802/j.cnki.zwbhxb.2014.03.013

Yu, Z., Guo, C., and Qiu, J. (2015). Precursor amino acids inhibit polymyxin E biosynthesis in *Paenibacillus polymyxa*, probably by affecting the expression of polymyxin E biosynthesis-associated genes. *Biomed Res. Int.* 2015:690830. doi: 10.1155/2015/690830

Yuan, H., Shi, B., Huang, T., Zhou, Z., Wang, L., Hou, H., et al. (2021). Biological control of pear Valsa canker caused by *Valsa pyri* using *Penicillium citrinum*. *Horticulturae* 7:198. doi: 10.3390/horticulturae7070198

Zhang, Q., Yong, D., Zhang, Y., Shi, X., Li, B., Li, G., et al. (2016). *Streptomyces rochei* A-1 induces resistance and defense-related responses against *Botryosphaeria dothidea* in apple fruit during storage. *Postharvest Biol. Technol.* 115, 30–37. doi: 10.1016/j.postharvbio.2015.12.013

Zhou, M. G., and Wang, J. (2001). Study on sensitivity base-line of *Fusarium graminearum* to carbendazim and biological characters of MBC-resistant strains. *Acta Phytopathol. Sin.* 31, 365–367. doi: 10.13926/j.cnki.apps.2001.04.014

Conflict of Interest: The authors declare that the research was conducted in the absence of any commercial or financial relationships that could be construed as a potential conflict of interest.

Publisher's Note: All claims expressed in this article are solely those of the authors and do not necessarily represent those of their affiliated organizations, or those of the publisher, the editors and the reviewers. Any product that may be evaluated in this article, or claim that may be made by its manufacturer, is not guaranteed or endorsed by the publisher.

frontiers in Microbiology

ORIGINAL RESEARCH
published: 07 February 2022
doi: 10.3389/fmicb.2022.796167

Efficacy of Dimethyl Trisulfide on the Suppression of Ring Rot Disease Caused by *Botryosphaeria dothidea* and Induction of Defense-Related Genes on Apple Fruits

Meng Sun[1,2,3,4†], *Yanxin Duan*[1,2,3,4†], *Jun Ping Liu*[1,2,3,4], *Jing Fu*[1,2,3,4] and *Yonghong Huang*[1,2,3,4*]

[1] College of Horticulture, Qingdao Agricultural University, Qingdao, China, [2] Laboratory of Quality and Safety Risk Assessment for Fruit (Qingdao), Ministry of Agriculture and Rural Affairs, Qingdao, China, [3] National Technology Centre for Whole Process Quality Control of FSEN Horticultural Products (Qingdao), Qingdao, China, [4] Qingdao Key Laboratory of Modern Agriculture Quality and Safety Engineering, Qingdao, China

OPEN ACCESS

Edited by:
Antonio Ippolito,
University of Bari Aldo Moro, Italy

Reviewed by:
Alejandro Hernández,
University of Extremadura, Spain
Soner Soylu,
Mustafa Kemal University, Turkey

***Correspondence:**
Yonghong Huang
gstshh@126.com

[†] These authors have contributed equally to this work

Specialty section:
This article was submitted to Food Microbiology, a section of the journal Frontiers in Microbiology

Received: 10 November 2021
Accepted: 07 January 2022
Published: 07 February 2022

Citation:
Sun M, Duan Y, Liu JP, Fu J and Huang Y (2022) Efficacy of Dimethyl Trisulfide on the Suppression of Ring Rot Disease Caused by Botryosphaeria dothidea and Induction of Defense-Related Genes on Apple Fruits. Front. Microbiol. 13:796167. doi: 10.3389/fmicb.2022.796167

Apple ring rot caused by *Botryosphaeria dothidea* is prevalent in main apple-producing areas in China, bringing substantial economic losses to the growers. In the present study, we demonstrated the inhibitory effect of dimethyl trisulfide (DT), one of the main activity components identified in Chinese leek (*Allium tuberosum*) volatile, on the apple ring rot on postharvest fruits. In *in vitro* experiment, 250 μL/L DT completely suppressed the mycelia growth of *B. dothidea*. In *in vivo* experiment, 15.63 μL/L DT showed 97% inhibition against the apple ring rot on postharvest fruit. In addition, the soluble sugar content, vitamin C content, and the soluble sugar/titratable acidity ratio of the DT-treated fruit were significantly higher than those of the control fruit. On this basis, we further explored the preliminary underlying mechanism. Microscopic observation revealed that DT seriously disrupted the normal morphology of *B. dothidea*. qRT-PCR determination showed the defense-related genes in DT-treated fruit were higher than those in the control fruit by 4.13–296.50 times, which showed that DT inhibited apple ring rot on postharvest fruit by suppressing the growth of *B. dothidea*, and inducing the defense-related genes in apple fruit. The findings of this study provided an efficient, safe, and environment-friendly alternative to control the apple ring rot on apple fruit.

Keywords: ***Allium tuberosum*, *Botryosphaeria dothidea*, biocontrol, defensive genes, fruit quality**

INTRODUCTION

Apple is one of the most critical and popular fruits around the world. However, apple ring rot caused by the latent pathogen *Botryosphaeria dothidea* has seriously threatened apple production in recent years. The pathogen infects branches and trunks, resulting in wart-like symptoms around lenticels. As the disease aggravates, the infected trunks and shoots die. *B. dothidea* also infects apple fruit, causing slightly sunken lesions with alternating tan and brown rings. Subsequently, the diseased fruit rots quickly with a sour smell and oozes brown mucus sometimes (Tang et al., 2012; Bai et al., 2015). The decayed fruit proportion caused by the disease usually ranges between

10 and 20% each year. However, it may reach 70% in seasons with conditions conducive to fungal development (Zhao et al., 2016).

In addition to apple fruits, *B. dothidea* also infects various fruit such as fig (*Ficus carica*) (Wang et al., 2020), olive (*Olea europaea* L.) (Korukmez et al., 2019), sweet cherry (*Prunus avium* L.) (Zhang et al., 2019), pomegranate (*Punica granatum* L.) (Gu et al., 2020), apricot (*Prunus armeniaca* L.) (Huang et al., 2019b), mulberry (*Morus alba* L.) (Huang et al., 2019a), pear (*Pyrus bretschneideri* Rehd.) (Sun et al., 2020), avocado (*Persea americana*) (Qiu et al., 2020), and kiwifruit (*Actinidia chinensis*) (Wang et al., 2021). Therefore, it is indispensable to develop efficient ways to prevent and control the spread of *B. dothidea*.

Cultivating resistant varieties is the most economical and effective approach for controlling apple ring rot caused by *B. dothidea*. Unfortunately, the major commercial cultivars like red fuji, golden delicious, gala, and red delicious are highly susceptible to *B. dothidea* (Guan et al., 2015). Therefore, fungicide application is still the primary method to control apple ring rot worldwide (Fan et al., 2016, 2019). Previous studies showed that synthetic fungicides including fludioxonil, fluazinam, pyrisoxazole (Song et al., 2018), difenoconazole, tebuconazole, prochloraz, trifloxystrobin (Dai et al., 2017), tebuconazole (Fan et al., 2016), and pyraclostrobin (Fan et al., 2019) exhibit great potential for inhibiting the apple ring rot. However, the overuse of synthetic chemical pesticides leads to the development of fungicide resistance and causes environmental pollution and health problems.

Therefore, it increasingly stimulates the research on a safer and more eco-friendly alternative means to control plant disease. Naturally derived bioactive compounds are one of the most promising ecological alternatives and have advantages over synthetic fungicides. Previous studies showed that pure monoterpenes in plants including cuminaldehyde, geraniol, and β-citronellol have promising antifungal effects against *B. dothidea* (Zhang et al., 2018). In addition, 32 essential oil monomers exhibit a varying inhibitory effect on *B. dothidea* (Li et al., 2021). The lemon (*Citrus limon* L.) essential oil contains limonene (61.68%), neral (21.66%), γ-pinene (10.23%), γ-terpinene (6.42%) and exhibits potent antifungal activity against *B. dothidea* (Ammad et al., 2018). 4-hydroxycinnamic acid from Moso bamboo (*Phyllostachys pubescens*) leaf shows good antifungal activity to *B. dothidea* (Liao et al., 2021). Matrine significantly inhibits the mycelial growth of *B. dothidea* (Pan et al., 2019). Chelidonine in *Chelidonium majus*, shows intense fungal activity against *B. dothidea* (Pan et al., 2017). Furocoumarins, phenylethyl esters, alcarindiol, and sesquiterpenoid from *Notopterygium incisum* exhibit antifungal activities against *B. dothidea* (Xiao et al., 2018). Several active components, including schisanhenol B, schizandrin A, schizarin D, schizandrin B, gomisin L, schizandrol A, schizandrol B, isoschizandrin, schisanlignone A, kadsulignan M identified from *Schisandra chinensis*, inhibit hyphal growth of *B. dothidea* and significantly inhibited the apple ring rot on fruits (Yi et al., 2016).

Our preliminary study found that the Chinese leek (*Allium tuberosum*) extract exhibited potent inhibition on the mycelia growth of *B. dothidea*, thereby significantly suppressing the incidence of apple ring rot on detached shoots and postharvest fruit (Zhao et al., 2017). However, the exact mechanism remains elusive. Therefore, in the present study, we tried to demonstrate the antifungal activity of dimethyl trisulfide (DT), one of the essential components in Chinese leek volatile, against apple ring rot on postharvest fruit. On this basis, we also attempted to explore the underlying mechanism involved in the DT inhibitory effect on apple ring rot from two aspects: fungus *B. dothidea* and the apple fruits.

MATERIALS AND METHODS

Experimental Material, Fungus, and Reagents

The apple fruit (*Malus domestica* Borkh. cv. Red Fuji) used in the experiments was purchased in the local supermarkets. The fruit with uniform sizes, no disease spots, and no mechanical damages was selected for the experiments. DT was provided by Cheng Du Micxy Chemical Co., Ltd., Chengdu, China. The fungal *B. dothidea* was isolated from diseased fruit in a apple orchards in Yantai city and identified by Sangon Biotech (Shanghai, China) (Fu, 2021), and it was kept in potato dextrose agar (PDA) medium.

Determination of the Inhibitory Effect of Dimethyl Trisulfide on the Mycelia Growth of *Botryosphaeria dothidea*

Various concentrations of DT (250, 125, 62.5, and 31.25 μL/mL) were prepared to verify the inhibitory effects of DT on the growth of *B. dothidea*. The experiment was performed referring to the previously published method with minor modifications (Kurt et al., 2011). Firstly, a mycelial disk (0.5 cm in diameter) was inoculated in the center of a Petri dish (9 cm in diameter, 70 mL in volume) containing 20 mL of PDA medium. After that, the various concentrations of DT (100 μL) were added onto the filter paper (2 cm × 2 cm) laid on the center of the Petri dish inner lid. Thus the actual DT concentrations in the Petri dish space were 500, 250, 125, and 62.5 μL/L, respectively. In addition, 100 μL sterilized water was used as control. The experiment was performed in six replicates. The inoculated Petri dishes were inverted and incubated at 28°C in the dark for 5 days. The fungal colony diameters were measured every day to evaluate the inhibitory effect of DT on mycelia growth. The area-under-curve (AUC) of fungal diameter was calculated using the following formula (Huang et al., 2012).

$$\mathrm{AUC} = \sum_{i=1}^{n-1} \left[\frac{X_{i+1} + X_i}{2} \right] t_{i+1} - t_i \qquad (1)$$

X is the inhibition. n is the number of evaluations, and the $(t_i\text{-}1 - t_i)$ is the time interval (days) between two consecutive evaluations.

The Inhibitory Effects of Dimethyl Trisulfide on the Incidence of Apple Ring Rot on Fruit

To assess the inhibitory effects of DT on the incidence of apple ring rot on fruit, we designed two experiments. The two experiments were the same except for the inoculation method.

Experiment 1

The healthy apple fruit was sterilized with 75% alcohol and then washed with sterilized distilled water three times. A mycelial disk (0.5 cm in diameter) was inoculated into a small hole (0.5 cm in diameter and 0.5 cm in depth) which was made at the fruit's equator with a sterilized hole puncher. Two inoculated fruits (0.5 L in volume) were placed into plastic boxes (4.5 L in volume). Then, 2 mL of DT at various concentrations (125, 62.5, and 31.25 μL/mL) were added to the petri dish lid placed at one of the corners of the plastic box. The same volume of sterilized water was used as a control. Thus the final DT concentration in the plastic box space was 62.5, 31.25, and 15.63 μL/L, respectively. The plastic boxes were sealed and incubated at 28°C in the dark. The experiment was repeated four times. The disease symptom was recorded, and the disease spot diameter was measured every day to evaluate the inhibitory effect of DT against apple ring rot. The AUC of disease spot diameters was calculated as the formula (1).

Experiment 2

Five mycelial disks (0.5 cm in diameter) were inoculated in 50 mL potato dextrose (PD) broth medium and incubated in a shaker at 28°C, 200 r/min for 48 h. The obtained mycelium pellets were broken into homogenate by ultrasound. The healthy apple fruit was sterilized with 75% alcohol and washed with sterilized distilled water three times. Then the fruit was inoculated with *B. dothidea* by dipping into the fungal homogenate for 15 min. Two inoculated apple fruit (0.5 L in volume) were placed in the plastic boxes (4.5 L in volume). Then 2 mL of DT at various concentrations (125, 62.5, and 31.25 μL/mL) were added into the petri dish lid placed at one of the corners of the plastic box. The same volume of sterilized water was used as a control. Thus the final DT concentration in the plastic boxes was 62.5, 31.25, and 15.63 μL/L, respectively. The plastic boxes were sealed and incubated at 28°C in the dark. The disease symptom was observed every day to evaluate the inhibitory effect of DT on apple ring rot.

Effects of Dimethyl Trisulfide on the Mycelial Morphology of the *Botryosphaeria dothidea*

A mycelial disk (0.5 cm in diameter) was inoculated on the center of the cellophane paper laid on the PDA medium (20 mL) contained in Petri dish (9 cm in diameter, 70 mL in volume). The Petri dishes were inverted and incubated at 28°C in the dark until the mycelium grew to half the medium surface. Then 100 μL DT (250 μL/L) was added onto the filter paper (2 cm × 2 cm) laid on the Petri dish's inner lid center. Thus, the actual DT concentration in the Petri dish space was 500 μL/L. 100 μL sterilized distilled water was used as a control. All the Petri dishes continued to be incubated at 28°C in the dark for 24 h. Then the cellophane paper with mycelia was cut into 1-cm-wide pieces and spread onto the glass slide. The mycelial morphology was observed using an inverted microscope (EVOS Auto 2, Thermo Fisher Scientific, San Jose, CA, United States) at 40×.

Effects of Dimethyl Trisulfide on the Internal Qualities of the Apple Fruit

The experiment consisted of four treatments, viz. (1) CK: The apple fruit was soaked in PD broth medium for 15 min. (2) Bd: The apple fruit was soaked in *B. dothidea* culture for 15 min. (3) DT: The apple fruit was soaked in 62.5 μL/L DT for 15 min. (4) DT + Bd: The apple fruit was soaked in 62.5 μL/L DT for 15 min, then were soaked in *B. dothidea* culture for 15 min following air-drying at room temperature for 1 h. All the fruits were put into plastic boxes and incubated at 28°C in the dark. Apple fruit was sampled at 0, 3, 6, 9, and 12 days to determine the dynamic changes of internal fruit quality indices, including total soluble solid (TSS), soluble sugar (SS), titratable acidity (TA), and vitamin C (VC), total soluble solid/titrable acidity (TSS/TA), and soluble sugar/titrable acidity (SS/TA). TSS content was determined using a PAL-1 type sugar concentration detector (ATAGO, Japan). SS content was determined using the anthrone colorimetric method. The TA content was determined by NaOH titration. VC content was determined by 2, 6-dichloroindophenol colorimetric (Yang L. et al., 2020). The experiment was performed in three replicates. The AUC of internal quality indices was calculated as the formula (1), where *X* is the contents of fruit internal quality indices.

Determination of the Expression of Defense Related-Genes Responded to Dimethyl Trisulfide

As previously described, four treatments (CK, DT, Bd, and Bd + DT) were performed. All the fruits were put into plastic boxes and incubated at 28°C in the dark. The disease symptoms were observed every day. 12 days later, a slight disease symptom emerged on the Bd-treated apple fruit. All the treated and control apple fruit were peeled around the equator with a sterilized paring knife. All the samples were stored at −80°C for later use.

The expressions of the defense-related genes including phenylalanine ammonia-lyase (PAL), glucanase_1 (GLU-1), glucanase_2 (GLU-2), glucanase_3 (GLU-3), peroxidase_1 (POD-1), peroxidase_2 (POD-2), polyphenol oxidase (PPO), catalase (CAT), and endochitinase (CHI) were determined by quantitative real-time PCR (qRT-PCR). We drew the gene sequence information of the nine genes mentioned above from the apple genome (ASM211411v1). The special primers were designed using primer 5 (**Table 1**) and synthesized by Sangon Biotech (Shanghai) Co., Ltd., Shanghai, China.

According to RNAprep Pure Plant Plus Kit [Tiangen Biotech (Beijing) Co., Ltd., Beijing, China], the RNA was extracted from the fruit samples. And the cDNA was synthesized using HiScript® III RT SuperMix for qPCR (+gDNA wiper) (Nanjing Vazyme

TABLE 1 | The primer sequences of defense-related genes and internal reference genes.

GeneName	Gene ID	Primers	Sequence (5′–3′)
PPO	NM_001319261.1	PPO -F	TCATGGCTCTTCTTCCCGTT
		PPO -R	GATTGGCAGATCGGAGCTTG
CHI	NM_001293894.1	CHI-F	GAGACTACTGGAGGATGGGC
		CHI-R	ATCCTTTCCGATTGCTTGGC
CAT	XM_008375181.3	CAT-F	CCTCGTGGTTTTGCAGTGAA
		CAT-R	GGAAGGTGAACATGTGCAGG
POD-1	XM_029099288.1	POD1-F	TCCTGTGCTGACATTTTGGC
		POD1-R	AATCTACATTTTGCCCGGCC
POD-2	XM_029091729.1	POD2-F	GTTGCACTCGTGATGTTGGT
		POD2-R	CAATCATGGAAGTGGAGGCG
PAL	XM_008368428.3	PAL -F	GCAGAGCAACACAACCAAGA
		PAL -R	CGTTAAAGCCCATGGTGAGG
GLU-1	NM_001293850.1	GLU1-F	GAGCCAGTGATTCAACGGAC
		GLU1-R	TGGAGGTTACTTCCAGGCAG
GLU-2	XM_008343526.2	GLU2-F	ATGTGGTGGCATGTGAGAGA
		GLU2-R	CTAGCAAACCCGACATCAGC
GLU-3	XM_029095631.1	GLU3-F	CCCTGATTCCAACCTTGCTG
		GLU3-R	AAATCCCTTGTCCGGTCCAT
Actin	XM_008393049.3	Actin-F	CTTCAATGTGCCTGCCATGTAT
		Actin-R	AATTTCCCGTTCAGCAGTAGTG

PPO, polyphenol oxidase; CHI, endochitinase; CAT, catalase; POD-1, peroxidase_1; POD-2, peroxidase_2; PAL, phenylalanine ammonia-lyase; GLU-1, glucanase_1; GLU-2, glucanase_2; GLU-3, glucanase_3.

Biotech Co., Ltd., Nanjing, China). qRT-PCR was performed using ABI7500 Thermal Cycler (Applied Biosystems, Foster City, CA, United States) to detect the expressions of the nine defense-related genes aforementioned. The reaction system (10 μL) contained 5 μL of 2× ChamQ SYBR Color qPCR Master Mix (Nanjing Vazyme Biotech Co., Ltd., Nanjing, China), 0.2 μL of each primer, 0.2 μL of the 50× ROX Reference Dye I, 1 μL of cDNA, 3.4 μL of the ddH_2O. The reaction conditions were as follows: 95°C for 30 s, followed by 40 cycles of 95°C for 10 s and 60°C for 30 s, then 95°C for 15 s, 60°C for 1 min and finally 95°C for 15 s. Actin was used as the internal reference gene, and the relative expression was calculated by $2^{-\Delta\Delta CT}$ method (Livak and Schmittgen, 2001). The experiment was performed in three replicates.

Statistical Analysis

Experimental data were analyzed using standard analysis of variance (ANOVA) followed by least significant difference tests ($p < 0.05$) using the software statistical analytical system (SAS 9.0). Standard errors were calculated for all mean values.

RESULTS

Dimethyl Trisulfide Inhibited the Mycelial Growth of *Botryosphaeria dothidea*

The results showed DT strongly inhibited the mycelia growth of the *B. dothidea*. The mycelia growth of the control was initiated on the first day and rapidly grew on successive days. On the fifth day, the fungal mycelia completely covered the whole surface of the Petri dish. But the DT-treated mycelia remained unchanged or grew slower than the control (**Figure 1**). Statistics showed that the colony diameters reduced with the increase of the DT concentration (**Figure 2A**). The inhibitory effect increased with DT concentration but decreased with incubation time. During the whole experimental period, 500 and 250 μL/L DT exhibited 100% inhibition against *B. dothidea*. 125 and 62.5 μL/L DT showed 93.5 and 69.0% inhibition on the first day, which sharply decreased to 18.3 and 8.75% on the fifth day, respectively (**Figure 2B**). The AUC of fungal colony diameters treated by various DT concentrations were reduced by 18.9–100% compared to that of control ($P < 0.0001$) (**Figure 2C**).

Dimethyl Trisulfide Disrupted the Mycelial Morphology of *Botryosphaeria dothidea*

Under a microscope, the control mycelia had complete morphology with uniform thickness, smooth surface, slender and full shape (**Figure 3A**). However, DT seriously deformed the normal mycelial morphology. The outline of the DT-treated mycelia became blurred, with more bifurcation at the top, similar to the chicken feet. And the mycelia also became curved and wrinkled. The front end expanded, forming a tumor-like structure. Some mycelia ruptured and dissolved, and the contents spilled (**Figures 3B–D**).

Dimethyl Trisulfide Inhibited the Incidence of Apple Ring Rot Disease Symptoms on Fruit

Experiment 1

The first 2 days after inoculation, disease spots gradually appeared around the control fruit's inoculating points. Three days later, the disease spots began to grow and developed rapidly. On the fifth day, the fruit was utterly rotten with a thick exudation on the surface and a sour smell. However, DT-treated apple fruit showed no disease symptoms during the early days of the experiment. After 5 days of inoculation, only mild disease spots appeared on the apple fruit treated with the low concentration DT (15.63 μL/L) (**Figure 4**). Statistical analysis showed that the disease spot diameter of the control fruit reached up to 10.03 cm on the fifth day, while that of fruit treated with a low DT concentration (15.63 μL/L) was 0.25 cm (**Figure 5A**), indicating a 97.5% inhibition. High DT concentrations (62.5 and 31.25 μL/L) exhibited 100% inhibition against the apple ring rot (**Figure 5B**). The AUC of disease spot diameter on fruit treated by the various DT concentrations was reduced by 98.5–100% compared to that of control ($P < 0.0001$) (**Figure 5C**).

Experiments 2

Only 1 day after inoculation, sparse mycelial colonies with different sizes appeared on the control fruit. During the first week, the colonies successively emerged and enlarged quickly, finally covering the whole fruit surface. The disease

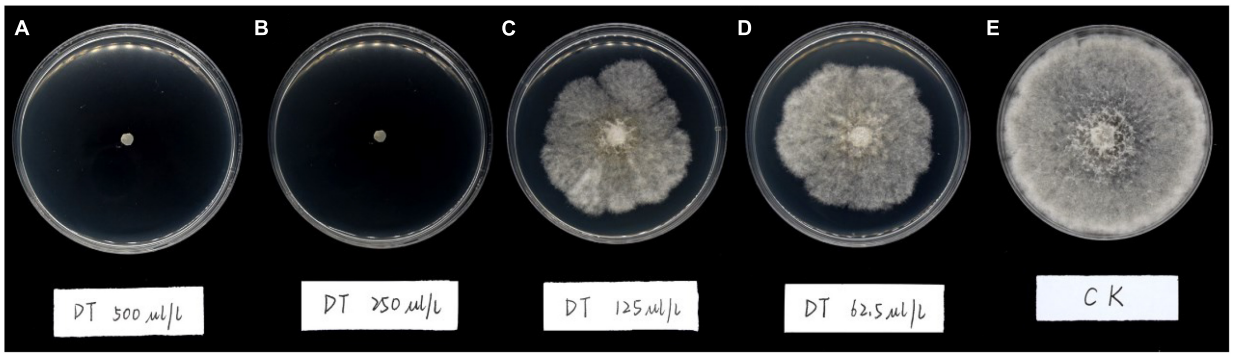

FIGURE 1 | The mycelial growth of *Botryosphaeria dothidea* on PDA medium containing various concentrations of dimethyl trisulfide for 5 days. **(A)** 500 μL/L, **(B)** 250 μL/L, **(C)**: 125 μL/L, **(D)** 62.5 μL/L, **(E)** control.

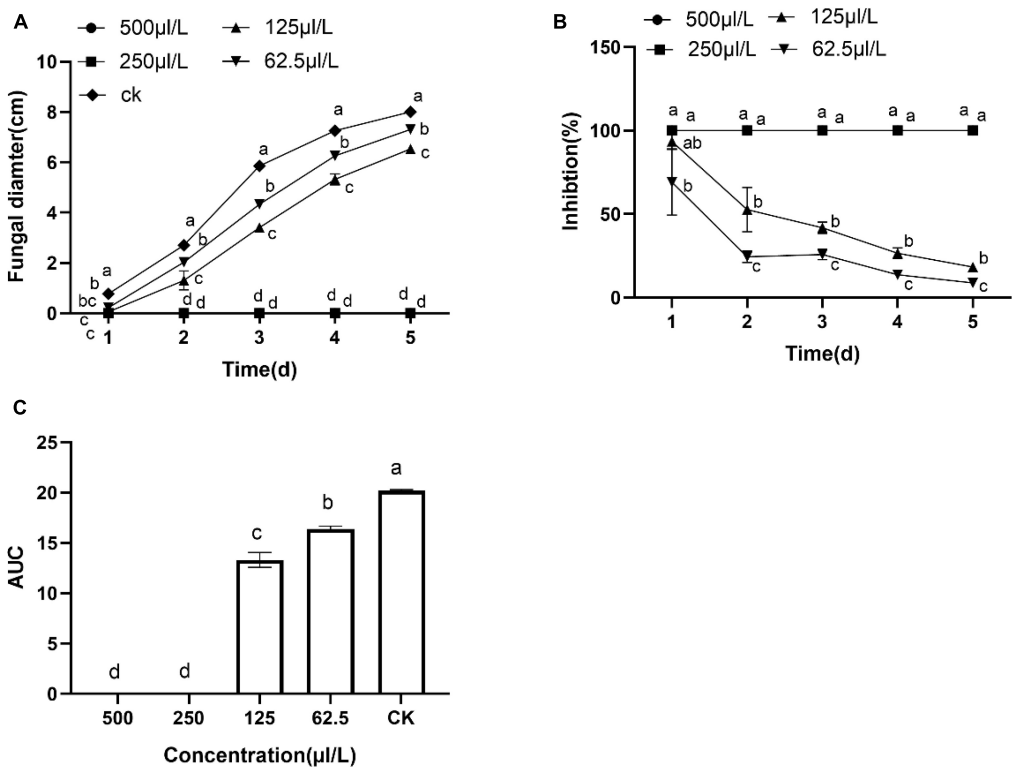

FIGURE 2 | The dimethyl trisulfide inhibition on the mycelia growth of *Botryosphaeria dothidea*. **(A)** The colony diameters of *Botryosphaeria dothidea* treated by the various concentration of dimethyl trisulfide. **(B)** The inhibition of various concentrations of dimethyl trisulfide against mycelia growth of *Botryosphaeria dothidea*. **(C)** The area-under-curve (AUC) of fungal colony diameters treated by various concentrations of dimethyl trisulfide. Different lowercase letters indicate a significant difference between treatments ($P < 0.05$).

spots gradually appeared across the fruit surface during the second week. They progressively expanded and joined together later, eventually leading to fruit decay during the third and fourth weeks. However, apple fruits treated with a low DT concentration (15.63 μL/L) showed no symptoms during the first week. During the second week, an average of 3 sparse mycelial colonies appeared on the fruit. On average, 10 sparse mycelial colonies appeared on the fruit during the third and fourth weeks. However, the apple fruit treated with higher DT concentrations (>31.25 μL/L) showed no obvious disease symptom and exhibited 100% inhibition against the apple ring rot throughout the experiment period (**Figure 6**).

Dimethyl Trisulfide Enhanced the Apple Fruit Quality

All the six fruit quality indices of the four treatments (CK, DT, Bd, and DT + Bd) showed an up-and-down trend, fluctuating

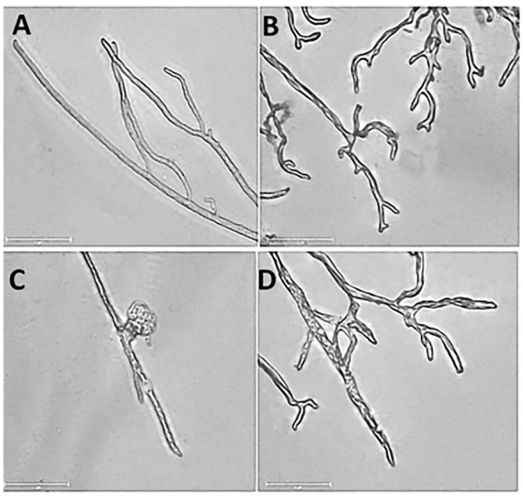

FIGURE 3 | The mycelial morphology of *Botryosphaeria dothidea*. **(A)** The mycelia of the untreated control. **(B–D)** The mycelia treated with 500 μL/L dimethyl trisulfide for 24 h.

with prolonged time (**Figure 7**). The AUC of fruit quality indices was used to evaluate DT's overall effect on the fruit quality. Compared to the control fruit (CK), DT treatment (DT) increased the SS content, SS/TA ratio and VC content by 4.22% ($P = 0.0124$), 16.59% ($P = 0.0209$), and 109.80% ($P < 0.0001$), respectively. Compared to the fruit inoculated with Bd (Bd), DT treatment (DT + Bd) significantly increased VC content by 86.13% ($P = 0.0499$), SS content by 3.67% ($P = 0.0346$), and also enhanced SS/TA ratio by 19.05% ($P = 0.0581$) (**Figure 8**).

Dimethyl Trisulfide Induced the Expression of Defense-Related Genes

Dimethyl trisulfide induced all the detected genes in apple fruit, six (GLU-1, GLU-2, POD-1, POD-2, CHI, and CAT) of which were significantly up-regulated (**Figure 9**). Compared with the control (CK), the six genes in DT-treated apple fruit (DT) were up-regulated by 14.91 (GLU-2) to 84.09 (CAT) times, with an average of 39.09 times. Compared to fruit inoculated with *B. dothidea* (Bd), the six genes in DT-treated apple fruit (Bd + DT) were increased by 4.13 (CHI) to 296.50 (POD-2) times, averaged 95.24 times. These results revealed that the DT markedly induces apple fruit's defense-related genes whether or not they were inoculated with *B. dothidea.*

DISCUSSION

Nowadays, extensive application of various synthetic fungicides is still the primary management strategy that effectively controls apple ring rot. But the pesticide residue resulted in potential harm to the environment, animals, even humans. Therefore, due to natural products' environment-friendly and low toxicity, developing natural fungicides from plants has attracted more attention worldwide. In the present study, we revealed that DT, one of the main components from Chinese leek, significantly suppressed apple ring rot on postharvest fruit. DT naturally existed in Chinese leek and other *Allium* plants. Plants of the *Allium* family, such as garlic (*Allium sativum*), onion (*Allium cepa*), and Chinese leek, have been cultivated for food since earliest times (Munday et al., 2003). And DT is widely distributed in foods and beverages such as broccoli, milk, cheese, whiskey, hineka, beer, and wine (Gijs et al., 2002; Isogai et al., 2009). Therefore, using DT to control apple ring rot is efficient and safe for humans, animals, and the environment, providing a possible way to control apple ring rot.

In the present study, we found that the DT inhibition at low concentration on the mycelia growth sharply decreased with the prolonged experimental time. For example, 125 and 62.5 μL/L DT showed 93.5 and 69.0% inhibition on the first day, but they decreased to 18.3 and 8.75% on the fifth day, respectively. That is because DT was highly volatile and quickly escaped from the Petri dishes into the air in a short period. In addition, DT interacted with the fungal mycelia and partly decomposed. The escape or decomposition rapidly decreased DT concentration in the petri dish. However, the remaining concentration was not sufficient to inhibit mycelial growth. To solve this problem in practical application, DT can be prepared into the slow-release formulation to maintain sustainable high inhibition.

To prove the inhibitory effect of DT on apple ring rot on postharvest fruit, we designed two inoculation methods, inoculating the apple fruit with a mycelial disk and socking

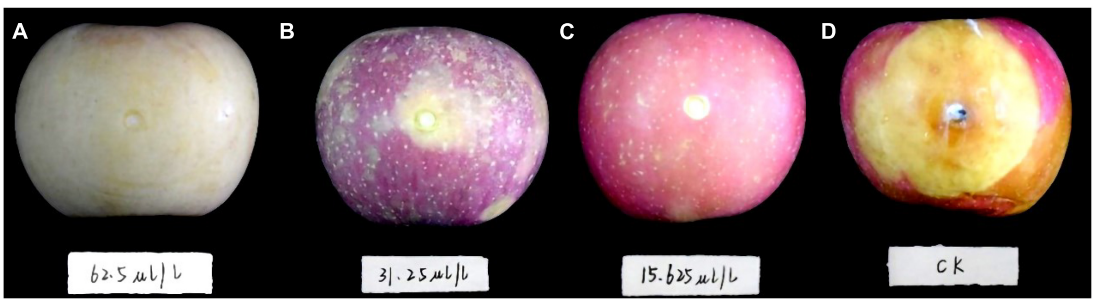

FIGURE 4 | The apple fruit was first inoculated with *Botryosphaeria dothidea* disk, subsequently treated with dimethyl trisulfide, then cultured at 28°C in the dark for 5 days. Apple fruits with different treatments exhibited varying degrees of disease symptoms. **(A)** 62.5 μL/L, **(B)** 31.25 μL/L, **(C)** 15.63 μL/L, **(D)** control.

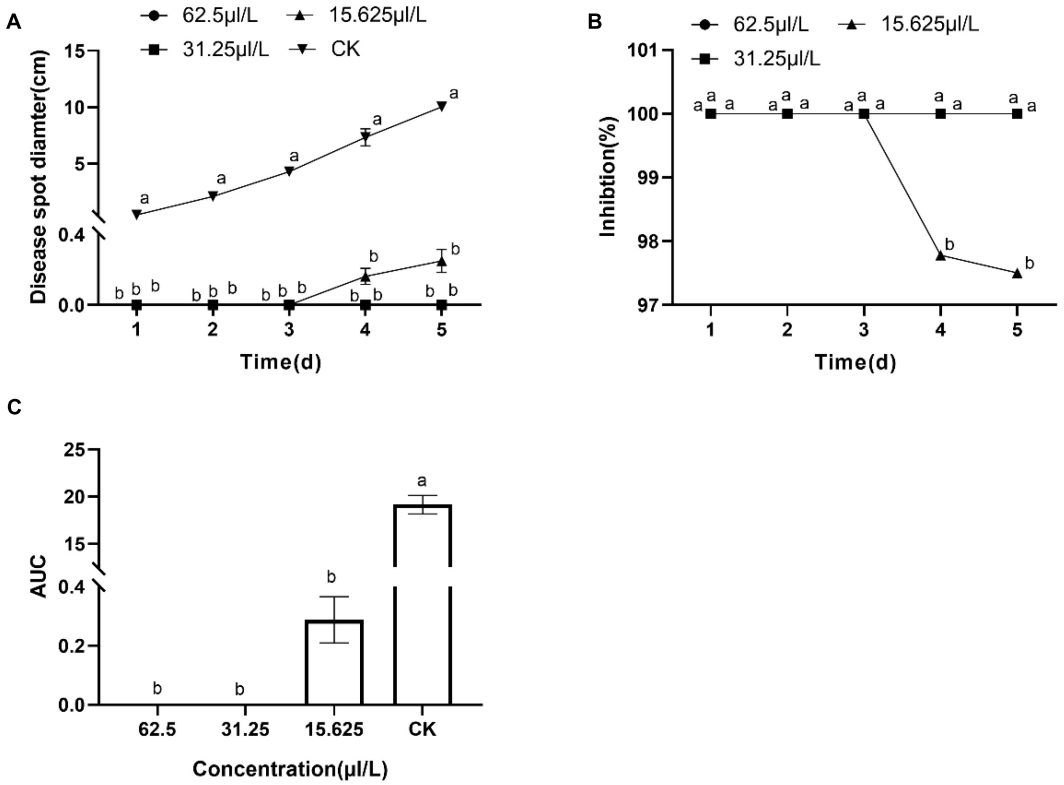

FIGURE 5 | The inhibitory effect of dimethyl trisulfide on the apple ring rot on apple fruit. **(A)** The disease spot diameter on apple fruits treated by various concentrations of dimethyl trisulfide. **(B)** The inhibition of various concentrations of dimethyl trisulfide against the apple ring rot on fruit. **(C)** The area-under-curve (AUC) of disease spot diameter on fruit treated by the various concentration of dimethyl trisulfide. Different lowercase letters indicate a significant difference between different treatments ($P < 0.05$).

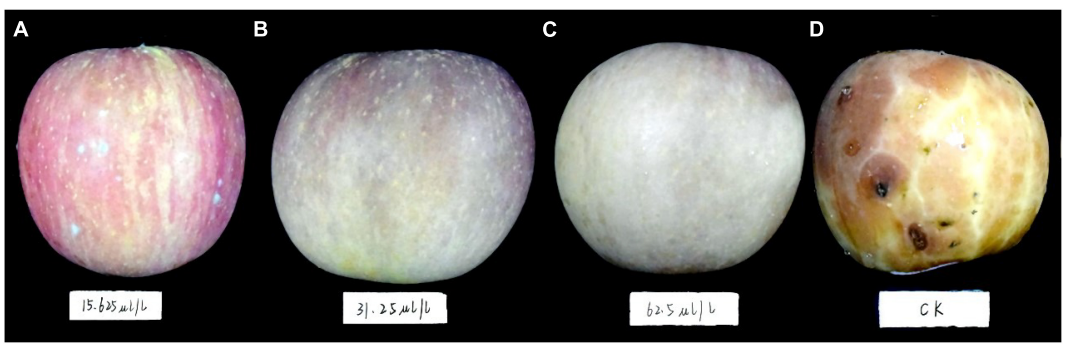

FIGURE 6 | The apple fruit was first dipped in a *Botryosphaeria dothidea* culture for 15 min, subsequently exposed to various concentrations of dimethyl trisulfide, then cultured at 28°C in the dark for 4 weeks. Apple fruits with different treatments exhibited varying degrees of disease symptoms. **(A)** 15.63 μL/L, **(B)** 31.25 μL/L, **(C)** 62.5 μL/L, **(D)** control.

the apple fruit in the *B. dothidea* culture for 15 min. The two experiments revealed that DT significantly suppressed the incidence of the disease. The high concentration (62.5 and 31.25 μL/L) of DT completely inhibited the disease, and the low concentration (15.63 μl/L) also showed more than 90% inhibition. However, the red skin color of apple fruit treated with high concentration (62.5 and 31.25 μL/L) DT somewhat faded, but that of the apple fruits treated with low concentration (15.63 μl/L) DT was perfectly maintained. Therefore, we suggest using lower DT concentration to treat apple fruit in practical application, dramatically maintaining the fruit color and preventing disease. Furthermore, the pathogen amount carried on the field fruit in the practical production was far lower than those artificially inoculated in our experiment. Thus, our present study demonstrated the potential application of DT as an alternative strategy against apple ring rot caused by *B. dothidea*.

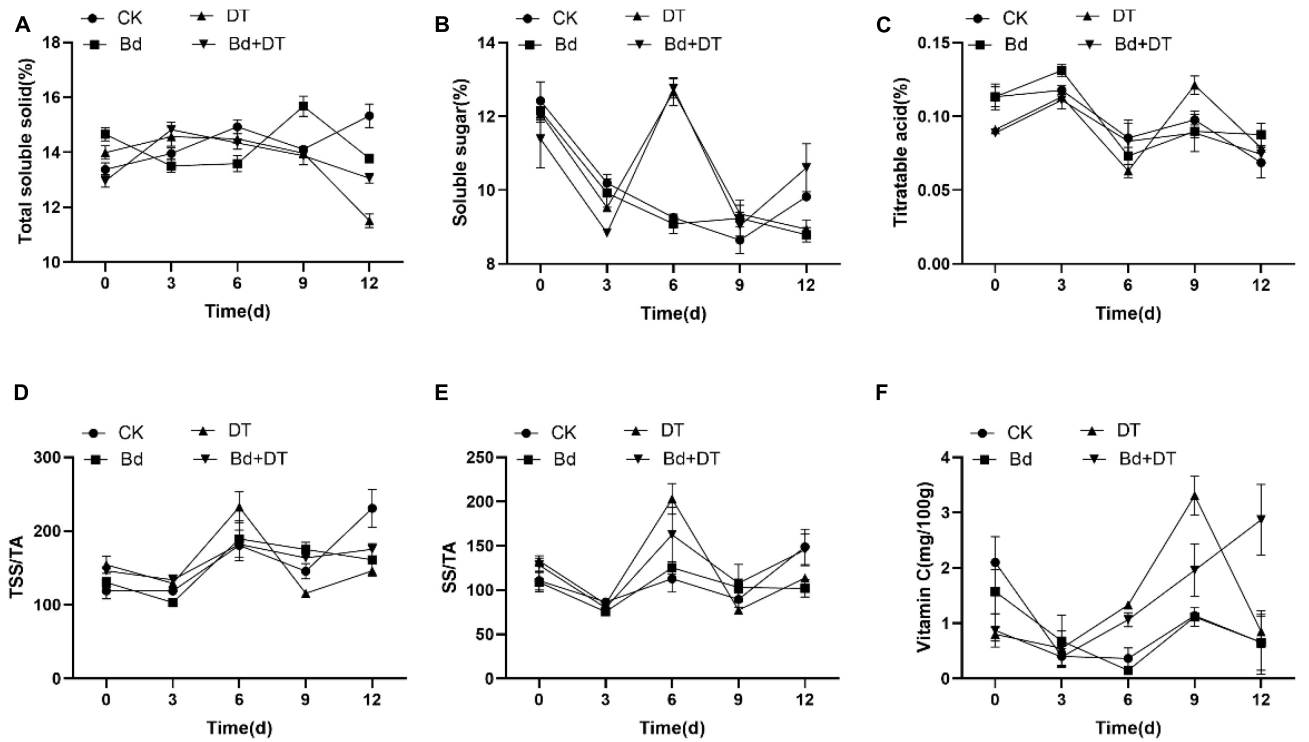

FIGURE 7 | The dynamic changes of internal quality indexes including total soluble solid **(A)**, soluble sugar **(B)**, titratable acidity **(C)**, TSS/TA **(D)**, SS/TA **(E)**, and vitamin C **(F)** in the different treatment fruit.

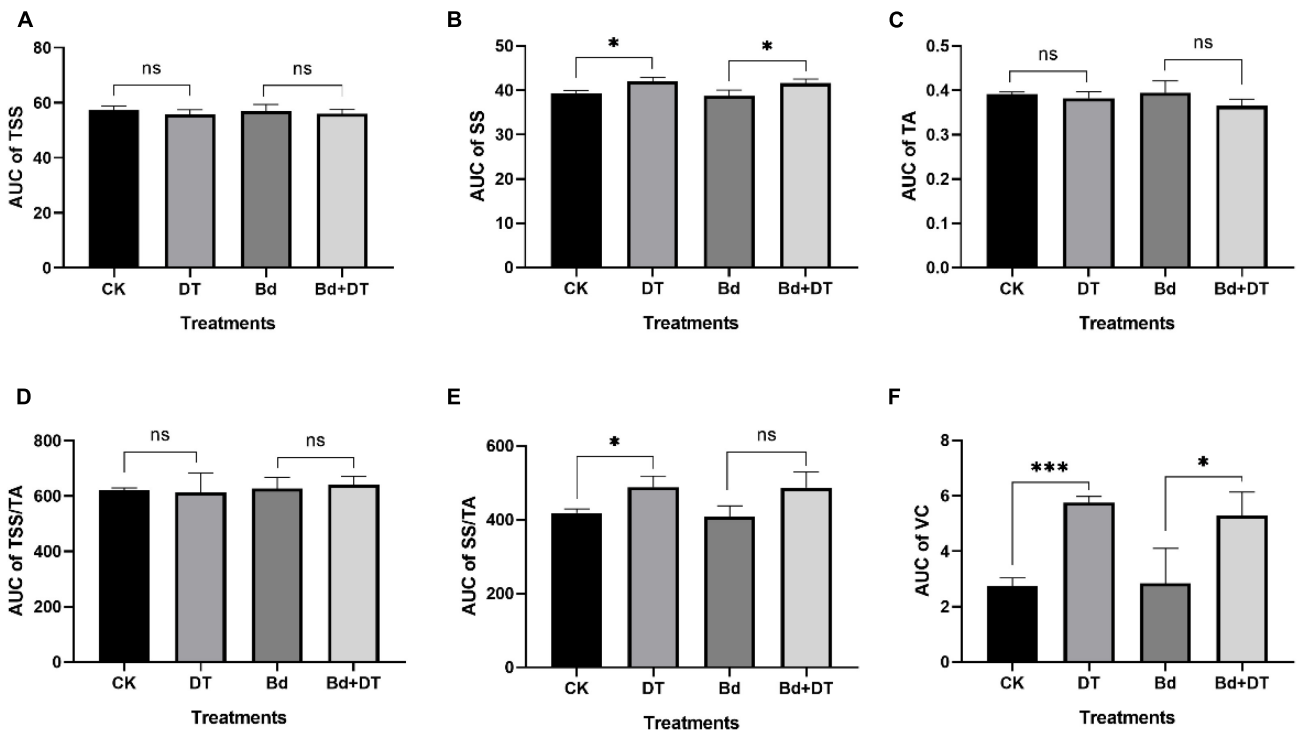

FIGURE 8 | The area-under-curve (AUC) of internal quality indexes including total soluble solid **(A)**, soluble sugar **(B)**, titratable acidity **(C)**, TSS/TA **(D)**, SS/TA **(E)**, and vitamin C **(F)** the different treatment fruit. $^{*}P < 0.05$, $^{***}P < 0.001$, ns $P > 0.05$.

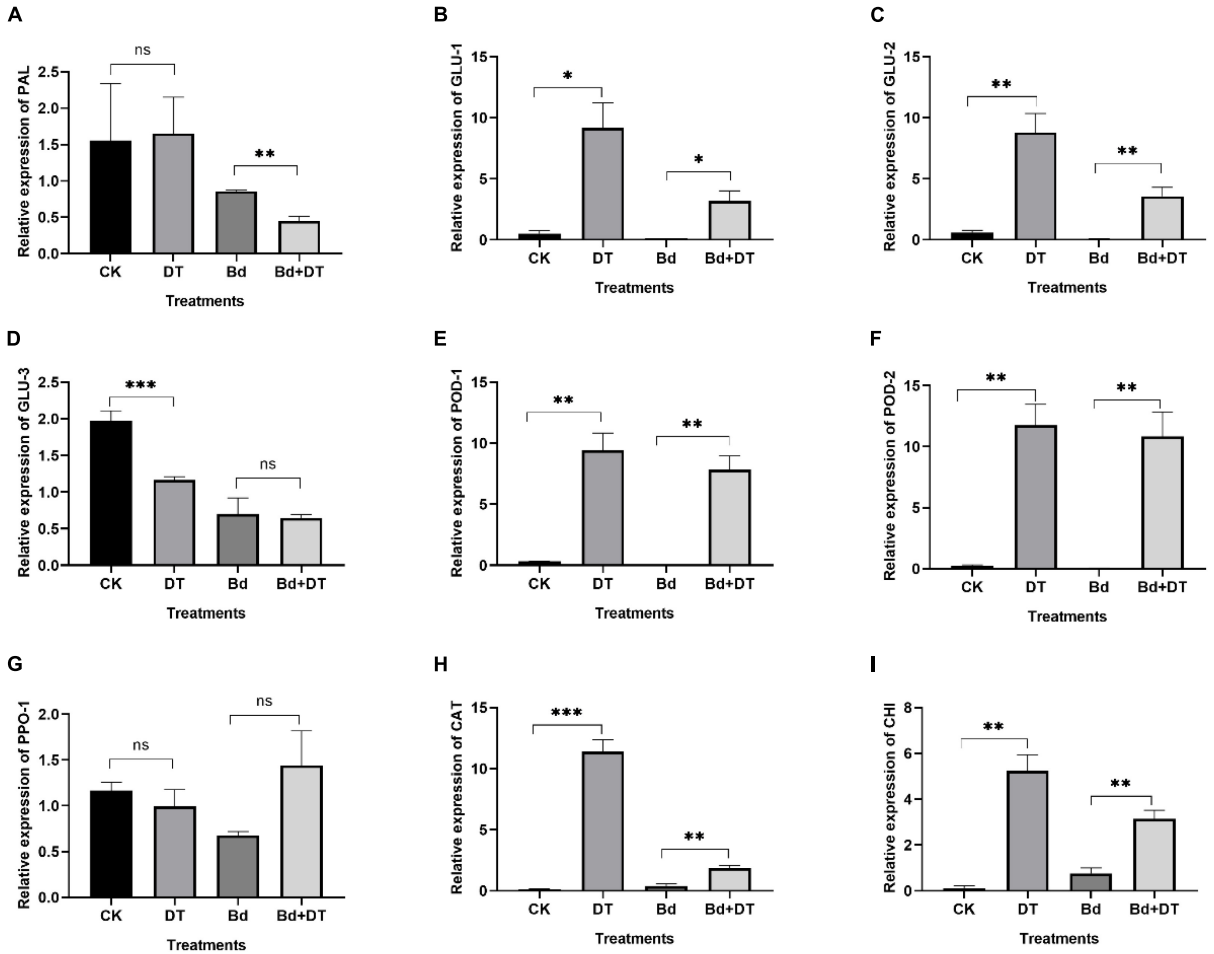

FIGURE 9 | The expression analysis of various defense-related genes including phenylalanine ammonia-lyase **(A)**, glucanase_1 **(B)**, glucanase_2 **(C)**, glucanase_3 **(D)**, peroxidase_1 **(E)**, peroxidase_2 **(F)**, polyphenol oxidase **(G)**, catalase **(H)**, endochitinase **(I)** in the DT-treated fruit. $^{*}P < 0.05$, $^{**}P < 0.01$, $^{***}P < 0.001$, ns $P > 0.05$.

The present study explored the underlying mechanism from the fungal *B. dothidea* aspect and the apple fruit aspect. From the findings in the present study, we deduced that DT inhibits the disease incidence by suppressing the growth of *B. dothidea* and inducing defense-related genes in apple fruit.

On the one hand, DT caused severe disruption to *B. dothidea* mycelia, leading to its slow growth or even death, further decreasing its vigor and amounts, thereby reducing the infection probability and ultimately suppressing the incidence of apple ring rot on apple fruit. The previous study showed that the essential oil aromatic plants, including origanum (*Origanum syriacum* L.), lavender (*Lavandula stoechas* L.), and rosemary (*Rosmarinus officinalis* L.), significantly inhibit the growth of *Phytophthora infestans* (Soylu et al., 2006) and *Botrytis cinerea* (Soylu et al., 2010) by causing considerable morphological degenerations of the fungal mycelia. Origanum contains carvacrol (79.8%) and *p*-cymene (8.2%), lavender contains camphor (20.2%), 1,8-cineole (35.5%), α-thujone (15.9%) and fenchone (13.5%), rosemary contains borneol (20.4%), camphor (19.5%), 1,8-cineole (17.4%) and linalool (6.1%) as the main components (Soylu et al., 2006). These components interfere with the enzymatic reactions of wall synthesis, resulting in considerable morphological alterations in mycelia such as cytoplasmic coagulation, vacuolations, hyphal shriveling, and protoplast leakage, finally affecting the fungal morphogenesis and growth (Rasooli et al., 2006; Soylu et al., 2006, 2010). Therefore, we believe the direct effect of DT on fungal *B. dothidea* mycelium may be an important factor inhibiting the ring rot disease on apple fruit.

On the other hand, DT significantly induced defense-related genes, including GLU-1, GLU-2, POD-1, POD-2, CHI, and CAT, by 4.13 to 296.49 times compared to the control. Previous studies revealed that the defense-related response played an essential role in improving the disease resistance of plants. GLU enhances the tolerant of rough lemon rootstock against foot rot (Sandhu et al., 2019), improves the inhibition of rice against *Rhizoctonia solani* (Kumar et al., 2018), reduces the rice sheath blight (Kaur et al., 2021), and confers tea tree

resistance against blister blight disease (Singh et al., 2018). POD is involved in the resistance response of coffee varieties to *Colletotrichum kahawae* (Diniz et al., 2019), potato to *P. infestans* (Yang Y. et al., 2020), *Arabidopsis thaliana* to *Botrytis cinerea*, *Colletotrichum higginsianum,* and *Pectobacterium carotovorum* (Zhao et al., 2019), *Citrus sinensis* to citrus bacterial canker (Li et al., 2020). CAT contributes maize to resistance against maize chlorotic mottle virus infection (Jiao et al., 2021), *Nicotiana tabacum* against *Chilli veinal mottle virus* infection (Yang T. et al., 2020). CHI enhances tobacco tolerance against *B. cinerea* (Navarro-Gonzalez et al., 2019), *Arabidopsis thaliana* resistance against the bacterium *Xanthomonas campestris* pv. *campestris* (Xcc) (Santos et al., 2019), and tomato resistance against *B. cinerea* (Zheng et al., 2018). According to the above studies, the significantly up-regulated POD, GLU, CHI, and CAT were probably critical in enhancing apple fruit resistance against *B. dothidea* infection.

In practical application, we can spray DT on the tree or the fruit during the growing season to control apple ring rot on branches or fruit. After harvesting, we can spray DT on fruit, dip the fruits in DT solution, or place DT in the corner of the fruit box to prevent apple ring rot on postharvest fruit. Chinese leek contains a large amount of DT or other organic sulfides. The essential oil of Chinese leek leaves contains disulfide compounds (64.9%) and trisulphide compounds (18.9%), the flower contains trisulphide compounds (34.0%) and disulfide compounds (20.2%), the essential oil of rhizome contains trisulphide compounds (47.3%), and the seed contains disulfide (32.4%) and tetrasulfide (5.2%) as the main constituents (Hu et al., 2013). These sulfides contained in Chinese leek, including allyl methyl sulfide, methyl disulfide, dimethyl trisulfide, and methyl allyl trisulfide (Zhao et al., 2017), diallyl disulfide, diallyl trisulfide, and diallyl tetrasulfide (Rattanachaikunsopon and Phumkhachorn, 2009), also exhibit vigorous and widely antifungal or antibacterial activity. Our previous study showed that Chinese leek significantly reduced the banana *Fusarium* wilt (Huang et al., 2012) by intercropping or rotating crops. Therefore, we can also intercrop Chinese leek in the orchard to control apple ring rot in practice production.

Besides Chinese leek, other *Allium* plants, including *A. sativum* (Natasya-Ain et al., 2018), *A. cepa* (Balamanikandan et al., 2015; Ortega-Ramirez et al., 2017), *Allium stipitatum* (Karunanidhi et al., 2017), *Allium saralicum* (Zangeneh M.M. et al., 2019), *Allium noeanum* (Shahriari et al., 2019), *Allium saralicum* (Zangeneh A. et al., 2019), *Allium hirtifolium* (Ismail et al., 2013), are reported to possess extensive antifungal or antibacterial activity. They also contain a large number of organic sulfides with intense antifungal activity. For example, propyl-propane thiosulfinate, propyl-propane thiosulfonate (Sorlozano-Puerto et al., 2020), methyl allyl thiosulphinate, E-ajoene and Z-ajoene from garlic (*A. sativum*), elephant garlic (*Allium ampeloprasum*), and onion (*A. cepa*) (Hughes and Lawson, 1991), Allicin (Bhattacharya et al., 2019), diallyl disulfide (Jin et al., 2021) from garlic (*A. sativum*), also exhibit vigorous and widely antifungal or antibacterial activity. These *Allium* plants are an excellent natural resource to control plant disease. However, they have been ignored for many years. For example, after harvesting garlic bulbs, the plant is often discarded in the field bank and the ditch, resulting in waste and pollution. We can take good advantage of these valuable resources by burying them in the soil around the tree, which controls the disease incidence and reduces pollution.

Perfect measures to control postharvest fruit diseases must have two fundamental characteristics: to effectively control disease occurrence and maintain fruit quality. In the present study, we demonstrate that DT showed a strong inhibitory effect on apple ring rot and significantly enhances SS and VC contents and the SS/TA ratio of the apple fruit, which suggests that DT is an ideal alternative strategy against postharvest apple ring rot.

CONCLUSION

In the present study, we demonstrated that DT, the main component of Chinese leek, significantly suppresses the mycelia growth of *B. dothidea* and inhibits the incidence of apple ring rot on postharvest fruit. Most importantly, DT significantly enhanced the soluble sugar content, vitamin C content, and soluble/titratable acidity ratio. We further found DT inhibited the apple ring rot by directly suppressing the pathogen growth and inducing the fruit's defense-related response. Therefore, it provides an efficient, safer, and environment-friendly alternative to control the apple ring rot on apple fruit.

DATA AVAILABILITY STATEMENT

The original contributions presented in the study are included in the article/supplementary material, further inquiries can be directed to the corresponding author.

AUTHOR CONTRIBUTIONS

YH contributed to the conception of the study and revised the manuscript. MS and YD wrote the manuscript, performed the experiments, and collected the data. JF experimented and collected the data. JL performed qRT-PCR validation. All authors contributed to the article and approved the submitted version.

FUNDING

This work was supported by the National Natural Science Foundation of China (31471864), the Natural Science Foundation of Shandong Province (ZR2020MC143), and the Qingdao Agricultural University High-level Personnel Startup Fund, China (6631115024).

REFERENCES

Ammad, F., Moumen, O., Gasem, A., Othmane, S., Hisashi, K. N., Zebib, B., et al. (2018). The potency of lemon (*Citrus limon* L.) essential oil to control some fungal diseases of grapevine wood. *Comptes Rendus Biol.* 341, 97–101. doi: 10.1016/j.crvi.2018.01.003

Bai, S., Dong, C., Zhu, J., Zhang, Y., and Dai, H. (2015). Identification of a xyloglucan-specific endo-(1-4)-beta-D-glucanase inhibitor protein from apple (*Malus* x *domestica* Borkh.) as a potential defense gene against *Botryosphaeria dothidea*. *Plant Sci.* 231, 11–19. doi: 10.1016/j.plantsci.2014.11.003

Balamanikandan, T., Balaji, S., and Pandiarajan, J. (2015). Biological synthesis of silver nanoparticles by using onion (*Allium cepa*) extract and their antibacterial and antifungal activity. *World Appl. Sci. J.* 33, 939–943. doi: 10.5829/idosi.wasj.2015.33.06.9525

Bhattacharya, S., Sen, D., and Bhattacharjee, C. (2019). In vitro antibacterial effect analysis of stabilized PEGylated allicin-containing extract from *Allium sativum* in conjugation with other antibiotics. *Process Biochem.* 87, 221–231. doi: 10.1016/j.procbio.2019.09.025

Dai, D. J., Wang, H. D., Wang, Y. P., and Zhang, C. Q. (2017). Management of Chinese hickory (*Carya cathayensis*) trunk canker through effective fungicide application programs and baseline sensitivity of *Botryosphaeria dothidea* to trifloxystrobin. *Austral. Plant Pathol.* 46, 75–82. doi: 10.1007/s13313-017-0465-4

Diniz, I., Azinheira, H., Figueiredo, A., Gichuru, E., Oliveira, H., Guerra-Guimarães, L., et al. (2019). Fungal penetration associated with recognition, signaling and defence-related genes and peroxidase activity during the resistance response of coffee to *Colletotrichum kahawae*. *Physiol. Mol. Plant Pathol.* 105, 119–127. doi: 10.1016/j.pmpp.2017.12.005

Fan, K., Wang, J., Fu, L., Li, X., Zhang, Y., Zhang, X., et al. (2016). Sensitivity of *Botryosphaeria dothidea* from apple to tebuconazole in China. *Crop Protect.* 87, 1–5. doi: 10.1016/j.cropro.2016.04.018

Fan, K., Wang, J., Fu, L., Zhang, G. F., Wu, H. B., Feng, C., et al. (2019). Baseline sensitivity and control efficacy of pyraclostrobin against *Botryosphaeria dothidea* isolates in China. *Plant Dis.* 103, 1458–1463. doi: 10.1094/PDIS-07-18-1214-RE

Fu, J. (2021). *Studies on the control and mechanism of volatiles from Chinese leek against apple ring rot*. Ph. D. thesis. Qingdao: Qingdao Agricultural University, 9–18.

Gijs, L., Chevance, F., Jerkovic, V., and Collin, S. (2002). How low ph can intensify β-damascenone and dimethyl trisulfide production through beer aging. *J. Agric. Food Chem.* 50, 5612–5616. doi: 10.1021/jf020563p

Gu, C., Yang, X., Al-Attala, M., Abid, M., Phyo, S., Zang, H., et al. (2020). First report of pomegranate fruit rot caused by *Botryosphaeria dothidea* in Anhui Province of China. *Plant Dis.* 104, 2736–2736. doi: 10.1094/PDIS-04-20-0790-PDN

Guan, Y., Chang, R., Liu, G., Wang, Y., Wu, T., Han, Z., et al. (2015). Role of lenticels and microcracks on susceptibility of apple fruit to *Botryosphaeria dothidea*. *Eur. J. Plant Pathol.* 143, 317–330. doi: 10.1007/s10658-015-0682-z

Hu, G., Sheng, C., Mao, R., Ma, Z., Lu, Y., and Wei, D. (2013). Essential oil composition of *Allium tuberosum* seed from China. *Chem. Nat. Compounds* 48, 1091–1093. doi: 10.1007/s10600-013-0476-5

Huang, Y. H., Wang, R. C., Li, C. H., Zuo, C. W., Wei, Y. R., Zhang, L., et al. (2012). Control of Fusarium wilt in banana with Chinese leek. *Eur. J. Plant Pathol.* 134, 87–95. doi: 10.1007/s10658-012-0024-3

Huang, Y., Meng, L. L., Liu, J., and Wang, C. X. (2019b). First report of shoot canker on apricot caused by *Botryosphaeria dothidea* in Shandong Province of China. *Plant Dis.* 103, 2945–2946. doi: 10.1094/PDIS-03-19-0522-PDN

Huang, Y., Meng, L., Liu, J., and Wang, C. X. (2019a). First report of *Botryosphaeria dothidea* causing shoot canker on mulberry in China. *Plant Dis.* 103, 1788–1789. doi: 10.1094/PDIS-01-19-0183-PDN

Hughes, B., and Lawson, L. (1991). Antimicrobial effects of *Allium sativum* L. (Garlic), *Allium ampeloprasum* L. (Elephant Garlic), and *Allium cepa* L.(Onion), garlic compounds and commercial garlic supplement products. *Phytother. Res.* 5, 154–158. doi: 10.1002/ptr.2650050403

Ismail, S., Jalilian, F. A., Talebpour, A. H., Zargar, M., Shameli, K., Sekawi, Z., et al. (2013). Chemical composition and antibacterial and cytotoxic activities of *Allium hirtifolium* Boiss. *BioMed Res. Int.* 2013:696835. doi: 10.1155/2013/696835

Isogai, A., Kanda, R., Hiraga, Y., Nishimura, T., Iwata, H., and Goto-Yamamoto, N. (2009). Screening and identification of precursor compounds of dimethyl trisulfide (DMTS) in Japanese sake. *J. Agric. Food Chem.* 57, 189–195. doi: 10.1021/jf802582p

Jiao, Z., Tian, Y., Cao, Y., Wang, J., Zhan, B., Zhao, Z., et al. (2021). A novel pathogenicity determinant hijacks maize catalase 1 to enhance viral multiplication and infection. *New Phytol.* 230, 1126–1141. doi: 10.1111/nph.17206

Jin, Z., Li, L., Zheng, Y., and An, P. (2021). Diallyl disulfide, the antibacterial component of garlic essential oil, inhibits the toxicity of *Bacillus cereus* ATCC 14579 at sub-inhibitory concentrations. *Food Control.* 126:108090. doi: 10.1016/j.foodcont.2021.108090

Karunanidhi, A., Ghaznavi-Rad, E., Jeevajothi Nathan, J., Abba, Y., van Belkum, A., and Neela, V. (2017). *Allium stipitatum* extract exhibits in vivo antibacterial activity against methicillin-resistant *Saphylococcus aureus* and accelerates burn wound healing in a full-thickness murine burn model. *Evidence Based Complementary Alternat. Med. eCAM* 2017:1914732. doi: 10.1155/2017/1914732

Kaur, R., Kalia, A., Lore, J. S., Kaur, A., Yadav, I., Sharma, P., et al. (2021). *Trichoderma* sp. endochitinase and β-1,3-glucanase impede *Rhizoctonia solani* growth independently, and their combined use does not enhance impediment. *Plant Pathol.* [Preprint]. doi: 10.1111/ppa.13381

Korukmez, N., Yildiz, F., Yayla, S., Gencer, R., and Akpinar, O. (2019). First report of fruit rot caused by *Botryosphaeria dothidea* on olive in Turkey. *J. Plant Pathol.* 102, 537–537. doi: 10.1007/s42161-019-00429-w

Kumar, R., Kumari, K., Hembram, K. C., Kandha, L., and Bindhani, B. K. (2018). Expression of an endo α-1, 3-Glucanase gene from *Trichoderma harzianum* in rice induces resistance against sheath blight. *J. Plant Biochem. Biotechnol.* 28, 84–90. doi: 10.1007/s13562-018-0465-7

Kurt, S., Gunes, U., and Soylu, E. M. (2011). In vitro and *in vivo* antifungal activity of synthetic pure isothiocyanates against *Sclerotinia sclerotiorum*. *Pest Manage. Sci.* 67, 869–875. doi: 10.1002/ps.2126

Li, J., Fu, S., Fan, G., Li, D., Yang, S., Peng, L., et al. (2021). Active compound identification by screening 33 essential oil monomers against *Botryosphaeria dothidea* from postharvest kiwifruit and its potential action mode. *Pest. Biochem. Physiol.* 2021:104957. doi: 10.1016/j.pestbp.2021.104957

Li, Q., Qin, X., Qi, J., Dou, W., Dunand, C., Chen, S., et al. (2020). CsPrx25, a class III peroxidase in *Citrus sinensis*, confers resistance to citrus bacterial canker through the maintenance of ROS homeostasis and cell wall lignification. *Horticult. Res.* 7:192. doi: 10.1038/s41438-020-00415-9

Liao, M., Ren, X., Gao, Q., Liu, N., Tang, F., Wang, G., et al. (2021). Anti-fungal activity of moso bamboo (*Phyllostachys pubescens*) leaf extract and its development into a botanical fungicide to control pepper phytophthora blight. *Sci. Rep.* 11:4146. doi: 10.1038/s41598-021-83598-y

Livak, K. J., and Schmittgen, T. D. (2001). Analysis of relative gene expression data using real-time quantitative PCR and the $2^{-\Delta\Delta CT}$ method. *Methods* 25, 402–408. doi: 10.1006/meth.2001.1262

Munday, R., Munday, J. S., and Munday, C. M. (2003). Comparative effects of mono-, di-, tri-, and tetrasulfides derived from plants of the *Allium* family: redox cycling in vitro and hemolytic activity and phase 2 enzyme induction in vivo. *Free Radic. Biol. Med.* 34, 1200–1211. doi: 10.1016/s0891-5849(03)00144-8

Natasya-Ain, R., Eirna-Liza, N., Jasmin, M., and Karim, M. (2018). Antibacterial activity of garlic extracts on fish pathogenic bacteria. *J. Environ. Biol.* 39, 808–812. doi: 10.22438/jeb/39/5(SI)/25

Navarro-Gonzalez, S. S., Ramirez-Trujillo, J. A., Pena-Chora, G., Gaytan, P., Roldan-Salgado, A., Corzo, G., et al. (2019). Enhanced tolerance against a fungal pathogen and insect resistance in transgenic tobacco plants overexpressing an endochitinase gene from *Serratia marcescens*. *Int. J. Mol. Sci.* 20:ijms20143482. doi: 10.3390/ijms20143482

Ortega-Ramirez, L. A., Silva-Espinoza, B. A., Vargas-Arispuro, I., Gonzalez-Aguilar, G. A., Cruz-Valenzuela, M. R., Nazzaro, F., et al. (2017). Combination of *Cymbopogon citratus* and *Allium cepa* essential oils increased antibacterial activity in leafy vegetables. *J. Sci. Food Agricult.* 97, 2166–2173. doi: 10.1002/jsfa.8025

Pan, J., Hao, X., Yao, H., Ge, K., Ma, L., and Ma, W. (2019). Matrine inhibits mycelia growth of *Botryosphaeria dothidea* by affecting membrane permeability. *J. For. Res.* 30, 1105–1113. doi: 10.1007/s11676-019-00883-3

Pan, J., Yang, Y., Zhang, R., Yao, H., Ge, K., Zhang, M., et al. (2017). Enrichment of chelidonine from *Chelidonium majus* L. using macroporous resin and its antifungal activity. *J. Chromatogr.* 1070, 7–14. doi: 10.1016/j.jchromb.2017.10.029

Qiu, F., Xu, G., Zhou, J., Zheng, F.-Q., Zheng, L., Miao, W., et al. (2020). First report of *Botryosphaeria dothidea* causing stem-end rot in avocado (Persea americana) in China. *Plant Dis.* 104, 286–287. doi: 10.1094/PDIS-07-19-1439-PDN

Rasooli, I., Rezaei, M. B., and Allameh, A. (2006). Growth inhibition and morphological alterations of *Aspergillus niger* by essential oils from *Thymus eriocalyx* and *Thymus x-porlock*. *Food Control.* 17, 359–364. doi: 10.1016/j.foodcont.2004.12.002

Rattanachaikunsopon, P., and Phumkhachorn, P. (2009). Potential of Chinese chive oil as a natural antimicrobial for controlling *Flavobacterium columnare* infection in Nile tilapia *Oreochromis niloticus*. *Fisher. Sci.* 75, 1431–1437. doi: 10.1007/s12562-009-0171-4

Sandhu, J. S., Nayyar, S., Kaur, A., Kaur, R., Kalia, A., Arora, A., et al. (2019). Foot rot tolerant transgenic rough lemon rootstock developed through expression of beta-1,3-glucanase from *Trichoderma* spp. *Plant Biotechnol. J.* 17, 2023–2025. doi: 10.1111/pbi.13152

Santos, C., Nogueira, F. C. S., Domont, G. B., Fontes, W., Prado, G. S., Habibi, P., et al. (2019). Proteomic analysis and functional validation of a *Brassica oleracea* endochitinase involved in resistance to *Xanthomonas campestris*. *Front. Plant Sci.* 10:414. doi: 10.3389/fpls.2019.00414

Shahriari, M., Hemmati, S., Zangeneh, A., and Zangeneh, M. M. (2019). Biosynthesis of gold nanoparticles using *Allium noeanum* Reut. ex Regel leaves aqueous extract; characterization and analysis of their cytotoxicity, antioxidant, and antibacterial properties. *Appl. Organometal. Chem.* 33:5189. doi: 10.1002/aoc.5189

Singh, H. R., Hazarika, P., Agarwala, N., Bhattacharyya, N., Bhagawati, P., Gohain, B., et al. (2018). Transgenic tea over-expressing *Solanum tuberosum* endo-1,3-beta-d-glucanase gene conferred resistance against blister blight disease. *Plant Mol. Biol. Rep.* 36, 107–122. doi: 10.1007/s11105-017-1063-x

Song, Y., Li, L., Li, C., Lu, Z., Men, X., and Chen, F. (2018). Evaluating the sensitivity and efficacy of fungicides with different modes of action against *Botryosphaeria dothidea*. *Plant Dis.* 102, 1785–1793. doi: 10.1094/pdis-01-18-0118-re

Sorlozano-Puerto, A., Albertuz-Crespo, M., Lopez-Machado, I., Gil-Martinez, L., Ariza-Romero, J. J., Maroto-Tello, A., et al. (2020). Antibacterial and antifungal activity of propyl-propane-thiosulfinate and propyl-propane-thiosulfonate, two organosulfur compounds from *Allium cepa*: in vitro antimicrobial effect via the gas phase. *Pharmaceuticals* 14:h14010021. doi: 10.3390/ph14010021

Soylu, E. M., Kurt, S., and Soylu, S. (2010). In vitro and *in vivo* antifungal activities of the essential oils of various plants against tomato grey mould disease agent *Botrytis cinerea*. *Int. J. Food Microbiol.* 143, 183–189. doi: 10.1016/j.ijfoodmicro.2010.08.015

Soylu, E. M., Soylu, S., and Kurt, S. (2006). Antimicrobial activities of the essential oils of various plants against tomato late blight disease agent *Phytophthora infestans*. *Mycopathologia* 161, 119–128. doi: 10.1007/s11046-005-0206-z

Sun, X., Pan, B., Wang, Y., Xu, W., and Zhang, S. (2020). Exogenous calcium improved resistance to *Botryosphaeria dothidea* by increasing autophagy activity and salicylic acid level in pear. *Mol. Plant Microbe Interact.* 33, 1150–1160. doi: 10.1094/MPMI-04-20-0101-R

Tang, W., Ding, Z., Zhou, Z. Q., Wang, Y. Z., and Guo, L. Y. (2012). Phylogenetic and pathogenic analyses show that the causal agent of apple ring rot in China is *Botryosphaeria dothidea*. *Plant Dis.* 96, 486–496. doi: 10.1094/PDIS-08-11-0635

Wang, L., Hou, H., Zhou, Z., Tu, H., and Yuan, H. (2021). Identification and detection of *Botryosphaeria dothidea* from kiwifruit (*Actinidia chinensis*) in China. *Plants* 10:lants10020401. doi: 10.3390/plants10020401

Wang, X., Zhang, X., Li, M., Ji, X., Feng, C., and Wang, F. (2020). First report of ficus carica bot rot caused by *Botryosphaeria dothidea* in China. *Plant Dis.* 104, 1869–1879. doi: 10.1094/PDIS-09-19-2039-PDN

Xiao, L., Zhou, Y. M., Zhang, X. F., and Du, F. Y. (2018). Notopterygium incisum extract and associated secondary metabolites inhibit apple fruit fungal pathogens. *Pest. Biochem. Physiol.* 150, 59–65. doi: 10.1016/j.pestbp.2018.07.001

Yang, L., Zhu, Z., Zhang, J., Gao, Y., Wang, X., Liu, G., et al. (2020). Response of kiwifruit yield and fruit quality to chloride-containing fertilizers. *Agronomy J.* 112, 1012–1020. doi: 10.1002/agj2.20074

Yang, T., Qiu, L., Huang, W., Xu, Q., Zou, J., Peng, Q., et al. (2020). Chilli veinal mottle virus HCPro interacts with catalase to facilitate virus infection in *Nicotiana tabacum*. *J. Exp. Bot.* 71, 5656–5668. doi: 10.1093/jxb/eraa304

Yang, Y., Jiang, R., Wang, H., Tian, Z., and Xie, C. (2020). StPOPA, encoding an anionic peroxidase, enhances potato resistance against *Phytophthora infestans*. *Mol. Breed.* 40:1. doi: 10.1007/s11032-019-1093-1

Yi, H., Chen, Y., Liu, J., Zhang, J., Guo, W., Xiao, W., et al. (2016). Extraction and separation of active ingredients in *Schisandra chinensis* (Turcz.) baill and the study of their antifungal effects. *PLoS One* 11:e0154731. doi: 10.1371/journal.pone.0154731

Zangeneh, A., Zangeneh, M. M., and Moradi, R. (2019). Ethnomedicinal plant-extract-assisted green synthesis of iron nanoparticles using *Allium saralicum* extract, and their antioxidant, cytotoxicity, antibacterial, antifungal and cutaneous wound-healing activities. *Appl. Organometal. Chem.* 34:5247. doi: 10.1002/aoc.5247

Zangeneh, M. M., Bovandi, S., Gharehyakheh, S., Zangeneh, A., and Irani, P. (2019). Green synthesis and chemical characterization of silver nanoparticles obtained using *Allium saralicum* aqueous extract and survey of in vitro antioxidant, cytotoxic, antibacterial and antifungal properties. *Appl. Organometal. Chem.* 33:4961. doi: 10.1002/aoc.4961

Zhang, L., Zhang, Q., Yang, P., Niu, Y., and Niu, W. (2019). First report of gummosis disease of sweet cherry caused by *Botryosphaeria dothidea* in China. *Plant Dis.* 103:1418-PDN

Zhang, Z., Xie, Y., Hu, X., Shi, H., Wei, M., and Lin, Z. (2018). Antifungal activity of monoterpenes against *Botryosphaeria dothidea*. *Nat. Prod. Commun.* 13:1934578X1801301. doi: 10.1177/1934578x1801301234

Zhao, G., Zhang, W., Zuo, C., and Huang, Y. (2017). Control effect of chinese leek extract and its main bioactive components on apple ring rot incidence. *Chin. J. Biol. Control* 33, 273–280. doi: 10.16409/j.cnki.2095-039x.2017.02.019

Zhao, L., Phuong, L. T., Luan, M. T., Fitrianti, A. N., Matsui, H., Nakagami, H., et al. (2019). A class III peroxidase PRX34 is a component of disease resistance in Arabidopsis. *J. General Plant Pathol.* 85, 405–412. doi: 10.1007/s10327-019-00863-9

Zhao, X., Zhang, G.-L., Li, B.-H., Xu, X.-M., Dong, X.-L., Wang, C.-X., et al. (2016). Seasonal dynamics of *Botryosphaeria dothidea* infections and symptom development on apple fruits and shoots in China. *Eur. J. Plant Pathol.* 146, 507–518. doi: 10.1007/s10658-016-0935-5

Zheng, Y., Wang, X., Liu, S., Zhang, K., Cai, Z., Chen, X., et al. (2018). The endochitinase of clonostachysrosea expression in *Bacillus amyloliquefaciens* enhances the *Botrytis cinerea* resistance of tomato. *Int. J. Mol. Sci.* 19:ijms19082221. doi: 10.3390/ijms19082221

Conflict of Interest: The authors declare that the research was conducted in the absence of any commercial or financial relationships that could be construed as a potential conflict of interest.

Publisher's Note: All claims expressed in this article are solely those of the authors and do not necessarily represent those of their affiliated organizations, or those of the publisher, the editors and the reviewers. Any product that may be evaluated in this article, or claim that may be made by its manufacturer, is not guaranteed or endorsed by the publisher.

frontiers in Microbiology

ORIGINAL RESEARCH
published: 02 March 2022
doi: 10.3389/fmicb.2022.828914

Chitosan Treatment Promotes Wound Healing of Apple by Eliciting Phenylpropanoid Pathway and Enzymatic Browning of Wounds

*Sabina Ackah[1], Sulin Xue[1], Richard Osei[2], Francis Kweku-Amagloh[3], Yuanyuan Zong[1], Dov Prusky[1,4] and Yang Bi[1]**

[1] College of Food Science and Engineering, Gansu Agricultural University, Lanzhou, China, [2] College of Plant Protection, Gansu Agricultural University, Lanzhou, China, [3] Department of Food Science and Technology, University for Development Studies, Tamale, Ghana, [4] Department of Postharvest Science of Fresh Produce, Agricultural Research Organization, Rishon LeZion, Israel

Chitosan is an elicitor that induces resistance in fruits against postharvest diseases, but there is little knowledge about the wound healing ability of chitosan on apple fruits. Our study aimed at revealing the effect of chitosan on the phenylpropanoid pathway by determining some enzyme activities, products metabolites, polyphenol oxidase activity, color (L^*, b^*, a^*), weight loss, and disease index during healing. Apple (cv. Fuji) fruits wounded artificially were treated with 2.5% chitosan and healed at 21–25°C, relative humidity = 81–85% for 7 days, and non-wounded fruits (coated and non-coated) were used as control. The result shows that chitosan treatment significantly decreased weight loss of wounded fruits and disease index of *Penicillium expansum* inoculated fruits. The activities of phenylalanine ammonia-lyase (PAL), cinnamic acid 4-hydroxylase (C4H), 4-coumaryl coenzyme A ligase (4CL), cinnamoyl-CoA reductase (CCR), and cinnamyl alcohol dehydrogenase (CAD) were elicited throughout the healing period by chitosan, which increased the biosynthesis of cinnamic acid, caffeic acid, ferulic acid, sinapic acid, *p*-coumaric acid, *p*-coumaryl alcohol, coniferyl alcohol, and sinapyl alcohol. Also, total phenol, flavonoid, and lignin contents were significantly increased at the fruits wounds. In addition, chitosan's ability to enhance polyphenol oxidase activity stimulated enzymatic browning of wounds. Although wounding increased phenylpropanoid enzymes activities before healing, chitosan caused higher enzyme activities for a significant healing effect compared with the control. These findings imply that chitosan accelerates apple wound healing by activating the phenylpropanoid pathway and stimulating enzymatic browning of wounds.

Keywords: chitosan, apple fruit, wound healing, phenylpropanoid metabolism, enzymatic browning

OPEN ACCESS

Edited by:
Khamis Youssef,
Agricultural Research Center, Egypt

Reviewed by:
Runqiang Yang,
Nanjing Agricultural University, China
Khaled A. El-Tarabily,
United Arab Emirates University, United Arab Emirates
M. Carmen Limon,
University of Seville, Spain

****Correspondence:***
Yang Bi
biyang@gsau.edu.cn

Specialty section:
This article was submitted to Food Microbiology, a section of the journal Frontiers in Microbiology

Received: *04 December 2021*
Accepted: *20 January 2022*
Published: *02 March 2022*

Citation:
Ackah S, Xue S, Osei R, Kweku-Amagloh F, Zong Y, Prusky D and Bi Y (2022) Chitosan Treatment Promotes Wound Healing of Apple by Eliciting Phenylpropanoid Pathway and Enzymatic Browning of Wounds. Front. Microbiol. 13:828914. doi: 10.3389/fmicb.2022.828914

INTRODUCTION

Apple (*Malus domestica* Borkh.) is the most economically widely produced fruit crop in temperate zones (Wang et al., 2018). However, apples are susceptible to mechanical injury during harvest and postharvest handling. Wounds formed on the fruit's surface create a channel for the invasion of pathogens that causes rot, which further results in excessive water evaporation (Gong et al., 2019). Apples have the ability of wound healing by accumulating lignin and polyphenols to prevent the

invasion of fungi (Zhang et al., 2020). However, the natural wound healing process takes a long time; therefore, rapid wound healing is critical for apple postharvest quality.

Chitosan is a chitin N-deacetylated derivative obtained from crustaceans' outer shells, mainly shrimps, crabs, krills, some fungi cell walls, etc. It is a natural polymer with a polycationic nature, non-toxic, biodegradable, excellent film-forming property, and antimicrobial effect (Deepmala et al., 2014; Silva and Pighinelli, 2017). Chitosan is used as an elicitor to induce resistance against postharvest diseases of horticultural crops (Romanazzi et al., 2017), such as gray mold caused by *Botrytis cinerea* in tomatoes, grapes, strawberries, apples, and peaches (Plainsirichai et al., 2014; Zhang et al., 2015; Gayed et al., 2017; Peian et al., 2021). Similarly, chitosan induced resistance to anthracnose caused by *Colletotrichum gloeosporioides* in citrus (Zhao et al., 2018), blue mold caused by *Penicillium expansum* in apples (Lu et al., 2014; Li et al., 2015), and green and blue mold caused by *Penicillium digitatum* and *Penicillium italicum* in orange (Zeng et al., 2010). Chitosan acts directly on the pathogens as a fungicide to destroy fungus (Li et al., 2015). Also, chitosan induces signal transduction pathways such as jasmonic acid (JA), salicylic acid (SA), ethylene (ET), and hydrogen peroxide to activate systemic acquired resistance of fruit in grapes and strawberries in response to stress (Gu et al., 2021; Peian et al., 2021). Moreover, chitosan residues bind to fruits cell membranes to stimulate the synthesis of phytoalexin and pathogenesis-related proteins: chitinase, β-1,3-glucanase, and lignin biosynthesis and activates reactive oxygen species generation in fruits (Li et al., 2015). Enzymatic browning, which results from the oxidation of phenolic compounds to quinones, is catalyzed by polyphenol oxidase (PPO) with brown pigmentation (Yan et al., 2018). Chitosan increases not only the synthesis of phenolic compounds but also PPO activity to stimulate browning in apples and citrus (Pilon et al., 2015; Zhao et al., 2018). Previous studies showed that chitosan elicited phenylalanine ammonia-lyase (PAL) activity to increase the content of phenolic compounds in tomatoes, grapes, and strawberries (Coqueiro et al., 2015; Romanazzi et al., 2017). Chitosan's efficacy in treating fruits has been demonstrated in numerous studies and has proven that chitosan coating can prevent deterioration and extend the shelf life of a range of fruits and vegetables (Plainsirichai et al., 2014; Li et al., 2015; Zhang et al., 2015; Gu et al., 2021). Moreover, the recent work by our team reveals that preharvest spraying with chitosan accelerated the wound healing process of muskmelons after harvesting by eliciting phenylpropanoid metabolism for the production of phenolic compounds and lignin at the wounded site (Li et al., 2021). Although chitosan antifungal effect has been demonstrated in many whole fruits and preharvest spraying with chitosan has been reported to promote wound healing in harvested muskmelons, there is no report on chitosan wound healing ability on apple fruits. Thus, this study aimed at exploring chitosan's effects on the wound healing of apple fruits. Fruits were artificially wounded, treated with 2.5% chitosan, and stored at room temperature of 20 ± 5°C, relative humidity (RH) = 81–85% to heal. The (1) weight loss of wounded/non-wounded fruits and disease index of *P. expansum* inoculated fruits were evaluated, (2) some important enzyme activities and products metabolites were determined, and (3) PPO activity and color (L^*, b^*, a*) of wounds during healing were subsequently analyzed.

MATERIALS AND METHODS

Fruit and Chitosan

Apple (*M. domestica* Borkh. cv. Fuji) fruits were harvested from a commercial orchard of Tiaoshan farm in Jingtai (37°380 N, 105°340 E, 1,671 m altitude), Gansu Province, China. Fruits that are free from disease and injury, uniform size, and maturity were sorted, and each fruit was netted with foam. The fruits were immediately packed in perforated paper boxes with each box containing 36 fruits, transported to Gansu Agricultural University, and stored at 2 ± 4°C, RH = 80–85%.

Water-soluble chitosan (degree of deacetylation ≥90%, WN Group of Publishers Ltd., Mansouriah, France) was used as treatment. Twenty-five gram of chitosan was completely dissolved in 1,000-ml H_2O to make a chitosan solution. The concentration of 2.5% chitosan used was based on preliminary test results.

Wounding and Treatment of Fruits

Wounding and treatment of apples were done according to Zhang et al. (2020). The fruits were first washed with water, disinfected using 0.1% (v/v) $NaClO_2$ for 3 min, then rinsed with water and allowed to dry. After drying, each fruit was disinfected with 75% ethanol. A sterilized scalpel (Deli, no. 2034, China) was used to make three wounds on the equatorial region of each fruit (circle 7.3–7.8-mm radius and 1-mm depth) and then soaked in 2.5% (w/v) chitosan for 10 min and allowed to dry on a clean surface. Two independent experiments were conducted in a completely randomized design with three replicates. The treatments were (i) wounded then treated with chitosan (W + chitosan), (ii) wounded then treated with distilled water (W + water), (iii) non-wounded and treated with chitosan (N + chitosan), and (iv) non-wounded and treated with distilled water (N + water). All fruits were kept in aerated poly-ET bags and subsequently stored at room temperature at 20–25°C, RH = 81–85% to heal.

Determination of the Rate of Water Loss

The determination of the weight loss of wounded and non-wounded fruits was done by weighing fruits gravimetrically according to Zhang et al. (2020) using an electronic scale (HZ electronic LLC, ST Hartford, CT, United States) on 0, 1, 3, 5, and 7 days of healing. The fresh weight change of apple fruits at each time point was divided by the initial weight and expressed as a percentage and recorded as the total weight loss. Ten fruits from each treatment were weighed at each time point and were repeated three times.

Determination of Diseases Index

The method reported by Zhang et al. (2020) for disease index was used. A spore suspension (1×10^5 spores/ml) of *Penicillium expansum* was prepared. Then, the wound surfaces of fruits were inoculated with 20-μl spore suspension on 0, 1, 3, 5, and 7 days of

healing. The inoculated fruits were then packed in aerated poly-ET bags and kept at 21–25°C, RH = 81–85% in the dark for incubation. Infected fruits were physically observed after 5 days of inoculation. The incidence was categorized in five levels based on the extent of fungi growth, that is: grade 4, fungi on all the wound surface; grade 3, fungi on three-fourths of wound surface; grade 2, fungi on a one-half area of wound surface; grade 1, fungi growth on a one-fourth area of wound surface; and grade 0, no fungi growth on the wound surface. Disease index was calculated using the formula, disease index = [Σ (the number of wounds at the disease level × the level of disease)]/4 × total wounds] × 100%. Ten wounds were evaluated at each time point and were repeated three times.

Determination of Wound Surface Color

The wound surface color was determined according to Dea et al. (2010) with slight modification. A colorimeter (X-Rite Ci6X, United States) was used to determine the color of the individual wounds of fruits on 0, 1, 3, 5, and 7 days of healing. L^* (lightness), a* (reddish–greenish), and b^* (yellowish–bluish), Chroma C* = [(a)2 + (b)2]1/2 and hue angle $h°$= [tan – 1(b*/a*)] data were collected to evaluate the wound surface color. Fifteen wounds were observed at each time point and were repeated three times.

Sampling

Fruits wound tissues were collected according to Zhang et al. (2020) after 0, 1, 3, 5, and 7 days of healing by carefully separating the scarred outmost tissue from the cut surface using a sterilized sharp blade. Tissues of non-wounded fruits were collected. Nitrogen (liquid) was used to freeze the collected tissues, ground with a grinder (IKA, no. A11, Germany) into a powdery form, and subsequently stored at −80°C until use.

Hydrogen Peroxide Content Assay

Hydrogen peroxide (H_2O_2) content was determined using a test kit from Suzhou Keming Biotechnology Co., Ltd., Suzhou, China. Extract solution (1 ml) was added to 0.1 g of frozen sample, then centrifuged at 8,000 × g at 4°C for 10 min. The supernatant was used as a crude enzyme. Other reagents were added as instructed. The result was expressed as μmol/g FW.

Assay of Some Enzymatic Activities

Phenylalanine ammonia-lyase activity was determined using the Koukol and Conn's (1961) method. Three milliliters of 100 mmol/L borate buffer (pH 8.8, 40 g/L polyvinylpyrrolidone, 2 mmol/L ethylenediaminetetraacetic acid, and 5 mmol/L β-mercaptoethanol) was added to 1-g frozen powder for 2 h to allow extraction, then centrifuged at 4°C at 8,000 × g for 30 min. The supernatant was used as a crude enzyme. PAL was assayed by adding 3 ml of 50 mmol/L borate buffer (pH 8.8) and 0.5 ml of 20 mmol/L L-phenylalanine to 0.5 ml of crude enzyme. Absorbance, optical density at a wavelength of 280 nm (OD_{290}) was measured immediately, and just after keeping in a 37°C water bath for 1 h, the second OD_{290} was measured. PAL activity was expressed as U/g FW, where $U = 0.01\ OD_{290}\ min^{-1}$.

Cinnamic acid 4-hydroxylase (C4H) activity was determined using a kit from Beijing Solarbio Science & Technology Co., Ltd., China. Extract solution (1 ml) was added to 0.5 g of frozen powder, centrifuged at 11,000 × g at 4°C for 15 min, and the collected supernatant was the enzyme solution. Regents were added as instructed. C4H activity was expressed as U/g FW, where $U = 0.01\ OD_{340}\ min^{-1}$.

4-Coumaryl coenzyme A ligase (4CL) activity was assayed using the method of Liu et al. (2014) with modifications. Three milliliters of extraction solution (Shanghai Yuanye Bio-Technology Co., Ltd., Shanghai, China) was added to 1 g of a frozen powder for 1 h and centrifuged at 8,000 × g for 30 min at 4°C, and the resulting supernatant was collected as the enzyme solution. An amount of 0.15 ml of 5-mM p-coumaric acid, 0.15 ml of 1-mM CoA, 0.15 ml of 50-mM adenosine triphosphate, and 0.45 ml of 15-mM $MgCl_2 \bullet 6H_2O$ was added to a 0.5-ml crude enzyme solution, kept for 30 min at 40°C. 4CL activity was expressed as U/g FW, where $U = 0.01\ OD_{333}\ min^{-1}$.

The activity of cinnamyl alcohol dehydrogenase (CAD) was determined using a test kit from Suzhou Keming Biotechnology Co., Ltd., Suzhou, China. Extract solution (1 ml) was added to 0.5 g of frozen powder, then centrifuged at 8,000 × g at 4°C for 10 min. Other reagents were added as instructed, and OD_{340} was measured as first OD, and second OD was measured after 5 min. CAD activity was expressed as nmol/min/g FW.

Cinnamoyl-CoA reductase (CCR) activity was determined using a test kit from Enzyme-Linked Immunosorbent Assay (ELISA) Co., Ltd., Suzhou, China. One milliliter of 10 mM pH 7.4 was added to 0.5 g of frozen powder, then centrifuged at 8,000 × g at 4°C for 15 min. The collected supernatant was the crude enzyme. Other reagents were added as instructed by the kit, and OD_{450} was measured. CCR activity was expressed as U/g FW, where $U = 0.01\ OD_{333}\ min^{-1}$.

The PPO and peroxidase (POD) activities were scientifically assayed according to the Venisse et al.'s (2002) method. An acetic acid–sodium acetate buffer (pH 5.5, containing 1 mmol/L polyethylene glycol, 1% Triton X-100, and 4% polyvinylpyrrolidone) was used as an extraction reagent. An amount of 5-ml extraction buffer was added to 2 g of frozen powder and kept for 30 min, centrifuged at 8,000 × g for 30 min at 4°C, and the collected supernatant was the enzyme solution. Then, 3 ml of 50 mmol/L acetic acid–sodium acetate buffer (pH 5.5) and 1 ml of 50 mmol/L catechol were added to 0.1 ml of the crude enzyme, and absorbance was immediately determined. The PPO activity was expressed as U/g FW, $U = 0.01\ OD_{420}\ min^{-1}$. To determine POD, 3 ml of 25 mmol/L guaiacol was added to 1 ml of a crude enzyme, after which 0.2 ml of 0.5 mol/L H_2O_2 was added, and the absorbance was determined. The POD activity was expressed as U/g FW, $U = 0.01\ OD_{470}\ min^{-1}$.

High-Performance Liquid Chromatography Analysis of Phenolic Acids and Monolignin Contents

The phenolic acids and monolignin contents were scientifically determined using the Zhao et al.'s (2006) method with slight modification. Three milliliters of 70% methanol was added to

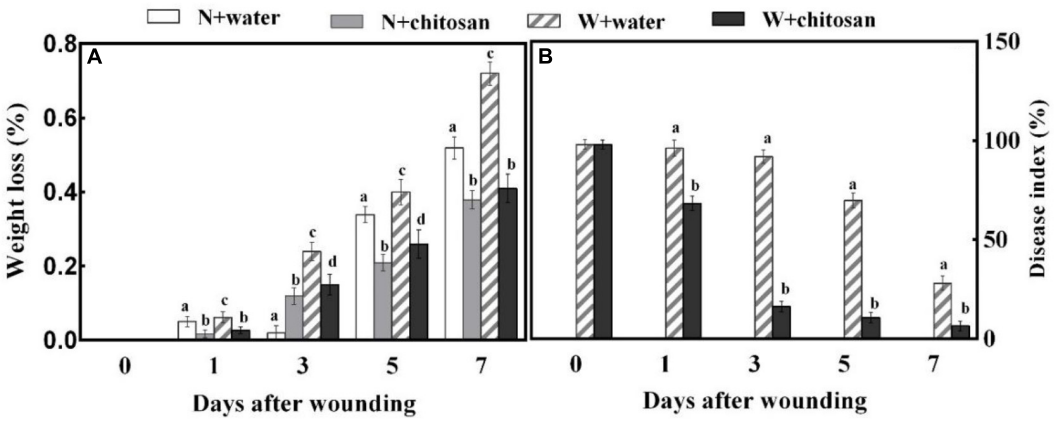

FIGURE 1 | Effect of chitosan treatment on weight loss **(A)** and disease index of inoculated fruit with *P. expansum* **(B)**. Non-wounded and treated with sterile water (N + water), non-wounded and treated with chitosan (N + chitosan), wounded and treated with sterile water (W + water), and wounded and treated with chitosan (W + chitosan). Vertical bars indicate standard error of means. Alphabets indicate significant differences ($p < 0.05$).

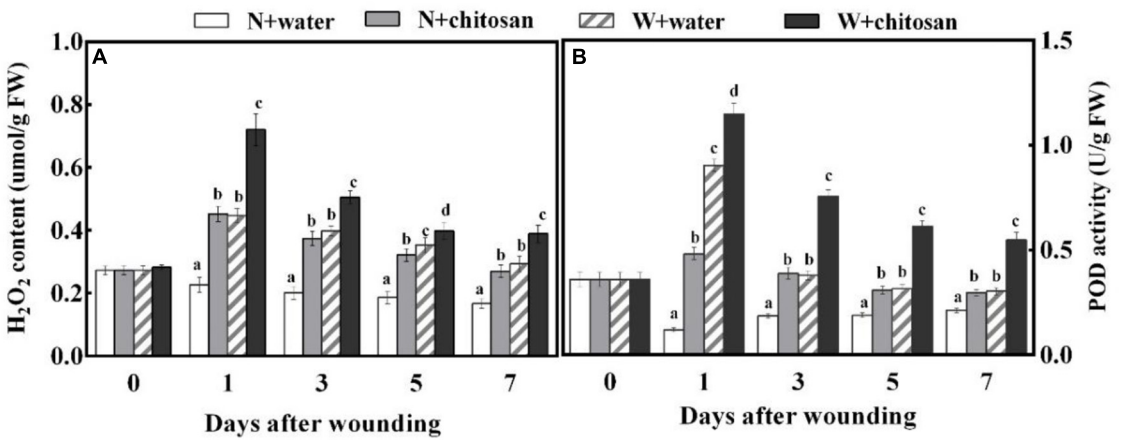

FIGURE 2 | Effect of chitosan treatment on H_2O_2 content **(A)** and POD activity **(B)**. Non-wounded and treated with sterile water (N + water), non-wounded and treated with chitosan (N + chitosan), wounded and treated with sterile water (W + water), and wounded and treated with chitosan (W + chitosan). Vertical bars indicate standard error of means. Alphabets indicate significant differences ($p < 0.05$).

3 g of sample tissues and undergoes ultrasonication for 30 min at 40 kHz before being centrifuged at 10,000 × *g* at 4°C for 20 min. The resultant supernatant was collected and concentrated under nitrogen before being diluted with 70% methanol to 1 ml. The resulting 1-ml solution was collected into an automatic injection (2 ml) bottle by filtering using an organic membrane medium of 0.45 μm. High-performance liquid chromatography was performed using Waters Symmetry C18 (4.6 × 250 mm, 5 μm) column. Methanol (A) and 1% acetic acid (B) mobile phase condition was as follows: gradient elution at 0–10 min, 30% A, 70% B; 10–12 min, 45% A, 55% B; 12–15 min, 65% A, 35% B; 15–18 min, 30% A, 70% B; and 18–20 min, 30% A, 70% B with a flow rate of 1 ml min^{-1} and injection volume of 10 μl, controlled at 25°C. Cinnamic acid, caffeic acid, ferulic acid, sinapic acid, and *p*-coumaric acid were detected at 276, 325, 322, 325, and 310 nm, respectively, and *p*-coumaryl alcohol, coniferyl alcohol, and sinapyl alcohol at 273, 263, and 273 nm, respectively. A standard curve of a standard sample under the same condition was set, and the concentration of all phenolic compounds was determined in comparison with the standard curve. The amount of substance (μg) to cause a change in absorbance per minute as compared with the standard sample was referred to as the individual contents. The various phenolic acids and monolignin contents were expressed as μg/g FW.

Determination of Total Phenol, Flavonoids, and Lignin Content

Scalbert et al.'s (1989) method was used to determine total phenols and flavonoid contents. Three grams of frozen tissues was carefully homogenized with a 5-ml solution of 0.5% acetic acid (CHCOOH) and 70% acetone (C_3H_6O) and then kept at 4°C for 24 h in the dark. The mixture was then centrifuged at 8,000 × *g* for 20 min at 4°C. The resulting supernatant was used for the determination of total phenol and flavonoid contents.

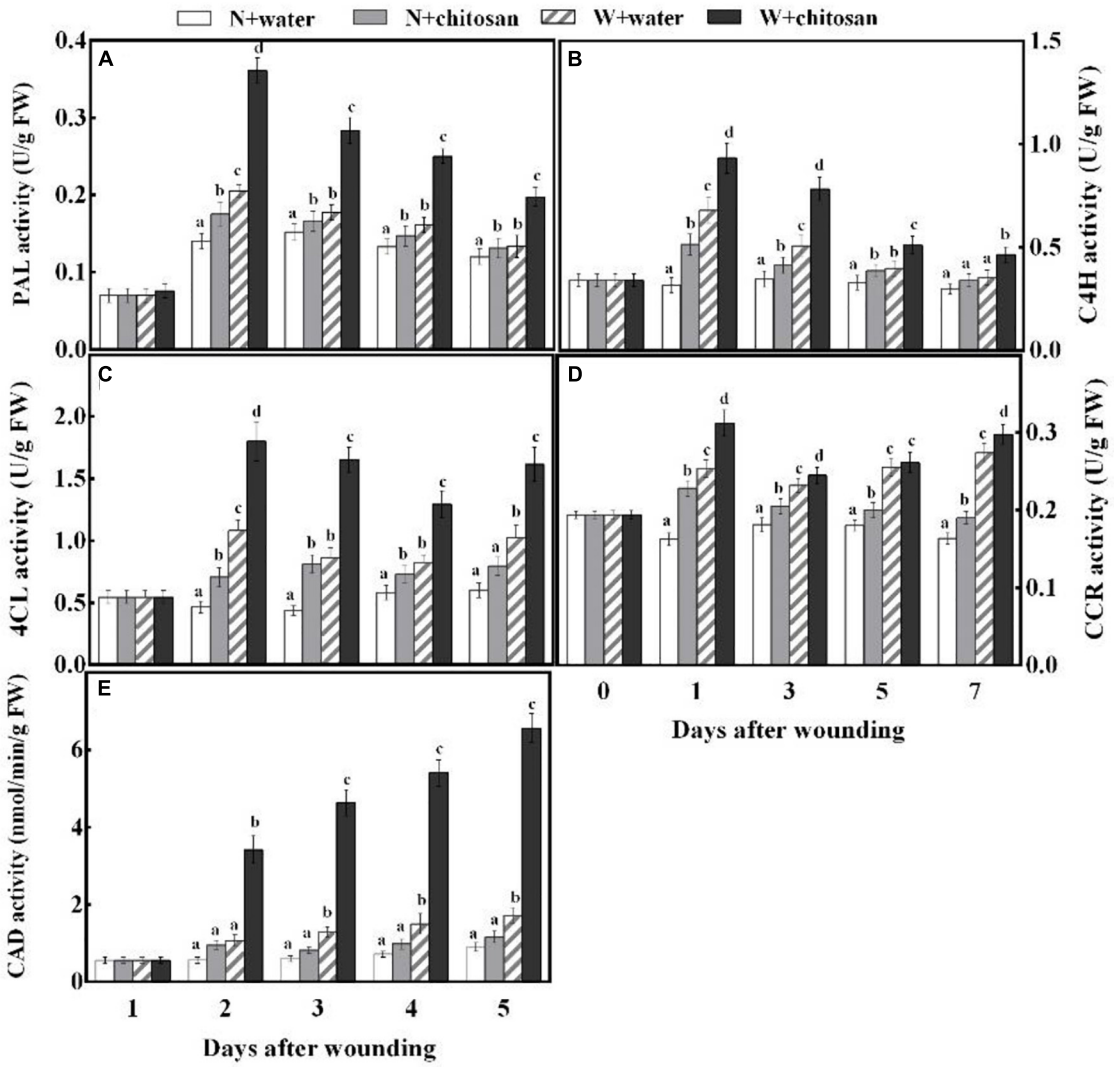

FIGURE 3 | Effect of chitosan treatment on activities of PAL **(A)**, C4H **(B)**, 4CL **(C)**, CCR **(D)**, and CAD **(E)**. Non-wounded and treated with sterile water (N + water), non-wounded and treated with chitosan (N + chitosan), wounded and treated with sterile water (W + water), and wounded and treated with chitosan (W + chitosan). Vertical bars indicate standard error of means. Alphabets indicate significant differences ($p < 0.05$).

Total phenol was determined by adding 2 ml of 0.1% (v/v) Folin–Ciocalteu's phenol chemical to 1-ml supernatant, then a volume of 2 ml of 7.5% Na_2CO_3 was added and heated for 5 min at 50°C. The absorbance, OD_{760}, was measured. To estimate total phenol content, a gallic acid standard curve was used, and the result was expressed as milligrams of gallic acid equivalents 100 g^{-1} FW. To determine flavonoid content, 0.25 ml of $AlCl_3 \bullet 6H_2O$ (10%) and 0.15 ml of $NaNO_2$ (5%) solution was mixed with a 3.5-ml crude enzyme. After 5 min, 1 ml of 1-M NaOH was also added. Absorbance was measured at 510 nm. A standard rutin curve was used to estimate the content of flavonoid and collectively expressed as milligrams of rutin equivalents 100 g^{-1} FW.

The method described by Hammerschmidt (1984) was used in this study to determine the lignin content. Three milliliters of 95% precooled was added to 1 g of the frozen powder, mixed very well, and centrifuged at 8,000 × *g* for 30 min at 4°C; the resulting precipitate was immediately collected (three times). After that, n-hexane–ethanol = 2:1 (v/v) was added to precipitate and again centrifuged three times continuously. The final precipitate collected was dried in an oven for 48 h, then 1 ml of 25% bromoacetic acid glacial acetic acid solution was added to the dried samples and held in a hot water bath (70°C) for 30 min before stopping the reaction with 1-ml NaOH (2 mol L^{-1}). Right after the addition of 2-ml glacial acetic acid, 0.1-ml hydroxylamine hydrochloride (7.5 mol/L) was added and immediately centrifuged. Finally, 0.5-ml supernatant was topped up with glacial acetic acid to 5 ml. The absorbance was immediately measured. The lignin content was expressed as OD_{280} g^{-1} FW.

Statistical Analysis

All the determinations mentioned earlier were repeated three times. Averages and standard errors (±SE) of data were calculated using Excel 2010. Significance differences were analyzed by analysis of variance (Duncan's multiple range test) using SPSS 20 (SPSS Inc., United States) ($p < 0.05$).

RESULTS

Chitosan Treatment Reduced Weight Loss and Disease Index of Fruits During Healing

Weight loss and disease index are crucial for evaluating the effect of wound healing on fruits. In this study, the weight loss for both chitosan treated and control fruits increased continuously during wound healing. On day 7, the weight loss of wounded chitosan-treated fruits was lower by 43% when compared with that of the control, but there was no significant difference compared with the non-wounded control (**Figure 1A**). The disease index of all fruits decreases as healing time increases, but the chitosan-treated fruits had a significantly lower disease index than the control fruits, which was 84.8% lower than the control at day 5 (**Figure 1B**). This is a clear indication that chitosan treatment promotes wound healing of apple fruits.

Effect of Chitosan Treatment on Hydrogen Peroxide Content and Peroxidase Activity

Hydrogen peroxide is an important signal molecule that induces a defense response. The H_2O_2 contents and POD activity of wounded fruits increased sharply on day 1 and declined gradually in all fruits, but the chitosan-treated fruits exhibited significantly higher values throughout the healing period. The H_2O_2 content on day 1 was 61% higher than the control, and POD activity was 94% more than the control on day 5, with a significant difference compared with their non-wounded fruits (**Figure 2**). These results show that chitosan treatment increases H_2O_2 content and POD activity at fruit wounds.

Chitosan Treatment Increased Phenylalanine Ammonia-Lyase, Cinnamic Acid 4-Hydroxylase, 4-Coumaryl Coenzyme A Ligase, Cinnamoyl-CoA Reductase, and Cinnamyl Alcohol Dehydrogenase Activities

Phenylalanine ammonia-lyase, C4H, 4CL, CCR, and CAD are important enzymes in the phenylpropanoid metabolism to aid in the production of phenolic and lignin. PAL and C4H activities peaked on day 1 and declined gradually from days 3 to 7 for both chitosan-treated and control wounded fruits, with the chitosan-treated fruits recording significantly higher activities throughout the healing period (**Figures 3A,B**), which were 76 and 56.3% higher than the control at days 1 and 3, respectively (**Figures 3A,B**). There were significant differences compared with their non-wounded fruits on days 1 and 3, respectively. 4CL activity increased sharply at the initial stage, declined on days 3 and 5, and finally increased on day 7 for all fruits, but the chitosan-treated fruits showed significantly higher activity, that is, 91% higher than the control at day 3, with a significant difference compared with their non-wounded fruits (**Figure 3C**). CCR activity increased sharply at the initial stage, declined on the third day, and increased gradually from days 5 to 7 for all wounded fruits, but the chitosan-treated fruits showed significantly higher activity, which was 23% higher than the control at day 1; however, there was a significant difference in comparison with its non-wounded fruits (**Figure 3D**). The CAD activity of both treated and control wounded fruits increased continuously throughout the healing period; however, the chitosan-treated fruits recorded significantly higher CAD activities than the control (**Figure 3E**). Moreover, there was a significant difference in comparison with its non-wounded fruits. The highest value of the treated fruits was recorded on the seventh day, which was 2.8-fold higher than the control (**Figure 3E**). The results earlier show that chitosan treatment effectively elicited the phenylpropanoid pathway by increasing the activities of PAL, C4H, 4CL, CCR, and CAD at the fruits' wounds during healing.

Chitosan Treatments Elevated Phenolic Acids, Total Phenol, and Flavonoid Contents

Phenolic acids are essential substrates for healing tissues formation, which also have antifungal and antioxidant properties. Cinnamic acid, ferulic acid, and *p*-coumaric acid contents of wounded chitosan-treated and control fruits increase as the healing time increases, but the chitosan-treated fruits showed significantly higher acid contents, which were 16.2, 58.3, and 74.1% more than the control on day 7, respectively. Moreover, there was a significant difference in comparison with their non-wounded fruits (**Figures 4A,C,D**). Caffeic acid and sinapic acid content increased sharply on the first day, declined on day 3, and increased gradually afterward for all fruits, but the chitosan-treated fruits recorded significantly higher acid contents compared with the control fruit. Caffeic acid was 96.3% higher than the control on day 1, and sinapic acid was 1.4 fold more than the control on day 7, with significant differences compared with their non-wounded fruits, respectively (**Figures 4B,E**). The total phenol content of all wounded fruits peaked on day 1 and declined gradually from days 3 to 7 (**Figure 4F**). However, the chitosan-treated fruits recorded higher contents than the controls. The total phenol content of chitosan-treated fruit was significantly high when compared with the control by 30% at day 3. Flavonoid content of wounded fruits increased sharply on day 1 and decreased gradually, but the treated fruits increased slightly on day 7 (**Figure 4G**). Flavonoid content of chitosan-treated fruit was significantly higher throughout the healing time, which was 53% more compared with the control at day 7, with a significant difference compared with its non-wounded fruits (**Figure 4G**).

The result indicates that chitosan treatment elevates the synthesis of five phenolic acids, total phenol, and flavonoid at the fruits' wounds during healing.

Chitosan Treatments Enhanced the Synthesis of Monolignins and Lignin

Coumaryl alcohol, coniferyl alcohol, and sinapyl alcohol are important monomers for the synthesis of lignin to increase the strength of cell walls. In this study, the contents of *p*-coumaryl alcohol, coniferyl alcohol, and sinapyl alcohol increased sharply on the first day, declined on day 3, and increased gradually afterward for both the treated and control fruits, but the chitosan-treated fruits recorded significantly higher contents compared with the control fruit (**Figures 5A–C**). *p*-Coumaryl alcohol content was 4.54-fold higher than the control fruits on day 3. On day 1, coniferyl and sinapyl alcohols were 1.13- and 1.56-fold higher than the control fruits, with significant differences compared to their non-wounded fruits, respectively (**Figures 5A–C**). The lignin content peaked on day 1 and declined gradually from days 3 to 7 for all fruits (**Figure 5D**). The chitosan-treated fruits recorded significantly higher content that was 33% more in comparison with the control at day 7, and when compared with its non-wounded fruits, there was a significant difference (**Figure 5D**). The result indicates that chitosan treatment promotes the synthesis of three lignin monomers and lignin of fruits during healing.

Chitosan Treatment Accelerates Enzymatic Browning at the Wound Surface

Browning at the wound surface is an indication of the oxidation of polyphenolic compounds. The activity of PPO peaked on day 1 and declined gradually from the third to the seventh day for all wounded fruits, but the chitosan-treated fruits showed significantly higher activity throughout the process of healing (**Figure 6A**). On day 7, chitosan-treated fruits had a significant increment of 35.1% compared with the control with significant difference compared with their non-wounded fruits (**Figure 6A**). Lightness (L^*) and hue angle values of both the treated and control fruits decrease as time increases; however, chitosan-treated fruits were significantly low when compared with the control fruits (**Figures 6B,F**). Reddish–greenish (a^*), yellowish–bluish (b^*), and chroma values of all fruits increase as healing time increases (**Figures 6C–E**). The treated fruits showed significantly higher values than the control, which were 1.3-fold, 13.4%, and 15.5% higher than the control for reddish–greenish (a^*), yellowish–bluish (b^*), and Chroma, respectively, at day 3 (**Figures 6C–E**). The results indicate that chitosan treatment accelerates enzymatic browning at the wound surface.

DISCUSSION

In this study, wounding increased weight loss as a result of stress. However, wounded fruit treated with chitosan effectively reduced the weight loss during healing by forming a protective film on the wound surface (**Figure 1**). Our results are in line with those of Plainsirichai et al. (2014), who discovered that chitosan could form a thin protective film directly on the fruit wound surface, thereby entirely or partially blocking spores on the surface to limit water transpiration. Chitosan films are also effective gas barriers, which modifies fruit's internal atmosphere by controlling the supply of O_2, CO_2, and moisture, thus reducing water transpiration and respiration and delaying ripening and senescence of fruits, which was evident in sweet cherries, strawberries, and pomegranates during storage (Pasquariello et al., 2015; Petriccione et al., 2015; Varasteh et al., 2017). In addition, lignin accumulation limits fruit water evaporation when formed on a wounded surface (Xue et al., 2019). Thus, the gradual accretion of lignin at the wound site of fruit in the present study also reduced water loss.

The results show that wounded fruit exhibited a high disease index compared with control. Chitosan-treated fruits had a significantly lower disease index than the control fruits (**Figure 1B**). Chitosan acts as a fungicidal treatment to destroy pathogens (Li et al., 2015). Chitosan can bind to plant defense proteins to induce phytoalexin and PR proteins: chitinase, β-1,3-glucanase, and lipoxygenase (Hidangmayum et al., 2019; Gu et al., 2021). For instance, chitinase, disease resistance protein, cellulose synthase-like protein E6, PPO, etc., were induced to stimulate the synthesis of PR proteins in grapes; however, these genes also stimulated H_2O_2, JA, SA, and ET biosynthesis to induce resistance and promote the formation of barrier tissues to prevent pathogen invasion (Peian et al., 2021). Lignin deposition at wounds by chitosan also contributes to the reduction of disease index because lignin is a defense polymer that restricts pathogen penetration or growth by depositing around the penetrating fungi (Xie et al., 2018). Therefore, it is suggested that chitosan reduced the disease index of inoculated fruits by acting as a fungicide, deposition of lignin, inducing phytoalexin and PR proteins production, and accumulation of phenol compounds at fruits' wound.

Phenylpropanoid metabolism aids wound healing by providing substrates for the synthesis of phenolic and monolignin with antifungal effects (Yang et al., 2020). PAL is a key enzyme initiating this metabolism by the deamination of L-phenylalanine to *trans*-cinnamic acid (Wang et al., 2020). *Trans*-cinnamic acid formed is directly hydroxylated by C4H to *p*-coumaric acid, which yields caffeic acid with the aid of *p*-coumaroyl shikimate 3-hydroxylase, and then caffeic acid is further generated into ferulic acid under *O*-methyltransferases. Sinapic acid is generated by converting ferulic acid into 5-hydroxyferulic acid by ferulic acid-5-hydroxylase, then further hydrolyzed by 5-hydroxyferulic acid *O*-methyltransferase into sinapic acid (Yang et al., 2020). These phenolic acids are converted to phenolic acids coenzyme A by 4CL and then catalyzed by CCR to yield corresponding aldehydes. The resulting aldehydes are catalyzed by CAD to form monolignins (*p*-coumaryl alcohol, coniferyl alcohol, and sinapyl alcohol) (Li et al., 2021). These phenolic acids and monolignin are precursors for suberin polyphenolic and lignin to strengthen cell walls. Coumaryl-CoA is also the precursor for the biosynthesis of flavonoids, which branch off from the phenylpropanoid pathway under the activities of chalcone

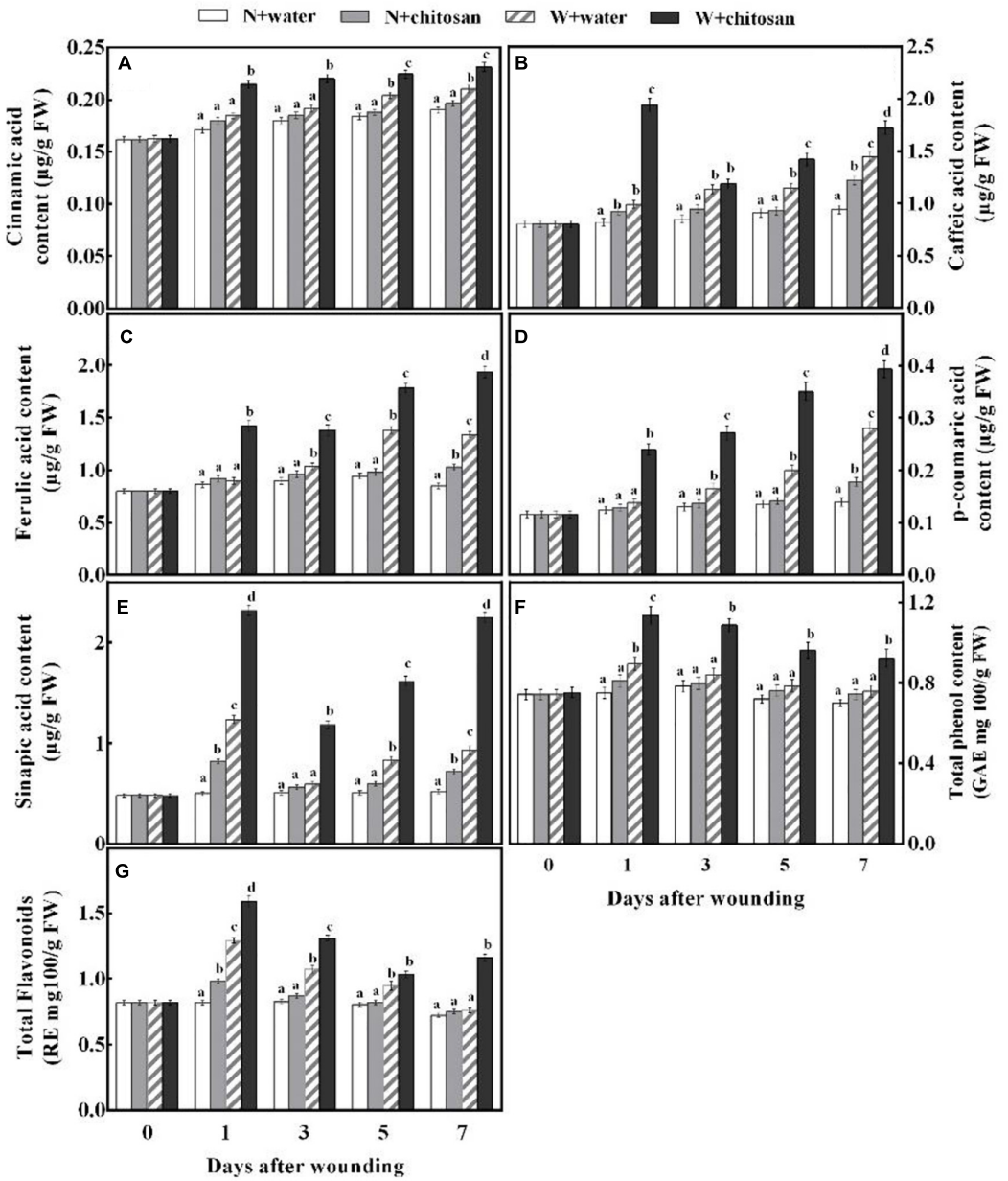

FIGURE 4 | Effect of chitosan treatment on contents of cinnamic acid **(A)**, caffeic acid **(B)**, ferulic acid **(C)**, *p*-coumaric acid **(D)**, sinapic acid **(E)**, total phenols **(F)**, and total flavonoids **(G)**. Non-wounded and treated with sterile water (N + water), non-wounded and treated with chitosan (N + chitosan), wounded and treated with sterile water (W + water), and wounded and treated with chitosan (W + chitosan). Vertical bars indicate standard error of means. Alphabets indicate significant differences ($p < 0.05$).

synthase and stilbene synthase (Waki et al., 2020). In the present study, wounded fruits increased the activities of PAL, C4H, 4CL, CCR, and CAD (**Figure 3**). However, wounded fruits treated with chitosan had higher PAL, C4H, 4CL, CCR, and CAD activities as well as cinnamic acid, *p*-coumaric acid, caffeic acid, ferulic acid, sinapic acid, flavonoids, and total phenol contents compared with the control, respectively (**Figures 3**, **4**). The current results agree with the work done by Li et al. (2021), where chitosan preharvest spraying increased the synthesis of cinnamic acid, *p*-coumaric acid, caffeic acid, ferulic acid, total phenol, and flavonoid contents at the wound site of harvested muskmelon by eliciting PAL and C4H activities. Chitosan is an elicitor that induces oxygen burst for the synthesis of H_2O_2 at the early stage of stress; however, the H_2O_2 induces PAL activity (Fooladi vanda et al., 2019). According to Lin et al. (2005), chitosan treatment increases the biosynthesis of signal molecules such as H_2O_2, JA, and SA by inducing the octadecanoid pathway to elicit PAL activity in rice cells. Furthermore, chitosan stimulates

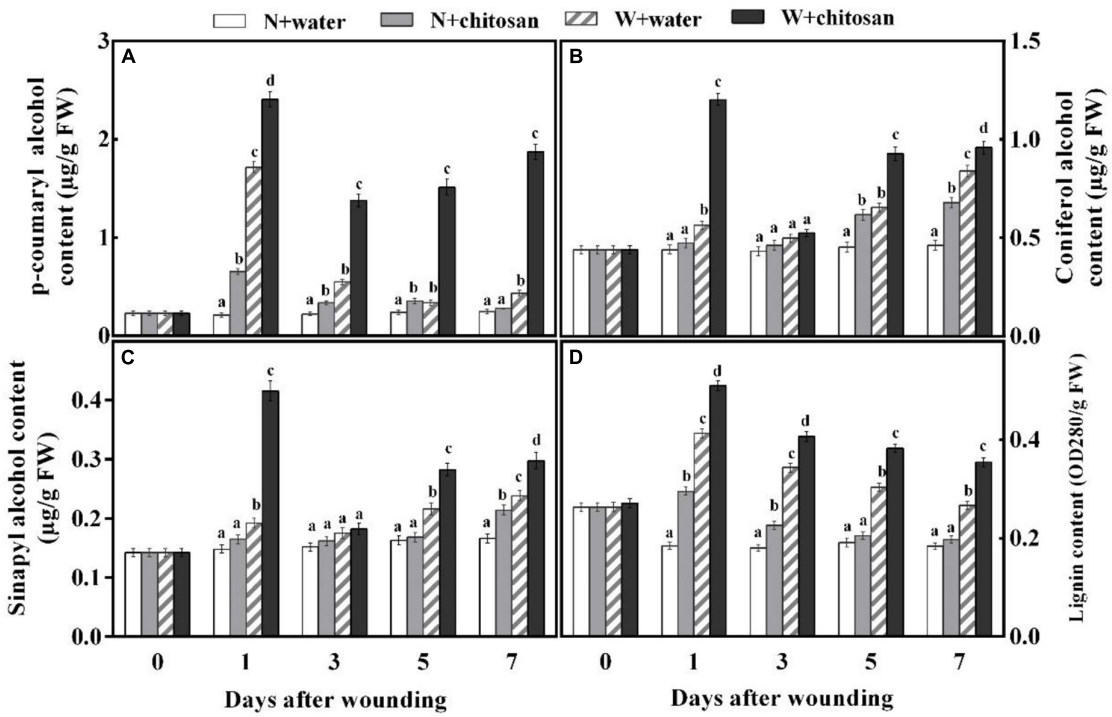

FIGURE 5 | Effect of chitosan treatment on contents of *p*-coumaryl alcohol **(A)**, coniferyl alcohol **(B)**, sinapyl alcohol **(C)**, and lignin **(D)**. Non-wounded and treated with sterile water (N + water), non-wounded and treated with chitosan (N + chitosan), wounded and treated with sterile water (W + water), and wounded and treated with chitosan (W + chitosan). Vertical bars indicate standard error of means. Alphabets indicate significant differences ($p < 0.05$).

defense at the transcriptional level by inducing *VvLOX*, *VvCOI1*, *VvAOC*, and *VvAOS* genes to increase the synthesis of H_2O_2, JA, SA, ET, and abscisic acid in grapes and strawberries to promote the synthesis of phenolic compounds (Peian et al., 2021). Flavonoids and some phenolic acids have a direct effect on pathogens by acting as phytoalexins to restrict mycelium and spore germination (Zhang et al., 2020). Lignin is considered an essential healing structure to strengthen cell walls in the scope of fruit wound healing (Xie et al., 2018). Monolignins (*p*-coumaryl alcohol, coniferyl alcohol, and sinapyl alcohol) are polymerized into *p*-hydroxyphenyl lignin, guaiacol lignin, and syringyl lignin linked by ether bonds into a structure known as polymer lignin, which is strong enough to prevent pathogen invasion (Yang et al., 2020; Zhu et al., 2021). Moreover, lignin accumulation is known to limit water evaporation and restrict pathogen infections (Xue et al., 2019). Our results show that chitosan treatment enhanced the synthesis of *p*-coumaryl alcohol, coniferyl alcohol, and sinapyl alcohol, which accumulated into lignin (**Figure 5**). Similarly, Zhao et al. (2018) reported that chitosan stimulated the accumulation of lignin at the fruit wound site. POD is involved in the polymerization of cinnamyl alcohols to form SPP and lignin *via* the POD-mediated free radical coupling process during lignification in the presence of H_2O_2 (Yang et al., 2020). Therefore, high H_2O_2 content by chitosan in this study not only induces PAL but also activates POD in the oxidative cross-linking between substrates for lignification. The results of our study agree with that of Zhao et al. (2018) and Li et al. (2021), who reported that chitosan elicits enzymes to promote healing of wounds by lignin accumulation in muskmelon and citrus. Thus, it is suggested that chitosan treatment may promote the phenylpropanoid pathway by inducing the synthesis of signal molecules pathways at the fruit's wound site to enhance the activities of enzymes and the synthesis of phenol compounds and lignin.

Polyphenol oxidase catalyzes the oxidation of tyrosine to quinones, which have stronger defensive power (Yan et al., 2018). Wounded fruits increased PPO activity. Moreover, our results show that wounded fruits treated with chitosan further increased the activity of PPO (**Figure 6A**). The activity of PPO not only induces resistance but is also the main cause of enzymatic browning in the presence of phenolic compounds (Xu et al., 2020). The phenolic compounds produced by the phenylpropanoid pathway are further catalyzed by PPO to produce quinones, causing browning. Therefore, the high accumulation of phenols and higher PPO activity in this present study led to the production of more quinones and enzymatic browning. Enzymatic browning reactions lead to the formation of water-soluble brown, gray, and black color pigments. The a^* and b^* values increased, whereas the L^* values decreased in this study (**Figure 6**), indicating a transition from white to black or brown. Similarly, Pilon et al. (2015) reported that chitosan activated browning in apples by the rapid activation of PPO. We, therefore, infer that chitosan first elicited the phenylpropanoid pathway to produce more phenol compounds and enhanced

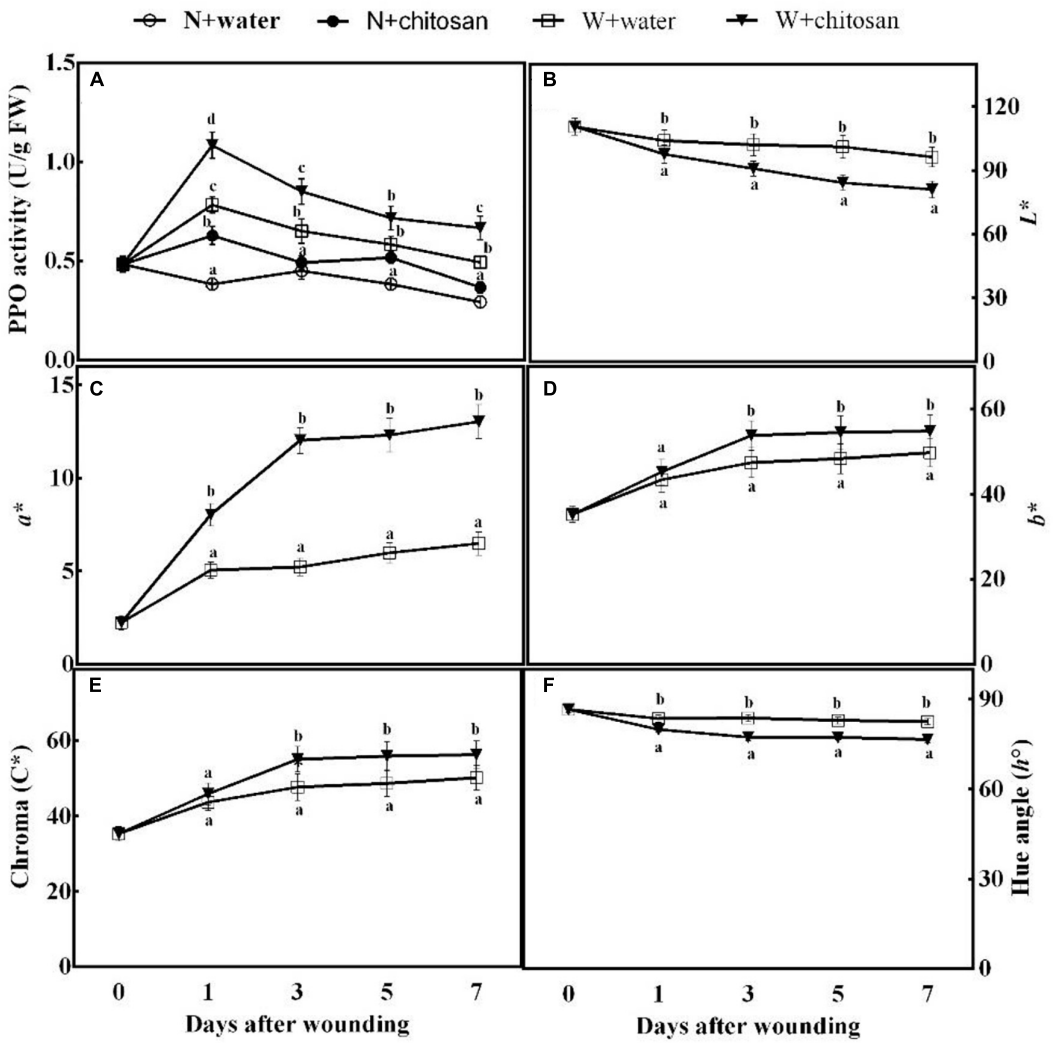

FIGURE 6 | Effect of chitosan treatment on PPO activity **(A)** and *L** **(B)**, *a** **(C)**, *b** **(D)**, Chroma *C** **(E)**, and hue angle *h*° **(F)**. Non-wounded and treated with sterile water (N + water), non-wounded and treated with chitosan (N + chitosan), wounded and treated with sterile water (W + water), and wounded and treated with chitosan (W + chitosan). Vertical bars indicate standard error of means. Alphabets indicate significant differences ($p < 0.05$).

PPO activity to stimulate the oxidation of phenols to quinones, causing color change (brown pigmentation) at the wound surface of fruits. Moreover, the quinones have a defense reaction against fungi (Xu et al., 2020), that can contribute to the reduction in disease (**Figure 6B**).

CONCLUSION

Chitosan treatment significantly elicited the activities of PAL, C4H, 4CL, CCR, and CAD and promoted the synthesis of cinnamic acid, ferulic acid, caffeic acid, *p*-coumaric acid, sinapic acid, *p*-coumaryl alcohol, coniferyl alcohol, and sinapyl alcohol, as well as total phenols, flavonoids, and lignin at the wounds of apples. Again, chitosan activated PPO activity, which stimulated enzymatic browning at fruit wounds. Moreover, the accumulation of phenolics and lignin polymer at wound surface prevented excessive water loss fruits and reduced disease index of *P. expansum* inoculated fruits. The findings in this study will add up knowledge in the scope of fruit wound healing and effective agricultural use of chitosan, considering its safe, edible, biodegradable, and non-toxic.

DATA AVAILABILITY STATEMENT

The raw data supporting the conclusions of this article will be made available by the authors, without undue reservation.

AUTHOR CONTRIBUTIONS

SA, SX, and RO designed the experimental setup, performed the experiments and analyzed the data. SA wrote the major part of

the article. YB designed the experiments, conceived the idea, and revised the article. YB, FK-A, YZ, and DP conceived the idea and revised the manuscript. All authors have read and agreed to the published version of the manuscript.

FUNDING

This research work was financed by the China–Israel (National Natural Science Foundation of China–Israel Science Foundation) project of the National Natural Science Foundation of China (31861143046 and 31660476).

ACKNOWLEDGMENTS

We would like to thank the China–Israel (National Natural Science Foundation of China–Israel Science Foundation) project of the National Natural Science Foundation of China.

REFERENCES

Coqueiro, D. S. O., de Souza, A. A., Takita, M. A., Rodrigues, C. M., Kishi, L. T., and Machado, M. A. (2015). Transcriptional profile of sweet orange in response to chitosan and salicylic acid. *BMC Genomics* 16:288. doi: 10.1186/s12864-015-1440-5

Dea, S., Brecht, J. K., Nunes, M. C. N., and Baldwin, E. A. (2010). Quality of fresh-cut "Kent" mango slices prepared from hot water or non-hot water-treated fruit. *Posthar. Biol. Technol.* 56, 171–180. doi: 10.1016/j.postharvbio.2010.01.007

Deepmala, K., Hemantaranjan, A., Singh, B., and Nishant Bhanu, A. (2014). A future perspective in crop protection: chitosan and its oligosaccharides. *Adv. Plants Agric. Res.* 1, 23–30. doi: 10.15406/apar.2014.01.00006

Fooladi vanda, G., Shabani, L., and Razavizadeh, R. (2019). Chitosan enhances rosmarinic acid production in shoot cultures of *Melissa officinalis* L. through the induction of methyl jasmonate. *Bot. Stud.* 60:26. doi: 10.1186/s40529-019-0274-x

Gayed, A. A. N. A., Shaarawi, S. A. M. A., Elkhishen, M. A., and Elsherbini, N. R. M. (2017). Pre-harvest application of calcium chloride and chitosan on fruit quality and storability of 'Early Swelling' peach during cold storage. *Ciênc. Agrotecnol.* 41, 220–231. doi: 10.1590/1413-70542017412005917

Gong, D., Bi, Y., Jiang, H., Xue, S., Wang, Z., Li, Y., et al. (2019). A comparison of postharvest physiology, quality and volatile compounds of 'Fuji' and 'Delicious' apples inoculated with *Penicillium expansum*. *Posthar. Biol. Technol.* 150, 95–104. doi: 10.1016/j.postharvbio.2018.12.018

Gu, N., Zhang, X., Gu, X., Zhao, L., Godana, E. A., Xu, M., et al. (2021). Transcriptomic and proteomic analysis of the mechanisms involved in enhanced disease resistance of strawberries induced by *Rhodotorula mucilaginosa* cultured with chitosan. *Posthar. Biol. Technol.* 172:111355. doi: 10.1016/j.postharvbio.2020.111355

Hammerschmidt, R. (1984). Rapid deposition of lignin in potato tuber tissue as a response to fungi non-pathogenic on potato. *Physiol. Plant Pathol.* 24, 33–42. doi: 10.1016/0048-4059(84)90071-7

Hidangmayum, A., Dwivedi, P., Katiyar, D., and Hemantaranjan, A. (2019). Application of chitosan on plant responses with special reference to abiotic stress. *Physiol. Mol. Biol. Plants* 25, 313–326. doi: 10.1007/s12298-018-0633-1

Koukol, J., and Conn, E. E. (1961). The metabolism of aromatic compounds in higher plants. *J. Biol. Chem.* 236, 2692–2698. doi: 10.1016/s0021-9258(19)61721-7

Li, H., Wang, Y., Liu, F., Yang, Y., Wu, Z., Cai, H., et al. (2015). Effects of chitosan on control of postharvest blue mold decay of apple fruit and the possible mechanisms involved. *Sci. Hortic.* 186, 77–83. doi: 10.1016/j.scienta.2015.02.014

Li, Z., Xue, S., Xu, X., Wang, B., Zheng, X., Li, B., et al. (2021). Preharvest multiple sprays with chitosan accelerate the deposition of suberin poly phenolic at wound sites of harvested muskmelons. *Posthar. Biol. Technol.* 179:111565. doi: 10.1016/j.postharvbio.2021.111565

Lin, W., Hu, X., Zhang, W., John Rogers, W., and Cai, W. (2005). Hydrogen peroxide mediates defense responses induced by chitosans of different molecular weights in rice. *J. Plant Physiol.* 162, 937–944. doi: 10.1016/j.jplph.2004.10.003

Liu, Y., Ge, Y., Bi, Y., Li, C., Deng, H., and Dong, B. (2014). Effect of postharvest acibenzolar-S-methyl dipping on phenylpropanoid pathway metabolism in muskmelon (*Cucumis melo* L.) fruits. *Sci. Hortic.* 168, 113–119. doi: 10.1016/j.scienta.2014.01.030

Lu, H., Lu, L., Zeng, L., Fu, D., Xiang, H., Yu, T., et al. (2014). Effect of chitin on the antagonistic activity of *Rhodosporidium paludigenum* against *Penicillium expansum* in apple fruit. *Posthar. Biol. Technol.* 92, 9–15. doi: 10.1016/j.postharvbio.2014.01.009

Pasquariello, M. S., Di Patre, D., Mastrobuoni, F., Zampella, L., Scortichini, M., and Petriccione, M. (2015). Influence of postharvest chitosan treatment on enzymatic browning and antioxidant enzyme activity in sweet cherry fruit. *Posthar. Biol. Technol.* 109, 45–56. doi: 10.1016/j.postharvbio.2015.06.007

Peian, Z., Haifeng, J., Peijie, G., Sadeghnezhad, E., Qianqian, P., Tianyu, D., et al. (2021). Chitosan induces jasmonic acid production leading to resistance of ripened fruit against *Botrytis cinerea* infection. *Food Chem.* 337:127772. doi: 10.1016/j.foodchem.2020.127772

Petriccione, M., Mastrobuoni, F., Pasquariello, M. S., Zampella, L., Nobis, E., Capriolo, G., et al. (2015). Effect of chitosan coating on the postharvest quality and antioxidant enzyme system response of strawberry fruit during cold storage. *Foods* 4, 501–523. doi: 10.3390/foods4040501

Pilon, L., Spricigo, P. C., Miranda, M., de Moura, M. R., Assis, O. B. G., Mattoso, L. H. C., et al. (2015). Chitosan nanoparticle coatings reduce microbial growth on fresh-cut apples while not affecting quality attributes. *Int. J. Food Sci. Technol.* 50, 440–448. doi: 10.1111/ijfs.12616

Plainsirichai, M., Leelaphatthanapanich, S., and Wongsachai, N. (2014). Effect of chitosan on the quality of rose apples (*Syzygium agueum* Alston) cv. tabtim chan stored at an ambient temperature. *APCBEE Procedia* 8, 317–322. doi: 10.1016/j.apcbee.2014.03.047

Romanazzi, G., Feliziani, E., Baños, S. B., and Sivakumar, D. (2017). Shelf life extension of fresh fruit and vegetables by chitosan treatment. *Crit. Rev. Food Sci. Nutr.* 57, 579–601. doi: 10.1080/10408398.2014.900474

Scalbert, A., Monties, B., and Janin, G. (1989). Tannins in wood: comparison of different estimation methods. *J. Agric. Food Chem.* 37, 1324–1329. doi: 10.1021/jf00089a026

Silva, R., and Pighinelli, L. (2017). Application of chitosan and buriti oil (*Mauritia Flexuosa* L.) in skin wound healing. *J. Appl. Biotechnol. Bioeng.* 3, 272–279. doi: 10.15406/jabb.2017.03.00056

Varasteh, F., Arzani, K., Barzegar, M., and Zamani, Z. (2017). Pomegranate (*Punica granatum* L.) fruit storability improvement using pre-storage chitosan coating technique. *J. Agric. Sci. Technol.* 19, 389–400.

Venisse, J. S., Malnoy, M., Faize, M., Paulin, J. P., and Brisset, M. N. (2002). Modulation of defense responses of *Malus* spp. during compatible and incompatible interactions with *Erwinia amylovora*. *Mol. Plant Microbe Interact.* 15, 1204–1212. doi: 10.1094/MPMI.2002.15.12.1204

Waki, T., Mameda, R., Nakano, T., Yamada, S., Terashita, M., Ito, K., et al. (2020). A conserved strategy of chalcone isomerase-like protein to rectify promiscuous chalcone synthase specificity. *Nat. Commun.* 11:870. doi: 10.1038/s41467-020-14558-9

Wang, C., Chen, L., Peng, C., Shang, X., and Lv, X. (2020). Postharvest benzothiazole treatment enhances healing in mechanically damaged sweet potato by activating the phenylpropanoid metabolism. *J. Sci. Food Agric.* 100, 3394–3400. doi: 10.1002/jsfa.10373

Wang, N., Jiang, S., Zhang, Z., Fang, H., Xu, H., Wang, Y., et al. (2018). *Malus sieversii*: the origin, flavonoid synthesis mechanism, and breeding of red-skinned and red- fleshed apples. *Hortic. Res.* 5:70. doi: 10.1038/s41438-018-0084-4

Xie, M., Zhang, J., Tschaplinski, T. J., Tuskan, G. A., Chen, J. G., and Muchero, W. (2018). Regulation of lignin biosynthesis and its role in growth-defense tradeoffs. *Front. Plant Sci.* 9:1427. doi: 10.3389/fpls.2018.01427

Xu, J., Zhou, L., Miao, J., Yu, W., Zou, L., Zhou, W., et al. (2020). Effect of cinnamon essential oil nanoemulsion combined with ascorbic acid on enzymatic browning of cloudy apple juice. *Food Bioprocess Technol.* 13, 860–870. doi: 10.1007/s11947-020-02443-8

Xue, H., Bi, Y., Prusky, D., Raza, H., Zhang, R., Zhang, S., et al. (2019). The mechanism of induced resistance against *Fusarium* dry rot in potato tubers by the T-2 toxin. *Posthar. Biol. Technol.* 153, 69–78. doi: 10.1016/j.postharvbio.2019.03.021

Yan, J., Deng, Y., Yu, J., Zhang, Y., and Chi, D. (2018). A study on JA- and BTH-induced resistance of *Rosa rugosa* 'Plena' to powdery mildew (*Sphaerotheca pannosa*). *J. For. Res.* 29, 823–831. doi: 10.1007/s11676-017-0481-9

Yang, R., Han, Y., Han, Z., Ackah, S., Li, Z., Bi, Y., et al. (2020). Hot water dipping stimulated wound healing of potato tubers. *Posthar. Biol. Technol.* 167:111245. doi: 10.1016/j.postharvbio.2020.111245

Zeng, K., Deng, Y., Ming, J., and Deng, L. (2010). Induction of disease resistance and ROS metabolism in navel oranges by chitosan. *Sci. Hortic.* 126, 223–228. doi: 10.1016/j.scienta.2010.07.017

Zhang, D., Wang, H., Hu, Y., and Liu, Y. (2015). Chitosan controls postharvest decay on cherry tomato fruit possibly via the mitogen-activated protein kinase signaling pathway. *J. Agric. Food Chem.* 63, 7399–7404. doi: 10.1021/acs.jafc.5b01566

Zhang, X., Zong, Y., Li, Z., Yang, R., Li, Z., Bi, Y., et al. (2020). Postharvest *Pichia guilliermondii* treatment promotes wound healing of apple fruits. *Posthar. Biol. Technol.* 167:111228. doi: 10.1016/j.postharvbio.2020.111228

Zhao, H., Dong, J., Lu, J., Chen, J., Li, Y., Shan, L., et al. (2006). Effects of extraction solvent mixtures on antioxidant activity evaluation and their extraction capacity and selectivity for free phenolic compounds in barley (*Hordeum vulgare* L.). *J. Agric. Food Chem.* 54, 7277–7286.

Zhao, Y., Deng, L., Zhou, Y., Ming, J., Yao, S., and Zeng, K. (2018). Wound healing in citrus fruit is promoted by chitosan and *Pichia membranaefaciens* as a resistance mechanism against *Colletotrichum gloeosporioides*. *Posthar. Biol. Technol.* 145, 134–143. doi: 10.1016/j.postharvbio.2018.07.007

Zhu, Y., Zong, Y., Liang, W., Sabina, A., Chai, X., Li, Y., et al. (2021). β- Aminobutyric acid treatment accelerates the deposition of suberin polyphenolic and lignin at wound sites of potato tubers during healing. *Posthar. Biol. Technol.* 179:111566. doi: 10.1016/j.postharvbio.2021.111566

Conflict of Interest: The authors declare that the research was conducted in the absence of any commercial or financial relationships that could be construed as a potential conflict of interest.

Publisher's Note: All claims expressed in this article are solely those of the authors and do not necessarily represent those of their affiliated organizations, or those of the publisher, the editors and the reviewers. Any product that may be evaluated in this article, or claim that may be made by its manufacturer, is not guaranteed or endorsed by the publisher.

frontiers in Microbiology

ORIGINAL RESEARCH
published: 03 March 2022
doi: 10.3389/fmicb.2021.802887

Endophytic Bacterium *Serratia plymuthica* From Chinese Leek Suppressed Apple Ring Rot on Postharvest Apple Fruit

Meng Sun[1,2,3,4], *Junping Liu*[1,2,3,4], *Jinghui Li*[1,2,3,4] *and Yonghong Huang*[1,2,3,4]*

[1] College of Horticulture, Qingdao Agricultural University, Qingdao, China, [2] Laboratory of Quality and Safety Risk Assessment for Fruit (Qingdao), Ministry of Agriculture and Rural Affairs, Qingdao, China, [3] National Technology Centre for Whole Process Quality Control of FSEN Horticultural Products (Qingdao), Qingdao, China, [4] Qingdao Key Laboratory of Modern Agriculture Quality and Safety Engineering, Qingdao, China

Apple ring rot caused by *Botryosphaeria dothidea* is an economically significant plant disease that spreads across the apple production areas in China. The pathogen infects apple fruits during the growing season and results in postharvest fruits rot during storage, which brings about a huge loss to plant growers. The study demonstrated that an endophytic bacterium *Serratia plymuthica* isolated from Chinese leek (*Allium tuberosum*) significantly suppressed the mycelial growth, severely damaging the typical morphology of *B. dothidea*, and exerted a high inhibition of 84.64% against apple ring rot on postharvest apple fruit. Furthermore, *S. plymuthica* significantly reduced the titratable acidity (TA) content, enhanced the soluble sugar (SS) content, vitamin C content, and SS/TA ratio, and maintained the firmness of the fruits. Furthermore, comparing the transcriptomes of the control and the *S. plymuthica* treated mycelia revealed that *S. plymuthica* significantly altered the expressions of genes related to membrane (GO:0016020), catalytic activity (GO:0003824), oxidation-reduction process (GO:0055114), and metabolism pathways, including tyrosine metabolism (ko00280), glycolysis/gluconeogenesis (ko00010), and glycerolipid metabolism (ko00561). The present study provided a possible way to control apple ring rot on postharvest fruit and a solid foundation for further exploring the underlying molecular mechanism.

Keywords: ***Serratia plymuthica*, *Botryosphaeria dothidea*, fruit quality, biocontrol, RNA-seq**

OPEN ACCESS

Edited by:
Sergio Ruffo Roberto, State University of Londrina, Brazil

Reviewed by:
Pingliang Li, Qingdao Agricultural University, China
Renato Vasconcelos Botelho, State University of Midwest Paraná, Brazil
Sozan El-Abeid, Agricultural Research Center, Egypt

***Correspondence:**
Yonghong Huang
gstshh@126.com

Specialty section:
This article was submitted to Food Microbiology, a section of the journal Frontiers in Microbiology

Received: *27 October 2021*
Accepted: *21 December 2021*
Published: *03 March 2022*

Citation:
Sun M, Liu J, Li J and Huang Y (2022) Endophytic Bacterium Serratia plymuthica From Chinese Leek Suppressed Apple Ring Rot on Postharvest Apple Fruit. Front. Microbiol. 12:802887. doi: 10.3389/fmicb.2021.802887

INTRODUCTION

Apple ring rot caused by *Botryosphaeria dothidea* is one of the devastating diseases spreading over China's central apple production region (Dong et al., 2021). *B. dothidea* infects branches, trunk, or fruits *via* lenticel or wound and results in warts in shoots and trunk or lesions in ripened fruits. As the disease progresses, it causes the infected trunk and shoots to die or fruits to rot (Bai et al., 2015). According to a previous report in 2009, the average occurrence of the apple ring rot is as high as 77.6% in 88 apple orchards across seven main apple production areas in China (Guo et al., 2009). Thus, the disease has been seriously threatening the healthy development of apple production in China. In addition, besides apple trees, *B. dothidea* can infect other essential fruit trees, such as pear (*Pyrus bretschneideri* Rehd.) (Sun et al., 2020), pomegranate (*Punica granatum* L.)

(Gu et al., 2020), apricot (*Prunus armeniaca* L.) (Huang et al., 2019b), kiwifruit (*Actinidia chinensis*) (Wang et al., 2021), sweet cherry (*Prunus avium* L.) (Zhang et al., 2019), and mulberry (*Morus alba* L.) (Huang et al., 2019a). Therefore, it is particularly important to develop ways to prevent and control the disease caused by *B. dothidea*.

Presently, chemical fungicides are still the most widely used methods to control apple ring rot, but it has hazards such as pollution to the environment and harm to human health and animals. Researchers have found that adopting antagonistic microbes is an efficient, safer, and environment-friendly way to control the disease. Previous studies show that *Bacillus amyloliquefaciens* PG12 (Chen et al., 2016), *Bacillus subtilis* 9407 (Fan et al., 2017), *Streptomyces rochei* A-1 (Zhang et al., 2016), *Streptomyces lavendulae* Xjy (Gao et al., 2016), *Paenibacillus polymyxa* APEC136 (Kim et al., 2016), *Bacillus atrophaeus* J-1 (Mu et al., 2020), and *Meyerozyma guilliermondii* Y-1 (Huang et al., 2021) efficiently suppress *B. dothidea* growth and reduce apple ring rot occurrence on fruits or apple trees.

Our previous study shows Chinese leek (*Allium tuberosum*) extract significantly suppresses the apple ring rot on apple shoots and fruits (Zhao et al., 2017) and reduces the occurrence of banana fusarium wilt caused by *Fusarium oxysporum* f. sp. *cubense* race 4 (*Foc*4) (Huang et al., 2012). Later, we isolated an endophytic bacterium from Chinese leek, identified as *S. plymuthica,* using 16 sRNA (Müller et al., 2013; Adam et al., 2016). Previous studies show that *S. plymuthica* has potent antifungal activity against several plant pathogens. *S. plymuthica* exerts striking inhibition against root rot on cucumber plant caused by *Pythium ultimum* (Benhamou et al., 2000). *S. plymuthica* strains IC1270 and IC14 control *Penicillium digitatum* (green mold) or *Penicillium italicum* (blue mold) on orange (Meziane et al., 2006). *S. plymuthica* A30 reduces blackleg development by 58.5% and transmission to tuber progeny as latent infection by 47-75% (Hadizadeh et al., 2019). *S. plymuthica* Sneb2001 shows a high lethal effect on the second-stage juveniles of *Meloidogyne incognita* (Zhao et al., 2021). However, to our knowledge, there are no reports concerning the effects of *S. plymuthica* on *B. dothidea*. Therefore, in the present study, we attempt to determine whether the endophytic bacterium *S. plymuthica* inhibits the apple ring rot on postharvest fruits caused by *B. dothidea* and preliminarily explore the underlying molecular mechanism, trying to provide a possible way to control apple ring rot.

MATERIALS AND METHODS

Experimental Materials

The apple fruit (*Malus domestica* Borkh. cv. Red Fuji) used in the experiments were purchased in the local supermarkets. The fruit with uniform sizes, no disease spots, and no mechanical damages was selected for the experiments. The *S. plymuthica* and the *B. dothidea* were kept on nutrient agar (NA) medium and potato dextrose agar (PDA) medium in the laboratory, respectively.

Determination of the Inhibition of *Serratia plymuthica* on the Growth of *Botryosphaeria dothidea*

PDA medium (20 ml) was poured into a 9-cm-diameter Petri dish. One fungal mycelium disc 0.5 cm in diameter was inoculated at 1/3 of Petri dish diameter. *S. plymuthica* culture (50 μl) (OD_{600} = 0.6) was added at 2/3 of Petri dish diameter. Sterilized water (50 μl) was used as untreated control. All the Petri dishes were inverted and incubated at 28°C for 3 days in the dark. The fungus mycelium diameters were measured every day to evaluate the inhibition of *S. plymuthica* on *B. dothidea* growth. The experiments were repeated three times, and five replicates were included for each sample in each experiment.

Observation of *Botryosphaeria dothidea* Mycelial Morphology Treated With *Serratia plymuthica*

A layer of cellophane was laid on a newly prepared PDA medium. One fungal mycelium disc (0.5 cm in diameter) was inoculated on the cellophane. *S. plymuthica* culture (50 μl) (OD_{600} = 0.6) was added onto a small piece of filter paper (1 × 1 cm), 1 cm away from the mycelium disc, over the cellophane. The fungal mycelium disc without *S. plymuthica* was used as an untreated control. The Petri dishes were inverted and incubated at 28°C in the dark. Twenty-four hours later, the cellophane with new mycelium was taken out from the Petri dishes, cut into 1 cm × 1 cm squares, and was observed under a microscope (EVOS Auto2, Thermo Fisher Scientific, United States).

The Inhibition of *Serratia plymuthica* Against Apple Ring Rot on Fruits Caused by *Botryosphaeria dothidea*

The apple fruits with uniform size, healthy, no mechanical injury were selected as experimental materials. After the fruit was sterilized with 70% ethanol, a tiny cavity (0.5 cm in diameter and 0.5 cm in depth) was made at the equator of the sterilized fruits using a sterilized puncher. Then, 50 μl *S. plymuthica* (OD_{600} = 0.6) was added into the small cavity. Then, 1 h later, one fungal mycelium disc (0.5 cm in diameter) was inoculated into the small cavity (*S. plymuthica* treated). The nutrient broth (NB) medium was used as a control. All the treated and the control fruits were placed in an incubator at 28°C for 5 days. The disease symptoms were recorded every day to evaluate the inhibition of *S. plymuthica* against apple ring rot caused by *B. dothidea*. The experiments were repeated three times, and 12 replicates were included for each sample in each experiment.

Effects of *Serratia plymuthica* on the Fruit Qualities

To determine whether *S. plymuthica* affected apple fruit quality, we designed four treatments in the experiment. (1) The apple fruits were soaked in PDB medium for 15 min (CK). (2) The apple fruits were soaked in *B. dothidea* culture for 15 min (Bd). (3) The apple fruits were soaked in *S. plymuthica* culture (OD_{600} = 0.6) for 15 min (Sp). (4) The apple fruits were firstly soaked in

S. plymuthica culture (OD_{600} = 0.6) culture for 15 min, and then they were aired at room for 1 h followed by soaking in *B. dothidea* culture for 15 min (Sp+Bd). All the fruits were set in an incubator at 28°C. Then, at 1, 3, 5, 7, and 9 days, fruits were sampled and peeled. Fruit firmness was measured at the fruit's equator with the FHM-5 fruit hardness tester (Takemura Electric Works Ltd., Tokyo, Japan). The pulp at the equator of the fruit was sampled to determine other internal quality indexes, including total soluble solid (TSS), soluble sugar (SS), titratable acidity (TA), vitamin C (VC), total soluble solid/titrable acidity (TSS/TA), and soluble sugar/titrable acidity (SS/TA). TSS content was determined using a PAL-1 type sugar concentration detector (ATAGO, Japan). SS content was determined using the anthrone colorimetric method. The TA content was determined by NaOH titration. VC content was determined by 2, 6-dichloroindophenol colorimetric (Yang et al., 2020). Three replicates were included for each sample in each sampling time point. The area-under-curve (AUC) of the internal quality indexes was calculated as the formula (Huang et al., 2012).

$$\mathrm{AUC} = \sum_{i=1}^{n-1} \left[\frac{X_{i+1} + X_i}{2} \right] (t_{i+1} - t_i) \quad (1)$$

X is fruit internal quality indexes. n is the number of evaluations, and (t_i-$_1$-t_i) is the time interval (days) between two consecutive evaluations.

RNA-Seq Analysis

A layer of sterilized cellophane was placed on the newly prepared PDA medium, on the center of which a mycelium disc (0.5 cm in diameter) of *B. dothidea* was inoculated. The Petri dish was sealed, inverted, and incubated at 28°C in the dark for 2 days. *S. plymuthica* culture (300 μl) (OD_{600} = 0.6) was sprayed on the mycelia. Sterilized water (300 μl) was used as control. The Petri dishes continued to be incubated in the same condition. Finally, 6 and 12 h later, the *S. plymuthica*-treated and the control mycelia were sampled for RNA-seq analysis and qRT-PCR verification.

Total RNA was extracted from *B. dothidea* mycelia using RNAprep Pure Plant Kit (Polysaccharides and Polyphenolics-rich) (Tiangen Biotech, Beijing). The quality and integrity of RNA samples were determined using a NanoDrop-2000 Spectrophotometer (Thermo Fisher Scientific, United States), agarose gel electrophoresis, and an Agilent Bioanalyzer 2100 bioanalyzer (Agilent Technologies, United States). The mRNA was isolated and fragmented into short segments (200–300 nt). The first-strand cDNA was generated by using the random hexamer-primed reverse transcription. Subsequently, the second strand was synthesized using RNase H and DNA polymerase I. Double-strand cDNA was purified and end-repaired, added with poly (A) tail, and ligated to sequencing linkers. The fragments were purified and then enriched by using PCR amplification to construct the final cDNA library. The library quality was detected with the Agilent Bioanalyzer 2100 bioanalyzer (Agilent Technologies, United States). The cDNA library was then sequenced *via* Illumina HiSeq^{TM} 2500. The data were deposited at the National Center for Biotechnology Information (accession PRJNA727902).

After sequencing, the low-quality reads and adapter sequences were removed from the raw data using Cutadapt (v2.10) (Martin, 2000). Then, the high-quality clean data were mapped to the *B. dothidea* genome (ASM1150312v2) with TopHat 2.1.1 (Trapnell et al., 2009). Gene expression levels were quantified based on HTSeq (Anders et al., 2015), the values of which were normalized by FPKM (Fragments Per Kilo bases per Million fragments) method. The differentially expressed genes (DEGs) analysis was performed by DESeq (Wang et al., 2010) with a threshold of $|\log2foldchang| > 1$ and $P < 0.05$. The DEGs were functionally annotated by mapping to the Gene Ontology (GO) (Ashburner et al., 2000), Kyoto Encyclopedia of Genes and Genomes (KEGG) (Kanehisa et al., 2016). We defined GO terms and KEGG pathways with a q-value < 0.05 as significantly enriched.

Quantitative Real-Time PCR Verification

DEGs were randomly selected for quantitative real-time PCR (qRT-PCR) to validate the quality of the sequencing data. The selected genes were extracted from the *B. dothidea* genome (ASM1150312v2), and the special primers were designed at the Primer Premier 5.0 software (**Table 1**). The cDNA was synthesized using the HiScript® lll RT SuperMix for qPCR (+gDNA wiper) reverse transcription kit (Vazyme Biotech, Nanjing, CN). According to the instructions of the ChamQ^{TM} SYBR Color qPCR Master Mix kit (Vazyme Biotech, Nanjing, CN), the expressions of selected genes were analyzed by ABI7500 thermal cycler (Applied Biosystems, CA). The total reaction system was 10 μl, including 5 μl of 2 × ChamQ SYBR Color qPCR Master Mix, 0.2 μl of each primer, 0.2 μl of the 50 × ROX Reference Dye I, 1 μl of cDNA, and 3.4 μl of the ddH_2O. The reaction conditions were following: 94°C for 5 min, followed by 30 cycles of 94°C for 30 s and 60°C for 30 s, then 72°C for 30 s, and a final extension at 72°C for 10 min. Actin was used as the internal reference gene, and the relative expression was calculated by $2^{-\Delta\Delta CT}$ method (Livak and Schmittgen, 2001). Three biological replicates were set up in the experiment.

Statistical Analysis

Experimental data were analyzed using standard analysis of variance (ANOVA) followed by least significant difference tests ($P < 0.05$) using the software statistical analytical system (SAS 9.0). Standard errors were calculated for all mean values.

RESULTS

Serratia plymuthica Significantly Inhibited the Mycelial Growth of *Botryosphaeria dothidea*

The *B. dothidea* mycelium discs inoculated on the PDA medium without *S. plymuthica* (control) began to grow on the first day and quickly expanded later. The mycelia covered the whole surface of the PDA medium after 3 day. But the *B. dothidea* mycelium discs treated with *S. plymuthica* grew more slowly than the control. Statistics showed the

mycelium diameters treated with *S. plymuthica* were 1.42, 3.83, and 3.93 cm at 1, 2, and 3 days, respectively, significantly smaller than those of the control. Compared to the control, *S. plymuthica* suppressed the growth of *B. dothidea* by 19.01% ($P = 0.0086$), 37.81% ($P < 0.0001$), and 52.50% ($P < 0.0001$) at 1, 2, and 3 days, respectively (**Figure 1A**). Furthermore, the

TABLE 1 | The qRT-PCR primers using in the study.

Gene	Forward primer sequence	Reverse primer sequence
BOTSDO06531	5′-ATGACCACACCACACTGCT-3′	5′-CTCCTTCTTCTGTTGCGACG-3′
BOTSDO00320	5′-AACAAACCGCTCGCTCAATC-3′	5′-CTGTTCTCCTCAATGCCGTG-3′
BOTSDO08455	5′-CGACGTCCTCCTCTACTTCC-3′	5′-GGCGTCTCGGTCCTACTG-3′
BOTSDO10612	5′-CAATGAGTCTCACCGCCATG-3′	5′-ACACAATTGACCGCGTTTCA-3′
BOTSDO00589	5′-TGCAATTCCTCACCCTCACC-3′	5′-GTTGTTGTGGCAGACGTAGG-3′
BOTSDO08313	5′-GCTTCAAGGCTTTCGAGGAC-3′	5′-TCGTACTGGTCCTTGTCACC-3′
BOTSDO02077	5′-CAAACCCTCACCATCCTCCT-3′	5′-CTGGATCAGGAAGGACAGCA-3′
BOTSDO04628	5′-CACTCCATCCTCTTCCTCCC-3′	5′-CGAGTTATCCCGCGAAATGG-3′
BOTSDO06884	5′-AAGAAGTTCCTCCAGCACGA-3′	5′-CATCCCACATAGCCGCATTC-3′
BOTSDO11898	5′-AATACGCCGCCAACATCTTC-3′	5′-CAGGTTGGAGACTAGGCGAA-3′
BOTSDO07469	5′-CTTCACCACCCTCCTCACC-3′	5′-TTCATGACGAAGCGGTTGAG-3′
BOTSDO08150	5′-GGTCTCCATCTTCCTTCGCT-3′	5′-CCAGATCAAGGAGGTGACGA-3′
BOTSDO13437	5′-CATTTCCTCCCTCAACGCAG-3′	5′-TCCCCTCTCCTTACTGCTCT-3′
BOTSDO01196	5′-GCTAGAGTCGAACGGGTACA-3′	5′-CGGGTCGACATCAATAGGGA-3′
BOTSDO11589	5′-CAAGGCTGCCACTGGAAAAT-3′	5′-CACGTCCAAAACAACCGGAT-3′
Actin	5′-GTTCAGACCGCCCTTTGCT-3′	5′-AGCCTTGCGACGGAACATA-3′

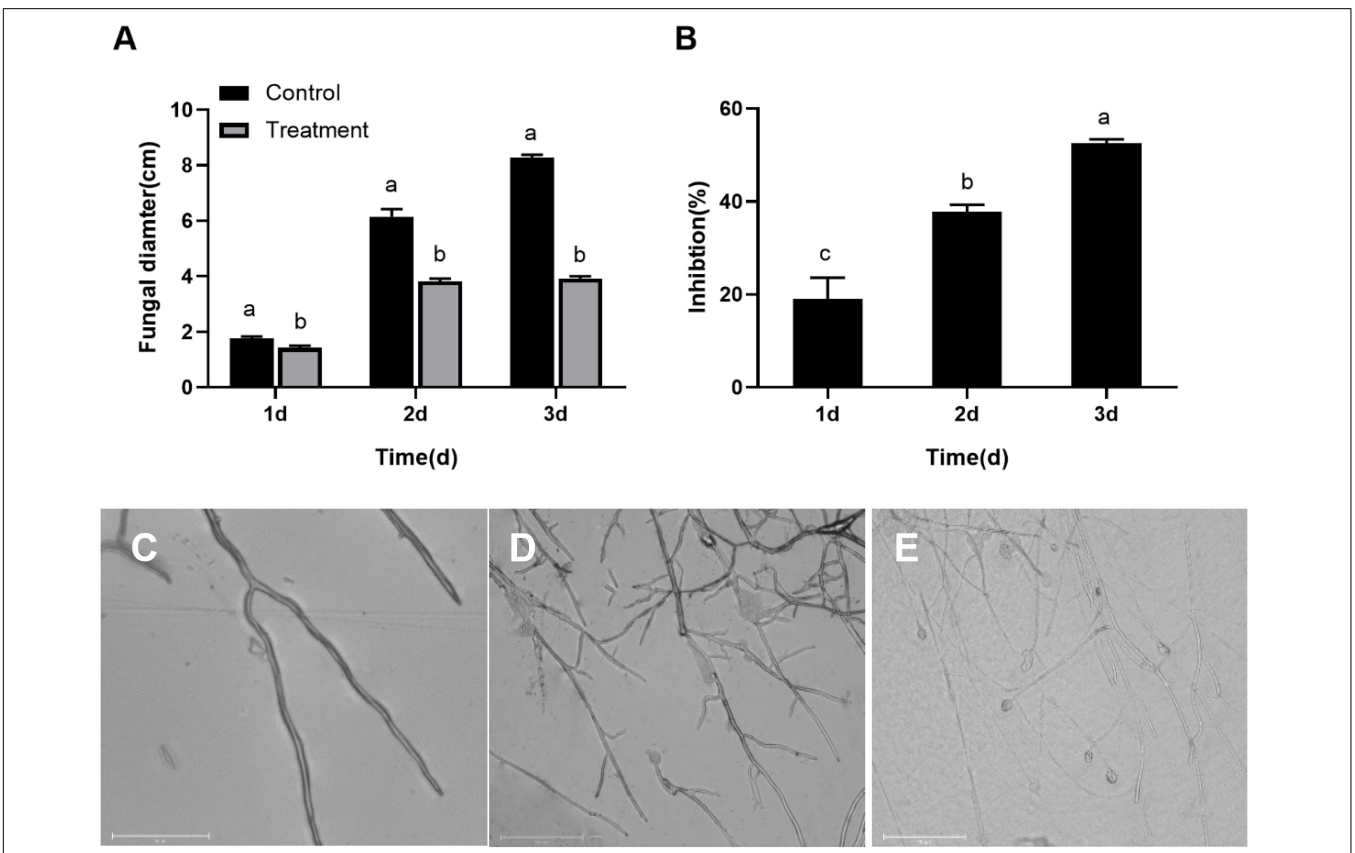

FIGURE 1 | *Serratia plymuthica* significantly inhibits the mycelial growth of *Botryosphaeria dothidea* **(A)**. The inhibition increases with the increase of the treatment time **(B)**. Compared to the untreated control **(C)**, *Serratia plymuthica* damages the mycelial morphology of *Botryosphaeria dothidea* **(D,E)**. Different lowercase letters indicate significant differences between treatments or different times ($P < 0.05$).

inhibition increased with the increase of the treatment time ($P < 0.0001$) (**Figure 1B**).

Serratia plymuthica Deformed the Typical Morphology of *Botryosphaeria dothidea* Mycelia

To identify whether *S. plymuthica* damaged the typical morphology of *B. dothidea* mycelia, we compared the control (**Figure 1C**) and the *S. plymuthica*-treated mycelia (**Figures 1D,E**). Under the microscope, the control mycelia had a smooth surface, with uniform sizes and fewer branches. But the *S. plymuthica*-treated mycelia showed abnormal morphology and became uneven in thickness. They showed more forks and swelled on the top end. In addition, some mycelia were so seriously damaged, resulting in a burst with the contents spilling out.

Serratia plymuthica Inhibited the Apple Ring Rot Occurrence on Fruits Caused by *Botryosphaeria dothidea*

All the *S. plymuthica*-treated and the untreated apple fruits showed slight disease symptoms at the inoculation sites 1 day later. But the disease spread at varying rates in the next few days. The disease spot diameter on the control fruit rapidly increased, almost as large as the height of the apple fruits 5 days later (**Figure 2A**). However, the disease symptom on the *S. plymuthica*-treated apple fruits developed slowly, and the disease spot diameter was smaller than the control (**Figure 2B**). Statistics analysis showed *S. plymuthica* significantly reduced the disease spot diameters on apple fruits compared to the control at 2 days ($P < 0.0001$), 3 days ($P = 0.0028$), 4 days ($P = 0.0025$), and 5 days ($P = 0.0002$) (**Figure 2C**), which showed *S. plymuthica* exhibited an efficient inhibition against the apple ring rot on fruits. In addition, the inhibition significantly increased with the duration of *S. plymuthica* treatment ($P = 0.0016$). On the first day, the inhibition was 37.04%. It reached 78.01% on the second day, then climbed as high as 84.64% on the subsequent days (**Figure 2D**).

Serratia plymuthica Enhanced the Fruit Quality Indexes of Apple Fruit

The seven indexes were determined to test the effects of *S. plymuthica* on the fruit quality. The results showed that all the indexes were variable during the experiment period, exhibiting an up- and down trend with the extension of the experiment time (**Figure 3**). The AUC showed whether the apple fruit was inoculated with *B. dothidea*, *S. plymuthica* significantly reduced TA content, enhanced SS content, TSS/TA ratio, and SS/TA ratio in apple fruits (**Figure 4**). Compared to the control (CK), TA

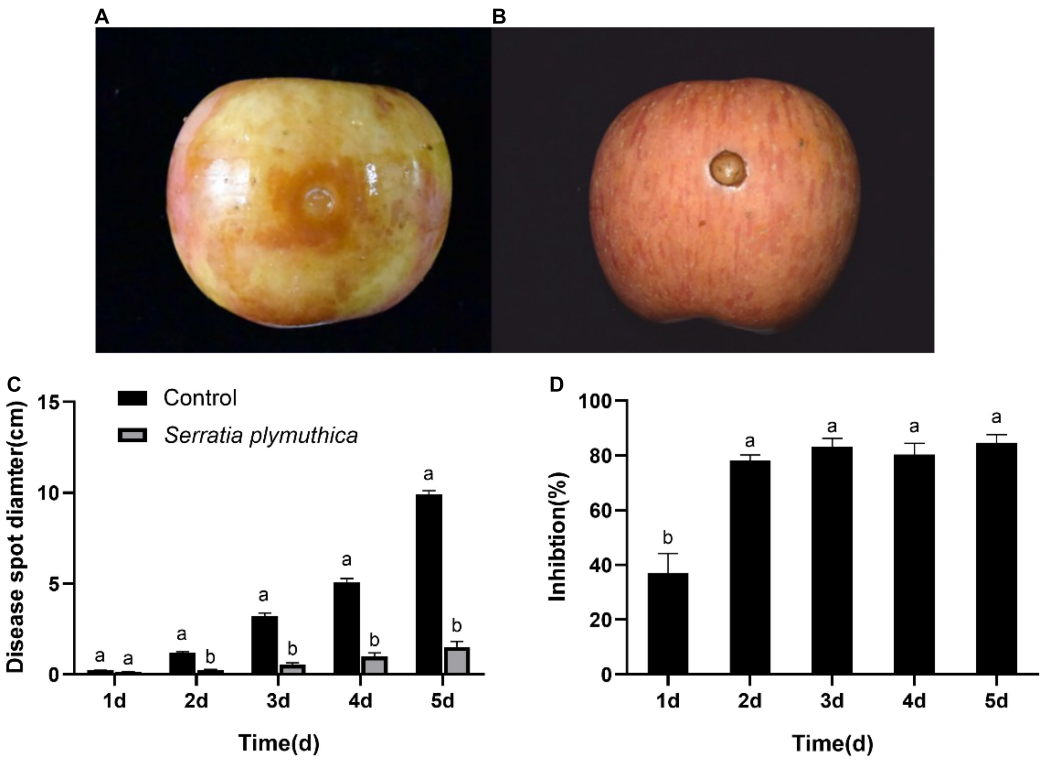

FIGURE 2 | The disease symptoms on the apple fruit inoculated with *Botryosphaeria dothidea*. The disease develops quickly on control fruits, and apple fruit rots 5 days later **(A)**. But the *Serratia plymuthica*-treated apple only shows slight disease symptoms **(B)**. *Serratia plymuthica* significantly reduces the disease spot diameter **(C)** and inhibits apple ring rot on postharvest fruits **(D)** caused by *Botryosphaeria dothidea*. Different lowercase letters indicate significant differences between treatments or different times ($P < 0.05$).

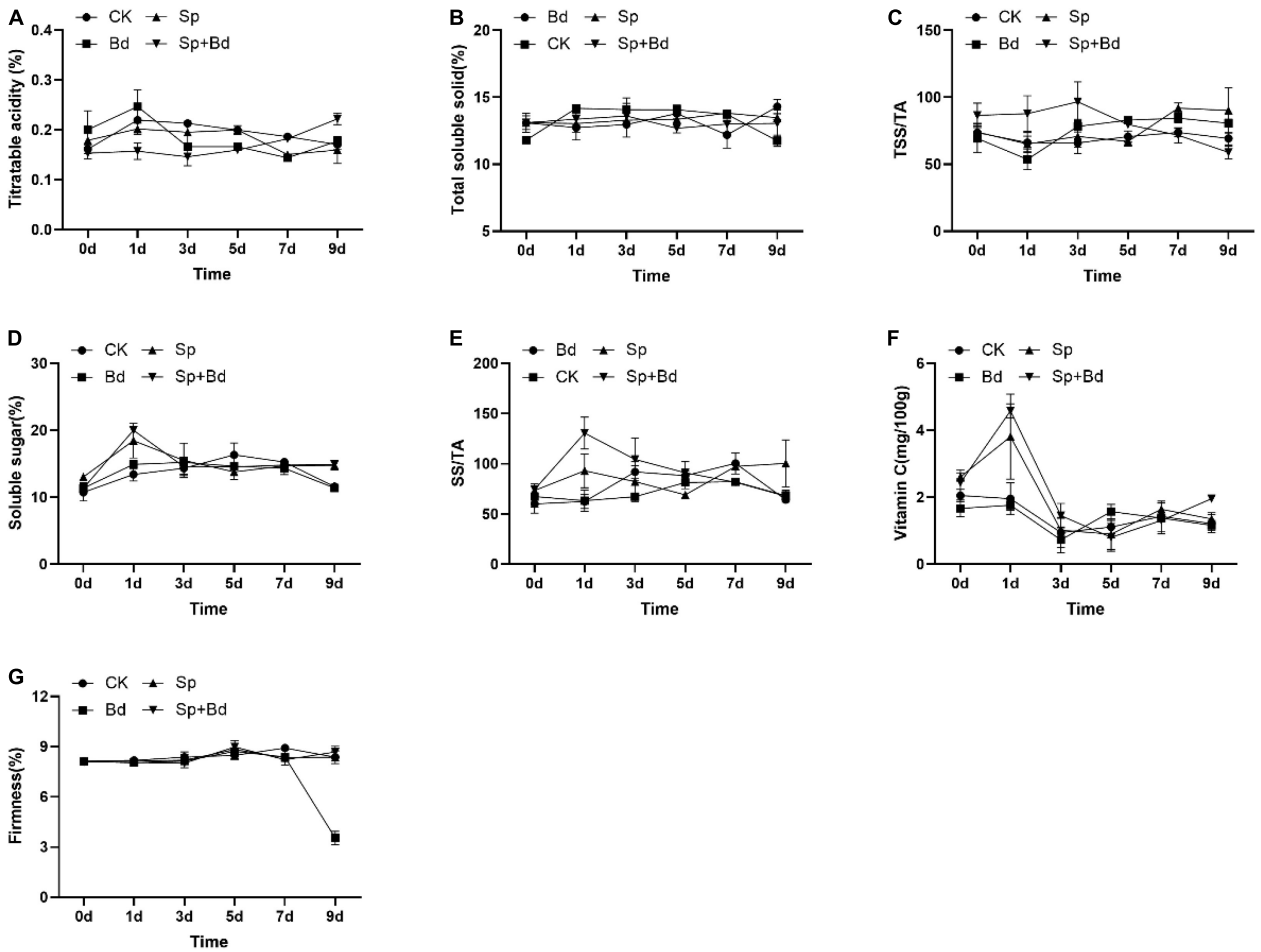

FIGURE 3 | The dynamic changes of fruit quality indexes including titratable acidity **(A)**, total soluble solid **(B)**, TSS/TA **(C)**, SS **(D)**, SS/TA **(E)**, vitamin C **(F)**, and firmness **(G)** in the different treatment fruits.

content in *S. plymuthica*-treated apple fruit (Sp) was reduced by 6.91% ($P = 0.0226$), and the SS content, TSS/TA ratio, and SS/TA ratio were enhanced by 8.27% ($P = 0.0307$), 8.28% ($P = 0.0149$), and 18.54% ($P = 0.0074$), respectively. In addition, compared to the control (Bd), TA content in *S. plymuthica*-treated apple fruit (Sp+Bd) was reduced by 8.69% ($P = 0.0329$), and the SS content, TSS/TA ratio, and SS/TA were enhanced by 9.39% ($P = 0.0036$), 9.20% ($P = 0.0352$), and 18.13% ($P = 0.0030$), respectively. Moreover, *S. plymuthica* also significantly improved VC content and maintained firmness when the apple fruit was inoculated with *B. dothidea*. The VC content and firmness in *S. plymuthica*-treated fruit (Sp+Bd) were 50.82% ($P = 0.0048$) and 6.55% ($P = 0.0085$) higher than that of control (Bd).

RNA-Seq Analysis and Differential Expression Gene Screening

After the raw data (35.02 Gb) were filtered to remove low-quality reads, the resulting high-quality clean data (26.97 Gb) were aligned to the *B. dothidea* reference genome (ASM1150312v2). Then, DEGs in the *S. plymuthica*-treated and the untreated control *B. dothidea* mycelium were screened by DESeq according to the screening criteria of $|\text{LogFoldChange}| > 1$ and $P < 0.05$ (**Supplementary Table 1**). At 6 h, 770 DEGs were obtained from comparison of T6h and CK6h samples, 440 (57.1%) of which were upregulated, and 330 (42.9%) downregulated. At 12 h, the DEGs were up to 890 (T12h_vs_CK12h), 429 (48.2%) of which were upregulated and 461 (51.8%) downregulated (**Figure 5**).

Gene Ontology Analysis

GO analysis revealed that at 6 h, DEGs were enriched into 838 items, among which 490 (58.5%), 43 (5.1%), and 305 (36.4%) belonged to biological process (BP), cellular component (CC), and molecular function (MF), respectively. At 12 h, DEGs were enriched into 901 items, of which 519 (57.6%), 51 (5.7%), and 331 (36.7%) belonged to BP, CC, and MF, respectively (**Supplementary Table 2**). In addition, analysis of the most enriched 10 items in each time point found that membrane (GO:0016020, CC), catalytic activity (GO:0003824, MF), and oxidation-reduction process (GO:0055114, BP) were the most enriched items at both 6 and 12 h (**Figure 6**).

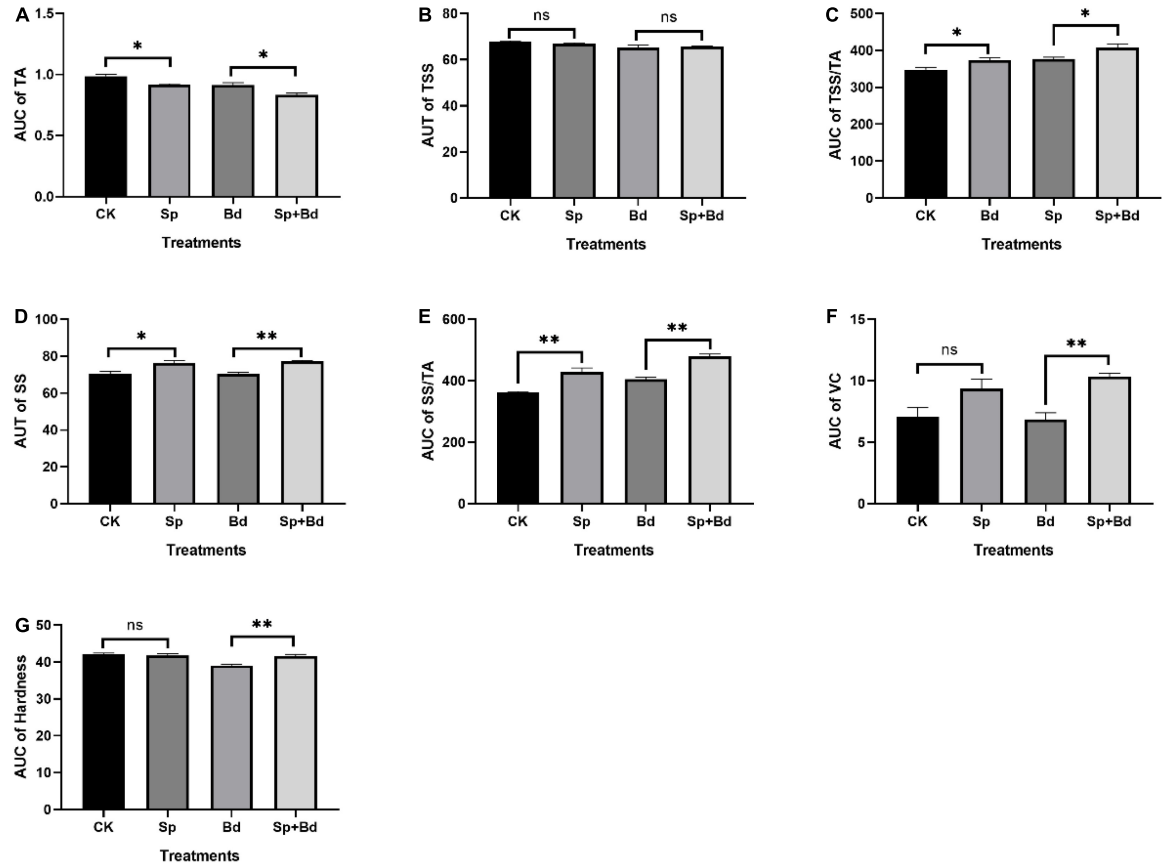

FIGURE 4 | The area-under-curve (AUC) of fruit quality indexes including titratable acidity **(A)**, total soluble solid **(B)**, TSS/TA **(C)**, SS **(D)**, SS/TA **(E)**, vitamin C **(F)**, and firmness **(G)** in the different treatment fruits. "*" means $P < 0.05$, "**" means $P < 0.01$, "ns" means $P < 0.05$.

Kyoto Encyclopedia of Genes and Genomes Analysis

KEGG analysis showed that at 6 h, DEGs were enriched in 71 KEGG pathways, among which 59 (83.10%) were metabolism pathways. At 12 h, DEGs were enriched into 68 KEGG pathways, of which 56 (83.58%) were metabolic pathways (**Supplementary Table 3**). Among the top 10 enriched pathways at each time point, six pathways including tyrosine metabolism (ko00280), arginine and proline metabolism (ko00330), pentose and glucuronate interconversions (ko00040), glycolysis/gluconeogenesis (ko00010), and glycerolipid metabolism (ko00561) and beta-alanine metabolism (ko00410) were the most enriched at both time points (**Figure 7**).

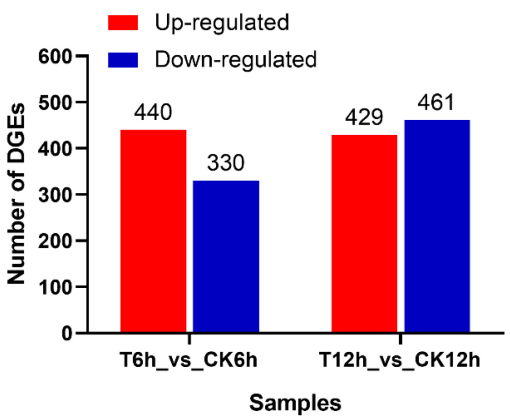

FIGURE 5 | Differentially expressed genes screening in *Botryosphaeria dothidea* treated by *Serratia plymuthica*.

Differentially Expressed Genes Related to Membrane

Cell membrane plays an essential role in maintaining integrated cell structure, cell substance synthesis and exchange, signal transduction, protein synthesis, and other cellular activities. GO analysis revealed a total of 256 DEGs were enriched into the GO term membrane (GO:0016020). Among these genes, 125 DEGs, including alternate oxidase (BOTSD010674), cytochrome P450 (BOTSD002023), GDSL-Type lipase (BOTSD000377), major facilitator superfamily (MFS) (BOTSD004416), and GPR1/FUN34/YaaH (GFY) (BOTSD007968), were significantly differentially expressed at both 6- and 12-h time point (**Figure 8**), highly responding to *S. plymuthica* treatment.

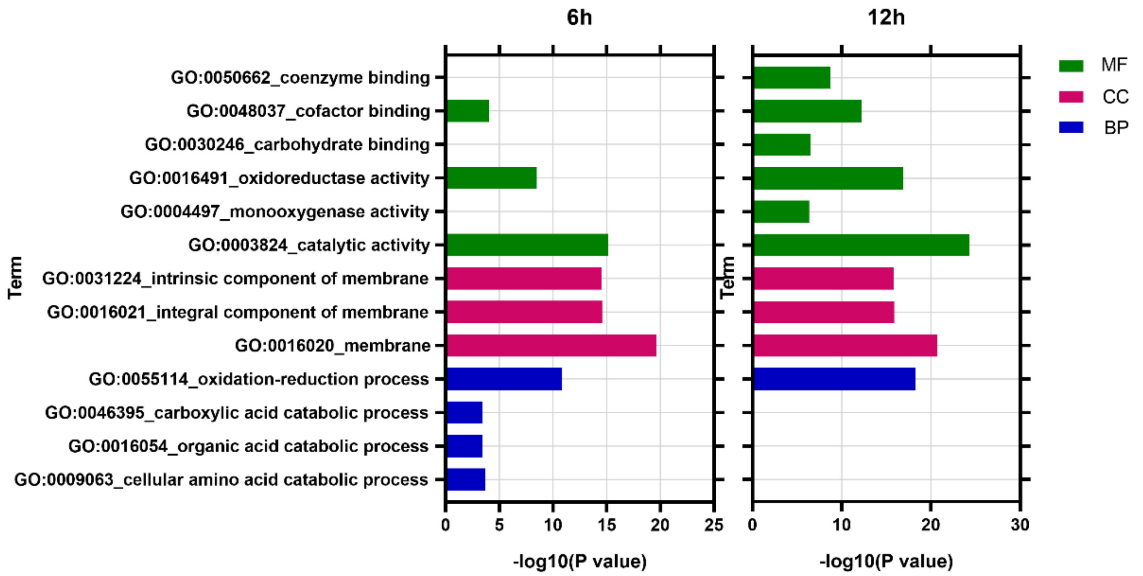

FIGURE 6 | GO enriched analysis of differentially expressed genes. MF, Molecular function; CC, cellular component; BP, biological process.

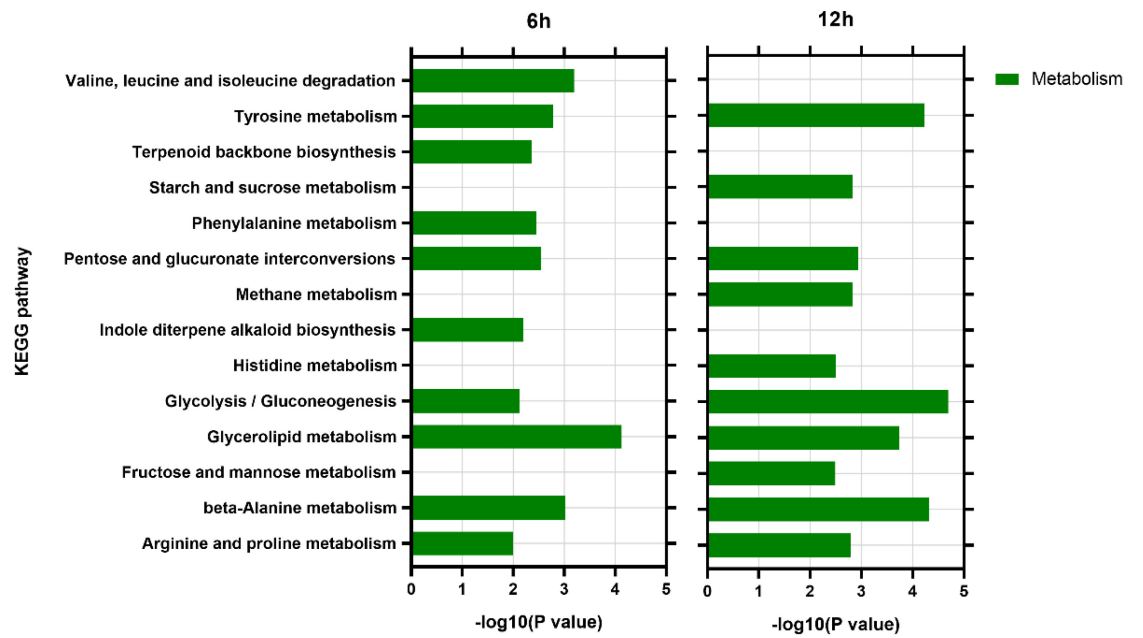

FIGURE 7 | Analysis of main KEGG pathways of differentially expressed genes.

Differentially Expressed Genes Related to Glycerolipid Metabolism

A total of 12 DEGs were involved in the glycerolipid metabolism. All the DEGs, including Aldo/keto reductase (BOTSDO04984), alcohol dehydrogenase (BOTSDO00477), and aldehyde dehydrogenase protein (BOTSDO10253, BOTSDO12847, BOTSDO01671), were significantly downregulated by *S. plymuthica* except glycerate kinase (BOTSDO03374) at both 6 and 12 h (**Figure 9A**), which revealed *S. plymuthica* slowed down the glycerolipid metabolism in *B. dothidea*.

Differentially Expressed Genes Associated With Glycolysis/Gluconeogenesis

The glycolysis/gluconeogenesis pathway contained 16 DEGs, 12 of which were significantly downregulated responding to *S. plymuthica* stress. These genes include alcohol

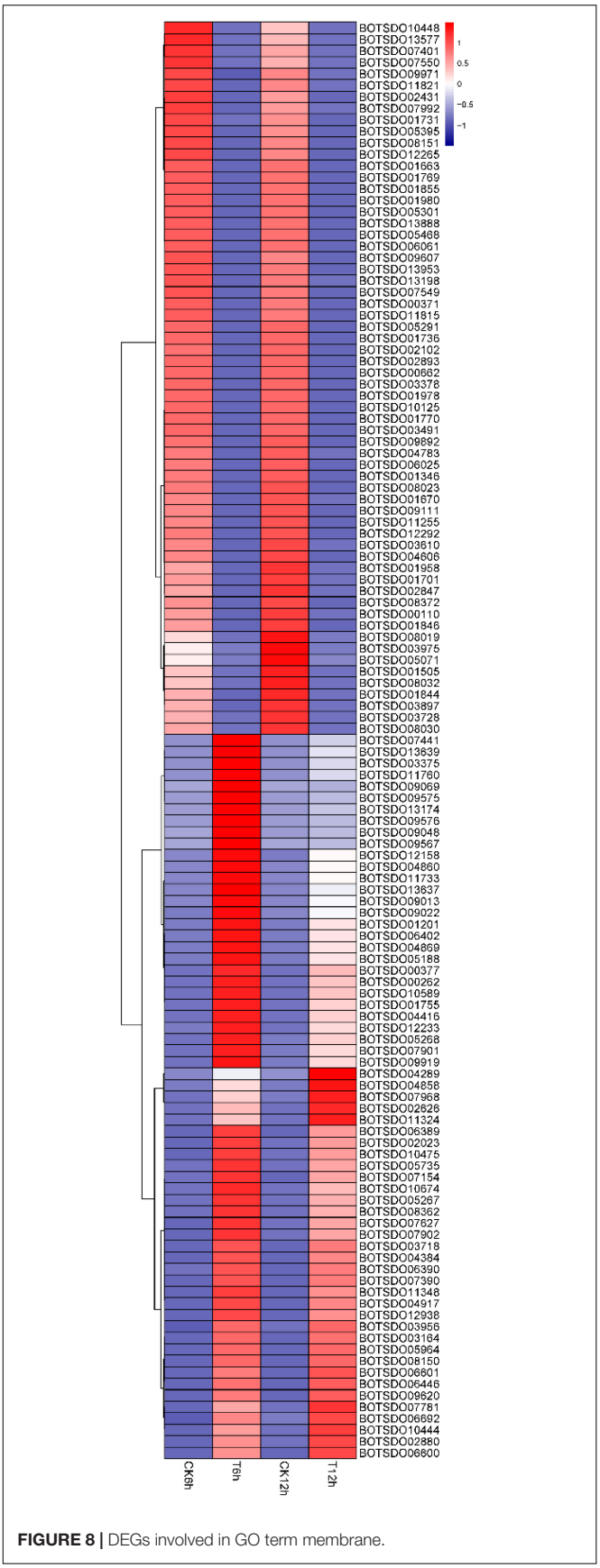

FIGURE 8 | DEGs involved in GO term membrane.

dehydrogenase superfamily zinc-containing (BOTSDO00371, BOTSDO00477, BOTSDO09499), aldehyde dehydrogenase protein (BOTSDO10253, BOTSDO12847, BOTSDO12850, BOTSDO01671), Aldo/keto reductase (BOTSDO04984), and DNA repair protein (BOTSDO03722). Except that, 4 DEGs such as phosphoglycerate mutase (BOTSDO07018, BOTSDO11212), thiamine pyrophosphate enzyme (BOTSDO07016), and hypothetical protein CC84DRAFT_425836 (BOTSDO09314) were upregulated responding to *S. plymuthica* (**Figure 9B**).

Differentially Expressed Genes Related to Tyrosine Metabolism

In the tyrosine metabolism pathway, a total of 14 DEGs were screened at both time points. Twelve DEGs consisting of copper amine oxidase (BOTSDO01717, BOTSDO10310, BOTSDO09755), fumarylacetoacetase (BOTSDO11171, BOTSDO06978, BOTSDO05479), alcohol dehydrogenase (BOTSDO00371, BOTSDO09499), and aldehyde dehydrogenase (BOTSDO12850) were significantly regulated compared to the responding control at 6 and 12 h. In contrast, the two DEGs, aspartate aminotransferase (BOTSDO07725) and the hypothetical protein MPH_00577 (BOTSDO02628), were upregulated at both time points (**Figure 9C**).

Quantitative RT-PCR Validation of RNA-Sequencing Data

To validate the RNA-seq results, we performed qRT-PCR on 15 genes differentially expressed between control and *S. plymuthica* treated mycelia (**Figure 10**). RNA-seq results showed that the 15 genes were upregulated by *S. plymuthica*, and qRT-PCR also revealed that those genes were upregulated by *S. plymuthica*. Though the gene change fold was not precisely the same, the changing trend was the same, which showed the qRT-PCR results were consistent with RNA-Seq results, thereby confirming the reliability of RNA-Seq data.

DISCUSSION

Apple ring rot is spreading across the orchards across China, seriously threatening the healthy development of apple fruit. In our preliminary study, we isolated an endophytic bacterium *S. plymuthica* from Chinese leek rhizome. The present study demonstrate that the *S. plymuthica* significantly suppresses the growth of *B. dothidea* and inhibits the apple ring rot on postharvest fruits. In addition, *S. plymuthica* also improves the fruit's quality. Therefore, the study provides a possible way to control the apple ring rot of postharvest fruits.

In the present study, the endophytic bacterial *S. plymuthica* exerts an antifungal activity of 52.5% against *B. dothidea* growth and suppresses the apple ring rot by 84.64%. Besides *S. plymuthica*, several species in *Serratia* sp. show potent antifungal activity. *Serratia* sp. isolated from *Bacopa monnieri* has effective inhibition against *Pythium myriotylum*, *Rhizoctonia solani*, *Sclerotium rolfsii*, *Phytophthora infestans*, and *Fusarium oxysporum* (Jimtha et al., 2017). *S. marcescens* significantly suppresses the

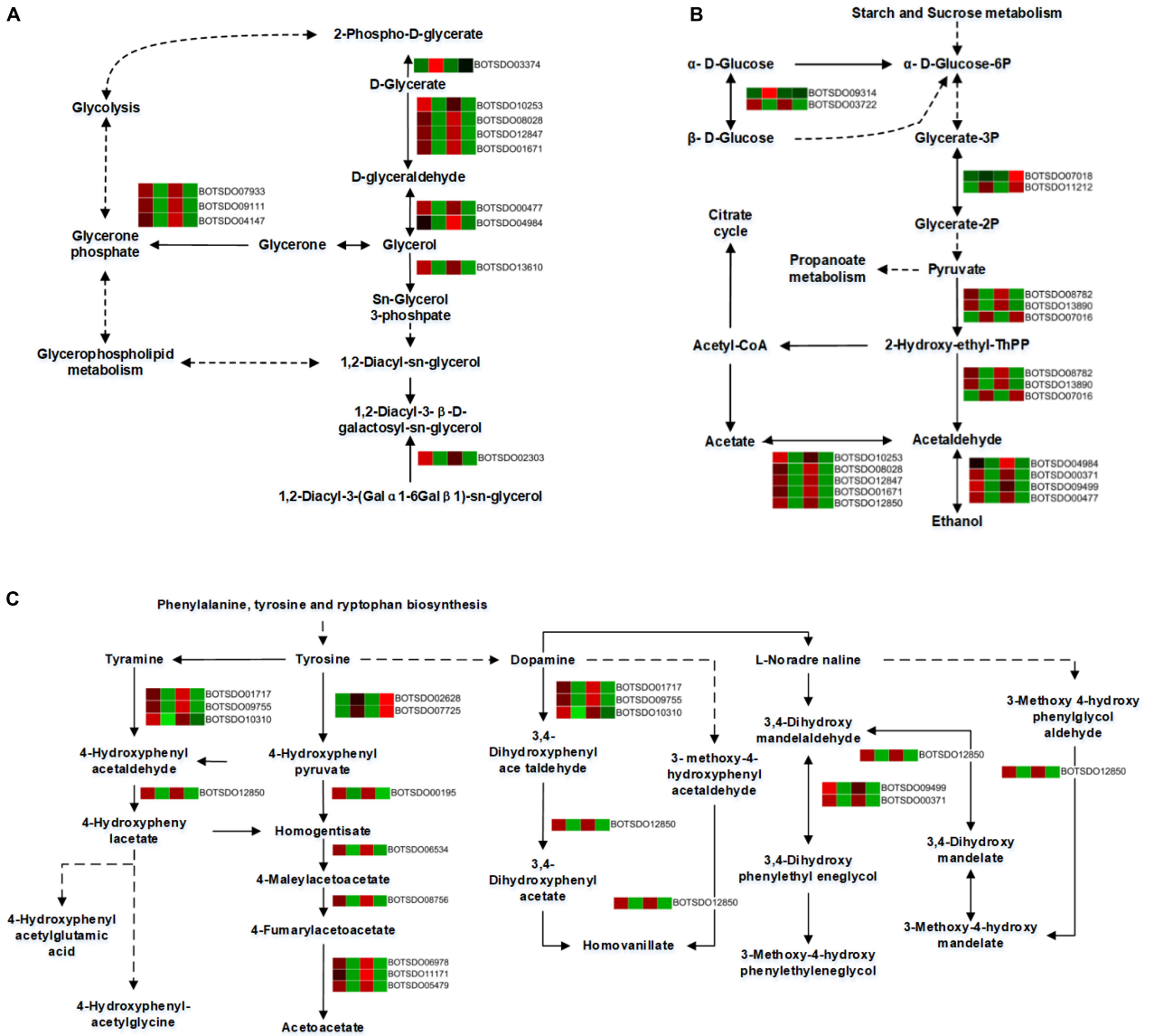

FIGURE 9 | DEGs involved in glycerolipid metabolism **(A)**, glycolysis/gluconeogenesis **(B)**, and tyrosine metabolism **(C)** by KEGG analysis.

growth of *Rhizoctonia solani*, *Fusarium oxysporum* (Do et al., 2017), and *Didymella applanata* (Duzhak et al., 2012). *S. rubidaea* exhibits high suppression against *Fusarium oxysporum* and *Colletotrichum gloeosporioides* (Nalini and Parthasarathi, 2014). *S. proteamaculans* 336x significantly suppresses the growth of *Gaeumannomyces graminis* var. *tritici*, and reduces the occurrence of wheat take-all (Wang et al., 2014). Together with all these previous studies, the present study suggests *Serratia* sp. is a good resource for developing antagonistic bacteria to prevent and control various plant pathogens.

To preliminary explore the molecular mechanism of the inhibition of *S. plymuthica* against *B. dothidea*, we screen 777 and 890 DEGs using RNA-seq from the comparisons of the control mycelia and the *S. plymuthica*-treated mycelia at 6 and 12 h, respectively. Among these DEGs, alternate oxidase (AOX), cytochrome P450 (CYP450), GDSL-Type lipase, MFS, and GFY, enriched into GO term membrane, highly responded to *S. plymuthica* at both time points. These membrane-related proteins can participate in the metabolism of many exogenous substances, including drugs and environmental stress, which is significant for maintaining normal cell growth and development. Alternative oxidase regulates the growth, development, and resistance to oxidative stress of *Sclerotinia sclerotiorum* (Xu et al., 2012). In addition, alternative oxidase gene improves the resistance of *Monascus ruber* to stressful conditions such as H_2O_2, high temperature, and alkaline buffer (Shao et al., 2017), and the resistance of *Vibrio fischeri* to nitric oxide, and enhances bacterial fitness and survival under stressful environmental conditions (Dunn, 2018). Cytochrome P450

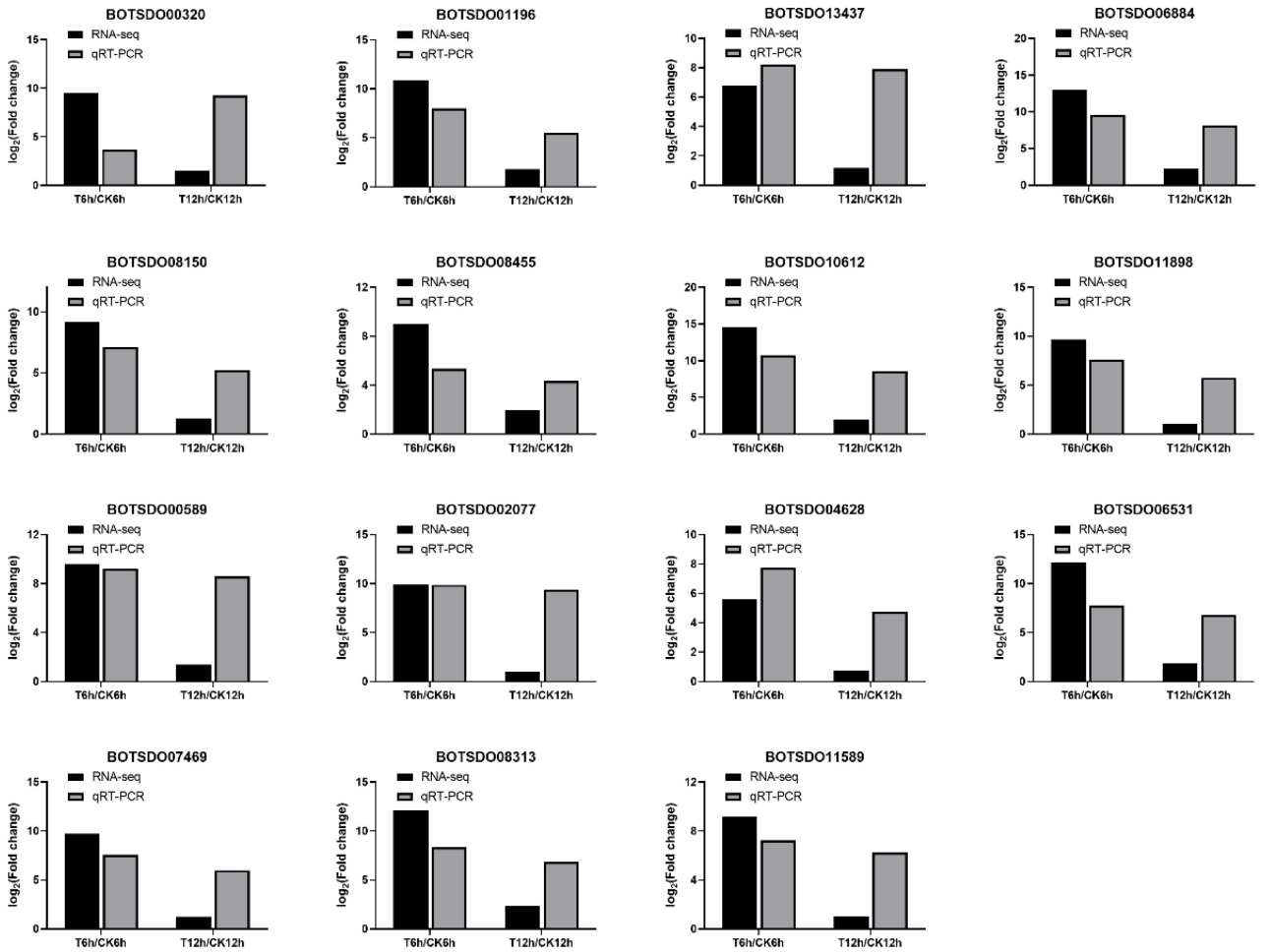

FIGURE 10 | qRT-PCR validation of 15 randomly selected differentially expressed genes identified by Illumina high throughput RNA-sequencing.

gene is required for the biosynthesis of the trichothecene toxin harzianum A in *Trichoderma* (Cardoza et al., 2019) and promotes cell survival of the sugarcane smut fungus *Sporisorium scitamineum* under oxidative stress (Cai et al., 2021). The GDSL lipase exhibits high tolerance against detergents and metal ions in *Geobacillus thermocatenulatus* (Jo et al., 2021). MFS gene mfs1 or mfs2 reduce the susceptibility to aminoglycosides, quinolones, and paraquat in *Pseudomonas aeruginosa* (Dulyayangkul et al., 2021) and play an essential role in resistance to toxicity, oxidants, and fungicides in *Alternaria alternata* (Lin et al., 2018). GFY gene *AcpA* in fungus *Aspergillus nidulans* (Robellet et al., 2008) is an essential component of mediated acetate transport.

In the present study, more than 83.00% of the KEGG pathway belong to the metabolic pathway. Glycerolipid metabolism, glycolysis/gluconeogenesis, and tyrosine metabolism are the most enriched pathways at both time points. We believe the inhibition of *S. plymuthica* against *B. dothidea* is closely related to these pathways. Previous studies show that DEGs such as alcohol dehydrogenase, aldehyde dehydrogenase gene, DNA repair protein, aspartate aminotransferases, and aldo/keto reductase contained in these pathways played a vital role in fungi. For instance, *Synechocystis* alcohol dehydrogenase sysr1 considerably increases tolerance in salt stress conditions (Yi et al., 2017), and *Botrytis cinerea* alcohol dehydrogenase *BcADH1* is required for fungal development, environmental adaptation, and its ability for full pathogenicity (DafaAlla et al., 2021). *ald1*, an aldehyde dehydrogenase gene in the fungus *Tricholoma vaccinum*, increases its tolerance to ethanol stress (Asiimwe et al., 2012). *Saccharomyces cerevisiae* DNA repair gene RAD6 is necessary to repair damaged DNA in stress situations (Madura et al., 1990). *Beauveria bassiana* aldo-keto reductase, Bbakr1, is involved in osmotic and salt stressors and oxidative and heavy metal (chromium) stress (Wang et al., 2018). Aspartate aminotransferase gene governs aspartate biosynthesis and nitrogen distribution in *Mycobacterium tuberculosis* (Jansen et al., 2020) and activates TOR complex 1 in fission yeast, improving cell growth and proliferation in response to nutritional signals (Reidman et al., 2019).

Good measures should not only control postharvest diseases on fruit but also maintain fruit quality. Previous studies show that alginate oligosaccharide (Bose et al., 2019), brassinosteroids

(Furio et al., 2019), acibenzolar-S-methyl (Li et al., 2020), ozone (Luo et al., 2019), and integration of ultraviolet-C with antagonistic yeast *Candida tropicalis* (Ou et al., 2016) strongly inhibit the disease occurrences on postharvest fruits, and also significantly improve these fruit qualities. In the present study, *S. plymuthica* significantly suppresses the occurrence of apple ring rot on postharvest fruit, reduces the TA content, increases the SS content, TSS/TA ratio, and SS/TA ratio, and maintains apple fruit's firmness. Thus, these previous studies and *S. plymuthica* used in the present study fulfill the criteria of good measure to control postharvest disease, which can kill two birds with one stone. In addition, the *S. plymuthica* is isolated from Chinese leek, a popular vegetable in China. Therefore, using the endophytic bacterium *S. plymuthica* to control apple ring rot on postharvest fruit is safer for humans and animals and more environment-friendly.

From the RNA analysis results, we deduce that *S. plymuthica* damages the membrane of *B. dothidea*, resulting in membrane-related gene expression altered and causing the oxidation-reduction imbalance, eventually leading to its amino acid, carbohydrate, and lipid, energy, and other metabolic disorders, which eventually affect the healthy growth of *B. dothidea*.

CONCLUSION

The present study demonstrates that the endophytic bacterium *S. plymuthica* isolated from Chinese leek significantly suppresses the growth of *B. dothidea*, and exerts a remarkable inhibition against apple ring rot on postharvest fruits. *S. plymuthica* reduces the TA content, increases the SS content, TSS/TA ratio, and SS/TA ratio, and maintains apple fruit's firmness. Furthermore, transcriptome analysis shows *S. plymuthica* mainly alters genes related to the metabolism pathway of *B. dothidea*. Thus, the study provides a possible way to control apple ring rot disease and lay a solid basis for further exploring the molecular mechanism of *S. plymuthica* inhibition against *B. dothidea*.

DATA AVAILABILITY STATEMENT

The RNA-seq data were deposited at the National Center for Biotechnology Information under accession number PRJNA727902.

AUTHOR CONTRIBUTIONS

YH contributed to the conception of the study and revised the manuscript. MS wrote the manuscript, performed the experiment, and collected the data. JPL and JHL experimented and collected the data. All authors contributed to the article and approved the submitted version.

SUPPLEMENTARY MATERIAL

The Supplementary Material for this article can be found online at: https://www.frontiersin.org/articles/10.3389/fmicb.2021.802887/full#supplementary-material

REFERENCES

Adam, E., Muller, H., Erlacher, A., and Berg, G. (2016). Complete genome sequences of the *Serratia plymuthica* strains 3Rp8 and 3Re4-18, two rhizosphere bacteria with antagonistic activity towards fungal phytopathogens and plant growth promoting abilities. *Stand. Genomic Sci.* 11:61. doi: 10.1186/s40793-016-0185-3

Anders, S., Pyl, P. T., and Huber, W. (2015). HTSeq - a Python framework to work with high-throughput sequencing data. *Bioinformatics* 31, 166–169. doi: 10.1093/bioinformatics/btu638

Ashburner, M., Ball, C. A., Blake, J. A., Botstein, D., Butler, H., Cherry, J. M., et al. (2000). Gene Ontology: tool for the unification of biology. *Nat. Genet.* 25, 25–29. doi: 10.1038/75556

Asiimwe, T., Krause, K., Schlunk, I., and Kothe, E. (2012). Modulation of ethanol stress tolerance by aldehyde dehydrogenase in the mycorrhizal fungus *Tricholoma vaccinum*. *Mycorrhiza* 22, 471–484. doi: 10.1007/s00572-011-0424-9

Bai, S., Dong, C., Zhu, J., Zhang, Y., and Dai, H. (2015). Identification of a xyloglucan-specific endo-(1-4)-beta-D-glucanase inhibitor protein from apple (*Malus x domestica* Borkh.) as a potential defense gene against *Botryosphaeria dothidea*. *Plant Sci.* 231, 11–19. doi: 10.1016/j.plantsci.2014.11.003

Benhamou, N., Gagné, S., Quéré, D. L., and Dehbi, L. (2000). Bacterial-mediated induced resistance in cucumber: beneficial effect of the endophytic bacterium *Serratia plymuthica* on the protection against infection by *pythium ultimum*. *Phytopathology* 90, 45–56. doi: 10.1094/PHYTO.2000.90.1.45

Bose, S. K., Howlader, P., Jia, X., Wang, W., and Yin, H. (2019). Alginate oligosaccharide postharvest treatment preserve fruit quality and increase storage life via Abscisic acid signaling in strawberry. *Food Chem.* 283, 665–674. doi: 10.1016/j.foodchem.2019.01.060

Cai, E., Li, L., Deng, Y., Sun, S., Jia, H., Wu, R., et al. (2021). MAP kinase Hog1 mediates a cytochrome P450 oxidoreductase to promote the *Sporisorium scitamineum* cell survival under oxidative stress. *Environ. Microbiol.* 23, 3306–3317. doi: 10.1111/1462-2920.15565

Cardoza, R. E., McCormick, S. P., Lindo, L., Kim, H.-S., Olivera, E. R., Nelson, D. R., et al. (2019). A cytochrome P450 monooxygenase gene required for biosynthesis of the trichothecene toxin harzianum A in *Trichoderma*. *Appl. Microbiol. Biotechnol.* 103, 8087–8103. doi: 10.1007/s00253-019-10047-2

Chen, X., Zhang, Y., Fu, X., Li, Y., and Wang, Q. (2016). Isolation and characterization of *Bacillus amyloliquefaciens* PG12 for the biological control of apple ring rot. *Postharvest Biol. Technol.* 115, 113–121. doi: 10.1016/j.postharvbio.2015.12.021

DafaAlla, T., Abdalla, M., El-Arabey, A. A., Eltayb, W. A., and Mohapatra, R. K. (2021). *Botrytis cinerea* alcohol dehydrogenase mediates fungal development, environmental adaptation and pathogenicity. *J. Biomol. Struct. Dyn.* [Epub Online ahead of print]. doi: 10.1080/07391102.2021.1971112

Do, T. T., Nguyen, T. T., Nguyen, T. L. S., and Le, H. T. (2017). Optimization, purification, and characterization of an extracellular antifungal protein from *Serratia marcescens* DT3 isolated from soil in Vietnam. *Turk. J. Biol.* 41, 448–457. doi: 10.3906/biy-1607-22

Dong, B. Z., Zhu, X. Q., Fan, J., and Guo, L. Y. (2021). The cutinase bdo_10846 play an important role in the virulence of *Botryosphaeria dothidea* and in inducing the wart symptom on apple plant. *Int. J. Mol. Sci.* 22:1910. doi: 10.3390/ijms22041910

Dulyayangkul, P., Satapoomin, N., Avison, M. B., Charoenlap, N., Vattanaviboon, P., and Mongkolsuk, S. (2021). Over-expression of hypochlorite inducible major facilitator superfamily (MFS) pumps reduces antimicrobial drug susceptibility by increasing the production of MeXY mediated by ArmZ in

pseudomonas aeruginosa. *Front. Microbiol.* 11:592153. doi: 10.3389/fmicb.2020.592153

Dunn, A. K. (2018). Alternative oxidase activity reduces stress in *Vibrio fischeri* cells exposed to nitric oxide. *J. Bacteriol.* 200, e00797–17. doi: 10.1128/JB.00797-17

Duzhak, A. B., Panfilova, Z. I., Duzhak, T. G., Vasyunina, E. A., and Shternshis, M. V. (2012). Role of prodigiosin and chitinases in antagonistic activity of the bacterium *Serratia marcescens* against the fungus *Didymella applanata*. *Biochemistry* 77, 910–916. doi: 10.1134/S0006297912080123

Fan, H., Ru, J., Zhang, Y., Wang, Q., and Li, Y. (2017). Fengycin produced by *Bacillus subtilis* 9407 plays a major role in the biocontrol of apple ring rot disease. *Microbiol. Res.* 199, 89–97. doi: 10.1016/j.micres.2017.03.004

Furio, R. N., Salazar, S. M., Martínez-Zamora, G. M., Coll, Y., Hael-Conrad, V., and Díaz-Ricci, J. C. (2019). Brassinosteroids promote growth, fruit quality and protection against Botrytis on *Fragaria x ananassa*. *Eur. J. Plant Pathol.* 154, 801–810. doi: 10.1007/s10658-019-01704-3

Gao, X., He, Q., Jiang, Y., and Huang, L. (2016). Optimization of nutrient and fermentation parameters for antifungal activity by *Streptomyces lavendulae* Xjy and its biocontrol efficacies against *Fulvia fulva* and *Botryosphaeria dothidea*. *J. Phytopathol.* 164, 155–165. doi: 10.1111/jph.12440

Gu, C., Yang, X., Al-Attala, M., Abid, M., Phyo, S., Zang, H., et al. (2020). First report of pomegranate fruit rot caused by *Botryosphaeria dothidea* in Anhui Province of China. *Plant Dis.* 104, 2736–2736. doi: 10.1094/PDIS-04-20-0790-PDN

Guo, L. Y., Li, J. Y., Li, B. H., Zhang, X. Z., Zhou, Z. Q., Li, G. X., et al. (2009). Investigations on the occurrence and chemical control of *Botryosphaeria* canker of apple in China. *Plant Prot.* 35, 120–123.

Hadizadeh, I., Peivastegan, B., Hannukkala, A., van der Wolf, J. M., Nissinen, R., and Pirhonen, M. (2019). Biological control of potato soft rot caused by *Dickeya solani* and the survival of bacterial antagonists under cold storage conditions. *Plant Pathol.* 68, 297–311. doi: 10.1111/ppa.12956

Huang, Y., Meng, L. L., Liu, J., and Wang, C. X. (2019b). First report of shoot canker on apricot caused by *Botryosphaeria dothidea* in Shandong province of China. *Plant Dis.* 103, 2945–2946. doi: 10.1094/PDIS-03-19-0522-PDN

Huang, Y., Meng, L., Liu, J., and Wang, C. X. (2019a). First report of *Botryosphaeria dothidea* causing shoot canker on mulberry in China. *Plant Dis.* 103, 1788–1789. doi: 10.1094/PDIS-01-19-0183-PDN

Huang, Y., Sun, C., Guan, X., Lian, S., Li, B., and Wang, C. (2021). Biocontrol efficiency of *Meyerozyma guilliermondii* Y-1 against apple postharvest decay caused by *Botryosphaeria dothidea* and the possible mechanisms of action. *Int. J. Food Microbiol.* 338:108957. doi: 10.1016/j.ijfoodmicro.2020.108957

Huang, Y. H., Wang, R. C., Li, C. H., Zuo, C. W., Wei, Y. R., Zhang, L., et al. (2012). Control of fusarium wilt in banana with Chinese leek. *Eur. J. Plant Pathol.* 134, 87–95. doi: 10.1007/s10658-012-0024-3

Jansen, R. S., Mandyoli, L., Hughes, R., Wakabayashi, S., Pinkham, J. T., Selbach, B., et al. (2020). Aspartate aminotransferase Rv3722c governs aspartate-dependent nitrogen metabolism in *Mycobacterium tuberculosis*. *Nat. Commun.* 11:1960. doi: 10.1038/s41467-020-15876-8

Jimtha, J. C., Jishma, P., Sreelekha, S., Chithra, S., and Radhakrishnan, E. K. (2017). Antifungal properties of prodigiosin producing rhizospheric *Serratia* sp. *Rhizosphere* 3, 105–108. doi: 10.1016/j.rhisph.2017.02.003

Jo, E., Kim, J., Lee, A., Moon, K., and Cha, J. (2021). Identification and characterization of a novel thermostable GDSL-Type lipase from *Geobacillus thermocatenulatus*. *J. Microbiol. Biotechnol.* 31, 483–491. doi: 10.4014/jmb.2012.12036

Kanehisa, M., Sato, Y., Kawashima, M., Furumichi, M., and Tanabe, M. (2016). KEGG as a reference resource for gene and protein annotation. *Nucleic Acids Res.* 44, D457–D462. doi: 10.1093/nar/gkv1070

Kim, Y. S., Balaraju, K., and Jeon, Y. (2016). Effects of rhizobacteria *Paenibacillus polymyxa* APEC136 and *Bacillus subtilis* APEC170 on biocontrol of postharvest pathogens of apple fruits. *J. Zhejiang Univ. Sci. B* 17, 931–940. doi: 10.1631/jzus.B1600117

Li, C., Zhang, J., Ge, Y., Li, X., Wei, M., Hou, J., et al. (2020). Postharvest acibenzolar-S-methyl treatment maintains storage quality and retards softening of apple fruit. *J. Food Biochem.* 44:e13141. doi: 10.1111/jfbc.13141

Lin, H.-C., Yu, P.-L., Chen, L.-H., Tsai, H.-C., and Chung, K.-R. (2018). A major facilitator superfamily transporter regulated by the stress-responsive transcription factor Yap1 is required for resistance to fungicides, xenobiotics, and oxidants and full virulence in *Alternaria alternata*. *Front. Microbiol.* 9:2229. doi: 10.3389/fmicb.2018.02229

Livak, K. J., and Schmittgen, T. D. (2001). Analysis of relative gene expression data using real-time quantitative PCR and the 2^{-the} method. *Methods* 25, 402–408. doi: 10.1006/meth.2001.1262

Luo, A., Bai, J., Li, R., Fang, Y., Li, L., Wang, D., et al. (2019). Effects of ozone treatment on the quality of kiwifruit during postharvest storage affected by *Botrytis cinerea* and *Penicillium expansum*. *J. Phytopathol.* 167, 470–478. doi: 10.1111/jph.12819

Madura, K., Prakash, S., and Prakash, L. (1990). Expression of the *Saccharomyces cerevisiae* DNA repair gene RAD6 that encodes a ubiquitin conjugating enzyme, increases in response to DNA damage and in meiosis but remains constant during the mitotic cell cycle. *Nucleic Acids Res.* 18, 771–778. doi: 10.1093/nar/18.4.771

Martin, M. (2000). Cutadapt removes adapter sequences from high-throughput sequencing reads. *EMBnet J.* 17, 10–12. doi: 10.14806/ej.17.1.200

Meziane, H., Gavriel, S., Ismailov, Z., Chet, I., Chernin, L., and Höfte, M. (2006). Control of green and blue mould on orange fruit by *Serratia plymuthica* strains IC14 and IC1270 and putative modes of action. *Postharvest Biol. Technol.* 39, 125–133. doi: 10.1016/j.postharvbio.2005.10.007

Mu, Y., Yue, Y., Gu, G., Deng, Y., Jin, H., and Tao, K. (2020). Identification and characterization of the *Bacillus atrophaeus* strain J-1 as biological agent of apple ring rot disease. *J. Plant Dis. Prot.* 127, 367–378. doi: 10.1007/s41348-020-00309-x

Müller, H., Fürnkranz, M., Grube, M., and Berg, G. (2013). Genome sequence of *Serratia plymuthica* strain s13, an endophyte with germination- and plant-growth-promoting activity from the flower of styrian oil pumpkin. *Genome Announc.* 1, e00594–13. doi: 10.1128/genomeA.00594-13

Nalini, S., and Parthasarathi, R. (2014). Production and characterization of rhamnolipids produced by *Serratia rubidaea* SNAU02 under solid-state fermentation and its application as biocontrol agent. *Bioresour. Technol.* 173, 231–238. doi: 10.1016/j.biortech.2014.09.051

Ou, C., Liu, Y., Wang, W., and Dong, D. (2016). Integration of UV-C with antagonistic yeast treatment for controlling post-harvest disease and maintaining fruit quality of *Ananas comosus*. *BioControl* 61, 591–603. doi: 10.1007/s10526-016-9740-5

Reidman, S., Cohen, A., Kupiec, M., and Weisman, R. (2019). The cytosolic form of aspartate aminotransferase is required for full activation of TOR complex 1 in fission yeast. *J. Biol. Chem.* 294, 18244–18255. doi: 10.1074/jbc.RA119.010101

Robellet, X., Flipphi, M., Pegot, S., Maccabe, A. P., and V'Elot, C. (2008). AcpA, a member of the GPR1/FUN34/YaaH membrane protein family, is essential for acetate permease activity in the hyphal fungus *Aspergillus nidulans*. *Biochem. J.* 412, 485–493. doi: 10.1042/BJ20080124

Shao, Y., Li, Q., Zhou, Y., and Chen, F. (2017). Effects of an alternative oxidase gene on conidia viability under external stresses in *Monascus ruber* M7. *J. Basic Microbiol.* 57, 413–418. doi: 10.1002/jobm.201600707

Sun, X., Pan, B., Wang, Y., Xu, W., and Zhang, S. (2020). Exogenous calcium improved resistance to *Botryosphaeria dothidea* by increasing autophagy activity and salicylic acid level in pear. *Mol. Plant-Microbe Interact.* 33, 1150–1160. doi: 10.1094/MPMI-04-20-0101-R

Trapnell, C., Pachter, L., and Salzberg, S. L. (2009). TopHat: discovering splice junctions with RNA-Seq. *Bioinformatics* 25, 1105–1111. doi: 10.1093/bioinformatics/btp120

Wang, H., He, Z., Luo, L., Zhao, X., Lu, Z., Luo, T., et al. (2018). An aldo-keto reductase, Bbakr1, is involved in stress response and detoxification of heavy metal chromium but not required for virulence in the insect fungal pathogen, *Beauveria bassiana*. *Fungal Genet. Biol.* 111, 7–15. doi: 10.1016/j.fgb.2018.01.001

Wang, L., Feng, Z., Wang, X., and Zhang, X. (2010). DEGseq: an R package for identifying differentially expressed genes from RNA-seq data. *Bioinformatics* 26, 136–138. doi: 10.1093/bioinformatics/btp612

Wang, L., Hou, H., Zhou, Z., Tu, H., and Yuan, H. (2021). Identification and detection of *Botryosphaeria dothidea* from kiwifruit (*Actinidia chinensis*) in China. *Plants* 10:401. doi: 10.3390/plants10020401

Wang, M., Xing, Y., Wang, J., Xu, Y., and Wang, G. (2014). The role of the chi1 gene from the endophytic bacteria *Serratia proteamaculans* 336x in the biological control of wheat take-all. *Can. J. Microbiol.* 60, 533–540. doi: 10.1139/cjm-2014-0212

Xu, T., Yao, F., Liang, W.-S., Li, Y.-H., Li, D.-R., Wang, H., et al. (2012). Involvement of alternative oxidase in the regulation of growth, development, and resistance to oxidative stress of *Sclerotinia sclerotiorum*. *J. Microbiol.* 50, 594–602. doi: 10.1007/s12275-012-2015-7

Yang, L., Zhu, Z., Zhang, J., Gao, Y., Wang, X., Liu, G., et al. (2020). Response of kiwifruit yield and fruit quality to chloride-containing fertilizers. *Agron. J.* 112, 1012–1020. doi: 10.1002/agj2.20074

Yi, S. Y., Ku, S. S., Sim, H. J., Kim, S. K., Park, J. H., Lyu, J. I., et al. (2017). An alcohol dehydrogenase gene from *Synechocystis* sp. confers salt tolerance in transgenic tobacco. *Front. Plant Sci.* 8:1965. doi: 10.3389/fpls.2017.01965

Zhang, L., Zhang, Q., Yang, P., Niu, Y., and Niu, W. (2019). First report of gummosis disease of sweet cherry caused by *Botryosphaeria dothidea* in China. *Plant Dis.* 103, 3283–3283.

Zhang, Q., Yong, D., Zhang, Y., Shi, X., Li, B., Li, G., et al. (2016). *Streptomyces rochei* A-1 induces resistance and defense-related responses against *Botryosphaeria dothidea* in apple fruit during storage. *Postharvest Biol. Technol.* 115, 30–37. doi: 10.1016/j.postharvbio.2015.12.013

Zhao, G., Zhang, W., Zuo, C., and Huang, Y. (2017). Control effect of Chinese leek extract and its main bioactive components on apple ring rot incidence. *Chin. J. Biol. Control* 33, 273–280. doi: 10.16409/j.cnki.2095-039x.2017.02.019

Zhao, J., Wang, S., Zhu, X., Wang, Y., Liu, X., Duan, Y., et al. (2021). Isolation and characterization of nodules endophytic bacteria *Pseudomonas protegens* Sneb1997 and *Serratia plymuthica* Sneb2001 for the biological control of root-knot nematode. *Appl. Soil Ecol.* 164:103924. doi: 10.1016/j.apsoil.2021.103924

Conflict of Interest: The authors declare that the research was conducted in the absence of any commercial or financial relationships that could be construed as a potential conflict of interest.

The reviewer PL declared a shared affiliation with the authors to the handling editor at the time of review.

Publisher's Note: All claims expressed in this article are solely those of the authors and do not necessarily represent those of their affiliated organizations, or those of the publisher, the editors and the reviewers. Any product that may be evaluated in this article, or claim that may be made by its manufacturer, is not guaranteed or endorsed by the publisher.

frontiers | Frontiers in Microbiology

ORIGINAL RESEARCH
published: 12 May 2022
doi: 10.3389/fmicb.2022.797234

Time Is of the Essence—Early Activation of the Mevalonate Pathway in Apple Challenged With Gray Mold Correlates With Reduced Susceptibility During Postharvest Storage

*Matthias Naets[1], Wendy Van Hemelrijck[2], Willem Gruyters[1†], Pieter Verboven[1], Bart Nicolaï[1,3], Wannes Keulemans[4], Barbara De Coninck[4] and Annemie H. Geeraerd[1]**

[1] Division of MeBioS, Department of Biosystems (BIOSYST), KU Leuven, Leuven, Belgium, [2] Research Station for Fruit Cultivation, Department of Mycology, Sint-Truiden, Belgium, [3] Flanders Centre of Postharvest Technology (VCBT), Leuven, Belgium, [4] Division of Crop Biotechnics, Department of Biosystems (BIOSYST), KU Leuven, Leuven, Belgium

Apple is typically stored under low temperature and controlled atmospheric conditions to ensure a year round supply of high quality fruit for the consumer. During storage, losses in quality and quantity occur due to spoilage by postharvest pathogens. One important postharvest pathogen of apple is *Botrytis cinerea*. The fungus is a broad host necrotroph with a large arsenal of infection strategies able to infect over 1,400 different plant species. We studied the apple-*B. cinerea* interaction to get a better understanding of the defense response in apple. We conducted an RNAseq experiment in which the transcriptome of inoculated and non-inoculated (control and mock) apples was analyzed at 0, 1, 12, and 28 h post inoculation. Our results show extensive reprogramming of the apple's transcriptome with about 28.9% of expressed genes exhibiting significant differential regulation in the inoculated samples. We demonstrate the transcriptional activation of pathogen-triggered immunity and a reprogramming of the fruit's metabolism. We demonstrate a clear transcriptional activation of secondary metabolism and a correlation between the early transcriptional activation of the mevalonate pathway and reduced susceptibility, expressed as a reduction in resulting lesion diameters. This pathway produces the building blocks for terpenoids, a large class of compounds with diverging functions including defense. 1-MCP and hot water dip treatment are used to further evidence the key role of terpenoids in the defense and demonstrate that ethylene modulates this response.

Keywords: ***Botrytis cinerea***, ***Malus* × *domestica (Borkh)***, **mevalonate (MVA) pathway, ethylene, phytopathology, RNAseq, hot water dipping**

OPEN ACCESS

Edited by:
Sergio Ruffo Roberto, State University of Londrina, Brazil

Reviewed by:
Fangcheng Bi, Guangdong Academy of Agricultural Sciences, China
Simona Marianna Sanzani, International Centre for Advanced Mediterranean Agronomic Studies, Italy

****Correspondence:***
Annemie H. Geeraerd
annemie.geeraerd@kuleuven.be

†Present address:
Willem Gruyters, Flemish Institute for Technological Research (VITO), Mol, Belgium

Specialty section:
This article was submitted to Food Microbiology, a section of the journal Frontiers in Microbiology

Received: *18 October 2021*
Accepted: *14 February 2022*
Published: *12 May 2022*

Citation:
Naets M, Van Hemelrijck W, Gruyters W, Verboven P, Nicolaï B, Keulemans W, De Coninck B and Geeraerd AH (2022) Time Is of the Essence—Early Activation of the Mevalonate Pathway in Apple Challenged With Gray Mold Correlates With Reduced Susceptibility During Postharvest Storage. Front. Microbiol. 13:797234. doi: 10.3389/fmicb.2022.797234

INTRODUCTION

Apple (*Malus* × *domestica* Borkh.) is the third most produced fruit with a global total of about 83 million tons in 2017 (Food and Agriculture Organization [FAO], 2019). It is a seasonal fruit harvested in autumn and subsequently stored under low temperature and controlled atmospheric conditions to ensure year round supply of high quality fruit. During this storage, part of the fruit is lost due to spoilage by postharvest pathogens. An exploratory study we conducted for commercially grown and managed "Nicoter" apple found that the model necrotroph *Botrytis cinerea* had the third highest incidence (Naets et al., 2020).

B. cinerea, commonly known as gray mold, has a host range spanning over 1,400 species (Elad et al., 2016). A survey about fungal phytopathogens held by the journal *Molecular Plant Pathology* among researchers in the field considered *B. cinerea* the second most important fungal pathogen (Dean et al., 2012). Being a necrotroph, *B. cinerea* kills host cells for nutrition using a diverse arsenal of cell wall degrading enzymes (CWDEs), toxins and effectors. The fungus manipulates the plant's defense response in his favor, inducing the hypersensitive response (HR) and programmed cell death (PCD), while suppressing other defense responses (Govrin and Levine, 2002; González et al., 2016).

Plants are under continuous threat of opportunistic and pathogenic microorganisms. During evolution, plants developed several mechanisms to recognize these attackers and mount a defense response. Recognition starts by surface-localized pattern recognition receptors (PRRs) or receptor-like proteins (RLPs) that bind well conserved microbe-associated molecular patterns (MAMPs) or damage-associated molecular patterns (DAMPs); the latter are formed from the plant itself by for instance breakdown of the cell wall. Recognition of MAMPs/DAMPs results in a signaling cascade that triggers innate immunity known as pathogen-triggered immunity (PTI) (Jones and Dangl, 2006; Boller and Felix, 2009). To circumvent PTI, pathogens can secrete effectors that prevent perception of MAMPs/DAMPs, e.g., ligands that bind chitin oligomers, or interfere with downstream signaling. This then results in effector-triggered susceptibility (ETS). As an answer to ETS, plants have evolved to recognize pathogen effectors through resistance (R) proteins, which are often nucleotide-binding leucine-rich repeat (NB-LRRs) proteins. Recognition of effectors then results in effector-triggered immunity (ETI), which often leads to cell death through the HR (Jones and Dangl, 2006; Boller and Felix, 2009). This classical zig-zag model does not hold for broad host necrotrophs (BHNs) such as *B. cinerea*, however. In this case, defense is quantitative (varying levels of susceptibility depending timing and intensity of an array of defense mechanisms) and variations in the level of susceptibility between species are thought to be linked to differences in innate immunity (Mengiste, 2012; Windram et al., 2012).

Most of this knowledge was established in model systems such as *Arabidopsis*, but a lot less research has been conducted on non-model systems. Transferring this knowledge becomes even trickier when studying fruit where for instance ethylene (ET) could have a dual role in defense and ripening. Still, understanding the defense response in fruit is fundamental, because losses due to pathogens can have an important economic impact.

Global transcriptome expression studies of domesticated apple have been carried out previously to investigate the interaction with the necrotrophic fungal pathogen *Pencillium expansum* (Vilanova et al., 2014; Ballester et al., 2017). Comparison with the incompatible *P. digitatum* showed that detoxification of reactive oxygen species (ROS) and upregulation of phenylpropanoid biosynthesis pathway play a crucial role (Vilanova et al., 2014). Comparing the response with that of the resistant *M. sieversii* demonstrated that a rapid activation of defenses could be a determinative factor in the outcome (Ballester et al., 2017).

In the current work, we wanted to deepen the knowledge about the defense response of apple. To this end, we present here the first global transcriptomic study of the *M.* × *domestica-B. cinerea* interaction in which we demonstrate the activation of PTI and secondary metabolism. We were able to correlate gene expression with infection success and thereby providing evidence for the importance of the early transcriptional activation of the mevalonate pathway that provides precursors for terpenoid biosynthesis. We further strengthen the case for the key role of terpenoids in defense through the use of 1-MCP and hot water dip (HWD) treatments, and demonstrate that ET plays a modulating role in this response.

MATERIALS AND METHODS

Plant and Fungal Material

Apples of cultivar "Jonagored" (an economically important variety in Flanders) were harvested randomly at commercial maturity according to guidelines by the Flanders Centre of Postharvest Technology on 26 September 2016 from a field in Rillaar (Beglium, 50.963293°N, 4.879464°E). The trees were planted in the winter of 2014 and were grafted onto an M9 rootstock. The plant density was 1.5 m by 3.75 m. A standard integrated pest management schedule was followed, except that 1 month prior to harvest no fungicide treatments were carried out. Harvested fruit were stored at 1°C with regular atmosphere (RA) until 29 September 2016 when atmospheric conditions were changed to controlled atmosphere (CA; 1% O_2 and 2.5–3.0% CO_2). The experiment was started after a total of about 15 w of storage. Apples were transferred to 22°C with RA 1 day prior to the start of the experiment. The apples used in the experiment had an average mass of 266 ± 6.1 g (mean ± se, n = 108) and respiration rate of 159 ± 7.4 nmol kg^{-1} s^{-1} (mean ± se, n = 5). Other quality measures are given in **Table 1** and indicate that apples had not ripened much since harvest where respiration rate was similar at levels of 165 ± 9.7 nmol kg^{-1} s^{-1} (mean ± se, n = 10). Fruit were not disinfected as our previous research indicated that this could result in a physiological response and damage to the fruit surface, both of them potentially able to bias the study results (Naets et al., 2018).

TABLE 1 | Average firmness, total soluble solids (TSS) content and hue of the batch of "Jonagored" apples at harvest (26 September 2016) and the start of the experiment (12 January 2017).

Side	Firmness (N)	TSS (%)	Hue (°)
Harvest			
Shadow	84 ± 3.6	15.4 ± 0.38	79 ± 3.5
Sun	88 ± 1.8	16.6 ± 0.31	
Start of experiment			
Shadow	94 ± 2.7	16.5 ± 0.24	87 ± 2.6
Sun	98 ± 2.2	17.5 ± 0.23	

Errors denote the standard error of the mean (Harvest: n = 20, Start of experiment: n = 15).

A *B. cinerea* B05.10 isolate was kindly provided by Julia Schumacher (Institut für Biologie and Biotechnologie der Pflanzen). The fungus was cultured on potato dextrose agar in the dark. After 5–7 days when the colony reached the periphery of the petri dish the culture was exposed to near-UV light overnight to induce sporulation and subsequently put back in the dark for another 5–7 days. Spores were harvested by flooding the plates with 5 mL of sterile distilled water. The suspension was filtered through glass wool and washed twice with 12 g L^{-1} potato dextrose broth (PDB) in order to remove any remaining mycelia. Finally, the spore concentration was adjusted to 10^6 conidia mL^{-1}.

RNAseq Experiment

Three wounds were made on the shadow side of the fruit at its equator with a depth of 10.5 mm and a diameter of 1.8 mm. This method had been shown to give reproducible infections. The side of the fruit was arbitrary, but important to fix, because previous research of us showed that the side of the fruit could have an effect on susceptibility to *B. cinerea* (Naets et al., 2019). Each wound was inoculated with either 2 μL of the spore suspension (which will be denoted as *B. cinerea* inoculated) or 12 g L^{-1} PDB (mock inoculated). The control consisted of samples from non-treated fruit (not wounded, not inoculated). The middle one of the three inoculated spots was sampled at specific time points post inoculation using a cork borer of size 8 (13.75 mm diameter). Samples were cut off at a depth of 15 mm and were immediately quenched in liquid nitrogen. The two outer spots were not sampled and, in the case of *B. cinerea* inoculated spots, were evaluated for lesion diameter 96 hpi (hours post inoculation) using a digital caliper. An example of a sampled apple at 96 hpi is given in **Supplementary Figure 1**.

Fruits were not treated (control), mock or *B. cinerea* inoculated. Immediately within the first 5 min after treatment (0), at 1, 12, and 28 hpi three biological replicates (apples) were sampled. This experiment was carried out in triplicate, thus giving 3 independent experiments with each 3 biological replicates per treatment per time point. The total number of samples available for sequencing was thus 36 (3 treatments ×x 3 replicates × 4 time points). Additionally, for the samples taken at 28 hpi, five biological replicates from each treatment were analyzed for metabolic changes by GC-MS and LC-MS to confirm transcriptomic results. The time point of 28 hpi was the earliest one where measurable differences in metabolite levels could reasonable be expected.

RNA Extraction and Sequencing

Total RNA was extracted by adding 800 μL of CTAB extraction buffer (2% CTAB, 2% PVP40, 100 mM Tris-HCl (pH8), 25 mM EDTA, 2 M NaCl, 0.5 g L^{-1} spermidine, 1% β-mercaptoethanol) to 150–200 mg finely crushed tissue sample. Subsequently, 80 μL N-laurylsarcosine sodium salt (20%) and a glass bead were added, and the mixture was incubated for 10 min in a thermomixer set at 70°C and 1,400 rpm. Next, 900 μL chloroform:isoamylalcohol (24:1) was added and the samples were centrifuged at 21,500 G and 22°C for 10 min. The supernatant was transferred to the gDNA eliminator spin column of the RNeasy Plus Mini kit from Qiagen (Manchester, United Kingdom). From here on, the manufacturer's guidelines for the kit were followed. Quality and concentration of the extracts were verified using a NanoDrop™ 2,000 (Leusden, Netherlands) and by gel electrophoresis. Equal amounts of RNA were pooled across experiments to obtain three unique replicates per treatment per time point. The pooled RNA was precipitated by adding 2 vol 100% ethanol and 0.1 vol 3 M sodium acetate (pH5.2–5.5), incubating at -80°C overnight, and centrifugating at 21,500 G. The precipitate was washed twice with 70% ethanol before being resuspended in nuclease free water. All A260/A280 and A260/A230 ratios were above 2. Pooled samples of with at least 4 μg RNA were sent to Polar Genomics (New York, United States) for sequencing. A stranded library was constructed for each sample with fragment lengths of 75 bp, as described by Zhong et al. (2011). Sequencing was performed on an Illumina Nextseq500 platform (San Diego, United States). Generated reads were cleaned up and subsequently aligned to the "Golden Delicious" ("Jonagold" is a cross of "Jonathan" and "Golden Delicious", and "Jonagored" is a color mutant of "Jonagold") apple genome (Daccord et al., 2017) and *B. cinerea* genome (Van Kan et al., 2017).

RNAseq Analysis

Statistical analysis was carried out in R (R Development Core Team, 2011). Differential expression analysis was performed using the DESeq2 package (Love et al., 2014). For each time point, differentially expressed genes (DEGs) were identified for the comparison of *B. cinerea* inoculated with control, and *B. cinerea* inoculated with mock inoculated fruit. DEGs were filtered for those showing at least twofold up or downregulation and subsequently filtered for those that were differentially regulated in both comparisons. The resulting DEGs were considered significantly differentially expressed. Heat maps for a specific enzyme were created from all genes coding for isozymes exhibiting significant differential expression on at least one time point by taking a weighted mean of the $\log_2$ fold change (LFC) as described by the following formula.

$$LFC = \frac{\sum_i \left[\left|d_{i1} + d_{i2}\right| \cdot LFC_i\right]}{\sum_i \left|d_{i1} + d_{i2}\right|}$$

In this formula d_{i1} and d_{i2} are the difference in expression in transcripts per million (TPM) for the i-th isozyme between

B. cinerea inoculated and control and *B. cinerea* inoculated and mock inoculated fruit, respectively.

Enrichment Analysis

Enrichment of specific functions was analyzed using significant DEGs as test set, and all genes exhibiting at least 1 TPM on average in control and mock inoculated samples were used as reference. Gene ontology (GO) enrichment analysis was carried out in BLAST2GO (Götz et al., 2008). Additionally, enrichment of pathways listed on the Kyoto Encyclopedia of Genes and Genomes (KEGG) database (Kanehisa, 2000) was tested. Enrichment of KEGG database pathways was scripted in R by mapping genes to their pathways, performing a Fisher exact test for each pathway, and correcting the *p*-values for multiple hypothesis testing using the Benjamini-Hochberg procedure.

Gas Chromatography Mass Spectrometry

Ground apple samples (15 appels, 28 hpi) were extracted with 1 mL of methanol at room temperature for 2.5 h, followed by centrifugation. Under vacuum, 450 μL of the supernatant was evaporated to dryness, and the obtained residue was derivatized for gas chromatography mass spectrometry (GC-MS) analysis by adding 10 μL of pyridine and 50 μL of N-Methyl-N-(trimethylsilyl) trifluoroacetamide (Sigma-Aldrich, Saint Louis, MO, United States). GC-MS analysis was carried out using a 7890B GC system equipped with a 7693A Automatic Liquid Sampler and a 7,250 Accurate-Mass Quadrupole Time-of-Flight MS system (Agilent Technologies, Santa Clara, CA, United States). 1 μL of the sample was injected in splitless mode with the injector port set to 280°C. Separation was achieved with a VF-5 ms column (30 m × 0.25 mm, 0.25 μm; Varian CP9013; Agilent Technologies) with helium carrier gas at a constant flow of 1.2 mL min^{-1}. The oven was held at 80°C for 1 min post-injection, ramped to 280°C at 5°C min^{-1}, held at 280°C for 5 min, ramped to 320°C at 20°C min^{-1}, held at 320°C for 5 min, and finally cooled to 80°C at 50°C min^{-1} at the end of the run. The MSD transfer line was set to 280°C and the electron ionization energy was 70 eV. Full EI-MS spectra were recorded between m/z 50–800 at a resolution of > 25,000 and with a solvent delay of 7.8 min. The resulting GC-MS chromatograms were converted to SureMass format, deconvoluted, and metabolites corresponding to the deconvoluted spectra were identified using the MassHunter Unknowns Analysis software package (Agilent Technologies) and the NIST 17 mass spectral library. A match factor of 75.0 was used as cut-off for compound identification. For each metabolite, a unique quantifier ion was chosen and used for quantification using the MassHunter Quantitative Analysis (for Q-TOF) software package (Agilent Technologies). In total, 285 metabolites were detected and quantified, of which 117 (41%) were identified based on their EI-MS spectra. Data post-processing was done with MetaboAnalyst 3.0.

Liquid Chromatography Mass Spectrometry

The ground apple samples were extracted with 1 mL of methanol at room temperature for 2.5 h, followed by centrifugation. Under vacuum, 450 μL of the supernatant was evaporated to dryness, and the obtained residue was re-suspended in 100 μL cyclohexane/100 μL MilliQ water. The samples were centrifuged, and 90 μL of the lower water phase was transferred to a 96-well plate for LC-MS analysis. LC-MS analysis was performed on an ACQUITY UPLC I-Class system (Waters) consisting of a binary pump, a vacuum degasser, an autosampler, and a column oven. Chromatographic separation was carried out on an ACQUITY UPLC BEH C18 (150 × 2.1 mm, 1.7 μm) column from Waters, and temperature was maintained at 40°C. A gradient of two buffers was used: buffer A (99:1:0.1 water:acetonitrile:formic acid, pH 3) and buffer B (99:1:0.1 acetonitrile:water:formic acid, pH 3), as follows: 95% A for 0.1 min decreased to 50% A in 30 min, decreased to 0% from 30 to 41 min. The flow rate was set to 0.35 mL min^{-1}, and the injection volume was 15 μL. The UPLC system was coupled to a Synapt G1 Q-TOF hybrid mass spectrometer (Waters). The LockSpray ion source was operated in negative electrospray ionization mode under the following specific conditions: capillary voltage, 3 kV; reference capillary voltage, 2.5 kV; cone voltage, 37 V; extraction cone, 3.5; source temperature, 120 °C; desolvation gas temperature, 400 °C; desolvation gas flow, 550 L h^{-1}; and cone gas flow, 50 L h^{-1}. The collision energy for full MS scan was set at 6 eV, for DDA MSMS ramped from 10 to 20 eV for low mass and from 20 to 45 eV for high mass. Mass range was set from 100 to 1,200 Da. Nitrogen (greater than 99.5%) was employed as desolvation and cone gas. Leucin-enkephalin (250 pg μL^{-1} solubilized in water:acetonitrile 1:1 [v/v], with 0.1% formic acid) was used for the lock mass calibration, with scanning every 1 min at a scan time of 0.1 s. Centroid data were recorded through Masslynx Software v4.1 (Waters). Data processing was performed with Progenesis QI software version 2.4 (Waters), data post-processing was done with MetaboAnalyst 3.0.

1-Methylcyclopropene and Hot Water Dipping Experiments

Apples from the same trees as the RNAseq experiment were harvested on 18 September 2018 and were either dipped the same day in water of 50°C for a duration of 5 min (HWD5) or exposed the next day to 625 nL L^{-1} 1-methylcyclopropene (1-MCP) at 1°C for 24 h. Fruit were subsequently transferred to the same CA conditions as described above. At regular time points, a sample of fruit was taken out of CA storage to carry out an inoculation experiment as described above. Samples for gene expression analysis were taken from both the sun and shadow side of non-inoculated fruit at harvest and after 29 w of CA storage for HWD5 treatment, and after 12 and 29 w of CA storage for 1-MCP treatment. It was decided to take two time points to evaluate if the fruit response diminished over time. Samples were taken with a cork borer of size 8 (13.75 mm diameter) and were divided into peel (0–3 mm) and flesh (4–15 mm) tissue.

Quantitative Reverse Transcription Polymerase Chain Reaction

cDNA was synthesized using the Quantitect Reverse Transcription kit (Qiagen, United Kingdom) following the manufacturer's specifications. RT-qPCR reactions were carried out with SsoAdvanced^{TM} Universal SYBR Green Supermix (Bio-rad, Belgium) and cycling settings: 95°C for 10 min followed by 40 cycles of 95°C for 10 s and 63°C for 30 s. As a reference we used ubiquitin-conjugating enzyme E2 (*UBC*) which was shown to have a stable expression in apple under a plethora of postharvest conditions (Storch et al., 2015). Primer sequences used are listed in **Supplementary Table 1**.

Temperature Simulations

Thermal simulations of heating and cooling of a single apple were performed in ANSYS 19.0 CFX (ANSYS, Inc., Canonsburg, Pennsylvania, United States). Fourier's second law of transient conduction was solved with constant uniform thermal properties. The thermal conductivity, specific heat and density of apple were 0.3972 W m^{-1} K^{-1}, 3,455 J kg^{-1} K^{-1} and 800 kg m^{-3}, respectively (Gruyters et al., 2018). For heating in water, it was assumed that the surface heat transfer coefficient was infinitely large, such that a Dirichlet boundary condition with a constant surface temperature of 50°C was implemented. During the cooling in air at 20°C, it was assumed that the surface heat transfer coefficient was 20 W $m^{-2}°C^{-1}$. The model equations were solved on the geometry of a "Jonagold" apple (a mutant of "Jonagored" for which a geometry was available) with an approximate diameter of 7 cm, of which a CAD surface was generated based on an X-ray computed tomography scan (Gruyters et al., 2018). A tetrahedral finite volumes mesh with 118,221 elements and 22,505 nodes was used for the numerical solution of the model in ANSYS. Transient simulations were performed with a second order backward Euler scheme with a time step of 10 s during heating and 30 s during cooling. The iterative convergence criterion was 10^{-7} RMS of the residual of the energy equation with a maximum of 10 iterations per time step. CPU time was 3 min 30 s for 5 min of heating on an Intel Xeon CPU E5-2630 0 @ 2.30 GHz. The following conditions were simulated: heating in water for 3, 4 and 5 min at 50°C, each time followed by air cooling at 20°C for 1 h.

RESULTS

RNA Sequencing

A total of 506,119,623 reads were generated using an Illumina Nextseq500 platform. After cleanup of the reads, a total of 470,274,412 high quality reads remained, averaging about 13 million reads per sample. An overview of the number of reads per sample and the amounts removed at each cleanup step is given in **Supplementary Table 2**. On average about 93 and 0.42% of the genes could be mapped to the *M.* × *domestica* and *B. cinerea* genome, respectively. The fraction of reads assigned to *B. cinerea* increased with time after inoculation and reached an average of 4.37% at 28 hpi.

Differential regulation of gene expression was tested using DESeq2 in R (Love et al., 2014). A total of 6,588 genes were identified as significantly upregulated of which 3,876 exhibited a fold change of more than 2 on at least one time point, and a total of 3,616 genes were identified as significantly downregulated of which 899 had a fold change of at least 2 on at least one time point (**Table 2**).

A principal component analysis (PCA) on the 500 most variable (standard setting of plotPCA function from DESeq2) apple genes after regularized log transformation demonstrates that the replicates had comparable results (**Figure 1**). Furthermore, plotting of replicate samples against one another (**Supplementary Figures 2–5**) showed high correlations averaging 98.8 ± 0.001% (se, n = 36). This proves the reproducibility of the assay and sequencing technique used.

The PCA biplot (**Figure 1**) shows that control samples of all time points cluster closely together, signifying that control samples did not display transcriptional changes on the same scale as the mock or *Botrytis* inoculated samples for the duration of the experiment. Furthermore, changes due to mock treatment were also much smaller than due to *Botrytis* inoculation. Samples taken immediately after administering the treatment were designated as 0 hpi, in practice, they were taken about 1–5 min after inoculation. The mock inoculated samples of 0 hpi were very similar to the control samples, while the *Botrytis* inoculated samples of 0 hpi were already clearly distinct from the control (**Figure 1**). This demonstrates that some responses upon pathogen recognition were very rapid. Mock and *Botrytis* inoculated samples of 1 hpi lie closely together in the plot, which indicates that the early wound and defense response strongly overlapped. This is reflected in the fact there were no DEGs at 1 hpi.

For a more in depth analysis, annotation data was obtained from the Genome Database for Rosaceae (GDR; Jung et al., 2004).[1] This database contains a list of KEGG ortholog annotations for about 24.6% of the apple genome. This translated to about 19.5% annotation of the expressed genes in our data (mean tpm > 1) and 26.3% of the DEGs. Also a list with GO annotation for 59.2% of the apple genome was obtained. This amounted to 63.5% of expressed genes and 69.2% of the DEGs. In the following when we talk about pathways, we mean the transcriptional regulation of these pathways.

For our analysis, we were guided by the results from an enrichment analysis of GO terms and KEGG pathways (**Supplementary Figure 6** and **Supplementary Tables 3**, **4**). This revealed upregulation of secondary metabolism, especially for phenylpropanoids and terpenoids, and a role for hormone regulation. A summary of key responses is given in **Figure 2** and **Supplementary Table 5** where a distinction is made between recognition, signaling, alteration of gene expression and defense response. Some key aspects will be discussed in brief below.

Pathogen Recognition

Induction of PTI through recognition of M/DAMPs is mediated by PRRs and RLPs. The largest family of plant receptors

[1] www.rosaceae.org

TABLE 2 | Differential expression analysis using DESeq2 in R.

Time point (hpi)	*Botrytis* inoculated vs. control	*Botrytis* inoculated vs. mock inoculated	Overlap	Abs (LFC) > 1
0	167 + 60	71 + 5	67 + 0	65 + 0
1	539 + 13	1 + 0	0 + 0	0 + 0
12	2,636 + 316	1,561 + 32	1,501 + 8	1,100 + 0
28	8,016 + 5,830	7,112 + 4,364	6,573 + 3,612	3,863 + 899
Overall (0, 1, 12, 28)	8,199 + 5,981	7,136 + 4,389	6,588 + 3,616	3,876 + 899

For each time point the number of genes up + downregulated are displayed for the comparison of Botrytis inoculated samples with the control, and Botrytis inoculated samples with mock inoculated samples. Additionally, the number of up + downregulated genes that overlap between those two comparisons is given, and the number of these genes that exhibited an absolute log_2 fold change of at least 1 compared to mock inoculation. Up + downregulated.

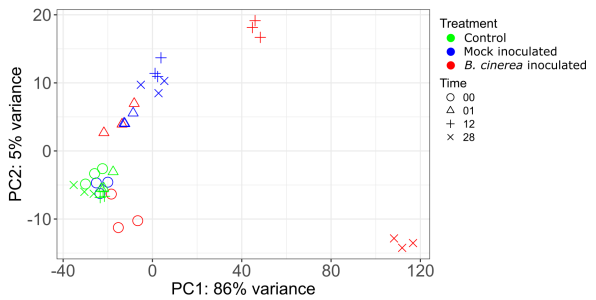

FIGURE 1 | Biplot of a PCA performed on the regularized log transformed counts of the top 500 most variable genes showing the position of each sample on PC1 and PC2.

are receptor-like kinases (RLKs), which are PRRs. One such RLK is the WALL-ASSOCIATED KINASE (WAK) that detects oligogalacturonides (OGs) (Decreux and Messiaen, 2005), DAMPs formed during breakdown of the plant cell wall by the fungus. Because no WAKs were annotated in the KEGG ortholog list obtained for apple from the GDR (Jung et al., 2004), we extracted WAK protein sequences from the Apple Gene Function and Gene Family Database (AppleGFDB, Zhang et al., 2013). We BLASTp searched these sequences in the new apple genome and used an *E*-value cutoff of 10^{-100}. This resulted in 47 WAK genes. Of these 47, we retrieved 17 in our DEG set. Chitin is the main component of the fungal cell wall. Chitin oligosaccharides can be detected by the plant's CHITIN ELICITOR RECEPTOR KINASE 1 (CERK1) (Miya et al., 2007). We retrieved four genes in the apple genome that were annotated with CERK1 and three of these were significantly upregulated in *B. cinerea* inoculated samples. In apple there are five genes annotated as the LEUCINE RICH REPEAT RECEPTOR-LIKE KINASE (LRR-RLK) BAK1. One of these, *MD08G1221700*, was significantly upregulated in our data (**Supplementary Table 5**).

Defense Signaling and Transcriptional Reprogramming

One of the earliest responses to pathogen recognition that occurs within the first minutes is the establishment of Ca^{2+} influx into the cell (Reddy et al., 2011), established by CYCLIC NUCLEOTIDE-GATED CHANNELS (CNGCs). Our data contains 11 out of 40 differentially regulated CNGCs. The Ca^{2+} signal is transduced by sensor relays, e.g., CALMODULIN (CaM; 5/16 significantly upregulated), and sensor responders, e.g., CALCIUM-DEPENDENT PROTEIN KINASE (CDPK; 6/32 differentially regulated) and Ca^{2+}/CaM-DEPENDENT PROTEIN KINASEs (CaMKs; 1/2 significantly upregulated). CDPKs can phosphorylate RESPIRATORY BURST OXIDASE HOMOLOGs (RBOHs; 1/8 significantly upregulated) and TFs (Reddy et al., 2011).

ROS are formed quickly upon wounding or pathogen challenge. They can have a direct role in stopping the pathogen by being directly toxic or by creating barriers through oxidative cross-linking of lignin precursors and cell wall glycoproteins (Torres, 2010). ROS also play an indirect role activating defense responses as second messengers. This is achieved by activating MITOGEN-ACTIVATED PROTEIN KINASE (MAPK) cascades. To achieve full activation of the MAPKs MPK3 and MPK6, OXI1 is required (Rentel et al., 2004). The apple genome has two genes that are annotated with OXI1 of which 2 were significantly upregulated. Two MPK3 and two MPK6 genes are annotated in the apple genome, and of these, respectively, one and zero genes were upregulated. The BAK1, CERK1 and WAK receptors also make use of MAPK signaling cascades that go through MAPK KINASE KINASE (MAPKKK), MAPK KINASE (MAPKK) and finally MAPK. Our expression set has two MAPKKK DEGs annotated with MEKK1, two MAPKK DEGs annotated with MKK2 and MKK9, and five MAPK DEGs annotated with MPK3, MPK4 (3 genes) and MPK7/14 (**Supplementary Table 5**).

Plant hormones play an important role in modulating plant responses to pathogens. Defense responses are regulated by the two major players salicylic acid (SA) and jasmonic acid (JA), while other hormones such as ET and abscisic acid (ABA) play a role in fine tuning the response (Pieterse et al., 2012; Bürger and Chory, 2019). In general, SA signaling confers resistance to (hemi-) biotrophic pathogens, and JA and ET signaling leads to resistance against necrotrophic pathogens. We found significant upregulation of JA biosynthetic genes coding for LIPOXYGENASE (LOX), ALLENE OXIDE SYNTHASE (AOS), ALLENE OXIDE CYCLASE (AOC), OXO-CIS-10,15-PHYTODIENOIC ACID REDUCTASE (OPR3) and 3-OXO-2-(CIS-2′-PENTENYL)-CYCLOPENTANE-1-OCTANOIC ACID-8:0 CoA LIGASE (OPCL1). SA biosynthesis can be achieved through the ISOCHORISMATE SYNTHASE (ICS) pathway or the PHENYLALANINE AMMONIA-LYASE (PAL) pathway. We found one gene annotated with ICS that was not

FIGURE 2 | Overview of gene expression responses of "Jonagored" apple to *B. cinerea* inoculation. BAK1, Brassinosteroid insensitive-associated receptor kinase 1; CERK1, Chitin elicitor receptor kinase 1; WAK, Wall-associated kinase-like; CNGC, Cyclic nucleotide gated channel; CDPK, Calcium-dependent protein kinase; CAMK, Ca^{2+}/calmodulin-dependent protein kinase; RBOH, Respiratory burst oxidase homolog; OXI1, Oxidative signal-inducible1 serine/threonine-protein kinase; MEKK, Mitogen-activated protein kinase kinase kinase; MKK, Mitogen-activated protein kinase kinase; MPK, Mitogen-activated protein kinase; ACS1/2/6, 1-Aminocyclopropane-1-carboxylate synthase 1/2/6; ACO, 1-Aminocyclopropane-1-carboxylate oxidase; ET, Ethylene; ETR, ET receptor; EIN3, ET-insensitive protein 3; ERF1, ET-responsive transcription factor 1; EREBP, ET-responsive element binding protein; SA, Salicylic acid; SGT SA glucosyltransferase; NPR1, Non-expresser of PR genes 1; TGA, TGACG binding factor 1; ABA, Abscisic acid; NCED1, 9-Cis-epoxycarotenoid dioxygenase 1; AAO3, Abscisic aldehyde oxidase; PP2C, Protein phosphatase 2C; SnRK2, Serine/threonine-protein kinase SRK2; ABA8H, ABA 8'-hydroxylase; ABF, ABA responsive element binding factor; JA, Jasmonic acid; LOX, Lipoxygenase; AOS, Allene oxide synthase; AOC, Allene oxide cyclase; OPR3, 12-Oxo-cis-10,15-phytodienoic acid reductase; OPCL1, 3-Oxo-2-(cis-2'-pentenyl)-cyclopentane-1-octanoic acid-8:0 CoA ligase; JAAH, Jasmonoyl-L-amino acid hydrolase; JAZ, JA ZIM domain protein; WRKY, Transcription factor WRKY; MYB, Myeloblastosis oncogene transcription factor; HSF, Heat shock transcription factor; NAC, NAM, ATAF1/2, and CUC transcription factor; Chi-B, basic endochitinase B; (+)-Neomenthol DH: (+)-Neomenthol dehydrogenase; CYP82G1, Cytochrome P450 family 82 subfamily G polypeptide 1; PAL, Phenylalanine ammonia-lyase; HSP70, Heat shock protein 70; PGIP, Polygalacturonase inhibiting protein; GST, Glutathione S-transferase.

differentially regulated. All four genes annotated as PAL were significantly upregulated. SA causes a redox change through activation of thioredoxins which leads to monomerization of NON-EXPRESSOR OF PR1 (NPR1), thereby facilitating its translocation to the nucleus. NPR1 then interacts with TGA transcription factors to effectuate changes in gene expression. DESeq2 analysis showed upregulated DEGs for NPR1 and TGA. Two of the four differentially expressed TGA genes identified by DESeq2 were upregulated and two were downregulated. Also biosynthesis of ET was upregulated with genes coding for 1-AMINOCYCLOPROPANE-1-CARBOXYLATE (ACC) SYNTHASE 1/2/6 (ACS1/2/6), ACC OXIDASE (ACO). ET signaling occurs by perception of ET by the ET RECEPTOR (ETR) localized in the endoplasmic reticulum. Binding of ET to the receptor causes inactivation of the ETR-CTR1 (CONSTITUTIVE TRIPLE RESPONSE 1) complex which leads to derepression of ET INSENSITIVE PROTEIN 2 (EIN2). EIN2 activates the transcription factor EIN3, which in turn causes transcription of other transcription factors such as ERF1. Our data shows upregulation of genes coding for ETR, EIN3, and ERF1 (**Supplementary Table 5**). An overview is provided in **Supplementary Figure 7**.

Signaling upon pathogen recognition should eventually lead to transcriptional reprogramming by activating or repressing transcription factors. Our data contained DEGs encoding transcription factors of several different families such as 5 WRKYs, 21 MYBs (myeloblastosis oncogene), 12 HSFs (heat shock factors) and 40 NACs (NAM, ATAF1/2, and CUC) (**Supplementary Table 5**).

Transcriptional Reprogramming of the Metabolism for Defense

Our data provides evidence (**Supplementary Table 6**) in support that primary metabolism is reprogrammed to provide energy for the defense response (Bolton, 2009). Photosynthesis was significantly downregulated with 6/17 genes coding for components of photosystem I, 4/32 genes coding for

components of photosystem II, 4/10 genes involved in light-harvesting complex I, and 6/20 genes involved in light-harvesting complex II significantly downregulated. Oxidation of fatty acids was upregulated (**Supplementary Figure 8**) with genes coding for LONG-CHAIN ACYL-CoA SYNTHETHASE (2/12), ACYL-CoA OXIDASE (2/6), ENOYL-CoA HYDRATASE/3-HYDROXYACYL- CoA DEHYDROGENASE (2/5), ACETYL-CoA ACYLTRANSFERASE 1 (2/3), and ACETYL-CoA C-ACETYLTRANSFERASE (2/3). Glycolytic activity was upregulated (**Supplementary Figure 9**) with DEGs for at 6-PHOSPHOFRUCTOKINASE 1 (PFK-1; 3/11), HEXOKINASE (1/9) and PYRUVATE KINASE (2/17). The final product of the glycolysis, pyruvate, is converted into acetyl-CoA by PYRUVATE DEHYDROGENASE (PDH). PDH is a complex of three enzymes (E1, E2, and E3) and E1 consists of two subunits (E1a and E1b). DEGs were identified for all of these components with 1 out of 3, 2 out of 3, 2 out of 9 and 1 out of 3 for E1a, E1b, E2, and E3, respectively. PDH is regulated by phosphorylation and dephosphorylation of E1a, respectively, inactivating and activating the complex. No DEGs were identified for PDH KINASE, while 8 out of 13 PDH PHOSPHATASE genes were significantly upregulated. Acetyl-CoA forms a crossroad in plant metabolism. This molecule is formed from oxidation of glucose, fatty acids and amino acids, and can be used as building block for biosynthesis of fatty acids, triglycerides, phospholipids, steroids and terpenoids. Acetyl-CoA can also be further oxidized in the tricarboxylic acid (TCA) cycle to yield precursors for the oxidative phosphorylation, thereby contributing to energy production. Our data shows significant upregulation of *citrate synthase, aconitate hydratase,* and *isocitrate dehydrogenase* indicating that the TCA cycle is upregulated.

Secondary metabolism denotes pathways that are not directly involved in vital life functions and entails a wide variety of metabolic pathways with diverging functions. One of them is the production of plant defense compounds including terpenoids and phenylpropanoids. Biosynthesis of terpenoids from acetyl-CoA starts by biosynthesis of the isoprenoid precursor isopentenyl pyrophosphate (IPP) through the mevalonate (MVA) pathway (cytosol; biosynthesis of sesquiterpenoids and triterpenoids; **Figure 3** and **Supplementary Table 6**) or the 2-C-Methyl-D-erythritol 4-phosphateZ (MEP) pathway (chloroplasts; biosynthesis of monoterpenoids, and diterpenoids). Our data shows a very distinct upregulation of the MVA pathway with significant upregulation of 2/2 HYDROXYMETHYLGLUTARYL-CoA (HMG-CoA) SYNTHASE (HMGS), 1/4 HMG-CoA REDUCTASE (HMGR), 2/2 MVA KINASE, 2/2 PHOSPHOMEVALONATE (MVA-5P) KINASE, and 2/2 MEVALONATEPYROPHOSPHATE (MVAPP) DECARBOXYLASE. The data suggests that IPP is further converted into sesquiterpenoids and triterpenoids with significant differential regulation of *farnesyl disphosphate* (FPP) *synthase* (*FPPS*; 4/4), FPP *farnesyltransferase* (*FPPFT*; 2/2), *squalene monooxygenase* (*SMO*; 10/15), *(-)-germacrene D synthase* (1/6), β-*amyrin synthase* (6/7) and β-*amyrin 28-monooxygenase* (8/14).

Phenylpropanoids are biosynthesized from phenylalanine (**Figure 4** and **Supplementary Table 6**). The key step in this pathway is the first conversion by PAL (**Dixon et al., 2002**). All of the four genes annotated with PAL were significantly upregulated in our data. Our data also shows differential regulation of C4H (TRANS-CINNAMATE 4-MONOOXYGENASE; 2/3), 4CL (4-COUMARATE:COA LIGASE; 2/7), C3H (4-COUMARATE 3-HYDROX YLASE; 2/3), HCT (4/17), COMT (CAFFEIC ACID/5-HYDROXYFERULIC ACID O-METHYLTRANSFERASE; 8/18), CALDH (CONIFERYL-ALDEHYDE DEHYDROGENASE; 1/5), CINNAMYL-ALCOHOL DEHYDROGENASE (10/20), PEROXIDASE (19/102), LACCASE (11/47), and CHALCONE ISOMERASE (CHI; 3/7).

Other metabolic responses detected in our data were differential regulation of cell wall metabolism with DEGs coding for 1,3-β-GLUCANASE (1/8), β-GLUCOSIDASE (8/46), CHITINASE (7/19), BASIC ENDOCHITINASE B (1/3) and POLYGALACTURONASE (PG) INHIBITING PROTEINs (PGIPs; 2/4) (**Supplementary Table 5**).

We attempted to verify some secondary metabolites by untargeted metabolomics. To this end, 5 of the sequenced samples of each treatment from 28 hpi were analyzed with GC-MS and LC-MS (**Supplementary Tables 8**, **9**). GC-MS analysis found significant accumulation of D-galacturonic acid, galactaric acid and glycerol, probably linked to pectin breakdown by *B. cinerea* polygalacturonases. Otherwise, almost no significant differences were found, likely due to this time point being too early for detecting significant metabolic changes.

Effectiveness of the Defense Response

In our experiment we sampled the middle of three inoculated spots. The outer spots were not sampled and the lesion diameter of these spots was recorded at 96 hpi. From other experiments we know that the correlation of the lesion diameter of the middle spot with the average of the outer two spots is about 88% ($p < 0.001$; **Supplementary Figure 10**). This allows us to correlate gene expression at a specific time point of sampling with later infection success, measured as lesion diameter at 96 hpi.

We analyzed the correlations between gene expression and infection severity at 96 hpi for the discussed pathways and found a striking image for the MVA pathway. This pathway showed a mostly negative correlation with infection success (i.e., higher expression led to lower susceptibility) and strong negative correlations occurred mostly at the early time points (**Figure 5**).

Effect of 1-Methylcyclopropene and HWD5 Treatment on Fruit Defense

In a next series of experiments we wanted to investigate the effect of a HWD of 5 min (HWD5), or 1-MCP treatment on the defense of apple against *B. cinerea*, and this as a function of time in CA storage. We carried out our pathogenicity assay on treated fruit after different durations of CA storage and found that both 1-MCP and HWD5 treatment lead to a significant increase in lesion diameter after 96 hpi (**Figure 6**).

We analyzed expression of *MPK3*, *MPK6*, *ERF1*, *PAL1*, *SMO1,* and two *SMO* homologs (denoted *SMO1* and *SMO2*) in peel and flesh tissue of control, HWD5 and 1-MCP treated fruit (**Figure 7**

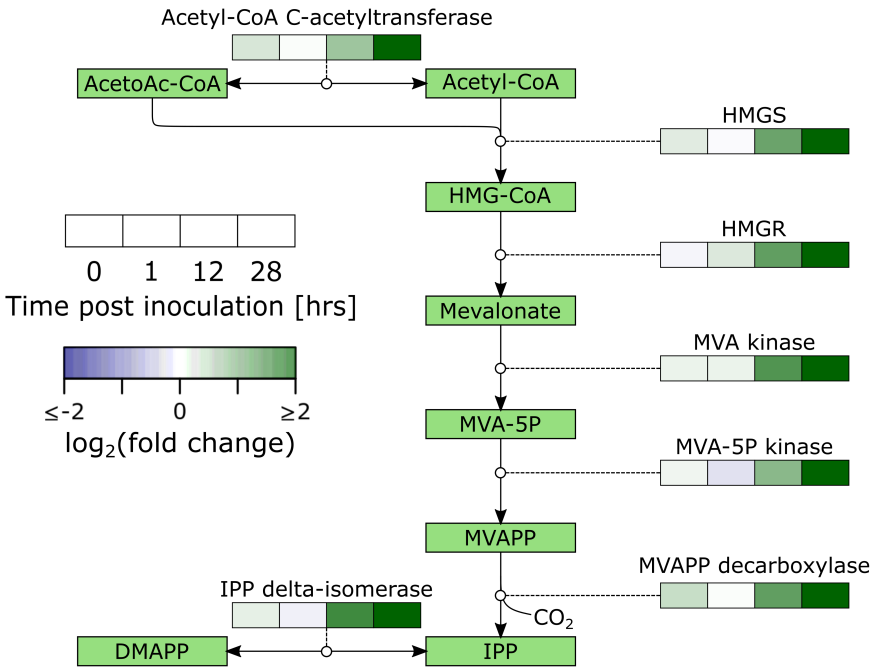

FIGURE 3 | Overview of the regulation of the mevalonate pathway in *B. cinerea* inoculated apples. Heat maps were constructed from genes with significant differential expression. AcetoAc-CoA, Acetoacetyl-CoA; HMG-CoA, Hydroxymethylglutaryl-CoA; HMGS, HMG-CoA synthase; MVA, Mevalonate; MVAPP, Mevalonatepyrophosphate; IPP, Isopentylpyrophosphate; DMAPP, Dimethylallylpyrophosphate.

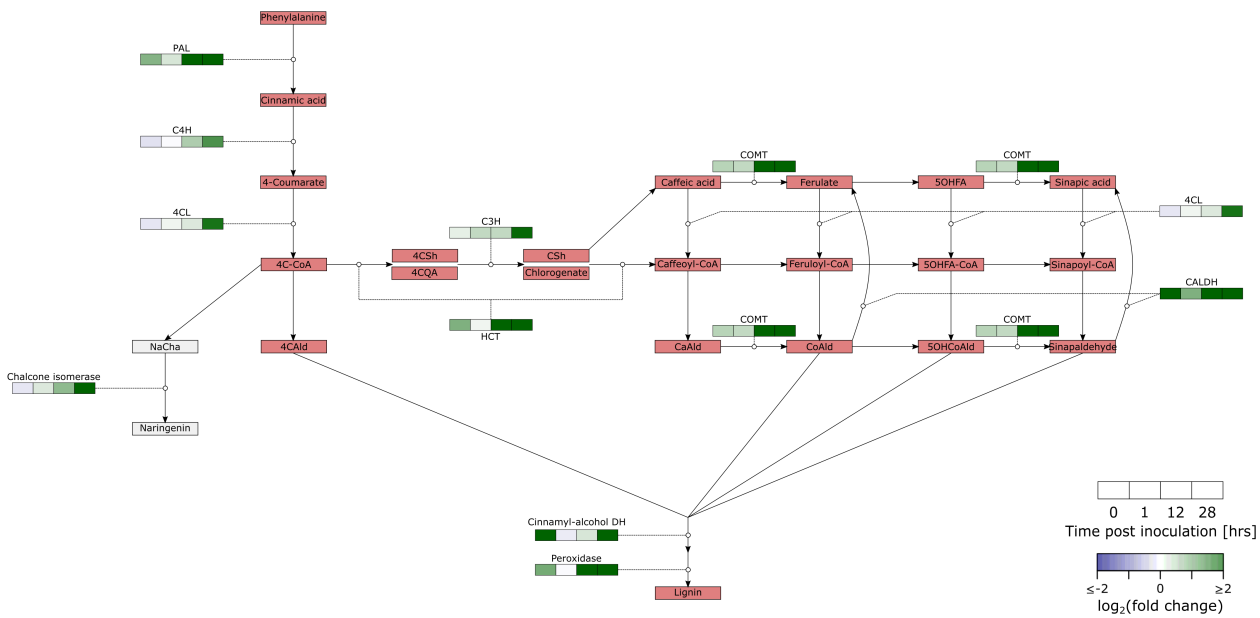

FIGURE 4 | Overview of the regulation of the phenylpropanoid pathway in *B. cinerea* inoculated apples. Heat maps were constructed from genes with significant differential expression. PAL, Phenylalanine ammonia-lyase; C4H, Trans-cinnamate 4-monooxygenase; 4CL, 4-Coumarate:CoA ligase; 4C-CoA, 4-Coumaroyl-CoA; C3H, 4-Coumarate 3-hydroxylase; HCT, Hydroxycinnamoyl-CoA shikimate:quinate hydroxycinnamoyl-transferase; COMT, Caffeic acid/5-hydroxyferulic acid O-methyltransferase; CALDH, Coniferyl-aldehyde dehydrogenase; 4CAld, 4-Coumaraldehyde; NaCha, Naringenin chalcone; 4CSh, 4-Coumaroyl shikimic acid; 4CQA, 4-Coumaroyl quinic acid; CSh, Caffeoyl shikimate; CaAld, Caffeylaldehyde; CoAld: Coniferaldehyde; 5OHFA, 5-Hydroxyferulic acid; 5OHCoAld, 5-Hydroxyconiferylaldehyde. Another class of secondary metabolic compounds are alkaloids. This is a diverse group of nitrogen containing molecules, often with a function in plant defense. Our expression set suggests that biosynthesis of tropane alkaloids is upregulated in *B. cinerea* infected tissue. ARGININE DECARBOXYLASE (AGD) was significantly upregulated (2/2). AGD converts Arginine into agmatine, which can be further converted into putrescine and finally tropinone. Our data contained 9 DEGs for TROPINONE REDUCTASE I (TR-I; 16 genes) which reduces tropinone to tropine.

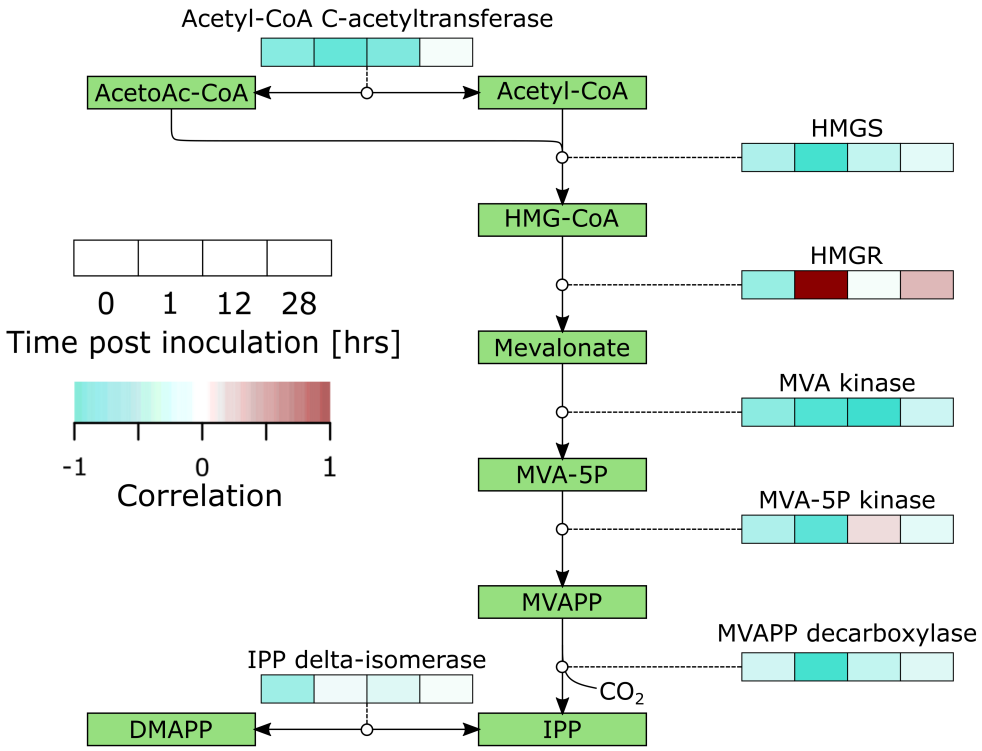

FIGURE 5 | Overview of correlations of the mevalonate pathway gene expression with lesion diameter at 96 hpi in *B. cinerea* inoculated apples. Heat maps were constructed from genes with significant differential expression. AcetoAc-CoA, Acetoacetyl-CoA; HMG-CoA, Hydroxymethylglutaryl-CoA; HMGS, HMG-CoA synthase; MVA, Mevalonate; MVAPP, Mevalonatepyrophosphate; IPP, Isopentylpyrophosphate; DMAPP, Dimethylallylpyrophosphate.

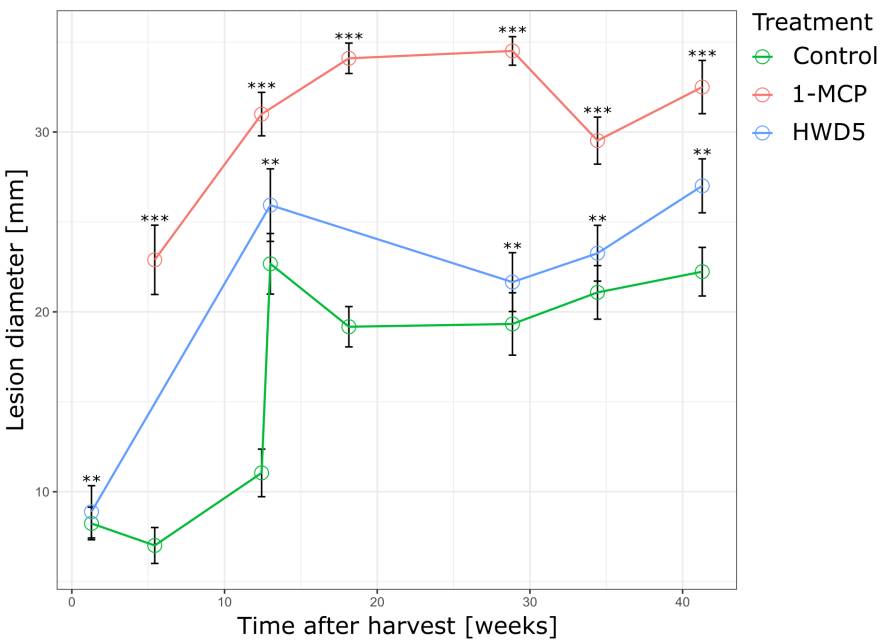

FIGURE 6 | Lesion diameter 96 hpi of pathogenicity assay performed at various time points throughout CA storage for control, HWD5 and 1-MCP treated apples inoculated with *B. cinerea*. Error bars denote the standard error of the mean ($n \geq 10$). Significant differences are indicated by an asterisk. $^{**}p < 0.01$ $^{***}p < 0.001$.

and **Supplementary Table 10**). HWD5 treatment caused only significant reductions in the peel. Expression of *MPK3*, *MPK6*, *PAL1*, *SMO1* and *SMO2* was affected at harvest. After 29 w of CA storage, only SMO1 still had a significantly lower expression compared to the control. 1-MCP treatment was able to also affect gene expression in flesh tissue, significantly reducing *ERF1* and *PAL1*, but only at 12 w in CA storage. In the peel, expression of *ERF1*, *PAL1* and *SMO1* was significantly reduced compared to the control at both 12 and 29 w. A PCA was performed on this expression data. The result demonstrates that peel has a clearly distinct expression pattern from flesh tissue and also reacts differently to the treatments (**Figure 8**).

The temperature profiles of the fruit during and after the HWD5 treatment were simulated (**Figure 9**). The fruit surface rapidly reaches 50°C, but the temperature shows a strong downward gradient along the radius toward the core. Diffusion of heat causes the inside of the fruit to reach its maximum temperature only after 5 min of dipping. For example, at a radial depth of 15 mm the temperature reaches 25.9°C at the end of the 5 min HWD, but still increases to a maximum of 29.1°C after the treatment.

DISCUSSION

Inoculation With *Botrytis cinerea* Caused Extensive Reprogramming of the Defense Response

The apple genome contains a total of 40,121 genes of which 25,912 were found to be expressed in our data (average expression over all samples > 1 tpm). A total of 10,204 genes (∼39.4% of expressed ones) were differentially expressed on at least one time point studied of which 7,489 exhibited a fold change of at least 2 (∼28.9% of expressed). A transcriptome time series analysis of *Arabidopsis* inoculated with *B. cinerea* found differential expression of about one-third of the *Arabidopsis* genome in the first 48 h (Windram et al., 2012). Our results demonstrate that also in apple extensive reprogramming of the transcriptome occurs upon inoculation with *B. cinerea* and that the extent to which this happened increased in the 28 hpi studied. Furthermore, this started already almost immediately after inoculation and includes some transcriptional activation of secondary metabolism (**Figures 1**, **2**). Almost four times as many genes were significantly upregulated than downregulated. Also in the case of lettuce (*Lactuca sativa*) and strawberry (*Fragaria* × *ananassa*) inoculated with *B. cinerea* a lot more upregulated genes were detected (De Cremer et al., 2013; Xiong et al., 2018).

Activation of Pathogen-Triggered Immunity in Inoculated Fruit

Our data shows clear evidence that *B. cinerea* inoculated fruit exhibited activation of PTI, which starts with pathogen recognition. In our data, we found upregulation of 12 WAK, 3 CERK1 and one BAK1 genes (**Figure 2** and **Supplementary Table 5**). In lettuce inoculated with *B. cinerea* 12 out of 21 annotated *WAKs* were significantly up or downregulated at 48 hpi (De Cremer et al., 2013). In our data, all differentially expressed *WAKs*, *CERK1s* and *BAK1* were significantly upregulated at 28 hpi and some already at 12 hpi. Brutus et al. (2010) found that *Arabidopsis* overexpressing *WAK1* exhibits enhanced resistance against *B. cinerea*. BAK1 on the other hand plays an important role in PTI signaling and is a negative regulator of cell death (He et al., 2007).

For PTI to manifest, this recognition then needs to be signaled. Evidence that this occurs is provided by the significant overrepresentation in upregulated DEGs of the GO terms protein phosphorylation at 12 and 28 hpi, calcium ion transport at 28 hpi and the KEGG pathway MAPK signaling pathway—plant at 28 hpi (**Supplementary Tables 3**, **4**). More specific evidence is provided by upregulation of 11 *CNGCs*, 5 *CaMs*, 6 *CDPKs*, 1 *CaMK*, 1 *RBOH* and a variety of *MAPKKKs*, *MAPKKs,* and *MAPKs* at 12 and/or 28 hpi (**Supplementary Table 5**). MEKK1, MKK1/MKK2, and MPK4 form a MAPK cascade that is important in the activation of effective defense against *B. cinerea* in *Arabidopsis* (Qiu et al., 2008). In our data we found two MEKK1, one MKK2 end 3 MPK4 genes that were significantly upregulated. MPK4 may then activate WRKY33 through MKS1, which in turn activates JA/ET responses (Zheng et al., 2006). All four annotated WRKY33 genes in the apple genome were significantly upregulated in our samples. WRKY33 in turn was found to antagonize SA signaling, thus preventing suppression of the JA pathway (Birkenbihl et al., 2012). The WRKY family TFs were the first to show significant overrepresentation around 18 hpi in *Arabidopsis* inoculated with *B. cinerea* (Windram et al., 2012).

Upregulated DEGs at 28 hpi displayed enrichment of regulation of hormone levels and at 12 and 28 hpi of alpha-linoleic acid metabolism (**Supplementary Tables 3**, **4**). This demonstrates that hormonal modulation of fruit defenses did in fact take place and suggests activation of the JA pathway. Closer inspection shows upregulation of JA biosynthesis genes (*LOX, AOS, AOC, OPR3, OPCL1*; **Supplementary Figure 7** and **Supplementary Table 5**). JA works synergistically with ET to coordinate defense responses against necrotrophic pathogens (Memelink, 2009; Bürger and Chory, 2019). Clear activation of ET biosynthesis (*ACS1/2/6, ACO)* and signaling (*ETR, EIN3, ERF1*) could be detected (**Supplementary Figure 7** and **Supplementary Table 5**). Time series analysis of *Arabidopsis* inoculated with *B. cinerea* showed that upregulation of ET biosynthesis through *ACS*, followed by ET signaling, was the first hormonal response at 14 hpi (Windram et al., 2012). We detected significant upregulation of *ACS* at 12 and 28 hpi.

Metabolic Reprogramming for Defense

Non-essential Processes for the Defense Were Downregulated

Downregulation of photosynthesis is a common local response in plant defense as a strategy to free up resources for the defense response and protect photosynthetic machinery from oxidative damage (Bolton, 2009). Our data confirms this with overrepresentation in downregulated DEGs of photosynthesis and biosynthesis of chlorophyll and antenna proteins at 28

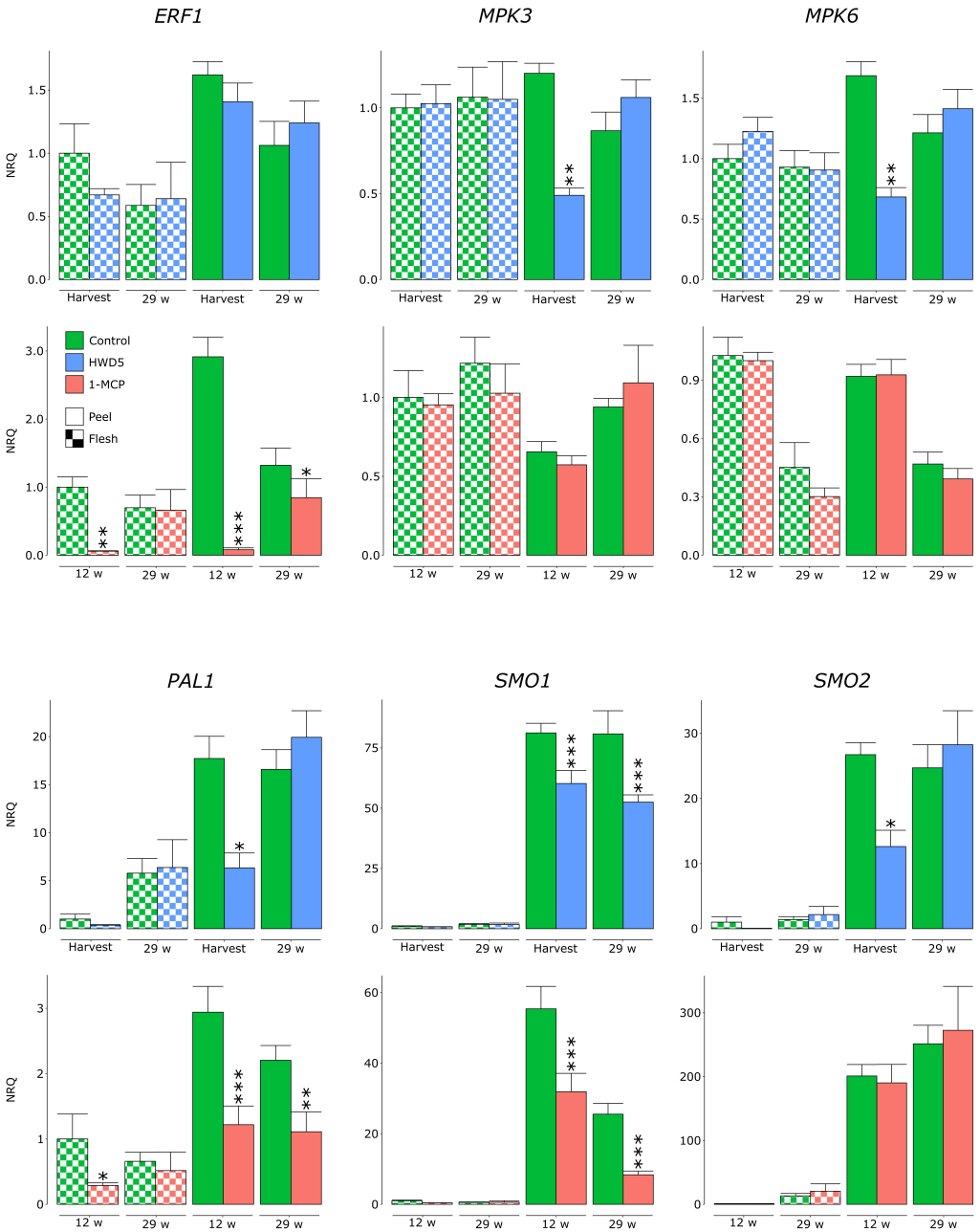

FIGURE 7 | Normalized relative quantities of genes analyzed in flesh and peel samples of "Jonagored" apples belonging to control, HWD5 or 1-MCP treatment. Samples were analyzed at harvest and after 29 w of CA storage (control, HWD5) or after 12 and 29 w of CA storage (control, 1-MCP). Error bars denote the standard errors of at least 6 biological replicates. Statistically significant differences with the control are denoted with asterisks: *$p < 0.05$ **$p < 0.01$ ***$p < 0.001$.

hpi. Photosynthesis and biosynthesis of chlorophyll were also downregulated in *Arabidopsis* inoculated with *B. cinerea* starting from 18 to 22 hpi, respectively (Windram et al., 2012).

Energy Production Was Transcriptionally Increased to Fuel the Defense

The defense response requires a lot of energy and this can be provided by the upregulation of β-oxidation of fatty acids, glycolysis, pyruvate metabolism, the PDH-bypass, acetyl-CoA biosynthesis, the TCA cycle and the γ-butyric acid (GABA) shunt (Bolton et al., 2008). Key genes of all these pathways were upregulated in our data. We found enrichment of the GO processes lipid metabolic process at 12 and 28 hpi, and acetyl-CoA biosynthetic process and KEGG pathway fatty acid degradation at 28 hpi in upregulated DEGs (**Supplementary Tables 3**, **4**), and upregulation of genes involved in all conversions of the β-oxidation (**Supplementary Figure 8** and **Supplementary Table 6**). Key regulatory points of the glycolysis [*PFK-1*,

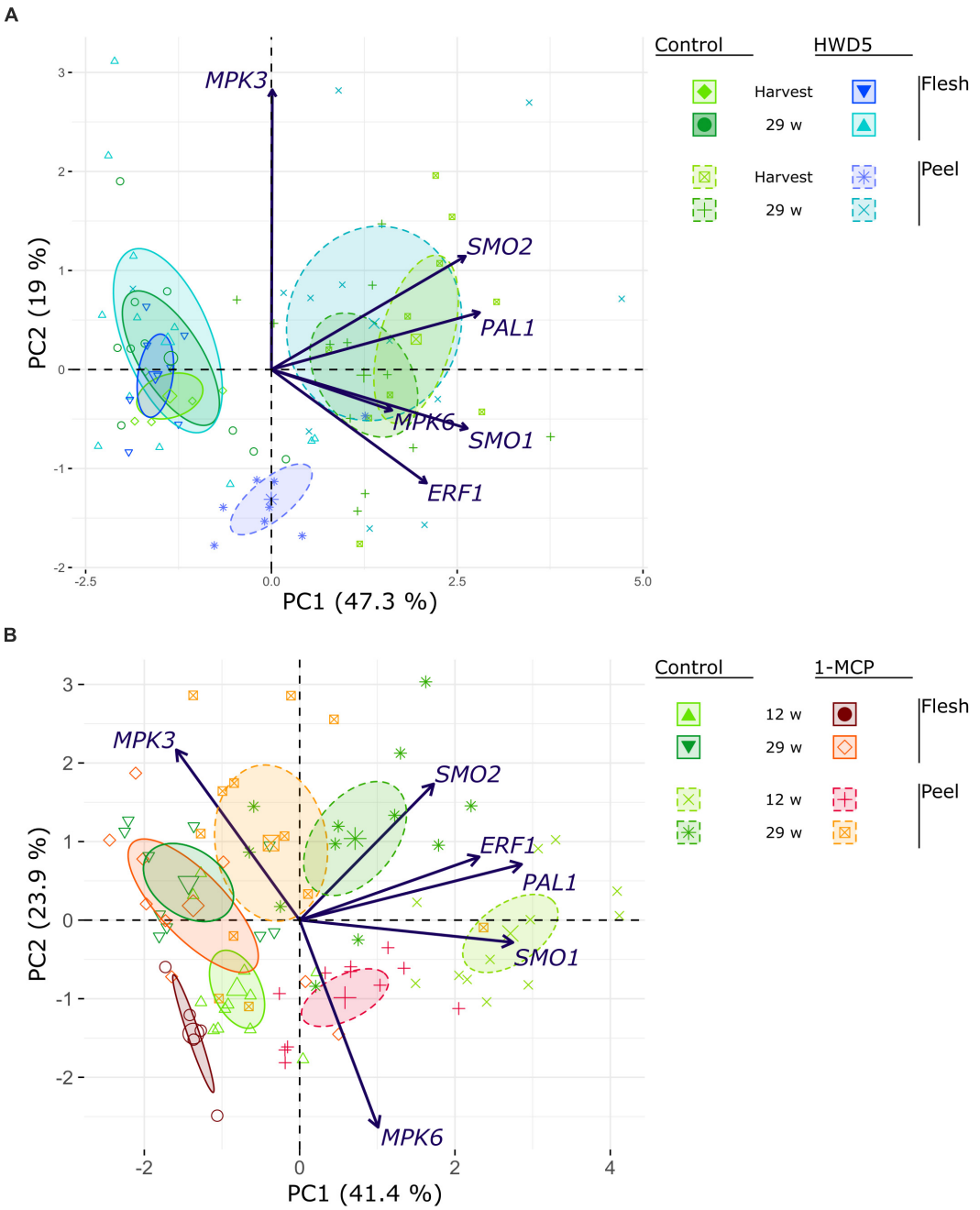

FIGURE 8 | PCA biplot of gene expression analyses performed on **(A)** control and HWD5 at harvest or after 29 w of CA storage, or **(B)** control and 1-MCP treated apples that had been stored with CA 13 or 29 w. Ellipses denote 95% confidence intervals.

hexokinase, *phosphoglycerate mutase* (*PGM*)] were significantly upregulated (**Supplementary Figure 9** and **Supplementary Table 6**). Our data shows significant upregulation of the transformation of pyruvate into acetyl-CoA by *PDH*, but also through the PDH-bypass that goes through *pyruvate decarboxylase* (*PDC*, 0/6), *aldehyde dehydrogenase* (*ALDH*, 2/10) and *acetyl-CoA synthethase* (2/2). This is confirmed by the overrepresentation of the GO term acetyl-CoA biosynthetic process in upregulated DEGs of 28 hpi (**Supplementary Table 3**). We suspect activation of the TCA cycle because of significant upregulation of *citrate synthase, aconitate hydratase* and *isocitrate dehydrogenase*. Lastly, upregulation of the GABA shunt is evident from significant upregulation of *glutamate dehydrogenase* (*GDH*) and *glutamate decarboxylase* (*GDC*). In conclusion, we demonstrated that on transcriptional level a clear activation of energy metabolism occurred in *B. cinerea* inoculated apples.

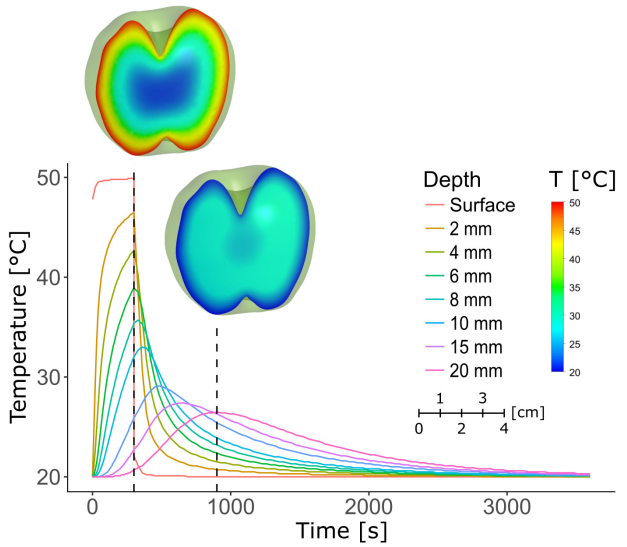

FIGURE 9 | Simulation of the temperature profile in an apple as a function of time during and after a 50°C HWD of 5 min. The first dashed line marks the end of the 5 min treatment, the second marks 15 or 10 min of air cooling after the treatment. Fruit heatmaps corresponding to the dashed lines show the temperature profile in the fruit at those time points.

Secondary Metabolism Was Activated

Our results show strong activation of terpenoid biosynthesis, which is supported by overrepresentation in upregulated DEGs of isoprenoid metabolic process and terpenoid backbone biosynthesis at 12 hpi, sesquiterpenoid and triterpenoid biosynthesis at 12 and 28 hpi, and monoterpenoid biosynthesis and diterpenoid biosynthesis at 28 hpi (**Supplementary Table 3**). Terpenoids play a role in plant defense as phytoanticipins and phytoalexins. Our data shows clear activation of the cytosolic MVA pathway (**Figure 3** and **Supplementary Table 6**) which points to biosynthesis of sesqui- and triterpenoids. This is supported by significant upregulation of *FPPS*, *FPPFT*, *SMO*, *(-)-germacrene D synthase*, β-*amyrin synthase* and β-*amyrin 28-monooxygenase*. The MVA pathway was also upregulated in the case of apple-*P. expansum* (Barad et al., 2016), tomato-*Colletotrichum gloeosporioides* (Alkan et al., 2015), lettuce-*B. cinerea* (De Cremer et al., 2013) and strawberry-*B. cinerea* (Xiong et al., 2018). Furthermore, ontogenic resistance in cucumber was linked to terpenoids and terpenoid glycosides in the peel (Mansfeld et al., 2017). *A. alternata* inoculated jujube displayed a red ring phenotype that contained the infection within. One pathway specifically upregulated in this red ring was terpenoid biosynthesis (Yuan et al., 2019). All of this evidence supports a prominent role of terpenoids in the defense response.

A common defense response in fruit is the activation of the phenylpropanoid pathway, e.g., apple-*P. expansum* (Vilanova et al., 2014), strawberry-*B. cinerea* (Xiong et al., 2018) and tomato-*C. gloeosporioides* (Alkan et al., 2015). This is confirmed in our samples by overrepresentation in upregulated DEGs of the GO term phenylpropanoid metabolic process at 0, 12 and 28 hpi, and KEGG pathway phenylpropanoid biosynthesis at 12 and 28 hpi (**Supplementary Tables 3**, **4**). All four homologs of the key enzyme regulating this pathway, PAL, were strongly upregulated in our samples (**Figure 4** and **Supplementary Table 5**). Furthermore, a lot of downstream enzymes in the pathway exhibited significant upregulation.

Early Activation of the Mevalonate Pathway Correlated With Reduced Susceptibility

Analysis of correlations between gene expression and infection success revealed that the MVA pathway had a strong negative impact on infection success (**Figure 5**). Especially early activation of this pathway seems to be important. When comparing the progenitor of domesticated apple (*M. sieversii* PI613981) resistant to *P. expansum* with the susceptible domesticated apple cultivar "Royal Gala," Ballester et al. (2017) found evidence that the early activation of defense responses was one critical factor for resistance. Vilanova et al. (2014) compared the defense of apple in response to a compatible (*P. expansum*) and incompatible (*P. digitatum*) pathogen. Their results showed that in the incompatible interaction, the phenylpropanoid pathway was upregulated faster and stronger. Furthermore, previous research of us has found a link between cell density and resistance in apple, possibly due to a correlation with biosynthetic capacity; meaning, fruit with a higher cell density may be able to mount a larger defense response in a given time (Naets et al., 2019). All this evidence indicates timing and magnitude of defense responses plays a key role in effective defense, and that, in the case of apple-*B. cinerea*, there is an important role for the MVA pathway.

Ethylene Signaling Affects Secondary Metabolism Needed for Defense

It is generally accepted that resistance against necrotrophs is modulated by JA/ET signaling (Pieterse et al., 2012; Bürger and Chory, 2019). We subjected apples to two treatments that can impact the ET component. 1-MCP is an ET perception inhibitor that strongly binds the ET receptor without activating it. Heat treatments can inactivate *ACS* and *ACO* which are heat labile, and even impact ET signaling by either inactivation of the receptors or affecting the downstream signaling (Lurie, 1998). For 1-MCP, this is confirmed by a significant reduction in *ERF1* expression in peel at 12 and 29 w and in flesh at 12 w. HWD5 did not significantly affect *ERF1* expression, but did significantly reduce *MPK3* and *MPK6* expression in peel tissue at harvest. *MPK3* and *MPK6* play a role in *Botrytis*-induced ET biosynthesis, but also in downstream activation of ET responsive genes (Jagodzik et al., 2018). *PAL1*, *SMO1*, and *SMO2* were tested as key genes for the phenylpropanoid and terpenoid biosynthesis. Both 1-MCP and HWD5 significantly affected expression of *PAL1* and *SMO1*, demonstrating that ET likely plays a role in regulating both pathways.

Both 1-MCP and HWD5 significantly increased lesion diameters 96 hpi and this for all tested time points throughout CA storage. Resistance against *B. cinerea* in *Arabidopsis* has been linked to the ability to confine the infection by cell wall modifications using hydroxycinnamates and monolignols. This

defense response was mediated by ET (Lloyd et al., 2011). Therefore, increased susceptibility in 1-MCP treated fruit could be a result of a lessened ability to confine the pathogen due to the significant reduction in *ERF1* and *PAL1* expression. *PAL1* was also significantly lowered in peel tissue of HWD5 treated fruit at harvest, but not at 29 w. It is possible that this resulted in a lower amount of PAL1 proteins, even after expression levels recovered. Both 1-MCP and HWD5 resulted in significantly lower expression of *SMO1* in peel tissue at each time point. The $\log_2$ reduction in peel tissue of 1-MCP treated fruit was -0.8 $\pm$ 0.29 and -1.61 $\pm$ 0.25 at 12 and 29 w, respectively, and in peel tissue of HWD5 treated fruit was -0.43 $\pm$ 0.15 and -0.62 $\pm$ 0.19 at harvest and 29 w, respectively. This difference in effect size could then also explain the difference in susceptibility increase. In practice *B. cinerea* can cause latent infections of flowers that then develop later during storage and fruit ripening (Dean et al., 2012), is able to directly infect fruit in the orchard *via* natural openings, operates as wound pathogen taking opportunity of wounds caused by insects, birds or postharvest handling (Droby and Lichter, 2007; Carisse, 2016), and can spread from fruit to fruit in the storage room in what is called nest rot (Snowdon, 1990). It can be expected that these different infection pathways, fruit maturity at infection, and disease development conditions may have their impact on these results.

CONCLUSION

In this work we presented an RNAseq study of *B. cinerea* inoculated apple. We demonstrate that drastic reprogramming occurs upon inoculation with differential expression of 28.9% of expressed genes. Part of this was a complete transcriptional reprogramming of the metabolism with a downregulation of photosynthesis and an upregulation of energy and secondary metabolism. Here we provided evidence of a correlation between an early activation of the mevalonate pathway that synthesizes precursors for terpenoids and reduced susceptibility. Further evidence for the importance of terpenoids in the defense response is provided by treating fruit with 1-MCP or HWD5. These treatments impacted ET perception and signaling, potentially related with the observed significantly larger lesions at 96 hpi. We demonstrated a significant reduction for both treatments in *SMO1* expression in peel tissue, a key gene in terpenoid biosynthesis. This evidence points to an important impact of terpenoid biosynthesis coordinated by ET signaling on apple defense against *B. cinerea*.

DATA AVAILABILITY STATEMENT

The data presented in the study are deposited in the GEO repository, accession number GSE195841.

AUTHOR CONTRIBUTIONS

MN: substantial contribution to conception and design, execution, analysis, and interpretation. WV: substantial contribution to acquisition of the data of the work. WG, PV, and BN: substantial contribution to analysis of the data. WK and AG: substantial contribution to design and interpretation. BD: substantial contribution to interpretation. All authors contributed to the article and approved the submitted version.

FUNDING

MN was funded by a Ph.D. grant of the Research Foundation Flanders (FWO; SB fellowship 3E140517).

ACKNOWLEDGMENTS

We would like to acknowledge Julia Schumacher (Institut für Biologie & Biotechnologie der Pflanzen) for the kind provision of the *B. cinerea* B05.10 isolate. Further, we would like to thank the Flanders Centre of Postharvest Technology (VCBT) for allowing us to use their storage facilities and ISO 17025 certified measurement possibilities for apple fruit quality parameters.

SUPPLEMENTARY MATERIAL

The Supplementary Material for this article can be found online at: https://www.frontiersin.org/articles/10.3389/fmicb.2022.797234/full#supplementary-material

REFERENCES

Alkan, N., Friedlander, G., Ment, D., Prusky, D., and Fluhr, R. (2015). Simultaneous transcriptome analysis of *Colletotrichum* gloeosporioides and tomato fruit pathosystem reveals novel fungal pathogenicity and fruit defense strategies. *New Phytol.* 205, 801–815. doi: 10.1111/nph.13087

Ballester, A. R., Norelli, J., Burchard, E., Abdelfattah, A., Levin, E., González-Candelas, L., et al. (2017). Transcriptomic response of resistant (PI613981–*Malus sieversii*) and susceptible ('Royal Gala') genotypes of apple to blue mold (*Penicillium expansum*) infection. *Front. Plant Sci.* 8:1981. doi: 10.3389/fpls.2017.01981

Barad, S., Sela, N., Kumar, D., Kumar-Dubey, A., Glam-Matana, N., Sherman, A., et al. (2016). Fungal and host transcriptome analysis of PH-regulated genes during colonization of apple fruits by *Penicillium expansum*. *BMC Genomics* 17:330. doi: 10.1186/s12864-016-2665-7

Birkenbihl, R. P., Diezel, C., and Somssich, I. E. (2012). *Arabidopsis* WRKY33 is a key transcriptional regulator of hormonal and metabolic responses toward *Botrytis cinerea* infection. *Plant Physiol.* 159, 266–285. doi: 10.1104/pp.111.192641

Boller, T., and Felix, G. (2009). A renaissance of elicitors: perception of microbe-associated molecular patterns and danger signals by pattern-recognition receptors. *Annu. Rev. Plant Biol.* 60, 379–406. doi: 10.1146/annurev.arplant.57.032905.105346

Bolton, M. D. (2009). Primary metabolism and plant defense—fuel for the fire. *Mol. Plant Microbe Interact.* 22, 487–497. doi: 10.1094/MPMI-22-5-0487

Bolton, M. D., Kolmer, J. A., Xu, W. W., and Garvin, D. F. (2008). Lr34 -mediated leaf rust resistance in wheat: transcript profiling reveals a high energetic demand supported by transient recruitment of multiple metabolic pathways. *Mol. Plant Microbe Interact.* 21, 1515–1527. doi: 10.1094/MPMI-21-12-1515

Brutus, A., Sicilia, F., Macone, A., Cervone, F., and De Lorenzo, G. (2010). A domain swap approach reveals a role of the plant wall-associated kinase 1 (WAK1) as a receptor of oligogalacturonides. *Proc. Natl. Acad. Sci. U.S.A.* 107, 9452–9457. doi: 10.1073/pnas.1000675107

Bürger, M., and Chory, J. (2019). Stressed out about hormones: how plants orchestrate immunity. *Cell Host Microbe* 26, 163–172. doi: 10.1016/j.chom.2019.07.006

Carisse, O. (2016). "Epidemiology and aerobiology of *Botrytis* spp," in *Botrytis – The Fungus, the Pathogen and Its Management in Agricultural Systems*, eds S. Fillinger and Y. Elad (Cham: Springer International Publishing), 127–148. doi: 10.1007/978-3-319-23371-0_7

Daccord, N., Celton, J. M., Linsmith, G., Becker, C., Choisne, N., Schijlen, E., et al. (2017). High-quality de novo assembly of the apple genome and methylome dynamics of early fruit development. *Nat. Genet.* 49, 1099–1106. doi: 10.1038/ng.3886

De Cremer, K., Mathys, J., Vos, C., Froenicke, L., Michelmore, R. W., Cammue, B. P., et al. (2013). RNAseq-based transcriptome analysis of *Lactuca Sativa* infected by the fungal necrotroph *Botrytis cinerea*. *Plant Cell Environ.* 36, 1992–2007. doi: 10.1111/pce.12106

Dean, R., Van Kan, J. A., Pretorius, Z. A., Hammond-Kosack, K. E., Di Pietro, A., Spanu, P. D., et al. (2012). The top 10 fungal pathogens in molecular plant pathology. *Mol. Plant Pathol.* 13, 414–430. doi: 10.1111/j.1364-3703.2011.00783.x

Decreux, A., and Messiaen, J. (2005). Wall-associated kinase WAK1 interacts with cell wall pectins in a calcium-induced conformation. *Plant Cell Physiol.* 46, 268–278. doi: 10.1093/pcp/pci026

Dixon, R. A., Achnine, L., Kota, P., Liu, C. J., Reddy, M. S., and Wang, L. (2002). The phenylpropanoid pathway and plant defence-a genomics perspective. *Mol. Plant Pathol.* 3, 371–390. doi: 10.1046/j.1364-3703.2002.00131.x

Droby, S., and Lichter, A. (2007). "Post-harvest botrytis infection: etiology, development and management," in *Botrytis: Biology, Pathology and Control*, eds Y. Elad, B. Williamson, P. Tudzynski, and N. Delen (Dordrecht: Springer Netherlands), 349–367. doi: 10.1007/978-1-4020-2626-3_19

Elad, Y., Vivier, M., and Fillinger, S. (2016). "Botrytis, the good, the bad and the ugly," in *Botrytis – the Fungus, the Pathogen and Its Management in Agricultural Systems*, eds S. Fillinger and Y. Elad (Cham: Springer International Publishing), 1–15. doi: 10.1007/978-3-319-23371-0_1

Food and Agriculture Organization [FAO] (2019). *FAOSTAT*. Available online at: www.fao.org/faostat (accessed November 8, 2019).

González, C., Brito, N., and Sharon, A. (2016). "Infection process and fungal virulence factors," in *Botrytis – the Fungus, the Pathogen and Its Management in Agricultural Systems*, eds S. Fillinger and Y. Elad (Cham: Springer International Publishing), 229–246. doi: 10.1007/978-3-319-23371-0_12

Götz, S., García-Gómez, J. M., Terol, J., Williams, T. D., Nagaraj, S. H., Nueda, M. J., et al. (2008). High-throughput functional annotation and data mining with the Blast2GO suite. *Nucleic Acids Res.* 36, 3420–3435. doi: 10.1093/nar/gkn176

Govrin, E. M., and Levine, A. (2002). Infection of *Arabidopsis* with a necrotrophic pathogen, *Botrytis cinerea*, elicits various defense responses but does not induce Systemic Acquired Resistance (SAR). *Plant Mol. Biol.* 48, 267–276. doi: 10.1023/A:1013323222095

Gruyters, W., Verboven, P., Diels, E., Rogge, S., Smeets, B., Ramon, H., et al. (2018). Modelling cooling of packaged fruit using 3D shape models. *Food Bioprocess Technol.* 11, 2008–2020. doi: 10.1007/s11947-018-2163-9

He, K., Gou, X., Yuan, T., Lin, H., Asami, T., Yoshida, S., et al. (2007). BAK1 and BKK1 regulate brassinosteroid-dependent growth and brassinosteroid-independent cell-death pathways. *Curr. Biol.* 17, 1109–1115. doi: 10.1016/j.cub.2007.05.036

Jagodzik, P., Tajdel-Zielinska, M., Ciesla, A., Marczak, M., and Ludwikow, A. (2018). Mitogen-activated protein kinase cascades in plant hormone signaling. *Front. Plant Sci.* 9:1387. doi: 10.3389/fpls.2018.01387

Jones, J. D. G., and Dangl, J. L. (2006). The plant immune system. *Nature* 444, 323–329. doi: 10.1038/nature05286

Jung, S., Jesudurai, C., Staton, M., Du, Z., Ficklin, S., Cho, I., et al. (2004). GDR (Genome Database for Rosaceae): integrated web resources for rosaceae genomics and genetics research. *BMC Bioinformatics* 5:130. doi: 10.1186/1471-2105-5-130

Kanehisa, M. (2000). KEGG: kyoto encyclopedia of genes and genomes. *Nucleic Acids Res.* 28, 27–30. doi: 10.1093/nar/28.1.27

Lloyd, A. J., William Allwood, J., Winder, C. L., Dunn, W. B., Heald, J. K., Cristescu, S. M., et al. (2011). Metabolomic approaches reveal that cell wall modifications play a major role in ethylene-mediated resistance against *Botrytis cinerea*. *Plant J.* 67, 852–868. doi: 10.1111/j.1365-313X.2011.04639.x

Love, M. I., Huber, W., and Anders, S. (2014). Moderated estimation of fold change and dispersion for RNA-Seq data with DESeq2. *Genome Biol.* 15:550. doi: 10.1186/s13059-014-0550-8

Lurie, S. (1998). Postharvest heat treatments. *Postharvest Biol. Technol.* 14, 257–269. doi: 10.1016/S0925-5214(98)00045-3

Mansfeld, B. N., Colle, M., Kang, Y., Jones, A. D., and Grumet, R. (2017). Transcriptomic and metabolomic analyses of cucumber fruit peels reveal a developmental increase in terpenoid glycosides associated with age-related resistance to *Phytophthora capsici*. *Hortic. Res.* 4:17022. doi: 10.1038/hortres.2017.22

Memelink, J. (2009). Regulation of gene expression by jasmonate hormones. *Phytochemistry* 70, 1560–1570. doi: 10.1016/j.phytochem.2009.09.004

Mengiste, T. (2012). Plant immunity to necrotrophs. *Annu. Rev. Phytopathol.* 50, 267–294. doi: 10.1146/annurev-phyto-081211-172955

Miya, A., Albert, P., Shinya, T., Desaki, Y., Ichimura, K., Shirasu, K., et al. (2007). CERK1, a LysM receptor kinase, is essential for chitin elicitor signaling in *Arabidopsis*. *Proc. Natl. Acad. Sci. U.S.A.* 104, 19613–19618. doi: 10.1073/pnas.0705147104

Naets, M., Bossuyt, L., De Coninck, B., Keulemans, W., and Geeraerd, A. (2020). Exploratory study on postharvest pathogens of 'Nicoter' apple in flanders (Belgium). *Sci. Hortic.* 260:108872. doi: 10.1016/j.scienta.2019.108872

Naets, M., van Dael, M., Vanstreels, E., Daelemans, D., Verboven, P., Nicolaï, B., et al. (2018). To disinfect or not to disinfect in postharvest research on the fungal decay of apple? *Int. J. Food Microbiol.* 266, 190–199. doi: 10.1016/j.ijfoodmicro.2017.12.003

Naets, M., Wang, Z., Verboven, P., Nicolaï, B., Keulemans, W., and Geeraerd, A. (2019). Size does matter – susceptibility of apple for grey mould is affected by cell size. *Plant Pathol.* 69:13097. doi: 10.1111/ppa.13097

Pieterse, C. M., Van der Does, D., Zamioudis, C., Leon-Reyes, A., and Van Wees, S. C. (2012). Hormonal modulation of plant immunity. *Annu. Rev. Cell Dev. Biol.* 28, 489–521. doi: 10.1146/annurev-cellbio-092910-154055

Qiu, J. L., Zhou, L., Yun, B. W., Nielsen, H. B., Fiil, B. K., Petersen, K., et al. (2008). *Arabidopsis* mitogen-activated protein kinase kinases MKK1 and MKK2 have overlapping functions in defense signaling mediated by MEKK1, MPK4, and MKS1. *Plant Physiol.* 148, 212–222. doi: 10.1104/pp.108.120006

R Development Core Team (2011). *R: A Language and Environment for Statistical Computing*, Vol. 1. Vienna: R Foundation for Statistical Computing.

Reddy, A. S. N., Ali, G. S., Celesnik, H., and Day, I. S. (2011). Coping with stresses: roles of calcium- and calcium/calmodulin-regulated gene expression. *Plant Cell* 23, 2010–2032. doi: 10.1105/tpc.111.084988

Rentel, M. C., Lecourieux, D., Ouaked, F., Usher, S. L., Petersen, L., Okamoto, H., et al. (2004). OXI1 kinase is necessary for oxidative burst-mediated signalling in *Arabidopsis*. *Nature* 427, 858–861. doi: 10.1038/nature02353

Snowdon, A. L. (1990). A colour atlas of post-harvest diseases and disorders of fruit and vegetables. volume 1: general introduction and fruits. *Exp. Agric.* 26:365. doi: 10.1017/S0014479700018573

Storch, T. T., Pegoraro, C., Finatto, T., Quecini, V., Rombaldi, C. V., and Girardi, C. L. (2015). Identification of a novel reference gene for apple transcriptional profiling under postharvest conditions." Edited by Boris Alexander Vinatzer. *PLoS One* 10:e0120599. doi: 10.1371/journal.pone.0120599

Torres, M. A. (2010). ROS in biotic interactions. *Physiol. Plant.* 138, 414–429. doi: 10.1111/j.1399-3054.2009.01326.x

Van Kan, J. A., Stassen, J. H., Mosbach, A., Van Der Lee, T. A., Faino, L., Farmer, A. D., et al. (2017). A gapless genome sequence of the fungus *Botrytis cinerea*. *Mol. Plant Pathol.* 8, 75–89. doi: 10.1111/mpp.12384

Vilanova, L., Wisniewski, M., Norelli, J., Viñas, I., Torres, R., Usall, J., et al. (2014). Transcriptomic profiling of apple in response to inoculation with a pathogen

(*Penicillium expansum*) and a non-pathogen (*Penicillium digitatum*). *Plant Mol. Biol. Rep.* 32, 566–583. doi: 10.1007/s11105-013-0676-y

Windram, O., Madhou, P., McHattie, S., Hill, C., Hickman, R., Cooke, E., et al. (2012). *Arabidopsis* defense against *Botrytis cinerea*?: chronology and regulation deciphered by high-resolution temporal transcriptomic analysis. *Plant Cell* 24, 3530–3557. doi: 10.1105/tpc.112.102046

Xiong, J. S., Zhu, H.-Y., Bai, Y.-B., Liu, H., and Cheng, Z.-M. (2018). RNA sequencing-based transcriptome analysis of mature strawberry fruit infected by necrotrophic fungal pathogen *Botrytis cinerea*. *Physiol. Mol. Plant Pathol.* 104, 77–85. doi: 10.1016/j.pmpp.2018.08.005

Yuan, S., Yan, J., Wang, M., Ding, X., Zhang, Y., Li, W., et al. (2019). Transcriptomic and metabolic profiling reveals 'Green Ring' and 'Red Ring' on jujube fruit upon postharvest alternaria alternata infection. *Plant Cell Physiol.* 60, 844–861. doi: 10.1093/pcp/pcy252

Zhang, S., Chen, G. H., Liu, Y., Chen, H., Yang, G., Yuan, X., et al. (2013). Apple gene function and gene family database: an integrated bioinformatics database for apple research. *Plant Growth Regul.* 70, 199–206. doi: 10.1007/s10725-013-9787-6

Zheng, Z., Qamar, S. A., Chen, Z., and Mengiste, T. (2006). *Arabidopsis* WRKY33 transcription factor is required for resistance to necrotrophic fungal pathogens. *Plant J.* 48, 592–605. doi: 10.1111/j.1365-313X.2006.02901.x

Zhong, S., Joung, J. G., Zheng, Y., Chen, Y. R., Liu, B., Shao, Y., et al. (2011). High-throughput illumina strand-specific RNA sequencing library preparation. *Cold Spring Harb. Protoc.* 6, 940–949. doi: 10.1101/pdb.prot5652

Conflict of Interest: The authors declare that the research was conducted in the absence of any commercial or financial relationships that could be construed as a potential conflict of interest.

Advantages of publishing in Frontiers

OPEN ACCESS
Articles are free to read for greatest visibility and readership

FAST PUBLICATION
Around 90 days from submission to decision

HIGH QUALITY PEER-REVIEW
Rigorous, collaborative, and constructive peer-review

TRANSPARENT PEER-REVIEW
Editors and reviewers acknowledged by name on published articles

Frontiers
Avenue du Tribunal-Fédéral 34
1005 Lausanne | Switzerland

Visit us: www.frontiersin.org
Contact us: frontiersin.org/about/contact

REPRODUCIBILITY OF RESEARCH
Support open data and methods to enhance research reproducibility

DIGITAL PUBLISHING
Articles designed for optimal readership across devices

FOLLOW US
@frontiersin

IMPACT METRICS
Advanced article metrics track visibility across digital media

EXTENSIVE PROMOTION
Marketing and promotion of impactful research

LOOP RESEARCH NETWORK
Our network increases your article's readership